Università degli Studi di Napoli Federico II

Ph.D. Program in

Civil System Engineering

XXXVI Cycle

Thesis for the Degree of Doctor of Philosophy

WASTE-BASED CHAIN ELONGATION FOR MEDIUM CHAIN FATTY ACIDS PRODUCTION

by

Samuel Gyebi Arhin

Scuola Politecnica e delle Scienze di Base

Dipartimento di Ingegneria Civile, Edile e Ambientale

Dissertation submitted: February 22, 2024

PhD supervisors: prof. ing. Giovanni Esposito

University of Naples Federico II

prof. ing. Alessandra Cesaro

University of Naples Federico II

prof. ing. Francesco Di Capua

University of Basilicata

PhD coordinator: prof. ing. Andrea Papola

Dedication

To my wife Selina Gyebi Arhin for her relentless support, love, encouragement, and sacrifice throughout this journey

"Na nea otumi yɛ ma ɛtra ade nyinaa ma ɛboro so kyɛn nea yɛsrɛ anaasɛ yesusuw sɛnea tumi a ɛyɛ yɛn mu adwuma no te no"

WASTE-BASED CHAIN ELONGATION FOR MEDIUM CHAIN FATTY ACIDS PRODUCTION

Ph.D. Thesis presented

for the fulfillment of the Degree of Doctor of Philosophy

in Civil Systems Engineering

by

Samuel Gyebi Arhin

January 2024

Approved as to style and content by

……..

Prof. ing. Giovanni Esposito, Advisor

…….

Prof. ing. Alessandra Cesaro, Co-advisor

…….

Prof. ing. Francesco di Capua, Co-advisor

Università degli Studi di Napoli Federico II

Ph.D. Program in Civil System Engineering

XXXVI cycle - Chairman: Prof. ing. Andrea Papola

Candidate's declaration

I hereby declare that this thesis submitted to obtain the academic degree of Philosophiæ Doctor (Ph.D.) in Civil Systems Engineering is my own unaided work, that I have not used other than the sources indicated, and that all direct and indirect sources are acknowledged as references.

Parts of this dissertation have been published in international journals and/or conference articles (see list of the author's publications).

…….

Samuel Gyebi Arhin

March 2024, Napoli

ENGLISH SUMMARY

The sustainable conversion of organic waste streams into biochemicals such as medium-chain fatty acids (MCFAs) represents a crucial node in the development of a circular economy and averting the negative impacts of unsustainable sources. The overarching goal of this PhD thesis was to investigate the valorization of food waste via chain elongation to generate MCFAs and optimize the process via the addition of another organic waste stream, namely lignocellulosic materials.

In the first place, acidogenic fermentation experiments were conducted to optimize the synthesis of electron acceptors and donors for the subsequent chain elongation phase. The pH, temperature, and food-to-microorganisms (F/M) ratio were identified as critical process lever for gearing the biochemical reactions in the acidogenic fermentation phase towards the desired intermediates for maximizing MCFAs production in the chain elongation phase. By manipulating these parameters, up to 719 ± 94 mgCOD/gVS of volatile fatty acids with desirable carbon chain lengths and 684 ± 34 mgCOD/gVS of lactic acid could be synthesized as electron acceptors and donor, respectively.

These intermediates from the acidogenic fermentation phase were then used as co-substrates with carbon monoxide (CO) and ethanol. Co-fermentation of CO and the acidogenic fermentation products improved MCFAs. CO at a partial pressure of 0.25 bar completely inhibited methanogenesis and availed more carbon for MCFA production, unveiling a sustainable chain elongation route without the participation of bioactive methanogenic inhibitors such as 2-bromoethanesulfonate. In the subsequent experiment, the potential co-operative effect of co-fermenting lactic acid derived from food waste acidogenic fermentation and ethanol on MCFAs production was assessed. At the optimum ratio, lactic acid and ethanol synergized to facilitate MCFAs production. Moreover, by capitalizing on the respective net proton consuming and net proton releasing behaviours of the lactate and ethanol-driven chain elongation, an in-situ buffering capability was activated to circumvent the need for external chemicals for pH control.

A key bottleneck found during chain elongation was the poor response of the microbiome to high CO partial pressures. Further research should focus on enhancing the resilience of the microbiome to high CO partial pressures.

SINTESI IN LINGUA ITALIANA

La conversione sostenibile dei flussi di rifiuti organici in sostanze biochimiche come gli acidi grassi a catena media (MCFA) rappresenta un nodo cruciale nello sviluppo di un'economia circolare e nella prevenzione degli impatti negativi delle fonti non sostenibili. L'obiettivo generale di questa tesi di dottorato è stato quello di studiare la valorizzazione degli scarti alimentari attraverso l'allungamento della catena di atomi di carbonio per generare MCFA e ottimizzare il processo attraverso l'aggiunta di un altro flusso di rifiuti organici rappresentato dai materiali lignocellulosici. In primo luogo, sono stati condotti esperimenti di fermentazione acidogenica per ottimizzare la sintesi di accettori e donatori di elettroni per la successiva fase di allungamento della catena di atomi di carbonio. Il pH, la temperatura e il rapporto cibo-microrganismi (F/M) sono stati identificati come parametri critici per orientare le reazioni biochimiche nella fase di fermentazione acidogenica verso gli intermedi desiderati al fine di massimizzare la produzione di MCFA. Manipolando questi parametri è stato possibile sintetizzare fino a 719 ± 94 mgCOD/gVS di acidi grassi volatili con lunghezze di catena carboniosa desiderabili e 684 ± 34 mgCOD/gVS di lattato rispettivamente come accettori e donatori di elettroni. Questi intermedi della fase di fermentazione acidogenica sono stati poi utilizzati come co-substrati con monossido di carbonio (CO) ed etanolo. La co-fermentazione di CO e dei prodotti di fermentazione acidogenica ha migliorato la produzione di MCFA. La presenza di CO ad una pressione parziale di 0.25 ha completamente inibito la metanogenesi ed ha messo a disposizione più atomi di carbonio per la produzione di MCFA, dando luogo ad un percorso di allungamento della catena carbonica più sostenibile in quanto realizzato senza l'utilizzo di inibitori metanogenici bioattivi come il 2-bromoethanesolfonato. Nell'esperimento successivo è stato valutato il potenziale effetto cooperativo della co-fermentazione del lattato derivato dalla fermentazione acidogena degli scarti alimentari e dell'etanolo per la produzione di MCFA, individuando il rapporto ottimale dei due donatori di elettroni per facilitare la produzione di MCFA. Inoltre, sfruttando i rispettivi comportamenti di consumo e rilascio netto di protoni durante le reazioni di allungamento della catena guidata rispettivamente dal lattato e dall'etanolo, è stata attivata una capacità tampone in situ per aggirare la necessità di sostanze chimiche esterne per il controllo del pH. Una importante limitazione all'uso di CO riscontrata durante la fase di allungamento della catena è stata la scarsa risposta del microbioma a pressioni parziali di CO elevate. Ulteriori ricerche dovrebbero concentrarsi sul miglioramento della resilienza del microbioma a pressioni parziali di CO elevate.

LIST OF PUBLICATIONS

The following publications are included in this thesis:

Paper I **S. G. Arhin,** A. Cesaro, F. Di Capua, G. Esposito

Recent progress and challenges in biotechnological valorization of lignocellulosic materials: towards sustainable biofuels and platform chemicals synthesis

Science of The Total Environment 857 (2023) 159333

Paper II **S. G. Arhin,** A. Cesaro, F. Di Capua, G. Esposito

Acidogenic fermentation of food waste to generate electron acceptors and donors towards medium-chain carboxylic acids production

Journal of Environmental Management 348 (2023) 119379

Paper III **S. G. Arhin,** A. Cesaro, F. Di Capua, V. Santala, M. Kokko, G. Esposito

Effect of carbon monoxide partial pressure on methanogenesis and medium-chain fatty acids from food waste effluents via mixotrophic cultures

Manuscript

Paper IV **S. G. Arhin,** A. Cesaro, F. Di Capua, G. Esposito

Facilitated medium-chain fatty acids production from food waste and ethanol co-fermentation: impact of lactate to ethanol ratio on chain elongation product spectrum

Manuscript

TABLE OF CONTENTS

Chapter 1

General introduction

1.1 The world's growing solid waste production: A critical concern

Solid waste generation is an inevitable outcome of human activities. Currently, the world's total solid waste production is estimated at 7–9 billion tonnes per annum (Chen et al., 2020). With the global population expected to reach nearly 10 billion people in 2050 (Suzuki, 2019), a surge in the total solid waste generation and the associated burden of solid waste management could be anticipated. In 2016, over 2 billion tonnes of the total solid waste emanated from municipal areas. Due to rapid population growth and urbanization, the quantity of municipal solid waste (MSW) is projected to reach 3.4 billion tonnes by 2050 (Kaza et al., 2018). This raises concerns because a substantial proportion the waste generated in 2016 were not managed in an environmentally friendly manner with close to 37 % landfilled and over 33 % openly dumped (Kaza et al., 2018). Under a business-as-usual scenario, it is projected that about 5.6 billion people will lack adequate access to basic waste management services by 2050 (Dixit et al., 2022).

The waste generation and disposal methods vary depending on several factors, including region and income level. While over one-third of the waste generated in high-income countries are recovered through compositing and recycling (Kaza et al., 2018), the primary disposal and management practices in low-income settings include open dumbing and burning (Mulya et al., 2022). Such improper waste management practices impact water and air quality, human life, and contributes to climate change (Khan et al., 2022). To mitigate the negative impacts of solid waste, proper waste management systems that integrates waste treatment with resource recovery is of the essence. Resources recovered from solid waste provide an excellent alternative to the finite fossil reserves because as an alternate energy source, solid waste burns cleaner than fossils fuels as emissions from solid waste facilities, including particulates, sulfur dioxide, mercury, lead, furan, etc., were found to be comparatively lower than those from fossil fuel facilities (Mukherjee et al., 2020). Thus, interest in exploring ways to better use solid waste have increased in countries all over the world (Ikhlayel, 2018; Scarlat et al., 2019). However, besides technical and economic feasibility, another crucial element in resource recovery and proper solid waste management systems is the propensity of the general populace to participate through household waste sorting and acceptance and use of recovered products (Holmgren et al., 2016; Nainggolan et al., 2019). Hence, education and a change of mindset to increase engagement in household waste sorting and patronage of recovered products is also essential to achieve a zero-waste circular economy.

1.1.1. Municipal solid waste production, composition and management in Europe

As one of the global frontrunners in policy development in waste management and circular economy – e.g., by introducing the Waste Framework Directive (European Commission, 2008), the European Green Deal (European Commission, 2019), etc.– member states of the European Union (EU) are progressively shifting their focus from MSW disposal to prevention and recycling. Altogether, MSW represents only about 10 % of the total waste generated in the EU (European Environment Agency, 2016). Notwithstanding, the amount of MSW generated in the EU is eminent, and moving MSW management up the waste hierarchy could enhance resource recovery, alleviate potential environmental burden and adverse impacts on human health, create jobs, and ensure a better overall waste management (European Environment Agency, 2016).

On the average, about 527 kg/capita of MSW were generated in the EU in 2021, representing a 12.9 % increase compared to the amount generated in 1995 (Eurostat, 2023). Notably**,** the amount varied considerably from 302 kg/capita in Romania to 835 kg/capita in Austria. Norway (799 kg/capita), Luxemburg (793 kg/capita), and Denmark (769 kg/capita) were among the countries with the highest production while Poland (362 kg/capita), Estonia (395 kg/capita), and Hungary (416 kg/capita) were among the least producers. Italy generated about 495 kg/capita, a 9.1 % increment from 1995. Despite the rise in the average per capita MSW production in the EU, the quantity landfilled has decreased considerably from 286 kg/capita in 1995 to 121 kg/capita in 2021 (~58 %). Meanwhile, the amount of MSW recycled, composted, and incinerated per capita between 1995 to 2021 have increased by 184, 196, and 98 %, respectively (**Fig 1.1**). Moreover, about 49 % of the total MSW generated were recycled in 2021 through material recycling and composting (Eurostat, 2023). Nonetheless, the average proportion of MSW landfilled in 2021 (c.a. 23 %) is still relatively higher than the 10 % target set for 2035 by the Landfill Directive (European Commission, 2023).

Typically, about 60 to 90 % of the total MSW generated in the EU emanate from households and consists of a diverse array of materials including plastics, paper, metal, glass, biowaste, batteries, etc. at various fractions (Salvetti, 2023). On the average, the plastics, paper and cardboard, metals, glass, and organic matter fractions are estimated at 12.4 %, 15.7 %, 5.1 %, 13.0%, and 37.4%, respectively, alongside other materials (Millas and Guerri, 2023). Based on its composition, MSW is broadly classified into three different categories (Eurostat, 2017). Category A consists of separately collected wastes from households including paper and

cardboard, textiles, plastics, glass, metals, biowaste (e.g., kitchen and garden wastes), hazardous household waste (e.g., spent solvents, photochemicals, pesticides, paints, batteries, detergents, etc.), other waste (e.g., edible oil and fat) and bulky waste. Category B is residual waste, which includes mixed waste from households and similar institutions except separately collected fractions in category A. Lastly, category C is made up of waste from municipal services such as waste from public bins and street sweepings, market cleansing waste, etc.

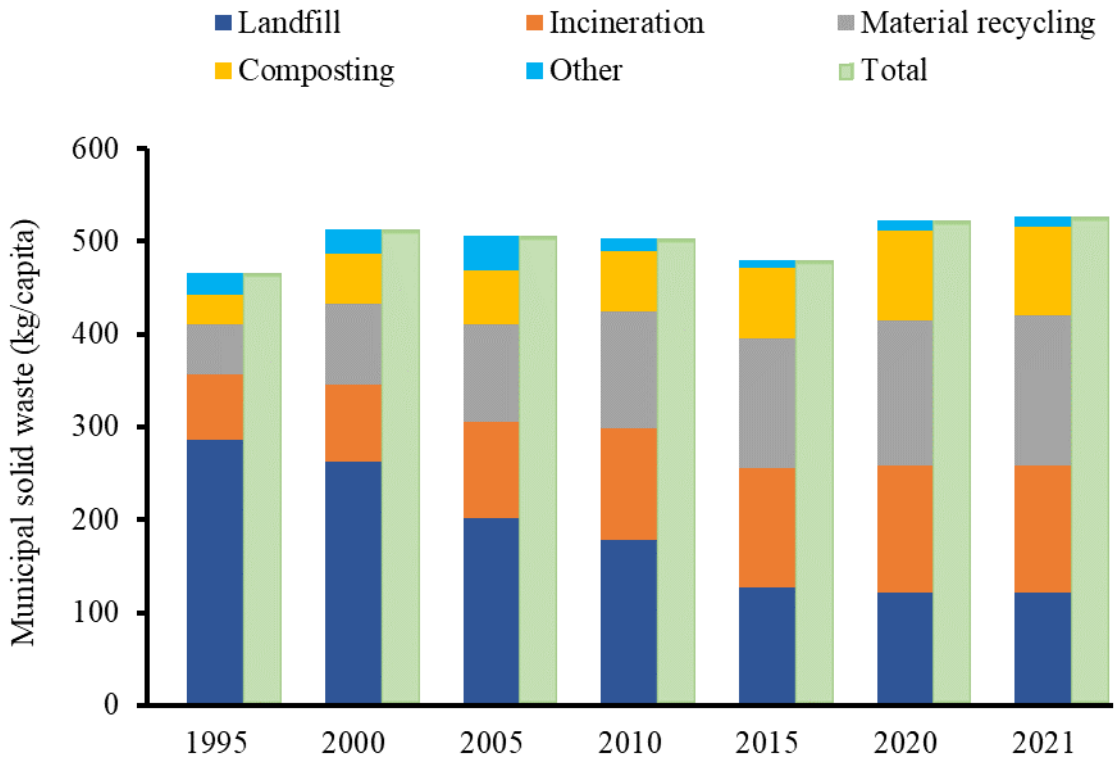

Fig. 1.1 Municipal solid waste management in the European Union. Adapted from Eurostat (2023).

1.1.1.1 Biowaste management in Europe

Biowaste, defined by the Waste Framework Directive (DIRECTIVE (EU) 2018/851, 2018) as "biodegradable garden and park waste, food and kitchen waste from households, offices, restaurants, wholesale, canteens, caterers and retail premises, and comparable waste from food processing plants", constitute about 40 % of the total MSW production in the EU (European Compost Network, 2017). With an estimated annual production between 118 to 138 million tonnes, biowaste is the single largest contributor to MSW production in the EU (European Compost Network, 2023; European Environment Agency, 2020). Due to its relatively large proportion, biowaste management plays a crucial role in the nascent circular economy concept

and meeting the EU target to recycle 65 % of MSW by 2035 (DIRECTIVE (EU) 2018/851, 2018). Thus, the implementation of separate collection of biowaste by all EU member states as stipulated in the Waste Framework Directive is vital for utilizing biowaste as a resource and diverting the biowaste fraction of MSW from landfills. Moreover, separating biowaste from residual waste could facilitate the recycling rate of other wastes, including plastics, glass, metal, and paper.

According to a recent survey, about 40 million tonnes per annum of municipal biowaste, representing about 17 % of the MSW, are separately collected and treated in the EU through composting and anaerobic digestion (Gilbert et al., 2022). Of this, the installed capacity for composting is about 66 %, while that of anaerobic digestion is 34 %. However, to meet the EU's 65 % MSW recycling target, it is projected that an increase in the treatment capacity of separately collected biowaste to about 78 million tonnes per annum is required. This means that the current number of treatment facilities of about 5800 plants would have to be doubled. Meanwhile, the gross domestic product (GDP) contributions gained through municipal biowaste processing could increase from € 739 million to € 145 billion with these increments in treatment facilities (Gilbert et al., 2022).

1.1.1.1.1 Food waste

According to the United Nations Environment Program (UNEP, 2021), food waste refers to food and its associated inedible parts removed from the human food supply chain in the manufacturing of food products, food retail, food service, and household, and could end up in one of the following final destinations: landfill, sewers, discards/litters/refuse, controlled combustion, anaerobic digestion/co-digestion, compost/ aerobic digestion, or land applications. Food loss, on the other hand, includes all livestock and crop human-edible commodity quantities that, directly or indirectly, completely exit the post-slaughter/harvest/production supply chain by being discarded, incinerated, or otherwise, and do not re-enter in any other utilization (e.g., as animal feed, industrial use, etc.) up to, and excluding, the retail level. Food losses also include those that occur during storage, transport, and processing. Food wastage encompasses food waste and food loss, and thus refer to any food lost by deterioration or waste (EU FUSIONS, 2016a).

Globally, nearly one-third of the food produced – about 1.3 billion tonnes – is lost or discarded across the supply chain each year, resulting in an economic loss of about USD 990 billion and

3.3 billion tonnes of carbon dioxide equivalent emissions (Bühlmann et al., 2022). The food waste generation in Europe is estimated at 88 million tonnes per annum (European Environment Agency, 2020), while those of the United States and China are about 37 to 78 and 121 to 145 million tonnes per annum, respectively (Dalke et al., 2021). In the EU and its member states, over 58 million tonnes (about 131 kg/capita) of food waste, with an economic value of € 132 billion, are generated annually (European Commission, 2023b). Food waste constitute over 60 % of the total biowaste production in the EU (European Environment Agency, 2020), and about 20 % of the total food produced in the EU is lost or wasted across the supply chain (European Commission, 2020). Also, over 54 % of the food waste generated in the EU emanate from households, and food waste arising from households, food service, and retail contribute about 70 % (European Commission, 2023b).

Wasting food does not only raise ethical and economic concerns but is also associated with biodiversity loss, climate change, depletion of resources, etc. Therefore, the European Commission has developed various roadmaps/action plans in line with the sustainable development goals (SDG) Target 12.3 that aims to halve the global per capita food waste production by 2030. For instance, measures to increase the sustainability of food distribution and consumption were highlighted in the Circular Economy Action Plan (European Commission, 2020). Another example is the Farm to Fork Strategy, a roadmap to build a sustainable EU food system in line with the aims of the European Green Deal (Rossi, 2022). The EU FUSIONS (Food Use for Social Innovation by Optimising Waste Prevention Strategies) Project also sought to significantly reduce food waste and ensure a more resources efficient Europe (EU FUSIONS, 2016b).

It is noteworthy that food waste and unavoidable food losses could occur at all stages of the food the supply chain and such losses are typically landfilled, causing environmental problems, including air pollution and greenhouse gas emissions (Byun et al., 2021). Thus, in line with the waste prevention hierarchy of the Waste Framework Directive (European Commission, 2023c), prevention and reduction should be the primary goal of all actors in the food chain, including food producers, processors, distributors, and ultimately consumers. Where surpluses cannot be prevented, redistributing to people in need should be the priority as estimates in 2018 suggest that about 110 million people in the EU were at risk of poverty and social exclusion and 38 million people were not able to afford a quality meal every second day (EU Platform on Food Losses and Food Waste, 2019). Food donation could help combat food poverty while reducing the amount of surplus food sent to industrial uses, waste treatment, and landfills. Donation of

surpluses to people should be followed by the conversion of food waste to animal feed. Another viable approach to manage food waste is its utilization in the industrial sector for bioenergy, biochemicals, and nutrients recovery. Food waste could be converted to energy via environmentally friendly technologies such as anaerobic digestion (AD) with reactor microbiome and the digestate obtained after the AD process could be applied as a fertilizer to enrich the soil (Zhang et al., 2024; Zhao et al., 2021). As of 2020, the installed infrastructural capacity for AD of food and garden waste in Europe was over 2000 plants with a digestion capacity of about 29 million tonnes per annum (Gilbert et al., 2022). Besides AD, composting could be used to recovery nutrients to be applied in the soil (Le Pera et al., 2023; Pérez et al., 2023), and over 3800 compost plants treating 42 million tonnes of food and garden waste per annum had been installed in Europe as of 2020 (Gilbert et al., 2022). Food waste can also serve as the carbon sources for the synthesis of several other valuable bio-based products such as biodiesel, bioethanol, single cell protein, polyhydroxylalkanoates, short-chain fatty acids, and medium-chain fatty acids among others (Arhin et al., 2023; Chacón et al., 2024; Hafid et al., 2022; Lahiri et al., 2023; Zeng et al., 2022).

1.2 Lignocellulosic wastes

Besides MSW, lignocellulosic wastes are another crucial waste stream whose valorization to biofuels and platform chemicals is essential to the circular economy and bioeconomy concept. Lignocellulosic biomass, also denoted as lignocellulosic materials (LCMs), emanate from several sources and could be divided into various groups, including agricultural residues (e.g., wheat straw, rice husks, corn stover), agro-industrial residues (e.g., wood chips, spent coffee grounds, orange peels, and paper pulp), industrial residues (e.g., newspaper, black liquor, skins and waste from palm oil mills), energy crops (e.g. switch grass, *Jatropha curcas*, *Miscanthus*), and residues from organic solid waste recycling plants (Güleç et al., 2023). They are made up of robust composite materials consisting typically of three different oxygen-containing high-molecular-weight organic polymers, namely, cellulose, hemicellulose, and lignin.

Cellulose, the main constituent of LCMs and the most abundant polymer in nature, is composed of D-glucose units linked by β-1,4-glycosidic bonds (Mika et al., 2018). The number of glucose units, i.e., the degree of polymerization, varies depending on the LCM (Soltanian et al., 2020). Cellulose is considered a semi-crystalline polymer having high-ordered crystalline and low-ordered amorphous domains, depending on the orientation of the cellulose molecules. The degree of crystallinity varies from 40% to 60% (Medronho and Lindman, 2015). The individual

cellulose molecules are not isolated in nature but are packed into larger aggregates called microfibrils (*ca*. 2–20 nm in diameter and 100–40,000 nm in length) with hydroxylic groups that form hydrogen bonds intra- and inter-microfibrils (Houfani et al., 2020; Mirmohamadsadeghi et al., 2021). The intramolecular hydrogen bonds ensure structural integrity, whereas the intermolecular hydrogen bonds allow linear polymer molecules to combine in sheet-like shapes. Because of its strong intermolecular hydrogen bonds between the hydroxyl groups, cellulose is insoluble in most organic solvents and water and is very resistant to biological degradation (Mirmohamadsadeghi et al., 2021; Soltanian et al., 2020).

In contrast to cellulose, comprised solely of glucose monomers, hemicellulose is an amorphous heteropolymer composed of pentoses (xylose and arabinose), hexoses (mannose, galactose, and glucose), and hexuronic acids (4-O-methyl-glucuronic, glucuronic, and galacturonic acids). These sugars are linked by either β-1,4-glycosidic or β-1,3-glycosidic bonds (Sharma et al., 2019). Depending on the dominant functional group, hemicelluloses are classified as xylans, xyloglucan, mannans, galactans, and β-1,3;1,4-glucans (Zhou et al., 2017). Xylan, composed primarily of xylose monomers, is the predominant hemicellulose in hardwoods and herbaceous biomass (Zhou et al., 2017). In general, hemicelluloses have a lower degree of polymerization than cellulose (about a few hundred), and their amorphous nature precludes the formation of ordered crystalline structures. Consequently, they are hygroscopic, hydrophilic, less stable, and more susceptible to chemical and microbial degradation (Houfani et al., 2020; Saha et al., 2019).

Lignin is also a complex tridimensional amorphous resin that enfolds the polysaccharide fibers layer and protects the inside carbohydrates and proteins from harm to water and microbial attacks, while conferring rigidity and recalcitrance to cell walls (Kumari and Singh, 2018; Zhang et al., 2017). The primary structure of the lignin polymer is not well defined: it is neither cross-linked, unbranched linear, nor linear with side chains (Zhu et al., 2016). The structure is formed by the oxidative coupling of three different hydroxycinnamyl alcohol monomers (monolignols): p-coumaryl (4-hydroxycinnamyl), coniferyl (3-methoxy 4-hydroxycinnamyl), and sinapyl (3,5-dimethoxy 4-hydroxycinnamyl) alcohols (Isikgor and Becer, 2015). These monolignols, also known as p-hydroxyphenyl (H), guaiacyl (G), and syringyl (S) units, respectively, are linked by a variety of covalent bonds, including different ether (e.g. α-O-4, β-O-4, and 4-O-5) and carbon-carbon bonds (e.g. β-β, β-5, and 5–5) (Li et al., 2015; Zhu et al., 2016). Their content in lignin differs in different types of plants, with softwood (gymnosperm)

lignin having mainly G-units, hardwood (angiosperm) lignin, a combination of G- and S-units, and grass lignin, a blend of all three aromatic units (Upton and Kasko, 2016). Besides these fundamental units, the lignin polymer can also feature non-canonical subunits such as: ferulates linking hemicellulose and lignin; acylated monolignols containing acetate, p-hydroxybenzoate, or p-coumarate moieties; ferulic acid; coniferaldehyde; sinapaldehyde; and 5-hydroxyconiferyl alcohol (Li et al., 2015).

Typically, cellulose and hemicellulose are enclosed in a lignin shelter and linked through hydrogen and covalent bonds forming a hydrophobic tridimensional structure, the "Lignin-Carbohydrate Complexes" (Ma et al., 2019). Their weight percentage in typical wood biomass varies and relates to the plant taxonomy, being in the range of 30–50%, 20–35%, and 15–30% for cellulose, hemicellulose, and lignin, respectively (**Table 1.1**).

As sugar-rich resources, cellulose and hemicellulose are suitable feedstocks for biofuels and biochemicals production, while lignin, the most prevalent source of aromatic building blocks in nature (Sun et al., 2018), is apt for bulk or functionalized aromatic compounds. Estimates indicate that the global production of lignin could adequately meet the global demand for aromatic compounds (Sheldon, 2014). Besides cellulose, hemicellulose, and lignin, trace amounts of extractive fractions (e.g., tannins, resins, and fatty acids), freely accessible carbohydrates, inorganic salts, and other substances such as vitamins, proteins, dyes, aromatic essences, certain oils, and flavors are also present in LCMs (Okolie et al., 2021).

Table 1.1. The proportion of cellulose, hemicellulose, and lignin in selected lignocellulosic biomass.

Biomass type	Lignocellulosic material	% Cellulose	% Hemicellulose	% Lignin	Reference
Crop residues	Corn stover	39.1	31.0	10.7	(Li et al., 2021)
	Rice straw	39.1	28.3	7.6	(Zhang et al., 2018)
	Briquetted wheat straw	45.9	28.6	16.5	(Rahman et al., 2018)
	Rape straw	45.5	21.8	17.1	(Gaballah et al., 2020)
	Pearl millet straw	36.4	25.3	15.4	(Kumar et al., 2019)
	Sugarcane bagasse	39.8	19.8	25.9	(Ying et al., 2019)
Grasses	Kans grass	40.0	24.1	3.2	(Rajak and Banerjee, 2018)
	Duckweed	12.0	9.6	9.5	(Zhang et al., 2021)
	Pennisetum hybrid	33.9	20.7	18.4	(Kang et al., 2018)
Softwood (gymnosperm)	Monterey pine	41.8	20.4	25.2	(Dong et al., 2018)
	Spruce	44.5	18.3	31.8	(Pielhop et al., 2015)
	Eastern red cedar	34.2	21.3	32.2	(Ramachandriya et al., 2013)
Hardwood (angiosperms)	Willow sawdust	35.6	21.5	28.7	(Alexandropoulou et al., 2017)
	Elmwood	43.6	23.0	26.3	(Noori and Karimi, 2016)
	Eucalyptus	39.8	13.1	34.5	(Kundu and Lee, 2016)
	Banana peels	16.1	10.2	22.1	(Palacios et al., n.d.)
	Watermelon rind	39.7	23.2	10.6	(Fakayode et al., 2020)

Waste from fruit processing industries	Coconut shell	17.9	56.3	25.8	(Rout et al., 2016)
	Hazelnut shell	27.6	28.9	39.9	(Şenol et al., 2020)

1.2.1 Global drivers for the development of lignocellulosic biorefineries

The word's energy demand is expected to double in 2050 to meet the needs of the growing human population (Güleç et al., 2023). Meanwhile, traditional resources such as fossil fuels still provide over 85 % of the global energy supply and about 66 % of the total electricity generation despite their well-known negative environmental impacts, including greenhouse gas emissions. According to the International Energy Agency (IEA), the total energy-related greenhouse gas emissions increased by 1.0 %, reaching a new all-time highest of 41.3 billion tonnes CO_2-equivalent in 2022 (IEA, 2023). This level of emissions is far beyond the global goal of net zero emissions by 2050 (IEA, 2021). Additionally, the World Health Organization (WHO) reported that 3 million people die every year from air pollution and only 10 % of the global population reside in areas that meet air quality standards (WHO, 2016).

In 2015, the Paris Climate Agreement was enacted by the 196 parties at the United Nations Climate Change Conference with the overarching goal to hold the global average temperature increase in this century to below 2 °C and pursue efforts to reduce the temperature increase even further to 1.5 °C compared to pre-industrial levels (United Nations Climate Change, 2023). However, to limit global warming to 1.5 °C, a 43% reduction in greenhouse gas emissions is required by 2030. This imply that to realize the goals on global warming and a net zero energy system, a rapid switch from conventional fossil resources and a surge in investments into clean energy, sustainable, and renewable energy resources worldwide is required in the coming years. Bio-based fuels and chemicals, having similar properties as their fossil-based counterparts, are widely seen as viable alternatives for various applications, including energy generation, transport, and industrial use. Nonetheless, the development of an efficient and sustainable bio-based economy depends highly on the feedstock used.

In this regard, LCMs are gaining attention for their widespread availability and lack of competition with human food supply, among other merits (Gaballah et al., 2020; Kiggundu et al., 2017; Kumar et al., 2019). LCMs comprise over 63 % of the global solid waste mass that is mostly poorly managed, leading to adverse environmental problems (Singh et al., 2022). Thus, the utilization of LCMs for fuels and platform chemicals generation would not only

address the environmental burden of improperly managed solid waste systems but also serve as a pathway towards a net zero energy system and abating the negative impacts of irreversible climate change. Moreover, the transformation of our energy system could create enormous amounts of clean energy jobs and lead to huge opportunities for the global economy (IEA, 2021).

1.2.2 Lignocellulosic biorefineries in Europe: State-of-the-art, challenges and prospects

From the viewpoint of environmental sustainability, many of the global drivers for a bio-based economy, including over-dependence on fossil resources, pollution, unsustainable use of forest and water resources, etc., are also relevant to the case of the EU. The ecological footprint of the EU is 4.7 global hectares per capita, which is double the size of its biocapacity (Hassan et al., 2019). Besides, the EU is directly impacted by the environmental concern of other regions through the impact of greenhouse gas emissions, or socio-economic pressures from over-exploitation of resource, global loss of biodiversity, etc. Driven by these concerns, the European Bioeconomy Strategy was launched in 2012 and updated in 2018, aiming to accelerate the deployment of a sustainable European bioeconomy, contribute towards the SDGs and help fulfil the aspiration of the Paris Agreement (European Commission, 2018).

Biorefinery represents an integral part of the Bioeconomy Strategy, which has sustainability and circularity at the core of its success. Currently, there are about 2,362 facilities in the EU utilizing biomass to generate bio-based chemicals, liquid biofuels, bio-based composite and fibres, biomethane, pulp and paper, timber, and starch, sugar and derived-products (Parisi, 2020). Of these, about 2186 are at the commercial-scale level while the remaining are pilot/demo and research and development (R&D) facilities. Amongst the commercial-scale facilities, about 402, 377, 273, and 115 produce bio-based chemicals, biomethane, liquid biofuels, and bio-composites, respectively. Moreover, about 194 of the commercial-scale facilities are integrated biorefineries generating multiple products. Regarding feedstock, agricultural resources are the most widely used in the commercial-scale facilities (150) while only 37 facilities utilize waste materials as feedstock. It must be stated that a significant number of those commercial biorefineries are so-called ‘first generation’ biorefineries that utilize human edible sugars, starch, oils, and fats. As of 2017, only 43 of these facilities were so-called ‘second generation’ biorefineries that utilize sustainable feedstocks such as LCMs, biowaste, and nonedible food and energy crops (Hassan et al., 2019). It is anticipated that the face-paced regulatory developments in the EU will accelerate the expansion of sustainable biorefineries in

the years ahead. For instance, the Renewable Energy Directive, which was amended in 2023 (DIRECTIVE (EU) 2023/2413, 2023) has set an overall EU renewable energy binding target of at least 42.5 % by 2030 but aims for a 45 % share of renewables in the EU energy consumption. Also, it is the goal of the EU Bioeconomy Strategy to build about 300 new sustainable biorefineries by 2030 (Carroll, 2022).

With these developments in mind, it is predicted that about 476 billion tonnes of LCMs would be needed to meet the demands of all bio-based industries in Europe in 2030 (S2Biom, 2016). Meanwhile, it is projected that about a billion dry tonnes of LCMs could be generated annually in Europe by 2030. Thus, the main challenge is not with the availability of feedstock, but the logistical challenges surrounding feedstock supply, including collection, drying, densification, transport, and storage. Such challenges could be addressed by the development of integrated logistic models capable of handling the supply chain bottlenecks, mapping of LCMs inventories, the development of machinery to handle large quantities of feedstock, and the establishment of centralized hubs for feedstock collection and storage, among others.

1.3 Overview of resources recovery from solid waste streams

As nations and authorities worldwide gradually embrace the circular economy concept, whereby recycling and reuse are major pillars for designing and optimization of products while the unsustainable consumption of natural resources is avoided, solid waste streams, including municipal biowaste and lignocellulosic biomass are deemed vital resources. These solid waste streams can be used for the production of various value-added products, including energy, chemicals, and nutrients. Various options have been developed over the years for the valorization of solid wate and the choice of a valorization approach depends on several factors, including the characteristics of the waste stream such as the biodegradable and non-biodegradable components. A detailed discussion on the potential valorization routes of solid waste focusing on LCMs is presented in **chapter 2**.

1.4 Thesis scope and objectives

1.4.1 Scope of the thesis

This thesis focused on green chemicals (MCFAs) biosynthesis from food waste via the carboxylates' platform using mixed-culture fermentation. The study aimed to generate high-value products from food waste to maximize the economic feasibility of food waste biorefinery.

Another organic waste stream, namely, LCMs, was considered as a co-substrate that could facilitate the generation of the product of interest (i.e., MCFAs).

The valorization approach employed for the project involved the conversion of food waste to short-chain fatty acids via acidogenic fermentation. Specifically, volatile fatty acids (VFAs) to act as the electron acceptors and lactic acid to serve as an electron donor were the targeted intermediates from food waste. Ethanol, generated via lignocellulosic pretreatment, saccharification, and fermentation was also targeted as the intermediate from lignocellulosic biomass. However, considering that ethanol could also be generated from syngas (CO, H_2, CO_2) derived via the thermochemical conversion of LCMs, the use of CO as an intermediate from LCMs was also explored. The generated intermediates from food waste and LCMs were co-fermented in a mixed-culture chain elongation systems to generate MCFAs. A schematic representation of the scope of the project is shown in **Fig. 1. 2**.

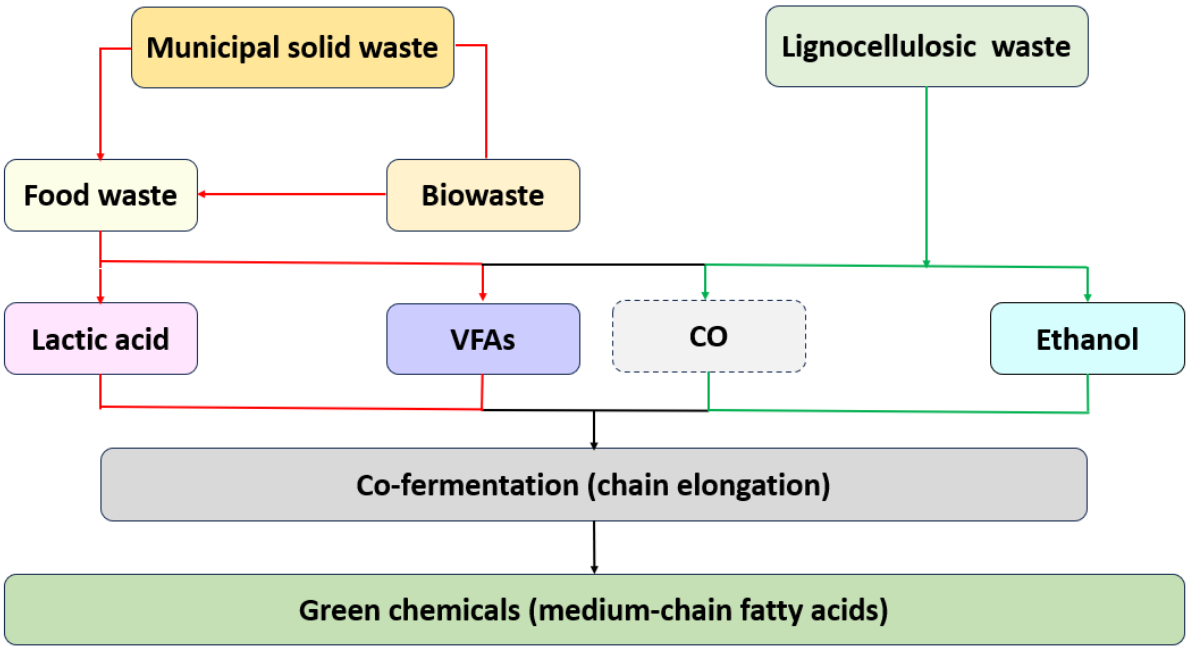

Fig 1.2. Scope of the thesis. VFAs: volatile fatty acids, CO: carbon monoxide.

1.4.2 Objectives of the study

The main objective of this PhD thesis was to investigate the valorization of food waste via chain elongation to generate MCFAs and optimize the process via the addition of another organic waste stream, namely LCMs. To this end, the potential synergistic effects of utilizing these waste streams for MCFAs production were assessed.

The following specific research objectives were addressed:

- Evaluate the recent scientific progress and challenges in the biorefinery of solid waste focusing on LCMs to unveil potential research gaps and limitations.
- Examine the conditions for maximizing the synthesis of electron acceptors and donors from food waste via acidogenic fermentation for subsequent utilization as reactants for generating MCFAs and perform a techno-economic assessment to compare MCFAs with other food waste valorization scenarios.
- Assess the impact of CO supplementation on methanogenesis and MCFAs production to understand the potential of utilizing syngas from LCMs pyrolysis and food waste acidogenic fermentation products for MCFAs production.
- Optimize the generation of ethanol from LCMs and investigate the potential co-operative effect of utilizing lignocellulosic ethanol and food waste acidogenic fermentation products for MCFAs synthesis.

A schematic representation of the objectives of the thesis and their interconnections are shown in **Fig. 1.3**. It is anticipated that the results of this study will contribute to resource recovery and circular economy through the generation of valuable platform chemicals food waste and LCMs. Moreover, the adoption of the valorization route explored in this study could enhance the economic viability and sustainability of food waste management systems, thus helping to mitigate the landfilling of food waste and its associated adverse health and environmental impacts.

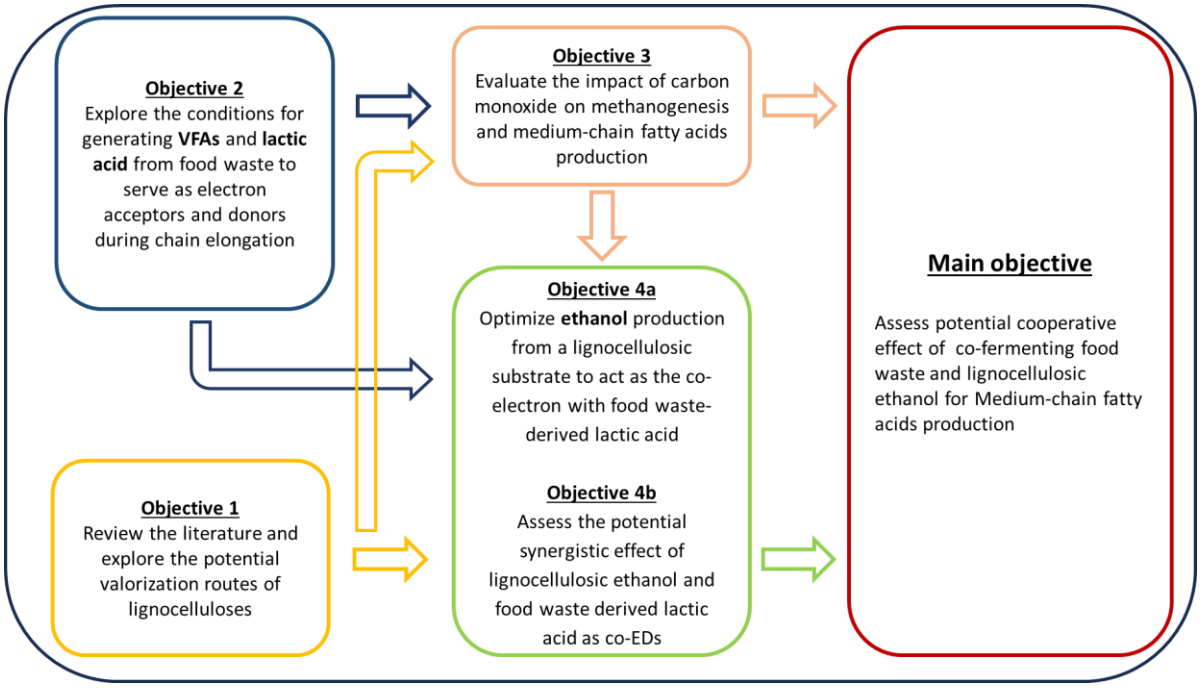

Fig.1.3. Schematic displays of the objectives of the thesis.

1.5 Thesis outline

The outline of this thesis is schematically shown in **Fig.1.4.**

Chapter 1 consists of a general introduction to the topic and a discussion on the scope, research objectives, and the outline of the thesis.

In **Chapter 2**, the recent scientific advances and challenges in the biological valorization of LCMs to biofuels and biochemicals are critically reviewed and presented. Additionally, the technoeconomic potential of lignocellulosic biorefineries and the relevance of carbon co-utilization to the economic sustainability of lignocellulosic biorefineries are highlighted.

Chapter 3 describes acidogenic fermentation experiments conducted to maximize the synthesis of electron acceptors and donors for MCFAs production. Considering that the product spectrum and concentration of acidogenic fermentation reactions are impacted by environmental conditions such as pH, temperature, and organic loading, the influence of these factors on the synthesis of electron acceptors and donors was examined. Based on the results obtained, a preliminary technoeconomic assessment on the feasibility of using the intermediates generated for MCFAs production was also performed.

Chapter 4 discusses the impacts of CO partial pressure on methanogenesis and MCFAs production using food waste acidogenic fermentation products as co-substrates. This section

aims at assessing the feasibility of coupling syngas generated from LCMs via thermochemical routes such as pyrolysis with the carboxylates' platform to facilitate MCFAs production. Considering that syngas is composed mainly of CO, H_2 and CO_2, and CO could both serve as a substrate and an inhibitor, the dual roles of CO in chain elongation systems were explored.

In **Chapter 5,** the potential synergistic effects of using lignocellulosic ethanol and food waste-derived lactic acid as co-electron donors in chain elongation systems are discussed. Experiments were initially performed to examine the conditions for generation ethanol from wheat straw. This was followed by acidogenic fermentation experiments to maximize the synthesis of lactic acid from food waste. Then, the effect of varying the ethanol to lactic acid mole ratio on MCFAs production was studied.

Lastly, **Chapter 6** presents a general discussion, future research perspective, and a concluding remark.

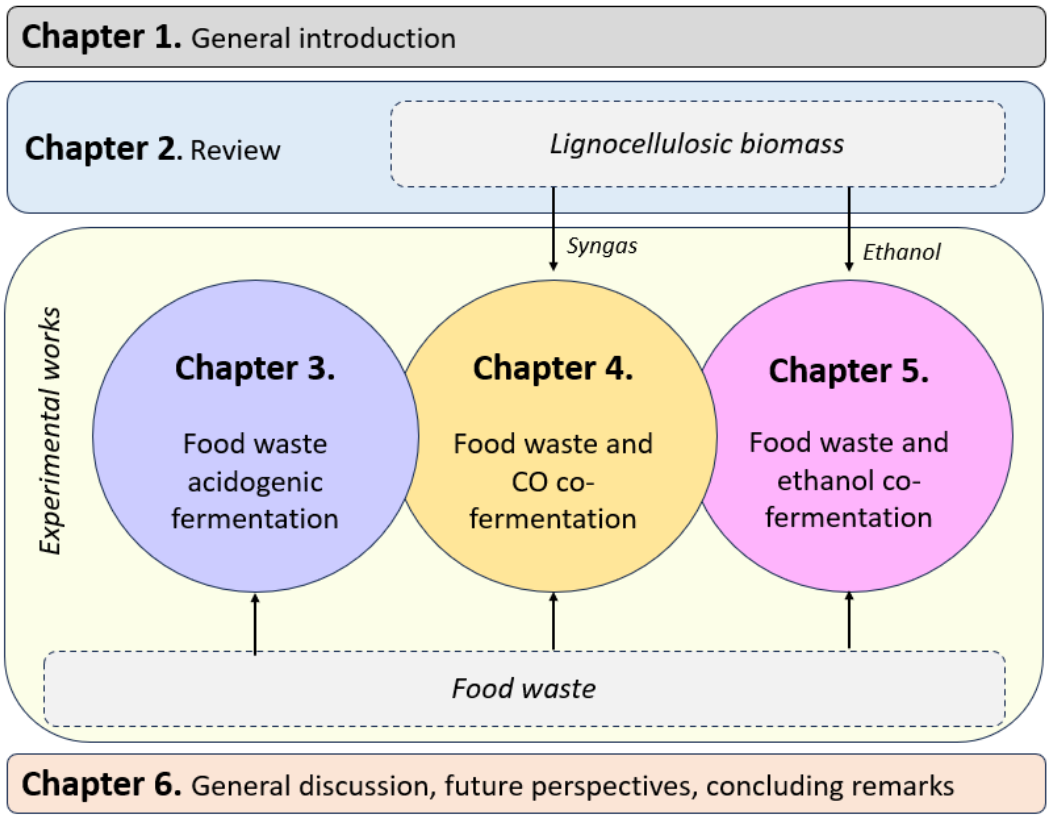

Fig 1.4. Schematic representation of the thesis outline.

References

Alexandropoulou, M., Antonopoulou, G., Fragkou, E., Ntaikou, I., Lyberatos, G., 2017. Fungal pretreatment of willow sawdust and its combination with alkaline treatment for enhancing biogas production. J Environ Manage 203, 704–713. https://doi.org/10.1016/j.jenvman.2016.04.006

Arhin, S.G., Cesaro, A., Di Capua, F., Esposito, G., 2023. Acidogenic fermentation of food waste to generate electron acceptors and donors towards medium-chain carboxylic acids production. J Environ Manage 348, 119379. https://doi.org/10.1016/j.jenvman.2023.119379

European Commission, 2018. Bioeconomy: the European way to use our natural resources. Action Plan 2018. Brussels. https://doi.org/10.2777/57931

Bühlmann, C.H., Mickan, B.S., Tait, S., Batstone, D.J., Mercer, G.D., Bahri, P.A., 2022. Lactic acid from mixed food waste fermentation using an adapted inoculum: Influence of pH and temperature regulation on yield and product spectrum. J Clean Prod 373. https://doi.org/10.1016/j.jclepro.2022.133716

Byun, J., Kwon, O., Park, H., Han, J., 2021. Food waste valorization to green energy vehicles: Sustainability assessment. Energy Environ Sci 14, 3651–3663. https://doi.org/10.1039/d1ee00850a

Carroll, S.G., 2022. Biorefineries – the engine of the bio-based economy [WWW Document]. Euractiv. URL https://www.euractiv.com/section/biomass/news/biorefineries-the-engine-of-the-bio-based-economy/ (accessed 1.1.24).

Chacón, M., Wongsirichot, P., Winterburn, J., Dixon, N., 2024. Genetic and process engineering for polyhydroxyalkanoate production from pre- and post-consumer food waste. Curr Opin Biotechnol. https://doi.org/10.1016/j.copbio.2023.103024

Chen, D.M.C., Bodirsky, B.L., Krueger, T., Mishra, A., Popp, A., 2020. The world's growing municipal solid waste: trends and impacts. Environmental Research Letters 15. https://doi.org/10.1088/1748-9326/ab8659

Dalke, R., Demro, D., Khalid, Y., Wu, H., Urgun-Demirtas, M., 2021. Current status of anaerobic digestion of food waste in the United States. Renewable and Sustainable Energy Reviews 151. https://doi.org/10.1016/j.rser.2021.111554

DIRECTIVE 2008/98/EC, 2008. DIRECTIVE 2008/98/EC OF THE EUROPEAN PARLIAMENT AND OF THE COUNCIL of 19 November 2008 on waste and repealing certain Directives.

DIRECTIVE (EU) 2018/851, 2018. DIRECTIVE (EU) 2018/851 OF THE EUROPEAN PARLIAMENT AND OF THE COUNCIL of 30 May 2018 amending Directive 2008/98/EC on waste (Text with EEA relevance).

DIRECTIVE (EU) 2023/2413, 2023. DIRECTIVE (EU) 2023/2413 OF THE EUROPEAN PARLIAMENT AND OF THE COUNCIL of 18 October 2023 amending Directive (EU) 2018/2001, Regulation (EU) 2018/1999 and Directive 98/70/EC as regards the promotion of energy from renewable sources, and repealing Council Directive (EU) 2015/652.

Dixit, A., Singh, D., Shukla, S.K., 2022. Changing scenario of municipal solid waste management in Kanpur city, India. J Mater Cycles Waste Manag. https://doi.org/10.1007/s10163-022-01427-4

Dong, C., Wang, Y., Zhang, H., Leu, S.Y., 2018. Feasibility of high-concentration cellulosic bioethanol production from undetoxified whole Monterey pine slurry. Bioresour Technol 250, 102–109. https://doi.org/10.1016/j.biortech.2017.11.029

EU FUSIONS, 2016a. Food waste definition [WWW Document]. URL https://www.eu-fusions.org/index.php/about-food-waste/280-food-waste-definition (accessed 12.25.23).

EU FUSIONS, 2016b. About FUSIONS [WWW Document]. URL https://www.eu-fusions.org/index.php/about-fusions (accessed 12.26.23).

EU Platform on Food Losses and Food Waste, 2019. Recommendations for Action in Food Waste Prevention.

European Commission, 2023a. Landfill waste [WWW Document]. URL https://environment.ec.europa.eu/topics/waste-and-recycling/landfill-waste_en (accessed 12.21.23).

European Commission, 2023b. Food Waste [WWW Document]. Food, Farming, Fisheries . URL https://food.ec.europa.eu/safety/food-waste_en (accessed 12.25.23).

European Commission, 2023c. Waste Framework Directive [WWW Document]. Energy, Climate change, Environment . URL https://environment.ec.europa.eu/topics/waste-and-recycling/waste-framework-directive_en (accessed 12.29.23).

European Commission, 2020. A new Circular Economy Action Plan. For a cleaner and more competitive Europe. Brussels.

European Commission, 2019. The European Green Deal.

European Compost Network, 2023. Bio-Waste in Europe [WWW Document]. URL https://www.compostnetwork.info/policy/biowaste-in-europe/ (accessed 12.22.23).

European Compost Network, 2017. Biowaste in the circular economy [WWW Document]. URL https://cor.europa.eu/en/events/Pages/Bio.aspx (accessed 12.22.23).

European Environment Agency, 2020. Bio-waste in Europe - turning challenges into opportunities.

European Environment Agency, 2016. Municipal waste management across European countries [WWW Document]. URL http://www.mzp.cz.

Eurostat, 2023. Municipal waste statistics: Statistics Explained [WWW Document]. URL https://ec.europa.eu/eurostat/statisticsexplained/

Eurostat, 2017. Guidance on municipal waste data collection, Eurostat – Unit E2 – Environmental statistics and accounts; sustainable development. [WWW Document]. URL https://ec.europa.eu/eurostat/documents/342366/351811/Municipal+Waste+guidance /bd38a449-7d30-44b6-a39f-8a20a9e67af2) (accessed 12.21.23).

Fakayode, O.A., Aboagarib, E.A.A., Yan, D., Li, M., Wahia, H., Mustapha, A.T., Zhou, C., Ma, H., 2020. Novel two-pot approach ultrasonication and deep eutectic solvent pretreatments for watermelon rind delignification: Parametric screening and optimization via response surface methodology. Energy 203. https://doi.org/10.1016/j.energy.2020.117872

Gaballah, E.S., Abomohra, A.E.F., Xu, C., Elsayed, M., Abdelkader, T.K., Lin, J., Yuan, Q., 2020. Enhancement of biogas production from rape straw using different co-pretreatment techniques and anaerobic co-digestion with cattle manure. Bioresour Technol 309. https://doi.org/10.1016/j.biortech.2020.123311

Gilbert, J., Clarity, C., Siebert, S., 2022. ECN DATA REPORT 2022. COMPOST AND DIGESTATE FOR A CIRCULAR BIOECONOMY. Overview of Bio-Waste Collection, Treatment & Markets Across Europe.

Güleç, F., Parthiban, A., Umenweke, G.C., Musa, U., Williams, O., Mortezaei, Y., Suk-Oh, H., Lester, E., Ogbaga, C.C., Gunes, B., Okolie, J.A., 2023. Progress in lignocellulosic biomass valorization for biofuels and value-added chemical production in the EU: A focus on thermochemical conversion processes. Biofuels, Bioproducts and Biorefining. https://doi.org/10.1002/bbb.2544

Hafid, H.S., Omar, F.N., Abdul Rahman, N., Wakisaka, M., 2022. Innovative conversion of food waste into biofuel in integrated waste management system. Crit Rev Environ Sci Technol. https://doi.org/10.1080/10643389.2021.1923976

Hassan, S.S., Williams, G.A., Jaiswal, A.K., 2019. Moving towards the second generation of lignocellulosic biorefineries in the EU: Drivers, challenges, and opportunities. Renewable and Sustainable Energy Reviews. https://doi.org/10.1016/j.rser.2018.11.041

Holmgren, K.E., Li, H., Verstraete, W., Cornel, P., 2016. State of the Art Compendium Report on Resource Recovery from Water.

Houfani, A.A., Anders, N., Spiess, A.C., Baldrian, P., Benallaoua, S., 2020. Insights from enzymatic degradation of cellulose and hemicellulose to fermentable sugars– a review. Biomass Bioenergy. https://doi.org/10.1016/j.biombioe.2020.105481

IEA, 2023. CO2 Emissions in 2022.

IEA, 2021. Net Zero by 2050 - A Roadmap for the Global Energy Sector.

Ikhlayel, M., 2018. Development of management systems for sustainable municipal solid waste in developing countries: a systematic life cycle thinking approach. J Clean Prod 180, 571–586. https://doi.org/10.1016/j.jclepro.2018.01.057

Isikgor, F.H., Becer, C.R., 2015. Lignocellulosic biomass: a sustainable platform for the production of bio-based chemicals and polymers. Polym Chem 6, 4497–4559. https://doi.org/10.1039/c5py00263j

Kang, X., Sun, Y., Li, L., Kong, X., Yuan, Z., 2018. Improving methane production from anaerobic digestion of Pennisetum Hybrid by alkaline pretreatment. Bioresour Technol 255, 205–212. https://doi.org/10.1016/j.biortech.2017.12.001

Kaza, S., Yao, L.C., Bhada-Tata, P., Van Woerden, Frank., 2018. What a Waste 2.0: A Global Snapshot of Solid Waste Management to 2050. Washington, DC.

Khan, S., Anjum, R., Raza, S.T., Ahmed Bazai, N., Ihtisham, M., 2022. Technologies for municipal solid waste management: Current status, challenges, and future perspectives. Chemosphere 288. https://doi.org/10.1016/j.chemosphere.2021.132403

Kiggundu, N., Arhin, S.G., Banadda, N., Kabenge, I., 2017. Impacts of Biofuel Policies on Welfare and Food Security: Assessing the Socioeconomic and Environmental Trade-offs in Sub-Saharan Africa. International Journal of Renewable Energy Research 7.

Kumar, S., Gandhi, P., Yadav, M., Paritosh, K., Pareek, N., Vivekanand, V., 2019. Weak alkaline treatment of wheat and pearl millet straw for enhanced biogas production and its economic analysis. Renew Energy 139, 753–764. https://doi.org/10.1016/j.renene.2019.02.133

Kumari, D., Singh, R., 2018. Pretreatment of lignocellulosic wastes for biofuel production: A critical review. Renewable and Sustainable Energy Reviews. https://doi.org/10.1016/j.rser.2018.03.111

Kundu, C., Lee, J.W., 2016. Bioethanol production from detoxified hydrolysate and the characterization of oxalic acid pretreated Eucalyptus (Eucalyptus globulus) biomass. Ind Crops Prod 83, 322–328. https://doi.org/10.1016/j.indcrop.2016.01.022

Lahiri, A., Daniel, S., Kanthapazham, R., Vanaraj, R., Thambidurai, A., Peter, L.S., 2023. A critical review on food waste management for the production of materials and biofuel. Journal of Hazardous Materials Advances. https://doi.org/10.1016/j.hazadv.2023.100266

Le Pera, A., Sellaro, M., Sicilia, F., Ciccoli, R., Sceberras, B., Freda, C., Fanelli, E., Cornacchia, G., 2023. Environmental and economic impacts of improper materials in the recycling of separated collected food waste through anaerobic digestion and composting. Science of the Total Environment 880. https://doi.org/10.1016/j.scitotenv.2023.163240

Li, C., Zhao, X., Wang, A., Huber, G.W., Zhang, T., 2015. Catalytic Transformation of Lignin for the Production of Chemicals and Fuels. Chem Rev. https://doi.org/10.1021/acs.chemrev.5b00155

Li, Y., Zhang, Z., Jiang, D., Jing, Y., Lu, C., Zhang, H., Zhang, Q., 2021. Continuous dark and photo biohydrogen production in a baffled bioreactor and electrons distribution analysis. Bioresour Technol 337. https://doi.org/10.1016/j.biortech.2021.125440

Ma, S., Wang, H., Li, J., Fu, Y., Zhu, W., 2019. Methane production performances of different compositions in lignocellulosic biomass through anaerobic digestion. Energy 189. https://doi.org/10.1016/j.energy.2019.116190

Medronho, B., Lindman, B., 2015. Brief overview on cellulose dissolution/regeneration interactions and mechanisms. Adv Colloid Interface Sci. https://doi.org/10.1016/j.cis.2014.05.004

Mika, L.T., Cséfalvay, E., Németh, Á., 2018. Catalytic Conversion of Carbohydrates to Initial Platform Chemicals: Chemistry and Sustainability. Chem Rev. https://doi.org/10.1021/acs.chemrev.7b00395

Millas, N., Guerri, S., 2023. Biowaste collection and valorisation: Problems and solutions [WWW Document]. waste-management-world.com. URL https://waste-management-world.com/collection-and-handling/biowaste-collection-and-valorisation-problems-and-solutions/ (accessed 12.22.23).

Mirmohamadsadeghi, S., Karimi, K., Azarbaijani, R., Parsa Yeganeh, L., Angelidaki, I., Nizami, A.S., Bhat, R., Dashora, K., Vijay, V.K., Aghbashlo, M., Gupta, V.K., Tabatabaei, M., 2021. Pretreatment of LCMs for enhanced biogas production: A review on influencing mechanisms and the importance of microbial diversity. Renewable and Sustainable Energy Reviews 135. https://doi.org/10.1016/j.rser.2020.110173

Mukherjee, C., Denney, J., Mbonimpa, E.G., Slagley, J., Bhowmik, R., 2020. A review on municipal solid waste-to-energy trends in the USA. Renewable and Sustainable Energy Reviews. https://doi.org/10.1016/j.rser.2019.109512

Mulya, K.S., Zhou, J., Phuang, Z.X., Laner, D., Woon, K.S., 2022. A systematic review of life cycle assessment of solid waste management: Methodological trends and prospects. Science of the Total Environment. https://doi.org/10.1016/j.scitotenv.2022.154903

Nainggolan, D., Pedersen, A.B., Smed, S., Zemo, K.H., Hasler, B., Termansen, M., 2019. Consumers in a Circular Economy: Economic Analysis of Household Waste Sorting Behaviour. Ecological Economics 166. https://doi.org/10.1016/j.ecolecon.2019.106402

Noori, M.S., Karimi, K., 2016. Detailed study of efficient ethanol production from elmwood by alkali pretreatment. Biochem Eng J 105, 197–204. https://doi.org/10.1016/j.bej.2015.09.019

Okolie, J.A., Nanda, S., Dalai, A.K., Kozinski, J.A., 2021. Chemistry and Specialty Industrial Applications of Lignocellulosic Biomass. Waste Biomass Valorization. https://doi.org/10.1007/s12649-020-01123-0

Palacios, A.S., Ilyina, A., Ramos-González, R., Aguilar, C.N., Luis Martínez-Hernández, J., Segura-Ceniceros, E.P., Lizeth Chávez González, M., Aguilar, M., Ballesteros, M., José, &, Oliva, M., Ruiz, H.A., n.d. Ethanol production from banana peels at high pretreated substrate loading: comparison of two operational strategies. https://doi.org/10.1007/s13399-019-00562-7/Published

Parisi, C., 2020. Distribution of the bio-based industry in the EU Database and visualisation, Publication of the Office of the European Union. https://doi.org/10.2760/745867

Pérez, T., Vergara, S.E., Silver, W.L., 2023. Assessing the climate change mitigation potential from food waste composting. Sci Rep 13. https://doi.org/10.1038/s41598-023-34174-z

Pielhop, T., Larrazábal, G.O., Studer, M.H., Brethauer, S., Seidel, C.M., Rudolf Von Rohr, P., 2015. Lignin repolymerisation in spruce autohydrolysis pretreatment increases cellulase deactivation. Green Chemistry 17, 3521–3532. https://doi.org/10.1039/c4gc02381a

Rahman, M.A., Møller, H.B., Saha, C.K., Alam, M.M., Wahid, R., Feng, L., 2018. Anaerobic co-digestion of poultry droppings and briquetted wheat straw at mesophilic and thermophilic conditions: Influence of alkali pretreatment. Renew Energy 128, 241–249. https://doi.org/10.1016/j.renene.2018.05.076

Rajak, R.C., Banerjee, R., 2018. An eco-friendly process integration for second generation bioethanol production from laccase delignified Kans grass. Energy Convers Manag 157, 364–371. https://doi.org/10.1016/j.enconman.2017.11.060

Ramachandriya, K.D., Wilkins, M., Atiyeh, H.K., Dunford, N.T., Hiziroglu, S., 2013. Effect of high dry solids loading on enzymatic hydrolysis of acid bisulfite pretreated Eastern redcedar. Bioresour Technol 147, 168–176. https://doi.org/10.1016/j.biortech.2013.08.048

Rossi, R., 2022. Taking the EU's "farm to fork" strategy forward. European Parliamentary Research Service.

Rout, T., Pradhan, D., Singh, R.K., Kumari, N., 2016. Exhaustive study of products obtained from coconut shell pyrolysis. J Environ Chem Eng 4, 3696–3705. https://doi.org/10.1016/j.jece.2016.02.024

S2Biom, 2016. Vision for 1 billion dry tonnes lignocellulosic biomass as a contribution to biobased economy by 2030 in Europe.

Saha, M., Saynik, P.B., Borah, A., Malani, R.S., Arya, P., Shivangi, Moholkar, V.S., 2019. Dioxane-based extraction process for production of high quality lignin. Bioresour Technol Rep 5, 206–211. https://doi.org/10.1016/j.biteb.2019.01.018

Salvetti, M., 2023. Municipal Waste Regulation in Europe: paving the road for upcoming challenges.

Scarlat, N., Fahl, F., Dallemand, J.F., 2019. Status and Opportunities for Energy Recovery from Municipal Solid Waste in Europe. Waste Biomass Valorization 10, 2425–2444. https://doi.org/10.1007/s12649-018-0297-7

Şenol, H., Erşan, M., Görgün, E., 2020. Optimization of temperature and pretreatments for methane yield of hazelnut shells using the response surface methodology. Fuel 271. https://doi.org/10.1016/j.fuel.2020.117585

Sharma, H.K., Xu, C., Qin, W., 2019. Biological Pretreatment of Lignocellulosic Biomass for Biofuels and Bioproducts: An Overview. Waste Biomass Valorization. https://doi.org/10.1007/s12649-017-0059-y

Sheldon, R.A., 2014. Green and sustainable manufacture of chemicals from biomass: State of the art. Green Chemistry. https://doi.org/10.1039/c3gc41935e

Singh, N., Singhania, R.R., Nigam, P.S., Dong, C. Di, Patel, A.K., Puri, M., 2022. Global status of lignocellulosic biorefinery: Challenges and perspectives. Bioresour Technol. https://doi.org/10.1016/j.biortech.2021.126415

Soltanian, S., Aghbashlo, M., Almasi, F., Hosseinzadeh-Bandbafha, H., Nizami, A.S., Ok, Y.S., Lam, S.S., Tabatabaei, M., 2020. A critical review of the effects of pretreatment methods on the exergetic aspects of lignocellulosic biofuels. Energy Convers Manag. https://doi.org/10.1016/j.enconman.2020.112792

Sun, Z., Fridrich, B., De Santi, A., Elangovan, S., Barta, K., 2018. Bright Side of Lignin Depolymerization: Toward New Platform Chemicals. Chem Rev. https://doi.org/10.1021/acs.chemrev.7b00588

Suzuki, E., 2019. World's population will reach nearly 10 billion by 2050 [WWW Document]. URL https://datatopics.worldbank.org/world-development-indicators/stories/world-population-will-continue-to-grow.html (accessed 12.5.23).

UNEP, 2021. FOOD WASTE INDEX REPORT 2021. Nairobi.

United Nations Climate Change, 2023. The Paris Agreement [WWW Document]. URL https://unfccc.int/process-and-meetings/the-paris-agreement (accessed 12.31.23).

Upton, B.M., Kasko, A.M., 2016. Strategies for the conversion of lignin to high-value polymeric materials: Review and perspective. Chem Rev. https://doi.org/10.1021/acs.chemrev.5b00345

WHO, 2016. Ambient air pollution: A global assessment of exposure and burden of disease.

Ying, W., Xu, G., Yang, H., Shi, Z., Yang, J., 2019. The sequential Fenton oxidation and sulfomethylation pretreatment for alleviating the negative effects of lignin in enzymatic saccharification of sugarcane bagasse. Bioresour Technol 286. https://doi.org/10.1016/j.biortech.2019.121392

Zeng, J., Zeng, H., Wang, Z., 2022. Review on technology of making biofuel from food waste. Int J Energy Res. https://doi.org/10.1002/er.7868

Zhang, H., Zhang, P., Ye, J., Wu, Y., Liu, J., Fang, W., Xu, D., Wang, B., Yan, L., Zeng, G., 2018. Comparison of various pretreatments for ethanol production enhancement from solid residue after rumen fluid digestion of rice straw. Bioresour Technol 247, 147–156. https://doi.org/10.1016/j.biortech.2017.09.065

Zhang, Q., Wang, S., Sun, H., Arhin, S.G., Yang, Z., Liu, G., Tong, Y.W., Tian, H., Wang, W., 2024. Anaerobic digestion + pyrolysis integrated system for food waste treatment achieving both environmental and economic benefits. Energy 288. https://doi.org/10.1016/j.energy.2023.129856

Zhang, X., Jiang, D., Zhang, H., Wang, Y., Zhang, Z., Lu, C., Zhang, Q., 2021. Enhancement of the biohydrogen production performance from mixed substrate by photo-fermentation: Effects of initial pH and inoculation volume ratio. Bioresour Technol 319. https://doi.org/10.1016/j.biortech.2020.124153

Zhang, Z., Song, J., Han, B., 2017. Catalytic Transformation of Lignocellulose into Chemicals and Fuel Products in Ionic Liquids. Chem Rev. https://doi.org/10.1021/acs.chemrev.6b00457

Zhao, Q., Arhin, S.G., Yang, Z., Liu, H., Li, Z., Anwar, N., Papadakis, V.G., Liu, G., Wang, W., 2021. pH regulation of the first phase could enhance the energy recovery from two-phase anaerobic digestion of food waste. Water Environment Research 93, 1370–1380. https://doi.org/10.1002/wer.1527

Zhou, X., Li, W., Mabon, R., Broadbelt, L.J., 2017. A critical review on hemicellulose pyrolysis. Energy Technology. https://doi.org/10.1002/ente.201600327

Zhu, H., Luo, W., Ciesielski, P.N., Fang, Z., Zhu, J.Y., Henriksson, G., Himmel, M.E., Hu, L., 2016. Wood-Derived Materials for Green Electronics, Biological Devices, and Energy Applications. Chem Rev. https://doi.org/10.1021/acs.chemrev.6b00225

Chapter 2

Recent progress and challenges in biotechnological valorization of lignocellulosic materials: towards sustainable biofuels and platform chemicals synthesis

S. G. Arhin, A. Cesaro, F. Di Capua, G. Esposito

Science of The Total Environment 857 (2023) 159333

2.1 Introduction

The fossil energy periods in human history marked by the advent of coal, crude oil, and natural gas in the 18th and 19th centuries represent a period of societal changes that led to improved production methods, productivity, mobility, and quality of life (Lee and Yang, 2019). However, our dependence on fossil resources is hampered by their rapid depletion and slender supply, high carbon emissions, anthropogenic climate change, and other environmental issues that imperil life on our planet (Mankar et al., 2021). It is thus imperative that we transition quickly from fossil resources to alternative sources of energy and carbon-based chemicals to ensure a more sustainable carbon economy. In this respect, research on renewable, eco-friendly, and reliable alternatives to fossil resources has gained scientific, industrial, and political attention in the 21st century. In particular, photosynthetic carbon captured in plant biomass is gaining attraction as an abundant source of clean, sustainable, and renewable carbon for fuels, chemicals, and functional materials synthesis (Liao et al., 2020). Substantial industrial and governmental investments have been made in recent decades to spur the commercialization of energy chemicals (e.g., bioethanol) and biomaterials (e.g., biodegradable plastics) synthesized from biomass. However, preliminary production paradigms focused on edible sugar and starch crops or oils as feedstocks, earning criticisms from the global research community (Kiggundu et al., 2017).

Notwithstanding, recent approaches centered on inedible LCMs, including agricultural wastes (e.g., wheat straw, rice husk, corn stover, sugarcane bagasse, etc.), forest residues (e.g., woodchips, sawdust, etc.), dedicated energy crops (e.g., switchgrass, *Miscanthus*, etc.) and so on, offer hope of meeting the global desire for bioderived chemicals and functional materials (Do et al., 2020; Mankar et al., 2021; Saif et al., 2021; Su et al., 2020). LCMs, consisting primarily of holocellulose (cellulose and hemicellulose) and aromatic macromolecules (lignin) (**Fig. 2.1**), are the most abundant biomass on earth, with an estimated annual production of nearly 200 billion tons (Sharma et al., 2022). Reports indicate only 8.2 billion tons of LCMs are currently utilized (Ashokkumar et al., 2022), suggesting LCMs have an enormous untapped potential that can be harnessed to meet the growing demand for carbon-based fuels and chemicals and alleviate the hegemony of the fossil-based economy. Hence, not surprisingly, many research groups have explored different innovative valorization methods, and over 200 value-added chemicals can now be synthesized from LCMs using various conversion techniques (Ashokkumar et al., 2022).

Biological conversion approaches–especially those catalyzed by a consortium of microbial species–have garnered attention as economically feasible and environmentally benign. Numerous anaerobes can metabolically funnel lignocellulosic monomers via complex reaction cascades into valuable fuels and commodity chemicals such as hydrogen gas, organic acids, bioalcohols, microbial lipids, and microbial proteins. However, the low bio-accessibility of LCMs due to the recalcitrant nature of plant cell wall components (Stinner et al., 2021), the structural complexity and compositional heterogeneity of lignocellulosic monomers, the limited flexibility of most wild-type product-forming microorganisms to co-metabolize different lignocellulosic monomers (Shahab et al., 2020), etc., are roadblocks that limit productivity, lead to carbon losses, and undesirable by-products formation. To overcome the recalcitrance of LCMs and increase the bioavailability of lignocellulosic monomers to product-forming microbes, innovative strategies for depolymerizing and disintegrating the lignocellulosic matrix via various pretreatment methods have been developed (Mankar et al., 2021; Stinner et al., 2021). Whatever the pretreatment route manipulating production setups and product-forming microorganisms to efficiently utilize the heterogenous mixture of carbon sources in LCMs (e.g., glucose, xylose, arabinose, mannose, galactose, monolignols, etc.) is essential to maximize profitability, ensure sustainability, and promote a circular economy. Accordingly, many research groups have focused on various strategies to maximize the co-utilization of all three major LCMs components and minimize carbon losses through carbon co-metabolism, carbon-flux redirection via genetic engineering, screening and isolation of novel microbial strains with high productivity, integrated biorefinery concepts to facilitate the co-production of various products as well as various techniques to address specific product-related challenges to increase productivity and generate products at competitive prices.

In this perspective, we present a comprehensive review of the recent advances in the biological valorization of LCMs to value-added fuels and chemicals, emphasizing the progress made to ensure the efficient conversion of the heterogeneous mixture of LCMs carbon sources into value-added products. We discuss the recent scientific progress in the bioconversion of LCMs into products such as biohydrogen, biomethane, biohythane, bioalcohols, biodiesel, carboxylic acids, bioplastics, and microbial proteins by providing insights into their production techniques and hurdles and suggesting how to address these limitations. Finally, we discuss the techno-economic potential of LCMs biorefineries and highlight the importance of carbon co-utilization to their commercial successes.

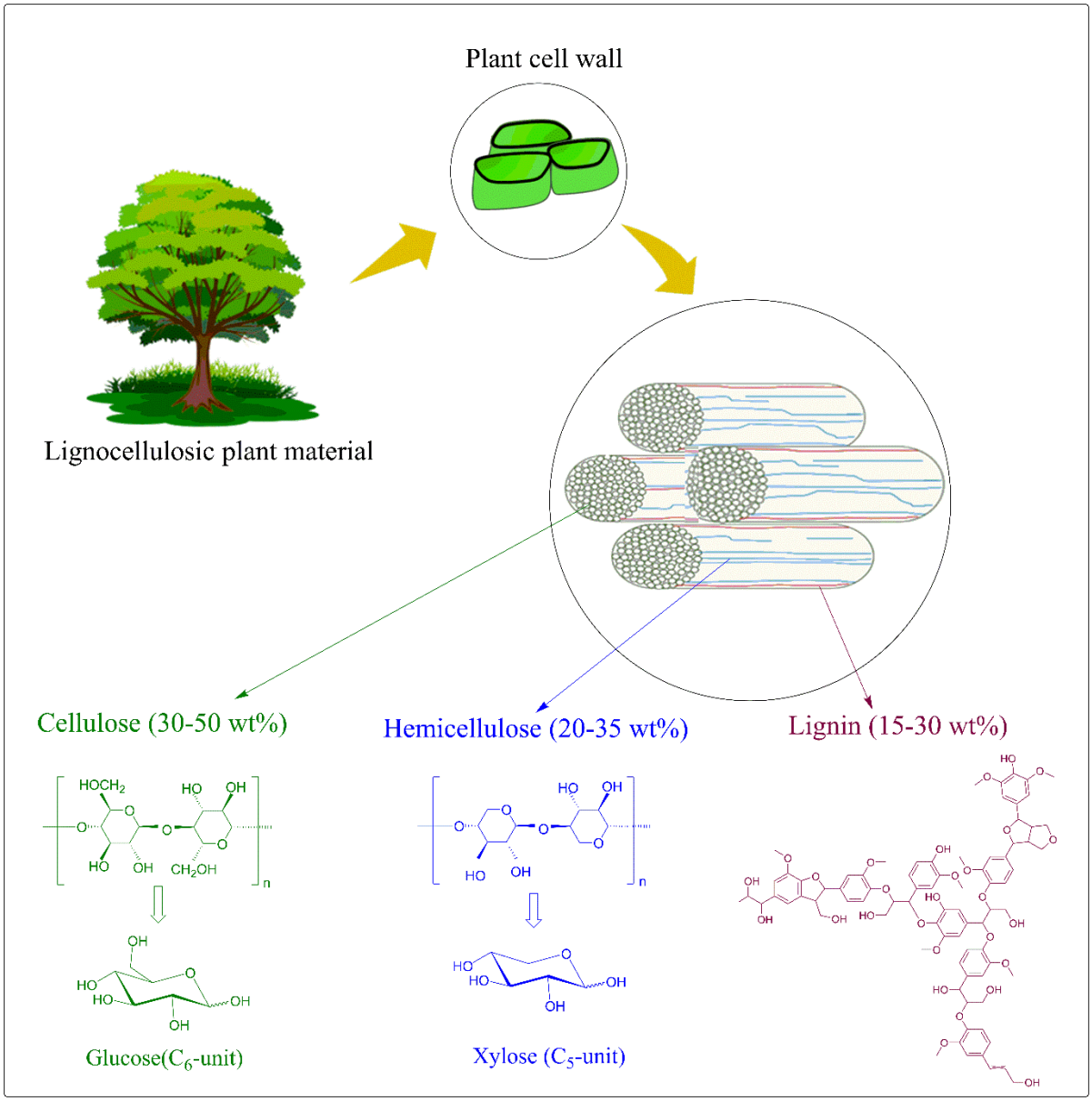

Fig. 2.1 Schematic illustration of the structure of lignocellulosic materials and their inherent recalcitrance.

2.2. Outlook on the biochemical valorization of lignocellulosic materials

Lignocellulosic biorefineries employ product-specific biochemical (e.g., fermentation and anaerobic digestion), thermochemical (e.g., pyrolysis and torrefaction), and hybrid (e.g., syngas fermentation) treatment routes to valorize LCMs. Biochemical conversion processes employ mild reaction conditions to convert LCMs fractions such as holocellulose into fermentable monosaccharide sugars via enzymatic or chemical hydrolysis, followed by microbial fermentation of the simple sugars to products such as ethanol. Given that biochemical processe operate under moderate conditions, are eco-friendly, and can generate various

replacements for petroleum-based products from LCMs by screening different enzymes and microorganisms, they are considered essential to long-term development and societal stability (Chen and Wang, 2016). Nonetheless, a dedicated process is required to fractionate the LCMs and expose polysaccharides for enzymatic hydrolysis. Fractionation can be realized via the so-called pretreatment processes, in which an LCMs is fragmented into its main components (i.e., cellulose, hemicellulose, and lignin) (Weidener et al., 2021).

Various pretreatment methods, including physical, chemical, physicochemical, biological, or a combination of these methods, have been employed to break down the lignocellulosic matrix and generate sugars for bioconversion **(Fig. 2.2)**. Additionally, thermochemical processes such as pyrolysis and gasification have also been explored as pretreatments for depolymerizing and disintegrating LCMs into bio-convertible intermediates, including CO, H_2, pyrolytic sugars, and carboxylic acids, that can be converted into high-value products using microorganisms.

After pretreatment, numerous value-added products can be synthesized from LCMs via biochemical conversion processes. In the subsequent sections, we critically discuss the recent advances in biosynthesis of some widely studied LCM-based products.

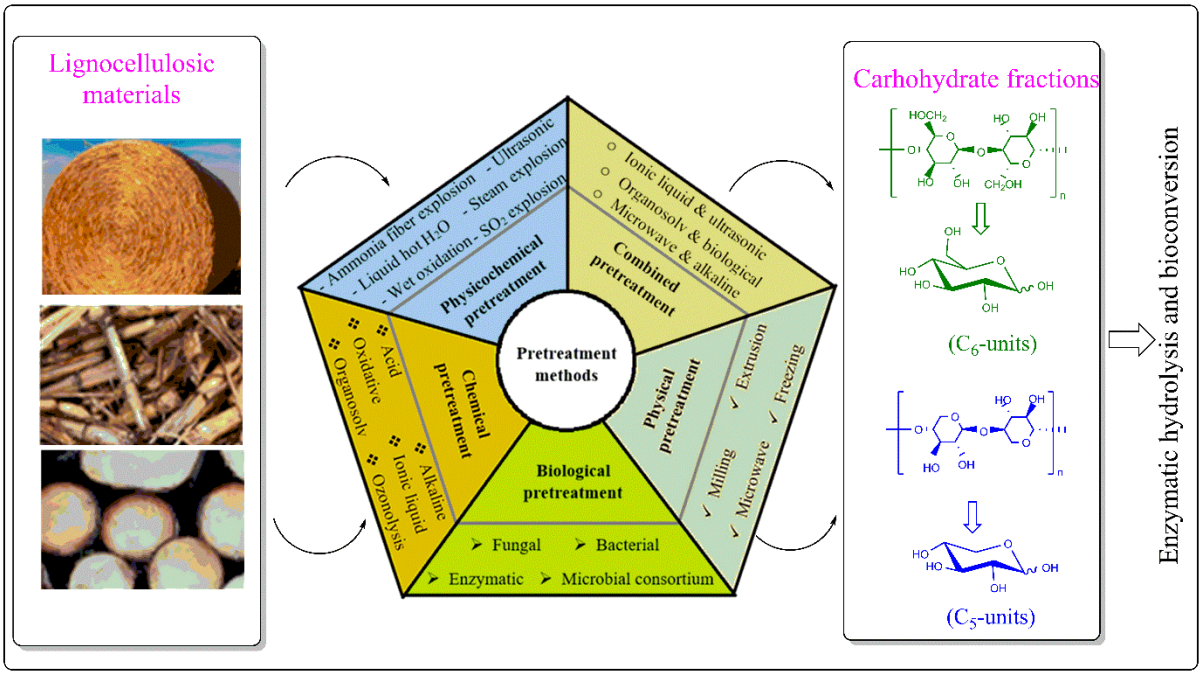

Fig. 2.2. Different pretreatment methods for releasing the carbohydrate fractions of lignocellulosic biomass for enzymatic hydrolysis and subsequent bioconversion to value-added carbon-based fuels and chemicals.

2.3 Advances in bioconversion of lignocellulosic materials to biofuels and biochemicals

2.3.1. Biohydrogen

Biohydrogen (H_2) has gained enormous attention as an energy carrier and potential transportation fuel because of its unique features such as high energy density (140 MJ/kg), clean and carbon-free nature, and wide applicability (Chen et al., 2021c; Khan et al., 2021). Although there are several methods for H_2 production, fermentative H_2 generation from LCMs presents several merits such as mild reaction conditions, cost effectiveness, renewability, and use of diverse substrates and microorganisms (Patel et al., 2021; Singh et al., 2021). Many LCMs, including cornstalk, sorghum, *Miscanthus*, *Arundo donax*, *Phragmites communis*, etc., have been proven to be viable substrates for fermentative H_2 production (Hu et al., 2021; Wei et al., 2021; Zhang et al., 2020b).

The process route for fermentative H_2 production from LCMs typically involves pretreatment, hydrolysis, and fermentation, and based on the reactor configuration in these processes, three main approaches for H_2 production currently exist (Bhatia et al., 2021; Yadav et al., 2020). The conventional approach, i.e., separate hydrolysis and fermentation (SHF), involves sequential hydrolysis and fermentation in two different reactors. This configuration allows operating conditions such as temperature to be optimized separately. However, the accumulation of monomeric sugars in the liquor could inhibit the hydrolysis process (Yadav et al., 2020). This drawback can be overcome by facilitating the bioconversion of pentoses and hexoses generated during hydrolysis to H_2 via integrated applications.

The most straightforward integrated concept, i.e., simultaneous saccharification and fermentation (SSF), in which hydrolysis and fermentation are performed in the same reactor, can increase H_2 production efficiency while eradicating the extra equipment and monitoring costs associated with SHF (Bhatia et al., 2021). However, operating conditions must be adjusted to meet the requirements of both hydrolysis and fermentation rather than a specific process. Also, hydrolytic enzymes used in SHF and SSF are produced in a separate process, which adds to production costs. To bypass this setback, the highly integrated consolidated bioprocessing (CBP), which involves the use of specific microbial consortia to simultaneously generate (hemi)cellulolytic enzymes for hydrolysis alongside monomeric sugars fermentation to H_2, was proposed. The CBP configuration possesses all the merits of SSF as well as saves

cost and time associated with enzyme production and the risk of enzyme contamination. The microbial consortia for CBP are selected based on the ability to degrade cellulose and hemicellulose and produce H_2. For example, Morales-Martinez et al. (2020) employed a syntrophic culture of bovine ruminal fluid, which has many microorganisms that can naturally degrade cellulose and hemicellulose by producing and excreting enzymes such as β-glucosidases, endoglucanases cellobiohydrolases, and cellodextrinases, and *Clostridium acetobutylicum*, a well-known H_2 fermenter that cannot effectively generate cellulolytic enzymes, to produce H_2 from agave biomass via CBP. Their results showed that at the optimum initial pH, temperature, inoculum ratio, and solid loading of 5.5, 35 °C, 1:2, and 10 %, respectively, about 150 mL H_2/g of biomass could be obtained in 264 h.

2.3.1.1. Fermentative H_2 production pathways

With regards to the fermentation process, four main technical conversion routes for fermentative H_2 production from LCMs are reported in the literature (Hu et al., 2021): (i) the light-dependent photo-fermentation (PF) process in which purple non-sulfur bacteria (PNSB) convert reducing sugars and organic acids to H_2 via a series of nitrogenase-catalyzed reactions (**Eqs. 2.1–2.7**), (ii) the dark-fermentation (DF) process in which anaerobes degrade complex carbohydrates to produce H_2 via hydrogenase-catalyzed reactions (Eqs. (**2.8–2.9**), (iii) the single-stage integrated system (alias dark-photo co-fermentation (DPCF)), in which DF and PF are performed simultaneously in the same bioreactor, and (iv) the two-stage sequential dark and photo-fermentation (SDPF) system in which DF and PF are performed successively in two separate bioreactors. PF is characterized by a high substrate conversion efficiency without VFAs formation because PNSB can utilize VFAs for H_2 production. Yet, the light-dependence and shielding effects (i.e., insufficient light penetration inside the bioreactor) make it uneconomical to produce H_2 from LCMs directly via PF (Hu et al., 2021). In contrast, DF does not require luminous energy, has a high H_2 production rate, and the anaerobes in DF can utilize different LCMs as carbon sources for H_2 production (Soares et al., 2020). However, H_2 yield is limited to about 33 % of the theoretical maximum (Nino-Navarro et al., 2020) due to the co-formation of VFAs and alcohols, which cannot be fully oxidized, thus diverging a considerable amount of the carbon present in the substrate to by-products formation.

To overcome the limitations of DF or PF in solitary and maximize H_2 yield and carbon utilization, the so-called integrated dark–photo-fermentation processes (i.e., DFCF and SDPF) were developed. **Table 2.1** highlights the H_2 yield from selected LCMs under various

fermentation modes, inoculum types, operating conditions, and pretreatments. Although comparative studies on DPCF and SDPF are rare, SDPF systems could be more effective because growth conditions for each bacteria group can be optimized and regulated separately, even though DPCF has lower implementation costs (Yadav et al., 2020). For instance, Zhang et al. (2020a) reported a higher H_2 yield in PF (141.42 mL/g total solids, TS) than in DF (36.08 mL/g TS) and DPCF (90.13 mL/g TS) from corn stover hydrolysate using photosynthetic bacteria HAU-M1 and dark fermentative bacteria *Enterobacter aerogenes*. The authors attributed the lower H_2 yield in DPCF to a compromised local mass transfer of the substrate as HAU-M1 was embedded and immobilized in DPCF but was suspended in PF. Thus, to maximize H_2 yield in DPCF bioreactors, it is essential to establish a syntrophic co-culture of anaerobes and PNSB (Wang et al., 2021).

Glucose pathway: $C_6H_{12}O_6 + 12H_2O$ (light energy)$\rightarrow 12H_2 + 6CO_2$ (**2.1**)

Acetic acid pathway: $CH_3COOH + 2H_2O \rightarrow 4H_2 + 2CO_2$ (**2.2**)

Lactic acid pathway: $CH_3CHOHCOOH + 3H_2O \rightarrow 6H_2 + 3CO_2$ (**2.3**)

Propionic acid pathway: $CH_3CH_2COOH + 4H_2O \rightarrow 7H_2 + 3CO_2$ (**2.4**)

Succinic acid pathway: $COOHCH_2CH_2COOH + 4H_2O \rightarrow 7H_2 + 4CO_2$ (**2.5**)

Malic acid pathway: $COOHCH_2CHOHCOOH + 3H_2O \rightarrow 6H_2 + 4CO_2$ (**2.6**)

Butyric acid pathway: $CH_3CH_2CH_2COOH + 6H_2O \rightarrow 10H_2 + 4CO_2$ (**2.7**)

Acetic acid pathway: $C_6H_{12}O_6 + 4H_2O \rightarrow 2CH_3COO^- + 4H^+ + 2HCO_3^- + 4H_2$ (**2.8**)

Butyric acid pathway: $C_6H_{12}O_6 + 2H_2O \rightarrow CH_3CH_2CH_2COO^- + 3H^+ + 2HCO_3^- + 2H_2$ (**2.9**)

Table 2.1 Selected studies on H_2 production from various lignocellulosic substrates under different fermentation modes.

Substrate	Mode of fermentation	Microorganisms	Fermentation conditions	Pretreatment method	H_2 yield	Ref.
Poplar (*Populus deltoides*)	DF (continuous)	Mixed culture	pH 7.0, temperature 37 °C, HRT 4d	Chemical pretreatment (i.e., 0.5% H_2SO_4 at 121 °C for 1h)	112 mL/g of dry poplar	Patel et al. (2021)
Energy Sorghum (*Sorghum bicolor* (L.) Moench, variety GN-04)	SDPF (semi-continuous)	DF by *Clostridium thermocellum* PF by *Rhodobacter sphaeroideswere*	Temperature 55 °C, sorghum loading of 20 g/L Temperature 37 °C, illumination with a 10 W halogen lamp	Milling (0.5 mm screen)	158 mL/g of sorghum added	Hu et al. (2021)
Corn stover	PF (batch)	Photosynthetic bacteria HAU-M1	Initial pH 6.5, temperature 30 °C, and light intensity 3500 Lux	Milling (60-mesh sieve)	141.42 mL/g TS	T. Zhang et al. (2020)
	DF (batch)	*Enterobacter aerogenes*	Initial pH 6.5, temperature 35 °C		36.08 mL/g TS	

	DPCF (batch)	HAU-M1 and *Enterobacter aerogenes* at a ratio of 3:1	Initial pH 6.5, light temperature 30 °C, and light intensity 3500 Lux		90.13 mL/g TS	
Corn stalk	PF (batch)	Photosynthetic bacteria HAU-M1	pH 5–7, temperature 30 °C, and light intensity 3000 Lux	N/A*	141.66 mL/g VS at pH 6	Lu et al. (2020)
Various kinds of energy grasses	PF (batch)	Photosynthetic bacteria HAU-M1	Initial pH 7.0, temperature 30 °C, light intensity 5000 Lux	Milling (particle size 180 nm)	147.64 mL/g TS	Y. Zhang et al. (2020)
Fruits-and-vegetables wastes and corn stover as co-substrates	DF (batch)	Mixed culture	Temperature 35 °C with orbital agitation (150 rpm)	Milling to 180 μm followed by dilute acid hydrolysis (i.e., 0.5% v/v HCl or H_2SO_4 at 120 °C for 120 min)	287.2 mL/g glucose (i.e., 2.31 mol/ mol glucose)	Rodríguez - Valderrama et al. (2020)
Corncob	DF (batch)	Mixed culture (i.e., bovine ruminal fluid bioaugmented with *C. acetobutylicum* at a ratio of 1:2)	pH 5.5, temperature 35 °C, 5% solids loading	Thermochemical pretreatment (i.e., 2% H_2SO_4 at 160 °C; 2% NaOH at 140 °C; 2% NaOCl at 140 °C; autohydrolysis: H_2O at 190 °C)	132 mL/g of biomass	Medina-Morales et al. (2021)

*N/A means not available

2.3.1.2 Strategies for maximizing fermentative H_2 yield

Besides bioreactor configuration, recent studies on fermentative H_2 production from LCMs have focused on various strategies for increasing H_2 yield such as novel microbial strains with higher biomass to H_2 conversion capabilities or bacteria strains that could co-produce H_2 and other bio-based products from LCMs to maximize carbon conversion without compromising H_2 yield. Wei et al. (2021) isolated a high temperature- and light-tolerant mutant, i.e., *Rhodobacter capsulatus* MX01, which could convert cornstalk hydrolysate to H_2 at a higher conversion efficiency (10.6%) compared to the wild-type strain. Also, *R. capsulatus* MX01 could perform PF in outdoor settings, which is vital for cost-effective, energy-saving, and eco-friendly practical applications. Verma et al. (2020) also isolated a new PNSB, *Rubrivivax benzoatilyticus* strain 'TERI-CHL1', for valorizing organic-rich DF effluent. A putative mutant of *Thermotoga neapolitana* DSMZ 4359^T, a well-known hyperthermophilic eubacterium with high H_2 yield from lignocellulosic hydrolysates, was identified to possess a new anaplerotic pathway to co-produce H_2 and lactic acid under capnophilic conditions (Pradhan et al., 2017). The mutant strain, TN-CMut, could grow on different LCMs carbon sources, including glucose, xylose, and arabinose, which makes it a great candidate for LCMs biorefineries aimed at sustainable bioproduction of H_2 and commodity chemicals such as lactic acid. Besides these studies, other researchers also aimed at genetically engineering and redirecting metabolic pathways of H_2 producers to facilitate H_2 yield. For example, Son et al. (2021) reported an

increased H_2 yield by overexpressing glucose-6-phosphate dehydrogenase and FeFe hydrogenase in *C. acetobutylicum*. The metabolically engineered *C. acetobutylicum* strains, CA-zwf(pIMP-zwf) and CA-hydA(pMTL-hydA), produced 1.2- and 1.4-fold higher H_2 yields than the wild-type, respectively. Chu et al. (2021) also demonstrated that the deletion of lactate dehydrogenase in *Klebsiella* sp. Strain Fsoil 024 could redirect NADH from the lactate pathway to H_2 synthesis. Despite recent advances in genetically modified H_2 fermenters, the stability of newly discovered and genetically modified stains needs rigorous testing beyond the laboratory scale for practical applications.

Additives such as biochar and nanomaterials, including nickel oxide (NiO), hematite (Fe_2O_3), magnetite (Fe_3O_4), and titanium dioxide (TiO_2) have also gained attention recently as tools for increasing fermentative H_2 yield from lignocellulosic hydrolysates. Such additives could facilitate H_2 production by (i) acting as co-factors on active sites of nitrogenase and hydrogenase, (ii) acting as oxygen scavengers, removing undesirable oxygen in anaerobic systems, (iii) stimulating electron transfer between functional microorganisms, (iv) absorbing inhibitors, and (v) facilitating microbial growth via immobilization (Srivastava et al., 2020). For instance, biochar derived from residual cornstalk could increase H_2 yield from cornstalk by 1.8-fold by providing a large specific surface area for bacterial attachment and promoting cellulolytic enzyme activity (Zhao et al., 2021). Green synthesized Fe_3O_4 and NiO nanoparticles could also facilitate Klebsiella sp. WL1316 catalyzed H_2 production from cotton stalk and rice straw hydrolysates by promoting hydrogenase and formate-hydrogen lyase (Q. Zhang et al., 2021a, 2021b). Additionally, phyto-fabricated nanoscale organic iron from *Eucalyptus viminalis* leaf extract could also improve H_2 production by *Rhodopseudomonas palustris* MP2 and *R. palustris* MP4 due to enhanced nitrogenase activities (Kanwal et al., 2020). Despite these promising outcomes, conflicting results on the influence of additives have also been reported. For instance, even though 20 mg/L Fe_3O_4 nanoparticles increased H_2 production in rice straw hydrolysate by 23.49%, adding 40 mg/L resulted in lower H_2 production (14.7%) than the control (0 mg/L) (Q. Zhang et al., 2021b).

It should be emphasized that although metal or metallic oxide nanoparticles could enhance the bioactivities of ferredoxin oxidordeuctase and hydrogenase, excessive concentrations could hinder hydrogenase activities and exhibit some toxic effects on hydrogen-producing bacteria. For example, Cheng et al. (2020) showed that adding 500 mg/L of Fe_3O_4 nanoparticles could cause the nanoparticles to infiltrate the cell walls and create holes on the surface of DF bacteria *E. aerogenes* ZJU1 cells due to oxidative stress. This phenomenon decreased hydrogenase

activities (by 31.8%), the NADH/NAD^+ ratio, and NADH-dependent H_2 production due to the enhancement of the ethanol pathway and the weakening of acetate and butyrate pathways. Consequently, the overall H_2 yield decreased (196.7 ± 4.8 mL/g glucose) compared to the control group (215.4 ± 4.3 mL/g glucose). Thus, such unfavorable results could be addressed by optimizing the concentration and particle size of additives to be used in H_2 bioreactors.

2.3.2. Biomethane

The bioconversion of LCMs to biomethane (CH_4) via AD is an extensively studied biotechnology for LCMs valorization and energy recovery because, compared to other conversion routes, AD is one of the most efficient ways to generate energy from biomass based on the energy-gained/input ratio (28.8 MJ/MJ) (Marta et al., 2020). Numerous recent studies have reported on the influence of various factors such as pretreatment, organic loading rate (OLR), hydraulic retention time (HRT), pH and buffering capacity, temperature, inoculum type, substrate co-digestion, bioreactor configuration, etc. on the stages of the AD process (i.e., hydrolysis, acidogenesis, acetogenesis, and methanogenesis) and ultimately CH_4 production. Several innovative pretreatment strategies, including the use of AD by-products such as liquid digestate and CO_2, for example, has been shown to increase monomeric sugar contents while reducing cellulose crystallinity (9.80 %) in corn straw, thus increasing the CH_4 yield (50.97 %) compared to the untreated corn straw (Ma et al., 2022). Oliva et al. (2021) also showed that methanol-organosolv pretreatment catalyzed by sulfuric acid could decrease the lignin content in hazelnut skin from 39.66 % to 34.73 % and increase the amount of bioavailable sugars, thereby increasing CH_4 yield (310.6 ± 22.2 mL/g VS) compared to the raw hazelnut skin (17.3 ± 32.3 mL/g VS). Regarding temperature, past studies suggest that hydrolysis at thermophilic conditions followed by methanogenesis at mesophilic conditions could be optimal for AD, as thermophilic temperatures could enhance the degradation of organic compounds while mesophilic temperatures exhibit better process stability and a more enriched microbial community (Kainthola et al., 2019). Additionally, the optimum range of alkalinity for AD is 2000–5000 mg CaCO3/L, with 1000 mg CaCO3/L being the lower limit of alkalinity required to provide a convenient buffering capacity (Ünyay et al., 2022). Also, the ideal pH range for hydrolysis, acidogenesis, acetogenesis, and methanogenesis is 6.0, 5.0–6.2, 6.0–7.0, and 6.5–7.5, respectively, with the optimal carbon-to-nitrogen (C/N) ratio ranging from 25 to 35 (D'Silva et al., 2021). Besides temperature, pH, alkalinity, and the C/N ratio, another crucial factor in AD is the OLR, which could significantly impact AD performance (Di Capua et al.,

2020). A high OLR could lead to H_2, NH_3, and VFAs accumulation and a drop in pH that could subsequently lower the reaction rate or even shut down the AD process. For example, in a long-term semi-continuous AD of switchgrass performed in a continuously stirred tank reactor (CSTR), Ünyay et al. (2022) reported that increasing the OLR from 0.75 to 1.0 g VS/(L.d) resulted in an almost similar CH_4 yield (148 and 157 mL/g VS, respectively). However, a further increase in the OLR to 1.5 g VS/(L.d) led to a drastic reduction in CH_4 yield (60 mL/g VS) due to switchgrass accumulation, which caused mixing problems and VFAs accumulation that led to a reduction in pH from time to time. **Table 2.2** summarizes the CH_4 yield from selected LCMs under varying operating conditions.

Table 2.2. Selected studies on CH_4 production from various lignocellulosic substrates.

Substrate	Mode of fermentation	Microorganisms	Fermentation conditions	Pretreatment conditions	CH_4 yield	Ref.
Corn straw	Batch	Mixed culture	Temperature 35 ± 1 °C, inoculum to substrate ratio 2 g VS/g VS	Liquid digestate at 55 or 170 °C with or without CO_2 (1 MPa) for 0.5 or 24 h	157.53 mL/g VS	Ma et al. (2022)
Hazelnut skin Spent coffee grounds Almond Shell	Batch	Mixed culture	Temperature 37 °C, pH 6.3–7.5, inoculum to substrate ratio 1.5 g VS/g VS	Organosolv (50% (v/v) water-methanol solution, with and without H_2SO_4 as the catalyst) at 130, 160, and 200 °C for 60 min	310.6 ± 22.2 mL/g VS 322.9 ± 19.5 mL/g VS 24.8 ± 2.6 mL/g VS	Oliva et al. (2021)
Wheat straw	Batch	Mixed culture	Temperature 37 ± 2 °C, inoculum to substrate ratio of 1.5 g VS/g VS	NMMO (i.e., 85% (w/w) at 120 °C for 3 h) Organosolv (i.e., 50% (v/v) ethanol at 180 °C for 1 h Alkaline (i.e., 1.6% (w/w) NaOH at 30 °C for 24 h)	304 ± 3 mL/g VS 316 ± 1 mL/g VS 315 ± 2 mL/g VS	Mancini et al. (2018)
Corn straw Wheat straw Sweet sorghum straw Rice straw	Batch	Mixed culture	Temperature 37 ± 1 °C, automatic stirring at 60 rpm, initial pH 7.0 ± 0.1	Grinding (1 mm sieve)	335.67 mL/g VS 265.98 mL/g VS 182.74 mL/g VS 161.74 mL/g VS	X. Dai et al. (2020)
Wheat straw and sunflower meal co-digestion	Batch	Mixed culture	Initial pH 7.1–7.5, mesophilic temperature	Thermal pretreatment at 120, 140, 160 and 180 °C for 1 h	433 NmL/g VS	Ayub and Hassan (2021)
Empty fruit bunches and palm oil mill effluent co-digestion	Semi-continuous solid-state	Mixed culture	Temperature 40 ◦C, substrate to inoculum ratio 2:1	Fungal pretreatment with *Volvariella volvacea* cultivated at 28–32 °C and 80–90% relative humidity	405.4 ± 7.1 mL/g VS	Mamimin et al. (2021)
Wheat straw	Batch and Continuous	Mixed culture bioaugmented with chitinolytic bacteria	Temperature 37 ± 2 °C, pH 6.4–7.4 HRT 25 d, mixing at 90 rpm, OLR 0.5 g/(L.d)	Fungal pretreatment with *Chaetomium globosporum* at 36 °C and 81% moisture content for 31 d	396 mL/g VS for batch AD and 92.9 mL/g VS d (163 mL/g VS d as biogas) for continuous AD	Yadav and Vivekanand (2021)

2.3.2.1. Increasing CH_4 production via direct interspecies electron transfer

For recalcitrant substrates such as LCMs, hydrolysis is considered the rate-limiting step in the AD process. Therefore, a pretreatment step is typically incorporated to improve the hydrolysis rate of the substrate (Mancini et al., 2018), which is then fermented into intermediates, including organic acids (mainly VFAs), alcohols, and H_2 via hydrolysis and acidogenesis. Consequently, VFAs accumulation could occur leading to a pH drop and even failure of the AD process (Ren et al., 2020). To ensure system stability, enhancing acetogenesis, acetate oxidation, and methanogenesis via the transfer of reducing equivalents such as H_2 and formate among the various functional microorganisms is essential for maintaining a thermodynamically stable environment and the syntrophism of AD cultures. For several decades, interspecies H_2/formate transfer (IHFT) in which H_2/formate serves as diffusible electron carriers has been recognized as the primary mechanism in syntrophic methanogenesis (Walker et al., 2020). However, IHFT is thermodynamically feasible only when the H_2/formate concentration is kept low.

Therefore, the relatively recent discovery of the possibility of direct interspecies electron transfer (DIET) from bacteria to methanogens offers new insight and opportunity to boost syntrophic metabolism in AD bioreactors and improve the process stability. Recent studies suggest that some bacteria could connect physically or electrically with methanogens to exchange electrons via electrically conductive cell components such as c-type cytochrome and e-pili (Shi et al., 2021a). This direct electron exchange (i.e., DIET) is deemed a more efficient electron transfer mechanism than IHFT because it is faster and more specific (Lovley, 2017). Consequently, DIET has been associated with more efficient VFAs and alcohol utilization for enhanced CH_4 production in AD bioreactors. For example, Shi et al. (2021a) demonstrated that corn straw-derived hydrochar could facilitate DIET between Methanosarcina sp. FDU0106 and Syntrophomonas sp. FDU0164 to increase the CH_4 production rate and yield by 30.8 % and 31.4 %, respectively. Saif et al. (2021) also showed that adding 2 g/L of biochar from walnut shell during anaerobic co-digestion of corn straw, wheat straw, and rice straw with cow dung could facilitate VFAs consumption via DIET and increase CH_4 yield by 56.97 %, 74.15 %, and 87.55 %, respectively. Similarly, Ma et al. (2020) observed that adding 15 g/L of rice husk biochar could increase the CH_4 production rate from sorghum by 25 % and shorten the lag phase time by 44 %, possibly due to DIET. In the DIET pathway to CH_4 synthesis, electron-donating microorganisms (exoelectrogens) oxidize VFAs (e.g., propionic acid, **Eq. 2.10**) and alcohols (e.g., ethanol, **Eq. 2.11**) to acetate, releasing electrons and protons, which are

subsequently metabolized by electron-accepting methanogens (electrotrophs) to reduce CO_2 to CH_4 (**Eq. 2.12**).

$$CH_3CH_2COOH + 3H_2O \rightarrow CH_3COO^- + HCO_3^- + H^+ + 3H_2 \quad (\mathbf{2.10})$$

$$CH_3CH_2OH + H_2O \rightarrow CH_3COO^- + 5H^+ + 4e^- \quad (\mathbf{2.11})$$

$$9H^+ + 8e^- + HCO_3^- \rightarrow CH_4 + 3H_2O \quad (\mathbf{2.12})$$

Although several methanogens, including *Methanospirillum* and *Methanosphaerula* might be involved in DIET (Jing et al., 2017), currently, *Methanosarcina barkeri* (Liu et al., 2012), *Methanothrix* (*Methanosaeta*) *harundinacea* (Rotaru et al., 2014), *Methanothrix concili* (Yang et al., 2019), and *Methanobacterium* sp. strain YSL (Zheng et al., 2020) are the methanogens confirmed with strong evidence to directly accept electrons via DIET. Also, *Geobacter metallireducens* (Liu et al., 2012; Rotaru et al., 2014; Zheng et al., 2020), *Geobacter lovleyi* (Yang et al., 2019), and *Syntrophus aciditrophicus* (Walker et al., 2020) are the bacteria demonstrated with strong evidence to donate electrons via DIET, although *Clostridium* (Ren et al., 2020), *Trichococcus* (Ren et al., 2020), *Thauera* (Jing et al., 2017), *Syntrophomonas* (Shi et al., 2021b) and others might also be involved in DIET.

In the absence of a recognized DIET bacteria, abiotic conductive materials such as biochar, hydrochar, and magnetite have been reported to act as electrical conduits, shuttling electrons to mediate DIET (Shi et al., 2021b; Zhang et al., 2018). This “battery” mechanism has been associated with enhanced CH_4 production in many recent studies where conductive materials were added to AD bioreactors (Shen et al., 2021). It is noteworthy that other studies have reported contradictory results where biochar addition, for instance, did not benefit CH_4 production (Ren et al., 2020). Properties of conductive materials such as the bulk electrical conductivity (EC) and electron-accepting/donating capacity (EADC) are often associated with the ability to mediate DIET (Shen et al., 2021). However, other studies argue that neither EC nor EADC but the abundance of surface oxygen-containing functional groups such as C−O, C==O, and C−OH is related to DIET (Ren et al., 2020; Shi et al., 2021b). These redox-active functional groups relate to quinone and hydroquinone moieties that can accept and donate electrons (Ren et al., 2020) and could partly explain the inconsistencies in the literature.

Based on the studies discussed, promoting DIET in AD bioreactors could enhance carbon conversion and increase CH_4 production from LCMs. However, research on conductive materials-mediated DIET is still in the infancy stage, and thus, requires more in-depth studies

to elucidate the mechanisms of electron transfer and determine potential practicalities and applicability. In this regard, molecular tools such as metaproteomics, metatranscriptomics, and metagenomics are becoming handy for unveiling metabolic pathways and key genes associated with DIET. However, multi-faceted approaches combining molecular analysis, kinetic modeling, and the intrinsic characteristics of conductive materials, including the crystallinity and redox-active surface functional groups could provide more detailed insights into conductive materials-mediated DIET and associated methanation.

2.3.3. Biohythane

Biohythane, a mixture of CH_4 and H_2 produced via anaerobic fermentation, has gained increased scientific and commercial interest in recent years as a sustainable vehicular fuel due to its higher combustion efficiency, lower pollutants emission, shorter fermentation time, and a more flexible H_2/CH_4 ratio compared to traditional biogas (Seengenyoung et al., 2019). Typically containing about 5–25 % of H_2 by volume (Ghimire et al., 2017), biohythane has been demonstrated as a versatile transport fuel and is considered a bridging solution in the transitioning from natural gas to H_2 as the ultimate energy carrier, i.e., the so-called "decarbonization" (Jiang et al., 2018). Recently, several feedstocks, including industrial sugars, cassava wastewater, parboiled rice wastewater, palm oil mill effluent, food wastes and other municipal solid wastes, microalgae (e.g., *Spirulina, Dunaliella, and Chlorella* sp.), and LCMs (e.g., sugarcane bagasse, rice husk, wheat straw, etc.) have been studied for biohythane production (Ghimire et al., 2017; Li et al., 2020; Rena et al., 2020; Yang et al., 2020a). LCMs remain one of the most promising feedstocks for biohythane production because of its high availability and relatively low cost (Kumari and Das, 2019).

1.3.3.1. Two-stage biohythane production

Conventionally, biohythane is produced from lignocellulosic hydrolysates via sequential DF and AD in two separate bioreactors. H_2 is generated in the DF stage, and the effluent containing VFAs and alcohols is converted to CH_4 via AD. Considering that the theoretical maximum H_2 yield from DF is limited to 4 mol-H_2/mol-hexose and the hydrolysis of LCMs is the rate-limiting step in CH_4 production, the physical separation of hydrolysis and H_2 production from methanogenesis in the two-stage anaerobic fermentation (TSAF) approach allows for fermentation conditions to be optimized separately for each microbial group, thus increasing the overall energy recovery and system stability, reducing fermentation time, and guaranteeing

a desired H_2/CH_4 ratio. For example, Dong et al. (2020) produced biohythane via TSAF of rice straw pretreated with NaOH/urea under outdoor cold-winter conditions and generated about 225 mL H_2/g sugar and 113 mL CH_4/g sugar, which was about 23 % and 190 % higher than that of conventional H_2 and CH_4 fermentation, respectively. Similarly, J. Li et al. (2020) assessed the feasibility and stability of generating biohythane from cornstalk in a semi-continuous pilot-scale study using TSAF without a hydrolysis step and achieved 25.02 mL H_2/g TS and 95.38 mL CH_4/g TS. Accordingly, the 18.47 % H_2 content in the biohythane gas makes it suitable for vehicular fuel and a vital reference point for future industrial applications. Mamimin et al. (2019) also demonstrated that two-stage co-digestion of palm oil mill effluent (POME) and palm oil solid waste residues could generate 26.5–34 m3 biohythane/ton waste, which was 67–114 % higher than that generated from POME mono-digestion.

Selecting the appropriate substrate for biohythane production is fundamental to maximizing productivity in TSAF. To this end, several LCMs, including wheat, rice, sorghum, sugarcane, corn, and cassava residues, peanut and hazelnut shells, and palm oil mill wastes have been used as substrates for two-stage biohythane production, with substrate co-digestion having better performances in terms of carbon utilization and overall biohythane yield due to better C/N ratio compared to substrate mono-digestion (Chen et al., 2021a; Mamimin et al., 2019). Aside from that, balancing the growth conditions of acidogens such as *Clostridium* sp., *Caldicellulosiruptor* sp., *Enterobacter* sp., and *Thermotoga* sp. in the first stage, and methanogens such as *Methanosarcina* and *Methanothrix* at high acetate concentrations (>1.2 mM) in the second stage is essential to maximize biohythane yield. Typically, in TSAF, the optimal pH and HRT for the first stage are 5–6 and 1–3 d, respectively, while pH 7–8 and HRT 10–15 d are considered optimal for the second stage, with the overall fermentation time ranging from 13 to 18 d (Lay et al., 2019). For temperature, some studies argue that temperature-phased TSAF systems consisting of thermophilic acidogenic and mesophilic methanogenic bioreactors could enhance biohythane yield due to enhanced growth of hydrogen-producing bacteria such as *Clostridium sensu stricto*_1 and *Thermoanaerobacterium* under thermophilic conditions. For instance, in a continuous TSAF study on biohythane production from rice straw and pig-manure co-digestion, the highest biohythane yield (i.e., 16.68 ± 1.88 mL H_2/g VS and 197.73 ± 11.77 mL CH_4/g VS) was obtained by operating the first stage bioreactor under thermophilic conditions and the second stage under mesophilic conditions (Chen et al., 2021a). The results showed that Thermoanaerobacterium and *C. sensu stricto_1* dominated the first stage thermophilic bioreactor leading to high H_2 production whereas *Methanobrevibacter*, a

hydrogenotrophic methanogen, dominated the microbial population when the first stage bioreactor was operated under mesophilic conditions causing a reduction in H_2 production. Liu et al. (2022) observed similar results in a long-term semi-continuous temperature-phased study on biohythane production from rice straw and pig-manure co-digestion that *C. sensu stricto_1* dominated the first stage bioreactor under thermophilic conditions. According to the authors, the highest biohythane yield, i.e., 73.09 ± 3.03 mL H_2/g VS and 235.81 ± 9.30 mL CH_4/g VS, was attained in the temperature-phased bioreactors at 6 % TS content and rice straw to pig manure ratio of 5:1.

2.3.3.2. Single-stage biohythane production

Despite the promising results on TSAF, to minimize the economic inputs and engineering complexities associated with operating two separate bioreactors, innovative single-stage reactors for biohythane production have also been proposed. For example, Yang et al. (2020a) proposed a multistage biohythane reactor that integrates an internal biofilm DF compartment with an external up-flow sludge blanket AD section in a single bioreactor unit. After hydrolysis and acidification in the inner zone filled with biocarriers, the liquid metabolites are driven by gravity and the pressure difference via a filter hole at the bottom into the granular sludge bed zone for CH_4 production. According to the authors, the bioreactor could generate 4.900 L H_2/(L.d) at pH 6 and 10.271 L CH_4/(L.d) at pH 6.5 and biohythane at an $H_2/(H_2 + CH_4)$ ratio of 16 % in the inner zone at initial pH of 6.5. Ta et al. (2020) also demonstrated an innovative single-stage DF reactor for biohythane production using a mixture of separately entrapped hydrogen-producing bacteria and methanogens. The hydrogen-producing bacteria and methanogens, cultivated independently for 2 weeks in two CSTRs, were entrapped in round-shaped beads. The hydrogenic beads were added to the single-stage reactor (operating in a continuous mode at pH 5.5, HRT 48 h, and temperature 37 °C) a week before the methanogenic beads, and at a biomass ratio of 2/3 (i.e., the ratio of hydrogenic/methanogenic beads), a peak biohythane production of 64.6 mL H_2/(L.d) and 395 mL CH_4/(L.d) was attained with 74.4 % chemical oxygen demand (COD) removal.

It is noteworthy that one of the main bottlenecks to overcome in single-stage biohythane systems is the conflict between H_2 generation and hydrogenotrophic CH_4 production. It is well known that within anaerobic microbiomes, H_2-producing bacteria generate H_2 that is consumed by hydrogenotrophic methanogens with CO_2 reduction to generate CH_4. Therefore, to increase H_2 yield, there is the need to suppress the growth of hydrogenotrophic methanogens. Yet

hydrogenotrophic methanogens have the crucial task of maintaining a low H_2 partial pressure, which is important for the metabolic reactions of methanogens. Thus, to obtain a desirable $H_2/(H_2 + CH_4)$ ratio in single-stage biohythane reactors, it is crucial to engineer the system to find the right balance between H_2 production and hydrogenotrophic methanogenesis. Aside from that, past studies also hinted that the effluent from single-stage biohythane reactors could have high COD concentrations that need further treatment (Nguyen et al., 2021). It is worth mentioning that research on single-stage production started in 2015 and thus remains in the infancy stage (Nguyen et al., 2021; Ta et al., 2020). Therefore, more in-depth studies are required to increase the process output and enhance carbon utilization. For instance, integrated biorefinery concepts combing single-stage biohythane production with other bioprocesses such as PF and aerobic digestion or pyrolysis of the solid digestate to generate fermentable intermediates could maximize the carbon conversion efficiency. Also, strategies for promoting H_2 and CH^4 yields in conventional AD or DF systems such as bioaugmentation (Sheng et al., 2021) and abiotic materials supplementation (Ma et al., 2020; Saif et al., 2021) could improve carbon conversion in single-stage biohythane reactors.

2.3.4. Bio-syngas production and bioconversion

Synthesis gas or syngas, a gaseous pyrogenic product containing H_2, CO, and CO_2, and generated via thermochemical conversion of LCMs, is considered essential energy and carbon source in biorefinery (Asimakopoulos et al., 2020, 2021). The yield and composition of syngas from LCMs depend on several controllable factors, including the type of LCMs, conversion process, feedstock co-processing, operating conditions (temperature, pressure, retention time), reactor configuration, presence of catalysts, etc. Therefore, a great deal of effort has been made in recent years to manipulate these parameters to enhance bio-syngas yield from LCMs and control the H_2/CO ratio in the syngas. For example, Jung et al. (2020) and Kim et al. (2021) explored the beneficial effects of CO_2-mediated catalytic and non-catalytic pyrolysis on syngas from rice husk, barnyard grass, and retinispora. Their results confirmed the gas-phase reaction between CO_2 and volatile organic compounds from LCMs pyrolysis as the main mechanism for enhanced CO formation, with lignin-rich substrates seemingly more susceptible to CO_2, thus having higher (nearly double) CO formation. Monir et al. (2018) and Liu et al. (2021a) also assessed the effect of coconut shell co-gasification with charcoal and pinewood co-pyrolysis with polycarbonate, respectively, and found that co-processing LCMs with other feedstocks has a synergistic impact on the H_2/CO ratio and total syngas yield.

2.3.4.1. Biological syngas conversion

Although syngas can be used directly in gas turbines to generate power after cleaning and conditioning, its utilization as a platform for value-added fuels and chemicals production is increasingly gaining attention. Since the invention of the Fischer–Tropsch synthesis (FTS), a broad array of liquid fuels and chemicals, including light olefins (e.g., ethylene, propylene, butylene), oxygenates (e.g., ethanol), wax, etc. have been obtained from syngas via the FTS pathway. However, some recent studies argue that microbiome catalyzed approaches could be more advantageous than the FTS pathway due to mild reaction conditions, robustness over syngas impurities, lower costs, and greater operational flexibility with regards to the H_2/CO molar ratio (Gunes, 2021; C. Li et al., 2021). It is well known that carboxydotrophic microorganisms can synthesize valuable metabolites (e.g., H_2, CH_4, etc.) from CO due to the presence of CO-dehydrogenase complex, a crucial enzyme for biological CO conversion characterized in anaerobes by the presence of Ni catalytic site (Andreides et al., 2021). Acetogens such as *Clostridium ljungdahlii* can catalyze the formation of acetyl coenzyme A (acetyl-CoA), the crucial intermediate for synthesizing valuable chemicals, including carboxylic acids, via the Wood-Ljungdahl pathway using H_2/CO as energy and carbon sources for CO_2 fixation. Hence, the bioconversion of LCM-derived syngas to biofuels and biochemicals has gained interest in recent years and has been adopted as an attractive route in pilot-, demo-, and near commercial-scale plants. For example, Liakakou et al. (2021) showed that *C. ljungdahlii* could convert syngas from lignin-rich residues (obtained from wheat straw after steam explosion pretreatment and enzymatic hydrolysis) to ethanol (0.02 g/L.h) and acetic acid (0.16 g/L.h) after removing inhibitors such as hydrogen sulfide (H_2S) and carbonyl sulfide (COS). Asimakopoulos et al. (2021) also converted syngas derived from gasified wood pellets to CH_4 using a mixed microbial consortium in a semi-pilot scale trickle bed reactor. The trickle bed reactor, connected in series with the fluidized bed gasifier and operating at 60 °C and pH 7, could convert the H_2 and CO in the 'real syngas' to CH_4 at conversion efficiencies of 100 % and 92.4 ± 0.6 %, respectively. Moreover, some commercial projects led by LanzaTech have demonstrated the feasibility of syngas fermentation to bioethanol, with over 90 % CO conversion efficiency and 95 % ethanol selectivity (Medeiros et al., 2020). **Table 2.3** highlights the results of some selected studies on the bioconversion of LCM-derived syngas into various value-added products.

Table 2.3. Selected studies on bioconversion of LCM-derived syngas to value-added fuels and chemicals.

Lignocellulosic feedstock	Syngas generation process	Bioreactor type and fermentation conditions	Microorganism	Targeted Product	Maximum productivity	Syngas conversion efficiency	Ref.
Lignin-rich feedstock from wheat straw	Gasification	Batch fermentation at 37 °C and pH 5.9 with continuous stirring at 800 rpm	*C. ljungdahlii* DSM 13528	Acetate and ethanol	240 ± 10 mg/L/h	55.9 ± 3.6 mol % total carbon fixation	Liakakou et al. (2021)
Beech wood	Gasification	Batch fermentation at 37 °C and pH 5.9 with continuous stirring at 800 rpm	*C. ljungdahlii* DSM 13528	Acetate and ethanol	270 ± 60 mg/L/h	55.4 ± 2.3 mol % total carbon fixation	Liakakou et al. (2021)
Wood pellets	Gasification	Continuous semi-pilot scale thermophilic trickle bed bioreactor	Mixed microbial consortium	Biomethane	380 ± 13 mL/L/h	100% H_2 and 92.4 ± 0.6% CO conversion	Asimakopoulos et al. (2021)
Forest residues	Co-gasification with charcoal (30%)	Tar-free bioreactor followed by feed-batch system at 37 °C and pH 4.0–6.0, and stirring speed 200 rpm	*Clostridium butyricum*	Bioethanol	1377.2 mg/L of syngas	N/A	Monir et al. (2020a)
Forest residues	Co-gasification with charcoal (30%)	Tar free fermenter in a continuous recycling fed mode at 37 °C and pH 4.0–6.5 with stirring at 200 rpm	*Saccharomyces cerevisiae*	Bioethanol	1405.8 mg/L of syngas	N/A	Monir et al. (2020b)
Empty fruit bunches of palm oil, coconut shell, and forest waste	Gasification	Tar free fermenter	*Clostridium butyricum* and *Saccharomyces cerevisiae*	Bioethanol	654.6 – 704.3 mg/L of syngas	N/A	Monir et al. (2022)

*N/A means not available

Regardless of the widespread acceptance of the biocatalytic syngas conversion process, the current fermentation process remains in the infancy stage and thus, has several challenges that need to be addressed to maximize carbon conversion such as the slow reaction rate and poor gas-to-liquid mass transfer, bacteria biomass washout, the lethal effect of high CO partial pressures on some functional groups (e.g., methanogens), and the inhibitory effect of syngas impurities such as H_2S, COS, tar, etc. (Asimakopoulos et al., 2020; Gunes, 2021; Lü et al., 2018). Some strategies have been proposed to surmount these limitations. For instance, Lü et al. (2018) demonstrated that carbonaceous additives such as biochar could boost methanogens'

resilience to CO and increase CH_4 production by 238 %. Other studies have also focused on bioreactor configurations to enhance mass transfer rates, and the results suggest that biofilm-based reactors such as trickle bed and membrane bioreactors provide higher mass transfer coefficients than bubble column and stirred tank bioreactors (Asimakopoulos et al., 2021). Also, with recent advances in metabolic engineering, syngas fermenters such as *C. ljungdahlii*, *Clostridium autoethanogenum*, *Clostridium carboxidivorans*, and *Acetobacter woodii* have been modified to increase product yield from syngas (Andreides et al., 2021). A hybrid bio-/chemo-catalytic approach incorporating the high specificity and reaction rate of chemical catalysts with the low cost and operational flexibility of microbiomes could also surmount the current limitations of conventional chemical and biological syngas conversion processes. Such hybrid systems could be designed to operate in the native cellular environment of microbiomes, thereby limiting operational costs, and the potential increment in productivity would warrant the cost of chemical catalysts employed.

2.3.5. C_2-C_{10} bioalcohols

The biotransformation of LCM-derived monomers into bioalcohols, the most commercialized biofuels compatible with current fuel infrastructures, continues to attract significant scientific and commercial attention. However, nearly all commercial bioethanol is derived from sugar- and starch-based (i.e., first-generation) feedstocks such as corn, sugarcane, cassava, and wheat, which could lead to an unbridgeable gap between energy supply and food security (Chen et al., 2021b). LCMs are the focal point of recent research on bioethanol production because, unlike first-generation feedstocks, bioethanol production from LCMs does not compete with human food production.

Despite the widespread interest in LCM-derived bioethanol, the process has many constraints that demand scientific attention. For instance, *Saccharomyces cerevisiae* and *Zymomonas mobilis*, both capable of converting D-glucose to ethanol with over 95 % maximum theoretical yield, remain the main chassis for current industrial-scale bioethanol production (Liang et al., 2020). However, wild-type strains of *S. cerevisiae* and *Z. mobilis* cannot innately ferment C_6 and C_5 sugar monomers simultaneously, which leads to waste of pentoses, typically xylose. For example, using bamboo biomass as a feedstock for bioethanol production, Song et al. (2022) observed that a significant fraction of xylose remained unused in the fermentation broth after fermentation with *S. cerevisiae*.

2.3.5.1. Facilitating carbon co-metabolism via co-culture fermentation

To avoid wasting pentoses during bioethanol production, several recent studies have focused on extracting hexoses and pentoses separately from LCMs followed by co-fermentation of the sugars using yeast co-cultures. For instance, Dionísio et al. (2021) proposed a strategy to promote the co-utilization of C_5 and C_6 sugars from sugarcane bagasse by using dilute sulfuric acid pretreatment to selectively solubilize the hemicellulosic fraction and recover xylose and arabinose, which were fermented to bioethanol by *Spathaspora passalidarum* NRRL Y-27907. The C_6-rich hydrolysate obtained from the solid residues was also converted to bioethanol by *S. cerevisiae* CAT-1 via a cell-recycle batch fermentation. The integration of the multiple processes increased bioethanol productivity by 361 %, with 86.11 % of the recovered xylose converted to bioethanol. Similarly Mishra and Ghosh (2020) proposed an acid-based fractional hydrolysis process with H_2SO_4 (1–30 % v/v) to separately extract glucose and xylose from kans grass biomass, which were converted into bioethanol (25.0 g/L) using a co-culture of *Z. mobilis* and *Scheffersomyces shehatae*.

It is noteworthy that the simultaneous co-fermentation of C_5 and C_6 sugars in the same bioreactor using yeast co-cultures could result in poor bioethanol yields possibly due to differences in culture conditions such as aeration requirements, initial sugar loading, and suppressed assimilation of C_5 sugars due to carbon catabolite repression (CCR) (Mishra and Ghosh, 2020). To overcome this, two main strategies have been developed: (i) separate fermentation of C_5 and C_6 in two bioreactors and (ii) two-stage sequential fermentation of C_5 and C_6 sugars in a single bioreactor. The main drawback of the separate bioreactors system is the need for additional monitoring and control during fermentation. Conversely, for the sequential fermentation approach, the presence of residual cells and ethanol from the first stage could affect sugar assimilation in the second stage (Kumar et al., 2022a, 2022b).

2.3.5.2. Genetic engineering of ethanologenic microbes to co-utilize C_5 and C_6 sugars

Besides yeast co-cultures, several other ethanologenic microorganisms, including *Escherichia coli* have also been studied for bioethanol generation from lignocellulosic hydrolysates. For example, Rojas-Chamorro et al. (2020) demonstrated that a monoculture of *E. coli* could generate higher concentrations of bioethanol (38.6 g/L) from the C_5 and C_6 sugars in brewers' spent grain hydrolysate than a co-culture of *Scheffersomyces stipitis* and *S. cerevisiae* (22.2 g/L), even though sugar consumption was more efficient in the co-culture. *E. coli* can grow in high concentrations of ethanol and co-ferment C_5 and C_6 sugars. However, in the presence of

both sugars, CCR can ensue leading to sequential consumption of the sugars and sometimes null utilization of the less preferred sugars, typically C_5 sugars. Therefore, attempts have been made to genetically engineer *E. coli* by demolishing the phosphotransferase system, which is responsible for CCR, or eliminating the fumarate reductase (*frdD*) and D-lactate dehydrogenase (*IdhA*) genes to redirect carbon-flux to ethanol synthesis. For example, Lopez-Hidalgo et al. (2021b) engineered an *E. coli* strain to overproduce ethanol and decrease lactic and succinic acid production by, firstly, deleting the *hycA* (a negative regulator of the formate regulon) in *E. coli* strain W3110 to obtain the WDH strain. Afterward, the *ldhA* and *frdD* genes were deleted in the WDH strain by transduction with bacteriophage P1. The new strain, *E. coli* W3110 (Δ*hycA* Δ*frdD* Δ*ldhA*), could achieve 0.32 ± 0.01 to 0.34 ± 0.06 g/g ethanol from xylose-dominant wheat straw and corn stover hydrolysates. Similar results were also obtained with the engineered strain *E. coli* WDH-LF (Δ*hycA* Δ*frdD* Δ*ldhA*), which could also achieve 0.48 ± 0.01 to 0.56 ± 0.08 g/g ethanol from a xylose-dominant wheat straw hydrolysate, generating more ethanol (+167 %) from glucose than the parenteral strain (Lopez-Hidalgo et al., 2021a).

Moreover, some studies have engineered *E. coli* for potential industrial production of C_3–C_4 bioalcohols, including propanol, isopropanol, and 1-butanol, and C_5–C_6 bioalcohols such as 1-pentanol, 2-methyl-1-butanol,1- hexanol, and 3-methyl-1-pentanol. For instance, Yang et al. (2020b) engineered an *E. coli* strain for isopropanol biosynthesis by combining genes from *C. acetobutylicum* (thlA, adc), *E. coli* (atoDA), and *Clostridium beijerinckii* (adh). The resulting strain, *E. coli* MG1655, could generate about 1.5 g/L of isopropanol. Eiben et al. (2020) also engineered *E. coli* to synthesize isopentanol from glucose by combining the isovaleryl-CoA biosynthesis pathway (LiuC, AibAB, and AibC) from *Myxococcus xanthus* with a butyryl-CoA reductase (AdhE2) from *C. acetobutylicum*. The resulting strain, *E. coli* XX03 (BW25113 Δ*adhE* Δ*ldhA* Δ*frdBC*), could produce 80.50 ± 8.08 mg/L of isopentanol. Furthermore, Kim et al. (2015) engineered *E. coli* JST07 (DE3) to synthesize C_6–C_{10} alcohols, including hexanol, octanol, and decanol, by overexpressing various enzymes responsible for medium-chain length alcohols production.

Despite the promising studies on genetic engineering of ethanologenic microbes for potential industrial production of various bioalcohols from LCMs, for sustainable LCM-based bioalcohol biorefinery, genetically modified strains must also be resilient to potential inhibitory compounds in lignocellulosic hydrolysates, able to quickly assimilate the various C_5–C_6 lignocellulosic sugars without CCR reactions, fast-growing, resilient to harsh environmental conditions, and utilize sugars from various LCMs with minimal or no pretreatment.

2.3.6. Biodiesel

Biodiesel, a mixture of long-chain fatty acid alkyl esters synthesized by a transesterification reaction between alcohol and triacylglycerols (TAG) of oils and fats in the presence of a catalyst, is the second-most abundantly produced biofuel after bioethanol. Biodiesel remains one of the most promising biofuels because, as a drop-in fuel, it can be used as a substitute or blended with different proportions of petroleum-based diesel. Moreover, biodiesel has many favorable characteristics such as renewability, sustainability, nontoxicity, high biodegradability, similar combustion properties to petroleum-based diesel, and low sulfate emission (Liu et al., 2021b). Conventional first-generation biodiesel is generated from edible oils from oleaginous plants such as soybean, rapeseed, coconut, oil palm, etc. However, the high raw material costs, accounting for about 75 % of the total production costs, remain an obstacle to plant oil-based biorefinery (Liu et al., 2021b, 2021a). Beyond this setback lies the ethical dilemma on food security vis-à-vis energy generation. Moreover, the industrialization of second-generation biodiesel that is based on non-edible oils and fats has yet to materialize since it cannot adequately meet the global demand. Hence, recent studies recommend microbial lipid or single-cell oil (SCO) produced by oleaginous microorganisms (OM) as a worthwhile alternative. Although every microbe can synthesize lipids, only those that can accumulate lipid content of up to 20 % of their dry cell weight are called OM (Miao et al., 2020). Several OM, including microalgae, molds, yeasts, and bacteria can accumulate over 20–70 % lipids in the form of TAG inside their cells, which can be converted into biodiesel through the transesterification process (Uthandi et al., 2021). Among the OM, the utilization of yeasts is considered more advantageous over mold and microalgae due to their fast growth rate, high lipid content without endo-toxin, easier industrial level scalability, and a wide range of substrates (Ananthi et al., 2019; Miao et al., 2020). The quantity of SCO that can be recovered from yeast, however, varies based on several factors, including the carbon source, C/N ratio, temperature, pH, etc. Estimates suggest that almost 80 % of the production cost is related to the carbon source used (Ananthi et al., 2019). Therefore, although there are many carbon sources, including glycerol and industrial sugars, LCMs are considered one of the most attractive carbon sources for the growth of OM due to their availability, potentially low cost, and renewability. For example, Slininger et al. (2016) estimated that biodiesel from switchgrass alone could replace over 20 % of United States diesel demand.

2.3.6.1. Enhancing C_5–C_6 sugars co-metabolism in oleaginous microorganisms

The process routes for SCO biosynthesis from LCM typically include pretreatment, hydrolysis of the pretreated biomass to generate fermentable sugars, and fermentation of the sugars to lipids using OM (Zan et al., 2021). Thus, a mixture of C_5–C_6 sugars comprised mainly of xylose and glucose is generated from the LCMs but xylose metabolism is typically repressed in the presence of glucose in most native OM (Valdés et al., 2020). However, as the starting materials for SCO biosynthesis, the co-utilization of LCM-derived sugars is a vital strategy to ensure the economic sustainability of SCO biorefinery. Therefore, several attempts have been made to isolate, screen, and identify novel OM with the genetic apparatus to co-ferment C_5– C_6 sugars. For example, Miao et al. (2020) identified a novel oleaginous yeast *Rhodotorula taiwanensis* strain AM2352 that could co-utilize xylose and glucose in corncob hydrolysate to generate SCO (55.8 g/kg corncob). Slininger et al. (2016) also screened 32 yeast isolates and identified four robust strains including, *Rhodosporidium toruloides* NRRL Y-1091, *Lipomyces tetrasporus* NRRL Y-11562, *Lipomyces kononenkoae* NRRL Y-7042, and *Saitoella coloradoensis* NRRL YB-2330 that can produce high lipid concentrations (>5 g/L) from both ammonia fiber expansion-pretreated corn stover and dilute acid pretreated post-frost switchgrass. Their results showed that *L. tetrasporus* NRRL Y-11562, *L. kononenkoae* NRRL Y-7042, and *R. toruloides* NRRL Y-1091 were able to consume acetic acid and co-utilized glucose, xylose, and arabinose for lipids accumulation, which makes them excellent candidates for SCO production from LCMs.

Alternatively, some studies have proposed selective fractionation approaches to recover xylose and glucose separately for fermentation by OM that can generate high lipid yields from both sugars such as *Lipomyces starkeyi*. For example, Di Fidio et al. (2021) proposed an integrated cascade process for *L. starkeyi* catalyzed SCO generation from two xylose- and glucose-rich giant reed (*Arundo donax* L.) hydrolysates. The xylose-rich hydrolysates were obtained by microwave-assisted hydrolysis of the hemicellulosic fraction of the giant reed biomass with the homogeneous catalyst $FeCl_3$ or the heterogeneous catalyst Amberlyst-70. The cellulose-rich solid residues were then subjected to enzymatic hydrolysis to obtain the glucose-rich hydrolysates. The results show that both cascade processes could generate about 8 g SCO per 100 g of raw biomass.

Additionally, some efforts have been made to engineer transporters and enzymes involved in xylose metabolism and develop recombinant OM. For example, Zan et al. (2021) demonstrated

that overexpressing xylose isomerase gene *xylA* or xylulokinase gene *xks1* in *Mucor circinelloides* during co-fermentation of glucose and xylose could increase xylose consumption by 25–37 % and enhance the lipid content by 8–28 %. Do et al. (2020) also engineered a xylose utilizing *Yarrowia lipolytica* strain YSXID that could produce high SCO (0.16 g/g) from *Miscanthus* hydrolysates containing xylose and glucose

2.3.6.2. Co-utilization of holocellulose and lignin for SCO production

Despite the advances made in the co-utilization of lignocellulosic sugars for SCO generation, a holistic approach that encompasses the utilization of polysaccharides and lignin for SCO biosynthesis could be more profitable to SCO biorefineries. However, studies on production regimes that co-utilized polysaccharides and lignin for SCO production are rare. Besides C_5–C_6 monomeric sugars, lignin and derivatives such as levoglucosan (i.e., 1,6-anhydro-β-D-glucopyranose, LG)–an anhydrous sugar derived from glucans via LCM pyrolysis–have also been demonstrated as viable carbon sources for OM. After depolymerization into various monomeric units, lignin can be funneled into lipids via "upper pathways" such as the β-ketoadipate pathway (Uthandi et al., 2021). For instance, Bhatia et al. (2019) demonstrated that *Rhodococcus* sp. YHY01 could utilize barley straw lignin as a carbon source to produce 0.051 g/L SCO with 39 % w/w SCO accumulation. However, co-fermentation with glucose resulted in reduced utilization of p-coumaric, cresol, and 2,6 dimethoxyphenol due to preferential utilization of glucose over phenolics, which affected lipids accumulation. Thus, further work is required to identify or engineer OM that can co-ferment polysaccharides and aromatics from LCM for SCO biosynthesis.

2.3.7. Bio-oil generation and bioconversion to biofuels

Bio-oil, a dark-brown liquid comprised of oxygenates such as phenols, alcohols, ketones, esters, aldehydes, acids, ethers, sugar derivatives, and furans obtained via thermochemical conversion of LCMs, is gaining attention as a promising biofuel because of its renewability, transportability, CO2 neutrality, relatively high energy density, and good secondary conversion performance (Guo et al., 2022). Bio-oil can be used in boilers, gas turbines, and gravity stoves for heat and power generation (Cai et al., 2021). However, because of its drawbacks, including high water, oxide, and acid content, high viscosity, low pH, and low calorific value compared with fossil oil, bio-oil cannot be utilized directly as a transport fuel (Guo et al., 2022). Several attempts have been made to improve the yield and quality of bio-oil for potential applications as a drop-in fuel. Chemical processes such as catalytic cracking, catalytic hydrogenation,

feedstock co-processing, CO2-assisted in-situ deoxygenation, and emulsification/micro-emulsification have been studied as strategies for upgrading LCM-derived bio-oil. Although significant advances have been made in upgrading the hydrocarbon selectivity and other fuel properties of bio-oil, reported calorific values after bio-oil upgrading (25.6–34.4 MJ/kg) are still lower than that of fossil oil (40 MJ/kg) (Guo et al., 2022; Jin et al., 2022; Xu et al., 2022). Thus, further investigations are required to make bio-oil competitive with fossil oil as a drop-in fuel.

2.3.7.1. Bioconversion of bio-oil as an alternative valorization route

Considering that bio-oil stems from the depolymerization and disintegration of cellulose, hemicellulose, and lignin, it contains numerous bioavailable carbon sources (e.g., C_2-C_6 sugars, hydroxy acids, oligomers, etc.) that can be converted into high-value products using microorganisms. Even though bio-oil consists of a wide variety of functional groups, it could be fractionated into two main stage fractions known as the bio-oil aqueous phase (BOAP) and a heavy water-insoluble phase, formed by pyrolytic lignin (Pollard et al., 2012). Thus, research interest in the bioconversion of various fractions of bio-oil, especially the BOAP, has grown over the years as an alternate valorization route. For example, Zhou et al. (2019) converted the BOAP of fast pyrolyzed corn stover to biogas (165 mL/L.d) using a *Methanosaeta* (58.1 %) and *Methanolinea* (25.3 %) dominant microbiome. Chang et al. (2021) also showed that LG, the most prevalent sugar in the BOAP, could be converted to bioethanol (0.43 g/g) using *E. coli*.

One of the main hurdles in the microbial valorization of LCM-derived bio-oil is the presence of inhibitors such as furans, phenols, and ketones that impede microbial growth. Therefore, to establish bio-oil as a platform for industrial biotechnology, a cluster of downstream detoxification strategies, including over-liming, oxidation, solvent extraction, and adsorption of inhibitors on absorbents such as activated carbon, has been proposed (Arnold et al., 2019; Zhou et al., 2019). However, the potential cost implications of these processes remain a concern. An alternate strategy is to develop robust microbial strains that could grow well and tolerate toxic compounds in bio-oil substrates. To this end, some effort has been made in recent years to isolate and/or engineer novel microbial strains that could tolerate inhibitors and convert bio-oil into value-added products. For example, Basaglia et al. (2021) examined 204 fungal and bacterial strains with potential industrial applications to identify the strains that could convert the BOAP of pyrolyzed fir wood pellet to value-added products while tolerating or

detoxifying inhibitory compounds in the BOAP. Their results showed that three fungal strains (i.e., *Ganoderma appianatum*, *Pleurotus ostreatus*, and *Trametes versicolor*) could metabolize the pure BOAP, although the possible involvement of these strains in the synthesis of value-added products is yet to be unveiled. The other bacterial and fungal isolates in the study required several dilutions of the BOAP to preserve cell visibility with S. cerevisiae strain L13, tolerating up to 1:5 (v/v) dilution and producing up to 8 g/L bioethanol and, thus, considered a promising candidate for future metabolic engineering and adaptive evolution strategies to enhance its resilience and productivity.

It must be stated that, although several eukaryotes (fungi and yeast) and bacterial species can metabolize the LG fraction of BOAP via the respective enzymes, LG kinase and LG dehydrogenase (**Fig. 2.3**), typical product-forming microbes such as *E. coli*, *Z. mobilis*, and *S. cerevisiae* cannot innately metabolize LG and require LG to be hydrolyzed into glucose via acid hydrolysis before assimilation. This indirect conversion route adds to the system's complexity and costs. Hence, some studies have attempted to engineer or isolate novel bacteria strains that can grow directly on LG as the carbon source for biotechnological applications. For instance, Chang et al. (2021) engineered new *E. coli* strains to directly utilize LG for bioethanol production by introducing levoglucosan kinase, pyruvate decarboxylase, and alcohol dehydrogenase genes into *E. coli*. The new strain *E. coli* LGE2 could reach about 78 % of the theoretical yield, although co-fermentation with other carbon sources did not benefit LG conversion. Arya et al. (2022) also isolated four bacteria species, *Paenibacillus athensensis* MEC069T, *Microbacterium* MEC084, *Shinella sumterensis* MEC087T, and *Klebsiella pneumoniae* subsp. *pneumoniae* MEC097, with the ability to degrade LG.

Despite these promising results, to establish bio-oil as a platform for industrial biotechnology, substantial research is still required in engineering or screening novel microorganisms that could grow directly on bio-oil carbon sources. Also, future studies should examine strategies for reducing the formation of bio-toxic compounds during pyrolysis and cost-effective downstream methods for removing these inhibitors from bio-oil.

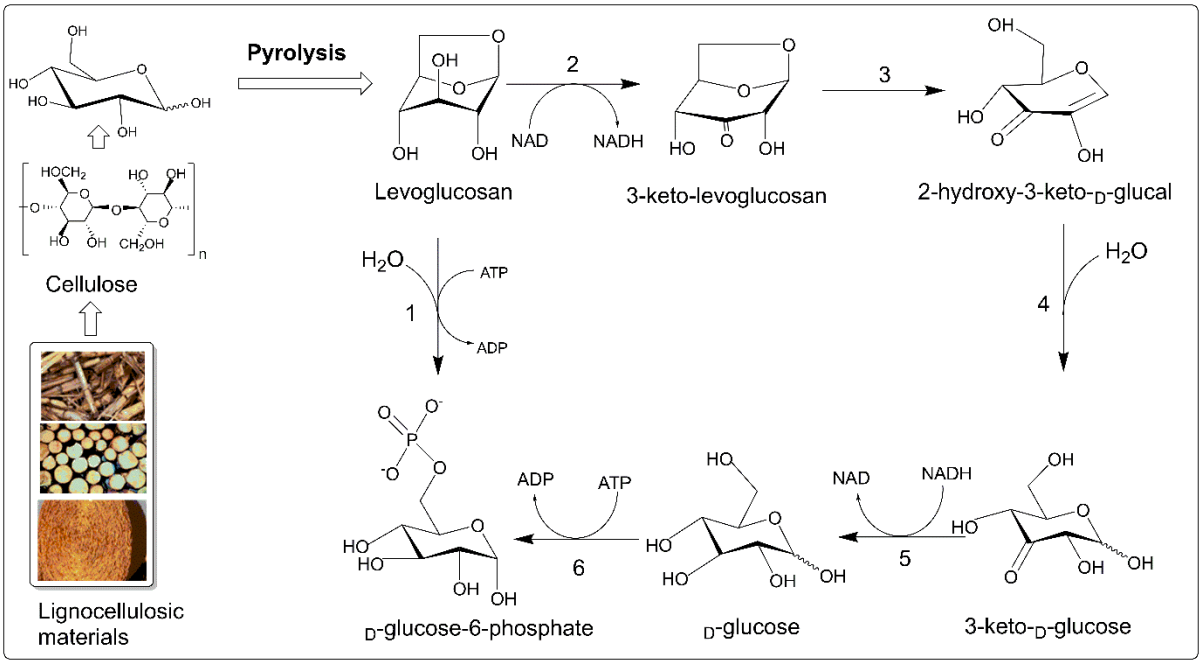

Fig. 2.3. Systemic pathways for levoglucosan production from lignocellulosic materials and subsequent metabolism by fungi and yeast via levoglucosan kinase (1) and proposed route for bacteria (*Bacillus smithii*) via levoglucosan dehydrogenase leading to the formation of intracellular D-glucose (2–5). Enzymes 1–6: levoglucosan kinase, levoglucosan dehydrogenase, β-eliminase, hydratase, reductase, and glucokinase, respectively. Metabolic routes are drawn as proposed by Arya et al. (2022).

2.3.8. Carboxylic acids

2.3.8.1. Short-chain carboxylic acids

Short-chain carboxylic acids (SCCAs) with two to five carbon atoms, including acetic, lactic, propionic, butyric, isobutyric, 2-methylbutyric, and valeric acids, are essential platform molecules currently derived from petrochemical sources. However, they have been suggested as potential bio-derived chemicals (Shahab et al., 2020). Acidogenic fermentation, a versatile biotechnology for generating SCCAs from lignocellulosic hydrolysates or LCM-derived syngas, is rapidly gaining attention as a promising valorization route for lignocellulosic biorefineries because SCCAs have acquired industrial value with widespread applications in pharmaceuticals, cosmetics, bioplastics, biofuels, food and agriculture, etc.

Several recent studies on acidogenic fermentation of lignocellulosic hydrolysates, including da Fonseca et al. (2021), Islam et al. (2021), Cubero-Cardoso et al. (2022), etc. have reported on the influence of various performance-enhancing strategies such as substrate pretreatment,

alkaline fermentation, high solid-state fermentation, substrate co-digestion, high OLR but short HRT, abiotic materials supplementation, bioaugmentation, etc. Moreover, some recent reviews such as Kumar et al. (2022a) have summarized the influence of operational parameters such as pH, temperature, OLR, substrate composition, additives, etc. on the performance of acidogenic bacteria such as *Firmicutes*, *Proteobacteria*, *Bacteroidetes*, and *Chloroflexi*. Yet, bio-SCCAs production from LCMs as a suitable alternative to existing petrochemical SCCA still faces several challenges. Firstly, the compositional heterogeneity of lignocellulosic sugars and the limited metabolic flexibility of many SCCAs fermenters result in low SCCAs concentrations (1–100 g/L) and undesirable by-products formation. To overcome this challenge, Shahab et al. (2020) proposed a method to metabolically funnel the complex mixture of lignocellulosic sugars into a central and versatile intermediate via a heterogeneous bioreactor system with spatial niches for cross-kingdom microbial consortia to prevail in an otherwise homogenous reactor environment. Using this heterogeneous bioreactor approach–with beechwood as the substrate and lactic acid as the central intermediate–Shahab et al. (2020) achieved about 196 kg of butyric acid per metric ton of beechwood.

2.3.8.2. Upgrading short-chain carboxylic acids into medium-chain carboxylic acids

Besides carbon co-utilization, another bottleneck in the LCMs–to–SCCAs pathway is the difficulty in separating and concentrating the individual acids from the fermentation broth. To circumvent this challenge, upgrading SCCAs to medium-chain carboxylic acids (MCCAs) containing 6 to 12 carbon atoms have emerged more recently as an attractive route. The growing interest in MCCAs is based on their versatility as platform chemicals, higher energy densities, and lower water solubilities when compared with SCCAs. For example, the energy content and market value of caproic acid are much higher than those of acetic, lactic, or butyric acid (**Table 2.4**). Also, SCCAs (excluding valeric acid with a solubility of 49.7 g/L) are completely miscible with water, but the solubilities of undissociated caproic and caprylic acids are 10.82 and 0.68 g/L, respectively. These relatively low solubilities allow for MCCAs to be harvested easily via phase separation. For instance, to bypass the lactic acid recovery process, Kleinsteuber and Dittrich-Zechendorf (2018) converted lactic acid from maize silage to MCCAs since these require less cost-intensive downstream processing and could generate extra income for biorefineries. Khor et al. (2017) also upgraded lactic acid produced from grass to caproic acid with a fermenting microbiome consisting mainly of *Clostridium IV* and *Lactobacillus*.

Table 2.4. Characteristics of some selected carboxylic acids and biofuels.

Metabolite	Molecular formula	Structure	Solubility in water (g/L) [a]	Energy content (kJ/mol)	Market value (US $/ton) [b]
Hydrogen	H_2	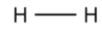	-	285.8	800–1800
Methane	CH_4		-	890.8	100–200
Ethanol	C_2H_5OH	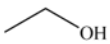	Miscible	1336.8	500–1000
Acetic acid	$C_2H_4O_2$		Miscible	876.1	400–800
Lactic acid	$C_3H_6O_3$	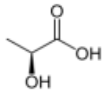	Miscible	1343.9	1000–2100
Butyric acid	$C_4H_8O_2$	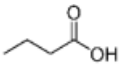	Miscible	2183.5	2000–2500
Caproic acid	$C_6H_{12}O_2$	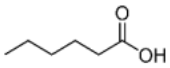	10.82	3492.2	2000–2500
Caprylic acid	$C_8H_{16}O_2$	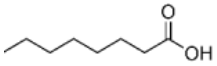	0.68	4799.9	3500–3900

[a] Adapted from Xu et al. (2018); [b] Adapted from K. Dai et al. (2020).

A specialized group of anaerobes, including *Clostridium* spp. (i.e*., C. kluyveri*, *C.* spp. *IV*, *C.* sp. *BS-1*, *C. sensu stricto*, and *C. carboxidivorans*), *Megasphaera* spp. (i.e., *M. hexanoica*, *M. elsdeni*, and *M.* sp. *MH*), *Eubacterium* spp. (i.e., *E. pyruvativorans*, and *E. limosum*), *Ruminococcaceae* CPB6, and *Rhodospirillum rubrum* are known to catalyze MCCAs biosynthesis via carbon-chain elongation. These bacteria gain energy by combining the oxidation of a reduced substrate such as ethanol or lactic acid to acetyl-CoA with the reductive elongation of acetyl-CoA with an SCCAs via the cyclic reverse β-oxidation (RBO) or fatty acid biosynthesis (FAB) pathways (**Fig. 2.4**). The RBO metabolic pathway is the model route for MCCAs biosynthesis and has been elucidated in the literature (Wu et al., 2020; Wang and Yin, 2022). However, recent studies indicate that a portion of the transformed acetyl-CoA does not enter the RBO pathway but converts to malonyl acyl carrier protein (malonyl-ACP), which goes into the FAB pathway for carbon chain extension with SCCA (Han et al., 2018; Wu et al., 2020, 2021b). Because the FAB pathway has more steps (due to acetyl-CoA conversion to malonyl-ACP; **Fig. 2.4**) and requires more energy (more ATP is committed to malonyl-ACP and ACP intermediates synthesis), the FAB pathway is often considered less efficient (Han et

al., 2018; Wang and Yin, 2022). However, some recent metagenomic studies suggest that FAB could be more active than RBO due to a higher relative abundance of enzymes involved in the FAB than the RBO pathway (Wu et al., 2020). Moreover, some chain elongation bacteria belonging to the genus *Clostridium* have all the functional enzymes for RBO and FAB (Wu et al., 2021b), suggesting that both pathways could simultaneously occur. Although currently, limited information exists on the degree of dominance of a specific metabolic pathway during chain elongation.

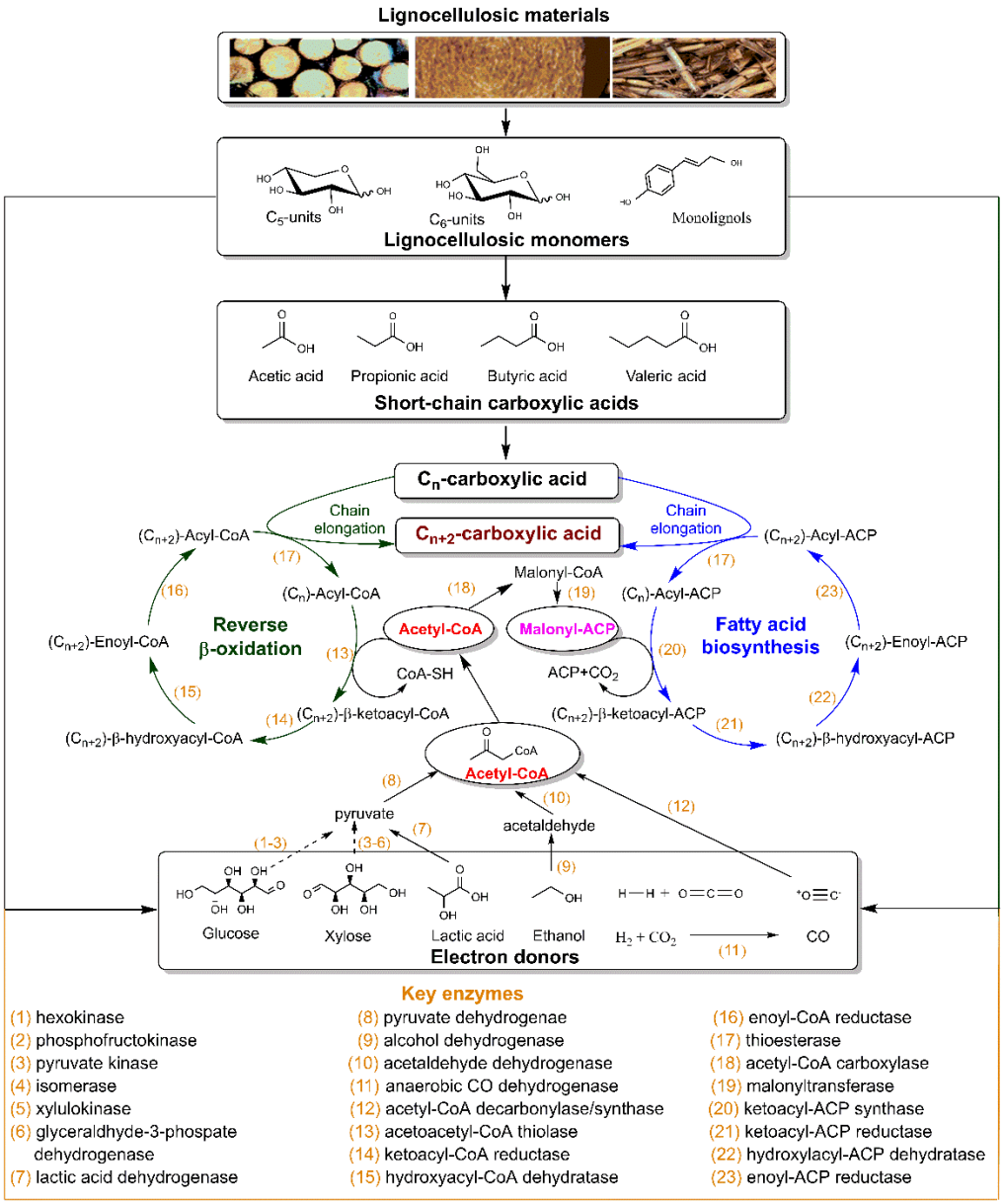

Fig. 2.4. Systematic pathways for medium-chain carboxylic acid production from lignocellulosic materials. Lignin conversion into electron acceptors (e.g., acetic, propionic, butyric acid) and electron donors (e.g., ethanol, CO, and H_2) could be achieved via

intermediates such as syngas. The reverse β-oxidation (in green) and fatty acid biosynthesis (in blue) metabolic pathways are adapted from Han et al. (2018), Wu et al. (2020), and Wang and Yin (2022).

From an economic and environmental sustainability viewpoint, LCMs are attractive substrates for MCCAs biosynthesis because LCMs are rich sources of both electron acceptors (EA) and electron donors, which produce the vital intermediate acetyl-CoA (**Fig. 2.4**). However, only a handful of studies have reported on MCCAs biosynthesis from LCMs (Yang et al., 2018; Yu et al., 2019), with the vast majority focusing on other organic residues such as waste activated sludge (Wu et al., 2021a, 2021b). The low utilization of LCMs for MCCAs production is probably due to the prerequisite pretreatment step for enhancing LCM biodegradability, which adds to the complexity of the system and the cost-benefit-sustainability nexus. Mild pretreatment could limit operation costs but sacrifice LCMs conversion efficiency and MCCAs selectivity (Khor et al., 2017). On the contrary, severe pretreatment may enhance biodegradability but negatively impact costs and release inhibitory compounds such as phenol and furfural, which may exacerbate the conversion efficiency.

2.3.8.3. Enhancing MCCA selectivity

The production process of MCCAs is sensitive to the growth of chain elongation bacteria. Therefore, a careful selection of operational parameters such as temperature and pH while minimizing the toxicity of both substrates and products could maximize the carbon conversion efficiency and increase MCCAs selectivity during LCMs conversion to MCCAs. The ideal temperature for chain elongation bacteria such as *C. kluyveri*, *M. elsdeni*, and *E. pyruvativorans* is about 39 °C (Reddy et al., 2018). However, optimal MCCA production was attained in open cultures at lower temperatures (30–37 °C) (Scarborough et al., 2018; Xu et al., 2018), possibly due to the enhanced mobility of cell membranes caused by the solvent characteristics of MCCAs. Also, the reported optimal pH range for the chain elongation bacteria is 5.5–7.4 (Reddy et al., 2018). When operating at a neutral pH, specific inhibition of other functional groups such as methanogens that may degrade the substrates and limit MCCAs selectivity is required. In contrast, a slightly acidic pH (e.g., 5.5) will inhibit methanogens and eliminate competition for the chain elongation bacteria. However, at a lower pH (i.e., closer to the pKa of MCCAs, 4.88 for caproic acid), the undissociated MCCAs constitute a vast component of the MCCAs pool (Candry et al., 2020). Thus, the toxicity of undissociated MCCAs can hinder the growth of functional bacteria, restricting products to moderate and low concentrations. Ge

et al. (2015) discovered in a long-term continuous bioreactor for converting dilute, undistilled corn-kernel ethanol to MCCA at pH 5.5 that the threshold concentration at which undissociated caproic acid exhibited toxicity was around 872 mg/L. Selective in situ extraction with solvent-based extraction techniques, for example, is vital in such situations to alleviate product toxicity.

Besides product toxicity, substrate toxicity is also a crucial operational factor to consider during MCCAs production. Ethanol is the most widely used electron donor for high-rate chain elongation. However, high concentrations of ethanol (>9.2 g/L) can inhibit microbiomes and MCCAs synthesis (Wu et al., 2018). Influent dilution with water or effluent recirculation could lessen substrate toxicity, yet these strategies sacrifice MCCAs selectivity (Liu et al., 2017). Currently, practical solutions to alleviating substrate toxicity include cell immobilization techniques to increase cell resilience (Zhang et al., 2021c).

An alternative strategy to potentially enhance the carbon conversion efficiency is a lignocellulosic biorefinery aimed at the co-production of MCCAs with other bio-based products. For instance, Scarborough et al. (2018) demonstrated that the production of caproic and caprylic acids from switchgrass stillage after ethanol distillation could improve the economic sustainability of biorefinery. The stillage, containing about 60 % of the COD of the fermented hydrolysate after ethanol distillation, was rich in glycerol, xylose, and acetic acid, which served as reactants for MCCAs synthesis. Sarkar et al. (2021) also demonstrated the feasibility of co-producing MCCAs and H_2 by open culture fermentation of brewery spent grains. However, it is noteworthy that a sufficiently high H_2 partial pressure in the headspace is crucial in the ethanol-guided chain elongation process to limit excessive ethanol oxidation, a competing biochemical process that impedes ethanol use for MCCAs production (Roghair et al., 2018a, 2018b). It is also worth mentioning that the effluent from chain elongation reactors often contains substantial amounts of SCCAs such as butyric acid (Liu et al., 2020). However, to our knowledge, no study has assessed the feasibility of extracting SCCA from MCCAs effluent or further converting MCCAs effluent into biofuels (e.g., butanol). Extraction of biofuels and biochemicals from MCCAs effluent could maximize resource recovery and shift MCCAs production towards a circular economy.

Overall, the studies discussed suggest that the bioconversion of LCM-derived SCCAs and electron donors to MCCAs presents an attractive route to circumvent cost-intensive SCCAs separation processes. However, further research is needed to maximize product selectivity and minimize carbon losses to competing bioprocesses.

2.3.9. Bioplastics

The ever-increasing demand, coupled with the negative environmental impacts of petrochemical-based (micro)plastics, has spurred scientific interest in bioplastics as alternatives. In particular, microbial funneling of LCM-derived compounds into polyesters of hydroxy alkanoic acids (alias polyhydroxyalkanoates; PHA) is not only deemed a sustainable approach to generate biodegradable plastics but also an important source of hydrocarbons for the production of fuels, chemicals, and materials after depolymerization and deoxygenation (Xu et al., 2021a). Numerous prokaryotes, including Pseudomonas putida, *Cupriavidus necator*, *Halogeometricum borinquense*, and *Bacillus megaterium* can accumulate PHA as cytoplasmic carbon and energy storage molecules in response to stressors such as osmotic pressure fluctuations, oxidative pressure, UV irradiation, high or low temperatures, etc. (Obruča et al., 2022; Xu et al., 2021a). Per the current knowledge, over 155 different PHA can be synthesized by prokaryotes, and these are classified as short-chain-length (scl), medium-chain-length (mcl), and long-chain-length (lcl) PHA, based on the number of carbon atoms per monomer (Raj et al., 2022). Scl-PHA such as poly (3- hydroxybutyrate) and poly (3-hydroxy valerate) contain 3–5C atoms and are the most abundantly produced PHA in prokaryotes. They are synthesized predominately by bacteria such as *C. necator* and *Aeromonas caviae* and exhibit thermoplastic properties but are often rigid, fragile, and crystalline (Taguchi and Matsumoto, 2021). In contrast, mcl-PHA consisting of 6–14C atoms, are synthesized by *Pseudomonas* spp. and are elastomers with low crystallinity, tensile strength, melting, and glass temperatures (Obruča et al., 2022). Lcl-PHA can also be synthesized by bacteria such as *Pseudomonas aeruginosa* and include polymers such as poly (3- hydroxypentadecanoate) that contain >14C atoms (Raj et al., 2022)

Currently, LCMs are one of the focal carbon sources for microbial PHA production. However, one of the principal drawbacks to the widespread commercialization of LCM-derived PHA is the high production costs, including the cost of commercial enzymes, since most wild-type PHA producers lack hydrolytic enzymes. Therefore, some recent studies have explored the low-cost hydrolysis process of AD as an option to circumvent the cost of commercial enzymes by converting LCMs into VFAs to be used as carbon sources for PHA producers. For instance, Brojanigo et al. (2022a) employed *C. necator* DSM 545 to convert the acidogenic effluent from rice milling residue into PHA (0.95 ± 0.02 g/L), alongside CH4 (493.27 ± 18.34 mL/g VS) from the solid fraction after acidification. Yet, considering PHA synthesis from a CBP perspective, Brojanigo et al. (2022b) engineered a recombinant amylolytic *C. necator* DSM

545 strain to generate PHA from rice residue (5.78 g/L) and purple sweet potato waste (3.65 g/L) by co-expressing the glucodextranase *G1d* from *Arthrobacter globiformis* I42 and the α-amylase *amyZ* gene from *Zunongwangia profunda* SM-A87 into *C. necator* DSM 545. The new strain, *C. necator* DSM 545 *#11*, exhibited an efficient hydrolytic activity (110.83 nkat/mL without antibiotics), demonstrating a way for one-step PHA biosynthesis from LCMs.

As observed for other LCM-based products, also for the synthesis of PHA from LCMs it should be emphasized that manipulating production setups or PHA producers to metabolically funnel all the complex heterogeneous carbon sources in LCMs into PHA could be crucial for the commercial sustainability of LCM-based PHA biorefinery because carbon co-metabolism could reduce carbon costs. However, most of the current literature on PHA production from LCMs has focused on utilizing either the monomeric sugars from starchy residues (Brojanigo et al., 2022b; Souza et al., 2022; Yan et al., 2021) or lignin as the sole carbon substrate (Morya et al., 2021; Xu et al., 2021a).

Studies on production regimes that co-utilize lignin and monomeric sugars for PHA biosynthesis are rare, plausibly due to the inability of most wild-type prokaryotes to innately co-utilize pentoses, hexoses, and lignin as carbon sources for PHA synthesis. For instance, *P. putida* is a widely known versatile mcl-PHA producer that can utilize different LCM-derived organics via various metabolic pathways, including the Embden–Meyerhof–Parnas, Entner–Doudoroff, and tricarboxylic acid cycle pathways (Xu et al., 2021b). Yet, *P. putida* KT2440 cannot innately metabolize pentoses. To bypass this limitation, Arreola-Vargas et al. (2021) employed the engineered strain C1J4 with overexpressed *phaC1* and *phaJ4* genes to co-ferment lignin and the sugar-rich hydrolysate from corn stover. Their results indicate that when combined at the appropriate ratio, holocellulose and lignin could synergize to maximize mcl-PHA production. Thus, future studies should consider such whole biomass conversion approaches, incorporating elements such as sustainability (life cycle assessment, LCA and energy-based methods) and economic assessments to comprehensively ascertain the beneficial effects of carbon co-metabolism on PHA biorefinery.

2.3.10. Microbial proteins

To safeguard the food supply of the growing human population and satisfy people's dietary lifestyle changes while minimizing the contribution of food production to anthropogenic climate change necessitate a shift from the linear economy-based agriculture that has an enormous environmental footprint to resource-efficient circular economy practices. One such

emerging biotechnology that has the potential to secure future high-quality protein supply is the so-called cellular agriculture (CA), in which microorganisms, grown over various carbon-based substrates, are used as alternatives for the traditional animal- and plant-sourced proteins (Peteghem et al., 2022; Voutilainen et al., 2021). Compared to traditional agriculture, CA is not limited by land size, water supply, and seasonality. Although CA is a relatively new term coined in 2015 (Nyyssölä et al., 2022), the concept of generating agricultural commodities from microorganisms has a long history in modern biotechnology. Commercially successful processes for microbial protein, including the Pekilo, Pruteen, and Quorn™ processes date back to the 70–80s (Nyyssölä et al., 2022; Voutilainen et al., 2021). The renewed commercial and scientific interest in CA, particularly food-grade microbial protein, is underpinned by the widespread desire for sustainable food production processes and a carbon-neutral economy.

Depending on the targeted product, microbial protein could be termed as single-cell protein (SCP) when proteins are derived from the entire cellular biomass or acellular protein when products secreted typically by genetically engineered microorganisms, such as drop-in substitutes for milk and eggs, are separated from the cellular biomass (Voutilainen et al., 2021). Various microorganisms, including bacteria (e.g., *Methylophilus methylotrophus*), fungi (e.g., *Fusarium venenatum*), yeasts (e.g., *Candida utilis*), and microalgae (e.g., *Chlorella vulgaris*) can produce SCP. Depending on the organism, the protein content could reach up to 80 % (dry weight basis) with higher fiber content and a favorable fatty acid profile compared to animal-sourced protein (Matassa et al., 2020; Upcraft et al., 2021). Over the years, a wide array of substrates, including fossil-based hydrocarbons (e.g., methanol and methane), food processing side streams (e.g., brewery spent grain and whey), and industrial sugars (e.g., glucose and fructose) have been used as energy and carbon source for SCP production (Moscariello et al., 2021; Peteghem et al., 2022). However, owing to their copious merits, LCMs are currently one of the favored substrates for SCP production. Several LCM, including industrial hemp (Moscariello et al., 2021), paper mulberry (Gu et al., 2022), rice straw (Upcraft et al., 2021), wheat straw (Voutilainen et al., 2021), and grass silage fiber (Pihlajaniemi et al., 2020) have been studied as substrates for SCP production in recent years. However, one of the main hurdles to producing food-grade SCP from LCM is the low yield of fermentable sugars using food-grade pretreatments, which impacts the economic viability of the process. For example, Upcraft et al. (2021) reported an overall glucose yield of 42.4 % with food-grade ionic liquid and cellulase enzyme compared to a 92.8 % yield with non-food certified ionic liquid. Economic assessment of their final SCP product showed a consumer price of approximately $21.80/kg

($173.02 per kg-protein), which is about five times the cost of chicken ($4.13/kg or 19.52 per kg-protein).

2.3.10.1. Enhancing carbon utilization during single-cell protein production

One potential strategy to bypass the challenge pose by the carbon costs and make lignocellulosic SCP production economically competitive with animal-sourced proteins is to co-produce fermentable sugars for SCP production alongside other valuable biochemicals from LCMs. For example, Gu et al. (2022) showed that autohydrolysis of paper mulberry could yield xylooligosaccharides (0.078 g/g raw materials), amino acids (0.018 g/g raw materials), and fermentable monosaccharides (0.201 g/g raw materials) that could be used to produce SCP (0.048 g/g raw materials). Their results showed that 9 out of the 17 amino acids observed were essential amino acids, including lysine, methionine, threonine, valine, etc., that could be recovered as animal feed.

Alternatively, depolymerizing and hydrolyzing the hemicellulosic fraction into fermentable sugars to be used as a co-carbon substrate alongside cellulosic hydrolysates could also be promising for SCP production. Magalhães et al. (2018) showed that a wild-type strain of *Candida tropicalis* (KP276650) could utilize the hemicellulosic hydrolysate of sugarcane bagasse as a carbon source for SCP production (0.17 g/g) with 60.05 % protein content. Drzymała et al. (2020) also indicated that a wild-type strain of *Y. lipolytica* (A101) could assimilate rye straw, rye bran, and oat bran hydrolysates comprised of pentoses and hexoses for SCP production (0.119, 0.104, 0.141 g/g, respectively, with 30.5–44.5 % protein content), although arabinose catabolism occurred only after glucose was completely consumed. Even though wild-type strains of *Y. lipolytica* have the enzymatic apparatus to metabolize pentoses, this pathway is often repressed due to CCR. Nonetheless, overexpressing pentose assimilation genes in native producers could favor pentose metabolism without the need for heterologous enzymes (Farias et al., 2022).

Furthermore, coupling thermochemical processes such as pyrolysis and gasification with CA by converting LCMs into energy- and resource-rich gaseous streams (e.g., CH_4, H_2, CO, CO_2, N_2, and NH_3) that are free of potential deleterious substances, including pathogens and metal, to be used as substrates for SCP producers could win consumer confidence while avoiding the need for food-grade pretreatments (Matassa et al., 2020; Moscariello et al., 2021). Such an

approach could ensure the complete valorization of the lignocellulosic matrix rather than selective utilization of cellulosic monomers for SCP production. Moreover, the bio-oil and biochar from pyrolysis, for example, could be recovered as valuable co-products, which would benefit the profitability of SCP biorefinery.

2.4. Techno-economic perspective of LCMs valorization

Even though technological advancements have been attained in LCM-based biorefinery processes using innovative valorization techniques, the successful implementation of these strategies depends on their commercial viability. The LCM-based biorefinery presents clear values in terms of environmental benefits and sustainability. Yet, it has demonstrated limited commercial success due to process complexities, inefficient pretreatment and saccharification processes, irregularities in the biomass supply chain as well as high capital and operating costs leading to scale-up challenges (Usmani et al., 2021). Techno-economic analysis (TEA) and LCA as performance indicators of industrial processes have been conducted over the years to assess the commercial feasibility of LCM-based biorefinery processes and guide research towards commercialization. Many recent TEA and LCA studies concur that, barring external incentives, the efficient utilization of all major LCMs components, including lignin valorization to a value-added co-product via integrated biorefinery processes, is vital for the commercial viability of LCM-based biorefineries. For example, for a biorefinery producing sugar from *Miscanthus* as a platform for various bio-based products, including bioethanol, hydrocarbons, and other valuable products, Ou et al. (2021) observed that the minimum selling price (MSP) of sugar to achieve a zero net present value (NPV) decreased from $446/metric ton to $342/metric ton when all three LCMs components were utilized, with the hemicellulose and lignin fractions converted into xylitol and polyol, respectively.

It must be stated that, although many factors influence the outcome of TEA, the feedstock cost remains one of the most fundamental drivers of profitability. Typically, feedstock costs are estimated at $22–85/t (Gunasekaran and Kumar, 2021), although costs exceeding this range (e.g., $163/t (Liao et al., 2020)) could be found in the literature depending on the type of LCM, accessibility, labor, fertilizer costs, and other local drivers such as inflation. Furthermore, the feedstock type determines the pretreatment technique to adopt, which is another vital determinant of profitability. For example, for herbaceous feedstocks such as sweet sorghum stalk, Dehghanzad et al. (2020) showed that enzymatic hydrolysis and fermentation of the untreated stalk after size reduction was the most economical scenario for biobutanol production

with a production cost of $0.39/L and 5.5 years investment payback time for a plant capacity of 100 kt/y dry sweet sorghum stalk. Nonetheless, the authors observed a compromise in the product yield, highlighting the need for further studies to maximize carbon conversion, product yield, and the profitability of the process. Some commonly used pretreatments for herbaceous feedstocks such as dilute acid, alkaline, steam explosion, liquid hot water, and ammonia fiber explosion are reported to cost about $0.07, 0.15, 0.05, 0.06, and 0.07 per liter of ethanol, respectively (Aui et al., 2021).

Besides feedstock and pretreatment, the downstream fermentation and product recovery processes are also key drivers of profitability. These processes impact the number and size of equipment, energy, chemical, and water consumption, enzyme costs, etc. Depending on the feedstock type and pretreatment used, capital costs linked with fermentation in bioethanol production could vary from M$187–501, equivalent to $0.55–2.36 per liter of ethanol. Also, commercially purchased enzymes could cost about $0.13 per liter of ethanol, while on-site generated enzymes cost less ($0.09/L ethanol). Recovering and reusing yeast could, however, lower fermentation-related costs (Aui et al., 2021).

2.5. Challenges and outlook

The development of feasible and economically sustainable biorefineries is the crux of the biofuel industry. Realizing this goal is fundamental for a world looking forward to an era beyond the fossil-based economy and its associated environmental impacts. LCMs have the potential to supply the carbon needed to meet the global demand for energy and other carbon-based chemicals currently derived from fossil-based feedstocks via sustainable conversion processes. However, the sustainability and economic competitiveness of the LCM-based biorefinery demand the efficient utilization of all major LCMs fractions for generating fuels and carbon-base chemicals. In this context, several attempts have been made in the past to enhance the conversion efficiency of LCMs carbon resources to fuels and chemicals. Yet, the complex structure and compositional heterogeneity of LCMs monomers remain a key hurdle to the efficient valorization of LCMs carbon. In recent years, various pretreatment approaches have been explored to maximize the bioavailability of LCM monomers to product-forming microorganisms and derive value from lignin. There is still the need to explore cost-effective methods that allow for the complete valorization of both polysaccharides and lignin in downstream processes.

Regarding efforts to ensure carbon co-metabolism, substantial progress has been made to facilitate the co-utilization of pentoses and hexoses by identifying novel microbes that can co-utilize pentoses and hexoses, employing co-cultures with different metabolic preferences, or engineered strains to avert CCR and the synthesis of undesired products. Nonetheless, more work is required in incorporating the lignin stream to ensure carbon-efficient utilization of LCMs and reduce carbon costs. For biotechnological applications such as the bioethanol industry that focus on LCMs pretreatment to generate fermentable sugars, utilizing the lignin stream for further production via fermentable intermediates such as syngas presents an opportunity to maximize profitability and minimize carbon losses. However, there is still the need to identify novel microbial strains that can resist inhibitory compounds in syngas and bioreactor setups that can overcome the gas-to-liquid mass transfer limitation during syngas fermentation.

Although significant progress has been made in recent years on performance-enhancing strategies, including substrate pretreatment, substrate co-digestion, operational parameters manipulation, abiotic materials supplementation, bioaugmentation, and carbon-flux redirection to maximize the yield and selectivity of value-added products, a considerable fraction of the carbon stream in LCMs is still channeled to by-products synthesis. Therefore, one potential strategy to overcome this challenge is an LCMs biorefinery aimed at multifaceted products via appropriately laidout conversion schemes (**Fig. 2.5**). For example, LCMs biorefineries that convert cellulosic hydrolysates into products such as bioethanol could couple bioethanol production with H_2 generation (Lopez-Hidalgo et al., 2021a, 2021b). The hemicellulosic fraction could be converted into sugar alcohols such as xylitol, arabitol, and galactitol, and the lignin fraction converted into platform chemicals such as syngas and bio-oil via pyrolysis or depolymerized into aromatics such as benzene, toluene, and xylenes. Adopting well-organized integrated biorefinery concepts could maximize carbon recovery, reduce carbon costs, and increase profitability. Moreover, closing the loop in such systems via digestate utilization is a pathway to a circular economy.

2.6. Conclusions

Photosynthetic carbon captured in LCMs can be converted into fuels, chemicals, and functional materials, providing an avenue to alleviate the hegemony of the fossil-based economy. However, the economic feasibility and sustainability of LCMs biorefinery necessitate the unabridged valorization of LCMs in an atom-efficient manner. Despite the progress made in

the biotechnological valorization of LCMs to various products, further research is needed to ensure the utilization of otherwise unused LCMs fractions via innovative bioreactor setups, screening and isolation of novel microbial strains, and genetic engineering of known product-forming microorganisms to enhance productivity. We recommend integrated biorefinery as a viable pathway to maximize profitability, ensure sustainability, and promote a circular economy.

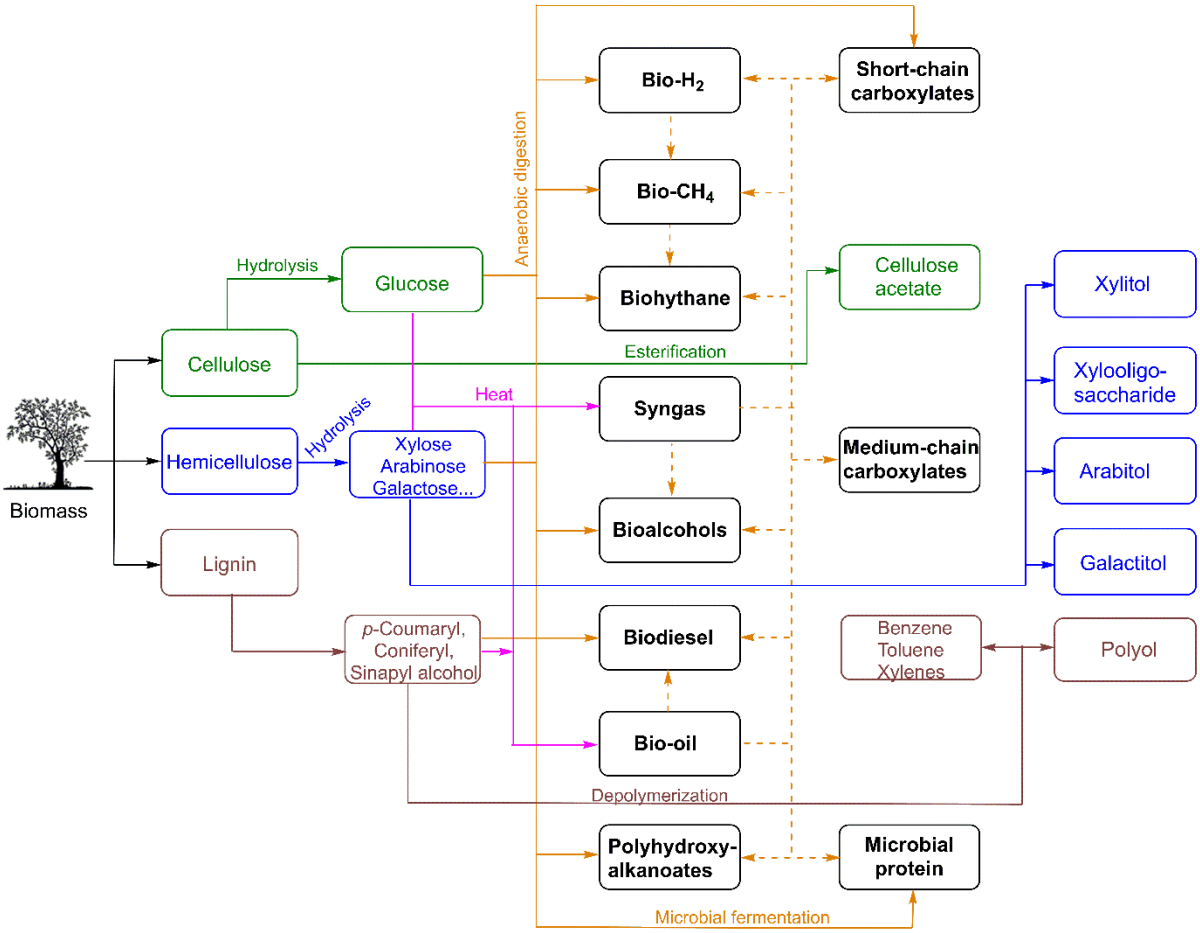

Fig. 2.5. An illustration of integrated biorefinery processes for generating multiple product streams from cellulose (green), hemicellulose (blue), lignin (brown), and all three lignocellulosic fractions (black) via microbial fermentation/anaerobic digestion (orange) or thermochemical processes (pink). Dashed lines (in orange) refer to interconnected products. The products shown in the figure are to serve as examples and are by no means exhaustive.

References

Ananthi, V., Prakash, G.S., Woong, S., Ravindran, B., 2019. Enhanced microbial biodiesel production from lignocellulosic hydrolysates using yeast isolates. Fuel 256, 115932. doi:10.1016/j.fuel.2019.115932

Andreides, D., Olsa, K., Pokorna, D., Zabranska, J., 2021. Biological conversion of carbon monoxide and hydrogen by anaerobic culture: Prospect of anaerobic digestion and thermochemical processes combination. Biotechnol. Adv. 107886. doi:10.1016/j.biotechadv.2021.107886

Arnold, S., Moss, K., Dahmen, N., Hausmann, R., 2019. Pretreatment strategies for microbial valorization of bio-oil fractions produced by fast pyrolysis of ash-rich lignocellulosic biomass. GCB Bioenergy 11, 181–190. doi:10.1111/gcbb.12544

Arreola-Vargas, J., Meng, X., Wang, Y., Ragauskas, A.J., Yuan, J.S., 2021. Enhanced medium chain length-polyhydroxyalkanoate production by co-fermentation of lignin and holocellulose. Green Chem. 2020, 8226–8237. doi:10.1039/d1gc02725e

Arya, A.S., Hang, M.T.H., Eiteman, M.A., 2022. Isolation and Characterization of Levoglucosan-Metabolizing Bacteria. Appl. Environ. Microbiol. 88, e01868-21.

Ashokkumar, V., Venkatkarthick, R., Jayashree, S., 2022. Recent advances in lignocellulosic biomass for biofuels and value-added bioproducts - A critical review. Bioresour. Technol. 344, 126195. doi:10.1016/j.biortech.2021.126195

Asimakopoulos, K., Kaufmann-elfang, M., Lundholm-h, C., Rasmussen, N.B.K., Grimalt-alemany, A., Gavala, H.N., Skiadas, I. V, 2021. Scale up study of a thermophilic trickle bed reactor performing syngas biomethanation. Appl. Energy 290, 116771. doi:10.1016/j.apenergy.2021.116771

Asimakopoulos, K., Łęż, M., Grimalt-alemany, A., Melas, A., 2020. Temperature effects on syngas biomethanation performed in a trickle bed reactor. Chem. Eng. J. 393, 124739. doi:10.1016/j.cej.2020.124739

Aui, A., Wang, Y., Mba-Wright, M., 2021. Evaluating the economic feasibility of cellulosic ethanol : A meta-analysis of techno-economic analysis studies. Renew. Sustain. Energy Rev. 145, 111098. doi:10.1016/j.rser.2021.111098

Ayub, A., Hassan, M., 2021. Enhancing biogas production through co-digestion and thermal pretreatment of wheat straw and sun flower meal. Renew. Energy 168, 1–10. doi:10.1016/j.renene.2020.11.149

Basaglia, M., Favaro, L., Torri, C., Casella, S., 2021. Is pyrolysis bio-oil prone to microbial conversion into added-value products? Renew. Energy 163, 783–791. doi:10.1016/j.renene.2020.08.010

Bhatia, S.K., Gurav, R., Choi, T.-R., Han, Y.H., Park, Y.-L., Park, J.Y., Jung, H.-R., Yang, S.-Y., Song, H.-S., Kim, S.-H., Choi, K.-Y., Yang, Y.-H., 2019. Bioconversion of barley straw lignin into biodiesel using Rhodococcus sp. Bioresour. Technol. 289, 121704. doi:10.1016/j.biortech.2019.121704

Bhatia, S.K., Jagtap, S. S., Bedekar, A. A., Bhatia, R. K., Rajendran, K., Pugazhendhi, A., Rao, C. V., Atabani, A. E., Kumar, G., Yang, Y. H., 2021. Renewable biohydrogen production from lignocellulosic biomass using fermentation and integration of systems with other energy generation technologies. Sci. Total Environ. 765, 144429. 10.1016/j.scitotenv.2020.144429

Brojanigo, S., Alvarado-Morales, M., Basaglia, M., Casella, S., Favaro, L., Angelidaki, I., 2022a. Innovative co-production of polyhydroxyalkanoates and methane from broken rice. Sci. Total Environ. doi:10.1016/j.scitotenv.2022.153931

Brojanigo, S., Gronchi, N., Cazzorla, T., Seng, T., Basaglia, M., Favaro, L., Casella, S., 2022b. Engineering Cupriavidus necator DSM 545 for the one-step conversion of starchy waste into polyhydroxyalkanoates. Bioresour. Technol. 347, 126383. doi:10.1016/j.biortech.2021.126383

Cai, J., Rahman, M., Zhang, S., Sarker, M., Zhang, X., Zhang, Y., Yu, X., Fini, E.H., 2021. Review on Aging of Bio-Oil from Biomass Pyrolysis and Strategy to Slowing Aging. Energy & Fuels 35, 11665−11692. doi:10.1021/acs.energyfuels.1c01214

Candry, P., Huang, S., Carvajal-arroyo, J.M., Rabaey, K., Ganigue, R., 2020. Enrichment and characterisation of ethanol chain elongating communities from natural and engineered environments. Sci. Rep. 10, 1–10. doi:10.1038/s41598-020-60052-z

Chang, D., Yu, Z., Islam, Z.U., Yang, Z., Thompson, I.P., 2021. Conversion efficiency of bioethanol from levoglucosan was improved by the newly engineered Escherichia coli. Env. Prog Sustain. Energy. 40, e13687. doi:10.1002/ep.13687

Chen, H., Huang, R., Wu, J., Zhang, W., Han, Y., Xiao, B., Wang, D., Zhou, Y., Liu, B., Yu, G., 2021. Biohythane production and microbial characteristics of two alternating mesophilic and thermophilic two-stage anaerobic co-digesters fed with rice straw and pig manure. Bioresour. Technol. 320, 124303. doi:10.1016/j.biortech.2020.124303

Chen, H., Wang, L., 2016. Technologies for Biochemical Conversion of Biomass, Elsevier Inc. Metallurgical Industry Press. doi:10.1016/B978-0-12-802417-1/00001-6

Chen, J., Zhang, B., Luo, L., Zhang, F., Yi, Y., Shan, Y., Liu, B., Zhou, Y., Wang, X., Lü, X., 2021. A review on recycling techniques for bioethanol production from lignocellulosic biomass. Renew. Sustain. Energy Rev. 149, 111370. doi:10.1016/j.rser.2021.111370

Chen, W., Farooq, W., Shahbaz, M., Raza, S., Ali, I., Al-ansari, T., Aishah, N., Amin, S., 2021. Current status of biohydrogen production from lignocellulosic biomass, technical challenges and commercial potential through pyrolysis process. Energy 226, 120433. doi:10.1016/j.energy.2021.120433

Cheng, J., Li, H., Ding, L., Zhou, J., Song, W., Li, Y.Y., Lin, R., 2020. Improving hydrogen and methane co-generation in cascading dark fermentation and anaerobic digestion: The effect of magnetite nanoparticles on microbial electron transfer and syntrophism. Chem. Eng. J. 397, 125394. doi:10.1016/j.cej.2020.125394

Chu, W., Xu, Y., Yang, J., Wu, Y., Wei, X., Hao, Y., Wang, S., Zhao, H., 2021. Effect of biohydrogen by overexpressing small RNA RyhB combined with ldh impairment in novel Klebsiella sp. FSoil 024. Int. J. Hydrogen Energy 46, 19303–19311. doi:10.1016/j.ijhydene.2021.03.087

Cubero-Cardoso, J., Russo, E., Serrano, A., Trujillo-Reyes, Á., Villa-Gomez, D., Esposito, G., Fermoso, F.G., 2022. Environmental Technology & Innovation Enhancing the recovery of volatile fatty acids from strawberry extrudate through anaerobic fermentation at different pH values. Environ. Technol. Innov. 28, 102587. doi:10.1016/j.eti.2022.102587

D' Silva, T.C., Isha, A., Chandra, R., Kumar, Virendra, Mohan, P., Subbarao, V., Kumar, R., Prakash, V., Singh, H., Ali, A., Kumar, Vinay, Kov, L., 2021. Enhancing methane production in anaerobic digestion through hydrogen assisted pathways – A state-of-the-art review. Renew. Sustain. Energy Rev. 151, 111536. doi:10.1016/j.rser.2021.111536

da Fonseca, Y.A., Silva, N.C.S., de Camargos, A.B., Silva, S. de Q., Wandurraga, H.J.L., Gurgel, L.V.A., Baeta, B.E.L., 2021. Influence of hydrothermal pretreatment conditions, typology of anaerobic digestion system, and microbial profile in the production of volatile fatty acids from olive mill solid waste. J. Environ. Chem. Eng. 9, 105055. doi:10.1016/j.jece.2021.105055

Dai, K., Zhang, W., Zeng, R.J., Zhang, F., 2020. Production of chemicals in thermophilic mixed culture fermentation: mechanism and strategy. Crit. Rev. Environ. Sci. Technol. 50, 1–30. doi:10.1080/10643389.2019.1616487

Dai, X., Hua, Y., Liu, R., Chen, S., Li, H., Dai, L., Cai, C., 2020. Biomethane production by typical straw anaerobic digestion: Deep insights of material compositions and surface properties. Bioresour. Technol. 313, 123643. doi:10.1016/j.biortech.2020.123643

Dehghanzad, M., Sha, M., Karimi, K., 2020. Whole sweet sorghum plant as a promising feedstock for biobutanol production via biorefinery approaches: Techno-economic analysis. Renew. Energy 158, 332–342. doi:10.1016/j.renene.2020.05.037

Di Capua, F., Spasiano, D., Giordano, A., Adani, F., Fratino, U., Pirozzi, F., Esposito, G., 2020. High-solid anaerobic digestion of sewage sludge: challenges and opportunities. Appl. Energy 278, 115608. doi:10.1016/j.apenergy.2020.115608

Di Fidio, N., Ragaglini, G., Dragoni, F., Antonetti, C., Galletti, A.M.R., 2021. Integrated cascade biorefinery processes for the production of single cell oil by Lipomyces starkeyi from Arundo donax L. hydrolysates. Bioresour. Technol. 325, 124635. doi:10.1016/j.biortech.2020.124635

Dionísio, S.R., Santoro, D.C.J., Bonan, C.I.D.G., Soares, L.B., Biazi, L.E., Rabelo, S.C., Ienczak, L., 2021. Second-generation ethanol process for integral use of hemicellulosic and cellulosic hydrolysates from diluted sulfuric acid pretreatment of sugarcane bagasse. Fuel 304, 121290. doi:10.1016/j.fuel.2021.121290

Do, S., Jiwon, Y., Gong, G., Kyong, J., Um, Y., Ok, S., Lee, H.S., 2020. High-yield lipid production from lignocellulosic biomass using engineered xylose-utilizing Yarrowia lipolytica. GCB Bioenergy 12, 670–679. doi:10.1111/gcbb.12699

Dong, L., Wu, X., Wang, Q., Cao, G., Wu, J., Zhou, C., Ren, N., 2020. Science of the Total Environment Evaluation of a novel pretreatment of NaOH/ Urea at outdoor cold-winter conditions for enhanced enzymatic conversion and hythane production from rice straw. Sci. Total Environ. 744, 140900. doi:10.1016/j.scitotenv.2020.140900

Drzymała, K., Mironczuk, A.M., Pietrzak, W., Dobrowolski, A., 2020. Rye and Oat Agricultural Wastes as Substrate Candidates for Biomass Production of the Non-Conventional Yeast Yarrowia lipolytica. Sustainability 12, 7704. doi:doi:10.3390/su12187704

Eiben, C.B., Tian, T., Thompson, M.G., Mendez-perez, D., Kaplan, N., Goyal, G., Chiniquy, J., Hillson, N.J., Lee, T.S., Keasling, J.D., 2020. Adenosine Triphosphate and Carbon Efficient Route to Second Generation Biofuel Isopentanol. ACS Synth. Biol. 9, 468–474. doi:10.1021/acssynbio.9b00402

Farias, D., Melo, A.H.F. de, da Silva, M.F., Bevilaqua, G.C., Ribeiro, D.G., Goldbeck, R., Forte, M.B.S., Forte, S., Maugeri-Filho, F., 2022. New biotechnological opportunities for C5 sugars from lignocellulosic materials. Bioresour. Technol. Reports 17, 100956. doi:10.1016/j.biteb.2022.100956

Ge, S., Usack, J.G., Spirito, C.M., Angenent, L.T., 2015. Long-Term n-Caproic Acid Production from

Yeast-Fermentation Beer in an Anaerobic Bioreactor with Continuous Product Extraction. Environ. Sci. Technol. 49, 8012−8021. doi:10.1021/acs.est.5b00238

Ghimire, A., Kumar, G., Sivagurunathan, P., Shobana, S., Saratale, G.D., Woo, H., Luongo, V., Esposito, G., Munoz, R., 2017. Bio-hythane production from microalgae biomass: Key challenges and potential opportunities for algal bio-refineries. Bioresour. Technol. 241, 525–536. doi:10.1016/j.biortech.2017.05.156

Gu, Y., Hu, Y., Huang, C., Lai, C., Ling, Z., Yong, Q., 2022. Co-production of amino acid-rich xylooligosaccharide and single-cell protein from paper mulberry by autohydrolysis and fermentation technologies. Biotechnol. Biofuels Bioprod. 15, 1–10. doi:10.1186/s13068-021-02095-6

Gunasekaran, M., Kumar, G., 2021. Lignocellulosic biomass as an optimistic feedstock for the production of biofuels as valuable energy source: Techno-economic analysis , Environmental Impact Analysis, Breakthrough and Perspectives. Environ. Technol. Innov. 24, 102080. doi:10.1016/j.eti.2021.102080

Gunes, B., 2021. A critical review on biofilm-based reactor systems for enhanced syngas fermentation processes. Renew. Sustain. Energy Rev. 143, 110950. doi:10.1016/j.rser.2021.110950

Guo, X., Yang, H., Wenga, T., Zhang, R., Liu, B., Chen, G., 2022. Catalytic fast pyrolysis of Arundo donax in a two-stage fixed bed reactor over metal-modified HZSM-5 catalysts. Biomass and Bioenergy 156, 106316. doi:10.1016/j.biombioe.2021.106316

Han, W., He, P., Shao, L., 2018. Metabolic Interactions of a Chain Elongation Microbiome. Appl. Environ. Microbiol. 84.

Hu, J., Cao, W., Guo, L., 2021. Directly convert lignocellulosic biomass to H2 without pretreatment and added cellulase by two-stage fermentation in semi-continuous modes. Renew. Energy 170, 866–874. doi:10.1016/j.renene.2021.02.062

Islam, S., Zhang, Z., Qu, S., Liu, Chun-lei, Guo, C., Liu, Chun-zhao, 2021. Coproduction of hydrogen and volatile fatty acids via integrated two-step fermentation of sweet sorghum stalks by alkaline and enzymatic treatment. Biomass and Bioenergy 145, 105923. doi:10.1016/j.biombioe.2020.105923

Jiang, H., Qin, Y., Gadow, S.I., Ohnishi, A., Fujimoto, N., Li, Y., 2018. Bio-hythane production from cassava residue by two-stage fermentative process with recirculation. Bioresour. Technol. 247, 769–775. doi:10.1016/j.biortech.2017.09.102

Jin, X., Lee, J.H., Choi, J.W., 2022. Catalytic co-pyrolysis of woody biomass with waste plastics: Effects of HZSM-5 and pyrolysis temperature on producing high-value pyrolytic products and reducing wax formation. Energy 239, 121739. doi:10.1016/j.energy.2021.121739

Jing, Y., Wan, J., Angelidaki, I., Zhang, S., Luo, G., 2017. iTRAQ quantitative proteomic analysis reveals the pathways for methanation of propionate facilitated by magnetite. Water Res. 108, 212–221. doi:10.1016/j.watres.2016.10.077

Jung, S., Kwon, D., Park, Y., Ho, K., Kwon, E.E., 2020. Power generation using rice husk derived fuels from CO2 -assisted catalytic pyrolysis over Co/Al2O3. Energy 206, 118143. doi:10.1016/j.energy.2020.118143

Kainthola, J., Kalamdhad, A.S., Goud, V. V., 2019. A review on enhanced biogas production from anaerobic digestion of lignocellulosic biomass by different enhancement techniques. Process

Biochem. 84, 81–90. doi:10.1016/j.procbio.2019.05.023

Kanwal, F., Tahir, A., Abdul, S., Shah, Q., Tsuzuki, T., Nisbet, D., Chen, J., Rehman, Y., 2020. Effect of phyto-fabricated nanoscale organic-iron complex on photo-fermentative hydrogen production by Rhodopseudomonas palustris MP2 and Rhodopseudomonas palustris MP4. Biomass and Bioenergy 140, 105667. doi:10.1016/j.biombioe.2020.105667

Khan, R., Mehran, M.T., Baig, M.M., Sarfraz, B., Raza, S., Bilal, M., Niazi, K., Zubair, M., 2021. 3D hierarchical heterostructured LSTN @ NiMn-layered double hydroxide as a bifunctional water splitting electrocatalyst for hydrogen production. Fuel 285, 119174. doi:10.1016/j.fuel.2020.119174

Khor, W.C., Andersen, S., Vervaeren, H., Rabaey, K., 2017. Electricity-assisted production of caproic acid from grass. Biotechnol. Biofuels 10, 1–11. doi:10.1186/s13068-017-0863-4

Kiggundu, N., Arhin, S.G., Banadda, N., Kabenge, I., 2017. Impacts of Biofuel Policies on Welfare and Food Security: Assessing the Socioeconomic and Environmental Trade-offs in Sub-Saharan Africa. Int. J. Renew. Energy Res. 7, 2162–2171.

Kim, J.-H., Jung, S., Lin, K.-Y.A., Rinklebe, J., Kwon, E.E., 2021. Comparative study on carbon dioxide-cofed catalytic pyrolysis of grass and woody biomass. Bioresour. Technol. 323, 124633. doi:10.1016/j.biortech.2020.124633

Kim, S., Clomburg, J.M., Gonzalez, R., 2015. Synthesis of medium - chain length (C6–C10) fuels and chemicals via β-oxidation reversal in Escherichia coli. J Ind Microbiol Biotechnol 42, 465–475. doi:10.1007/s10295-015-1589-6

Kleinsteuber, S., Dittrich-Zechendorf, M., 2018. Carboxylic acid production from ensiled crops in anaerobic solid-state fermentation - trace elements as pH controlling agents support microbial chain elongation with lactic acid. Eng. Life Sci. 447–458. doi:10.1002/elsc.201700186

Kumar, A., Pilli, S., Bhunia, P., Tyagi, R.D., Surampalli, R.Y., Zhang, T.C., Kim, S., Pandey, A., 2022. Dark fermentation: Production and utilization of volatile fatty acid from different wastes- A review. Chemosphere 288, 132444. doi:10.1016/j.chemosphere.2021.132444

Kumar, R.S., Singh, P., Ghosh, S., 2022. Sequential fermentation for enhanced volumetric productivity of bioethanol from mixed sugars. Fuel 308, 121984. doi:10.1016/j.fuel.2021.121984

Kumari, S., Das, D., 2019. Biohythane production from sugarcane bagasse and water hyacinth: A way towards promising green energy production. J. Clean. Prod. 207, 689–701. doi:10.1016/j.jclepro.2018.10.050

Lay, C., Kumar, G., Mudhoo, A., Lin, C., Leu, H., Shobana, S., 2019. Recent trends and prospects in biohythane research: An overview. Int. J. Hydrogen Energy 45, 5864–5873. doi:10.1016/j.ijhydene.2019.07.209

Lee, J., Yang, J., 2019. Global energy transitions and political systems. Renew. Sustain. Energy Rev. 115, 109370. doi: 10.1016/j.rser.2019.109370

Li, C., Zhu, X., Angelidaki, I., 2021. Syngas biomethanation: effect of biomass-gas ratio, syngas composition and pH buffer. Bioresour. Technol. 342, 125997. doi:10.1016/j.biortech.2021.125997

Li, J., He, J., Si, B., Liu, Z., Zhang, C., Wang, Y., Xing, X., 2020. A pilot study of biohythane production from cornstalk via two-stage anaerobic fermentation. Int. J. Hydrogen Energy 45, 31719–31731.

doi:10.1016/j.ijhydene.2020.08.253

Liakakou, E.T., Infantes, A., Neumann, A., Vreugdenhil, B.J., 2021. Connecting gasification with syngas fermentation: Comparison of the performance of lignin and beech wood. Fuel 290, 120054. doi:10.1016/j.fuel.2020.120054

Liang, L., Liu, R., Freed, E.F., Eckert, C.A., 2020. Synthetic Biology and Metabolic Engineering Employing Escherichia coli for C2–C6 Bioalcohol Production. Front. Bioeng. Biotechnol. 8, 1–8. doi:10.3389/fbioe.2020.00710

Liao, Y., Koelewijn, S.-F., Bossche, G. Van den, Aelst, J. Van, Bosch, S. Van den, Renders, T., Navare, K., Nicolaï, T., Aelst, K. Van, Maesen, M., Matsushima, H., Thevelein, J.M., Acker, K. Van, Lagrain, B., Verboekend, D., Sels, B.F., 2020. A sustainable wood biorefinery for low–carbon footprint chemicals production. Science (80-.). 367, 1385–1390.

Liu, B., Kleinsteuber, S., Centler, F., Harms, H., Sträuber, H., 2020. Competition Between Butyrate Fermenters and Chain-Elongating Bacteria Limits the Efficiency of Medium-Chain Carboxylate Production. Front. Microbiol. 11, 1–13. doi:10.3389/fmicb.2020.00336

Liu, F., Rotaru, A.E., Shrestha, P.M., Malvankar, N.S., Nevin, K.P., Lovley, D.R., 2012. Promoting direct interspecies electron transfer with activated carbon. Energy Environ. Sci. 5, 8982–8989. doi:10.1039/c2ee22459c

Liu, R., Chen, X., Zhang, K., Han, Y., Tong, Y., Wang, J., Xiao, B., Liu, J., 2022. Effect of mixing ratio and total solids content on temperature-phased anaerobic codigestion of rice straw and pig manure: Biohythane production and microbial structure. Bioresour. Technol. 344, 126173. doi:10.1016/j.biortech.2021.126173

Liu, X., Raj, K., Burra, G., Wang, Z., Li, J., Che, D., Gupta, A.K., 2021. Towards enhanced understanding of synergistic effects in co-pyrolysis of pinewood and polycarbonate. Appl. Energy 289, 116662. doi:10.1016/j.apenergy.2021.116662

Liu, W., Mao, W., Zhang, C., Liu, L., Zhang, Z., Guo, C., Lin, J., 2021. Effective and economic microbial lipid biosynthesis for biodiesel production by two-phase whole-cell biocatalytic process. J. Clean. Prod. 298, 126798. doi:10.1016/j.jclepro.2021.126798

Liu, Y., He, P., Shao, L., Zhang, H., Lü, F., 2017. Significant enhancement by biochar of caproate production via chain elongation. Water Res. 119, 150–159. doi:10.1016/j.watres.2017.04.050

Lopez-Hidalgo, A.M., Hernandez, V.E.B., Leon-Rodriguez, A. De, 2021a. Scale-up of hydrogen and ethanol co-production by an engineered Escherichia coli. Fuel 300, 121002. doi:10.1016/j.fuel.2021.121002

Lopez-Hidalgo, A.M., Magaña, G., Rodriguez, F., Leon-rodriguez, A. De, Sanchez, A., Futuros, L. De, Guadalajara, U., Avanzada, D.I., Investigación, C. De, Estudios, D., Politécnico, I., 2021b. Co-production of ethanol-hydrogen by genetically engineered Escherichia coli in sustainable biorefineries for lignocellulosic ethanol production. Chem. Eng. J. 406, 126829. doi:10.1016/j.cej.2020.126829

Lovley, D.R., 2017. Happy together: microbial communities that hook up to swap electrons. ISME J. 11, 327–336. doi:10.1038/ismej.2016.136

Lu, C., Tahir, N., Li, W., Zhang, Z., Jiang, D., Guo, S., Wang, J., Wang, K., Zhang, Q., 2020. Enhanced buffer capacity of fermentation broth and biohydrogen production from corn stalk with Na2HPO4/ NaH2PO4. Bioresour. Technol. 313, 123783. doi:10.1016/j.biortech.2020.123783

Lü, F., Guo, K., Duan, H., Shao, L., He, P., 2018. Exploit Carbon Materials to Accelerate Initiation and Enhance Process Stability of CO Anaerobic Open-Culture Fermentation. ACS Sustain. Chem. Eng. 6, 2787−2796. doi:10.1021/acssuschemeng.7b04589

Ma, H., Hu, Y., Kobayashi, T., Xu, K.Q., 2020. The role of rice husk biochar addition in anaerobic digestion for sweet sorghum under high loading condition. Biotechnol. Reports 27, e00515. doi:10.1016/j.btre.2020.e00515

Ma, S., Wang, H., Wang, B., Gu, X., Zhu, W., 2022. Biomethane enhancement from corn straw using anaerobic digestion by-products as pretreatment agents: A highly effective and green strategy. Bioresour. Technol. 344, 126177. doi:10.1016/j.biortech.2021.126177

Magalhães, C.E.B., Souza-Neto, M.S., Astolfi-Filho, S., Matos, I.T.S.R., 2018. Candida tropicalis able to produce yeast single cell protein using sugarcane bagasse hemicellulosic hydrolysate as carbon source. Biotechnol. Res. Innov. 2, 19–21. doi:10.1016/j.biori.2018.08.002

Mamimin, C., Chanthong, S., Leamdum, C., O-thong, S., 2021. Improvement of empty palm fruit bunches biodegradability and biogas production by integrating the straw mushroom cultivation as a pretreatment in the solid-state anaerobic digestion. Bioresour. Technol. 319, 124227. doi:10.1016/j.biortech.2020.124227

Mamimin, C., Kongjan, P., O-thong, S., 2019. Enhancement of biohythane production from solid waste by co-digestion with palm oil mill effluent in two-stage thermophilic fermentation. Int. J. Hydrogen Energy 44, 17224–17237. doi:10.1016/j.ijhydene.2019.03.275

Mancini, G., Papirio, S., Lens, P.N.L., Esposito, G., 2018. Increased biogas production from wheat straw by chemical pretreatments. Renew. Energy 119, 608–614. doi:10.1016/j.renene.2017.12.045

Mankar, A. R., Pandey, A., Modak, A., Pant, K. K., 2021. Pretreatment of lignocellulosic biomass: A review on recent advances. Bioresour. Technol. 334, 125235. doi:10.1016/j.biortech.2021.125235

Marta, K., Paulina, R., Magda, D., Anna, N., Aleksandra, K., 2020. Evaluation of Ultrasound Pretreatment for Enhanced Anaerobic Digestion of Sida hermaphrodita. BioEnergy Res. 13, 824–832.

Matassa, S., Papirio, S., Pikaar, I., Hülsen, T., Leijenhorst, E., Esposito, G., Pirozzia, F., Verstraete, W., 2020. Upcycling of biowaste carbon and nutrients in line with consumer confidence: the “full gas ”route to single cell protein. Green Chem. 22, 4912–4929. doi:10.1039/d0gc01382j

Medeiros, E.M. De, Noorman, H., Maciel, R., Posada, J.A., 2020. Production of ethanol fuel via syngas fermentation: Optimization of economic performance and energy efficiency. Chem. Eng. Sci. X 5, 100056. doi:10.1016/j.cesx.2020.100056

Medina-Morales, M.A., Cruz-Andrade, L.E.D. la, Paredes-Pena, L.A., Morales-Martinez, T.K., Garza, J.A.R.-D. la, Moreno-Davila, I.M., Tamayo-Ordonez, M.C., Rios-Gonzalez, L.J., 2021. Biohydrogen production from thermochemically pretreated corncob using a mixed culture bioaugmented with Clostridium acetobutylicum. Int. J. Hydrogen Energy 6, 25974–25984. doi:10.1016/j.ijhydene.2021.04.046

Miao, Z., Tian, X., Liang, W., He, Y., Wang, G., 2020. Bioconversion of corncob hydrolysate into microbial lipid by an oleaginous yeast Rhodotorula taiwanensis AM2352 for biodiesel production. Renew. Energy 161, 91–97. doi:10.1016/j.renene.2020.07.007

Mishra, A., Ghosh, S., 2020. Saccharification of kans grass biomass by a novel fractional hydrolysis method followed by co-culture fermentation for bioethanol production. Renew. Energy 146, 750–759. doi:10.1016/j.renene.2019.07.016

Monir, M.U., Aziz, A.A., Khatun, F., Yousuf, A., 2020a. Bioethanol production through syngas fermentation in a tar free bioreactor using Clostridium butyricum. Renew. Energy 157, 1116–1123. doi:10.1016/j.renene.2020.05.099

Monir, M.U., Aziz, A.A., Kristanti, R.A., Yousuf, A., 2018. Gasification of lignocellulosic biomass to produce syngas in a 50 kW downdraft reactor. Biomass and Bioenergy 119, 335–345. doi:10.1016/j.biombioe.2018.10.006

Monir, M.U., Aziz, A.A., Yousuf, A., 2022. Integrated technique to produce sustainable bioethanol from lignocellulosic biomass. Mater. Lett. X 13, 100127. doi:10.1016/j.mlblux.2022.100127

Monir, M.U., Aziz, A.A., Yousuf, A., Alam, M.Z., 2020b. Hydrogen-rich syngas fermentation for bioethanol production using Sacharomyces cerevisiea. Int. J. Hydrogen Energy 45, 18241–18249. doi:10.1016/j.ijhydene.2019.07.246

Morales-Martinez, T.K., Medina-Morales, M.A., Ortiz-Cruz, A.L., Rodriguez-De la Garza, J.A., Moreno-Davila, M., Lopez-Badillo, C.M., Rios-Gonzalez, L., 2020. Consolidated bioprocessing of hydrogen production from agave biomass by Clostridium acetobutylicum and bovine ruminal fluid. Int. J. Hydrogen Energy 45, 13707–13716. doi:10.1016/j.ijhydene.2019.11.089

Morya, R., Sharma, A., Kumar, M., Tyagi, B., Shekhar, S., Shekhar, I., 2021. Polyhydroxyalkanoate synthesis and characterization: A proteogenomic and process optimization study for biovalorization of industrial lignin. Bioresour. Technol. 320, 124439. doi:10.1016/j.biortech.2020.124439

Moscariello, C., Matassa, S., Esposito, G., Papirio, S., 2021. From residue to resource: The multifaceted environmental and bioeconomy potential of industrial hemp (Cannabis sativa L.). Resour. Conserv. Recycl. 175, 105864. doi:10.1016/j.resconrec.2021.105864

Nino-Navarro, C., Chairez, I., Christen, P., Canul-chan, M., García-pe, E.I., 2020. Enhanced hydrogen production by a sequential dark and photo fermentation process: Effects of initial feedstock composition, dilution and microbial population. Renew. Energy 147, 924–936. doi:10.1016/j.renene.2019.09.024

Nguyen, M.-L.T., Hung, P., Vo, T., Lay, C.-H., Lin, C.-Y., 2021. Effect of food to microorganisms (F/M) ratio on biohythane production via single-stage dark fermentation. Int. J. Hydrogen Energy 46, 11313–11324. doi:10.1016/j.ijhydene.2020.06.127

Nyyssölä, A., Suhonen, A., Ritala, A., Oksman-Caldentey, K.-M., 2022. The role of single cell protein in cellular agriculture. Curr. Opin. Biotechnol. 75, 102686. doi:10.1016/j.copbio.2022.102686

Obruča, S., Dvořák, P., Sedláček, P., Koller, M., Sedlář, K., Pernicová, I., Šafránek, D., 2022. Polyhydroxyalkanoates synthesis by halophiles and thermophiles: towards sustainable production of microbial bioplastics. Biotechnol. Adv. doi:10.1016/j.biotechadv.2022.107906

Oliva, A., Tan, L.C., Papirio, S., Esposito, G., Lens, P.N.L., 2021. Effect of methanol-organosolv pretreatment on anaerobic digestion of lignocellulosic materials. Renew. Energy 169, 1000–1012. doi:10.1016/j.renene.2020.12.095

Ou, L., Dou, C., Yu, J., Kim, H., Park, Y., Lee, E.Y., Kelley, S., Park, S., 2021. Techno-economic analysis of sugar production from lignocellulosic biomass with utilization of hemicellulose and

lignin for high-value co-products. Biofuels, Bioprod. Bioref. 15, 404–415. doi:10.1002/bbb.2170

Patel, S.K.S., Gupta, R.K., Das, D., Lee, J., Kalia, V.C., 2021. Continuous biohydrogen production from poplar biomass hydrolysate by a defined bacterial mixture immobilized on lignocellulosic materials under non-sterile conditions. J. Clean. Prod. 287, 125037. doi:10.1016/j.jclepro.2020.125037

Peteghem, L. Van, Sakarika, M., Matassa, S., Pikaar, I., Ganigu, R., Rabaey, K., 2022. Towards new carbon–neutral food systems: Combining carbon capture and utilization with microbial protein production. Bioresour. Technol. 349, 126853. doi:10.1016/j.biortech.2022.126853

Pihlajaniemi, V., Ellilä, S., Poikkimäki, S., Nappa, M., Rinne, M., Lantto, R., Siika-aho, M., 2020. Comparison of pretreatments and cost-optimization of enzymatic hydrolysis for production of single cell protein from grass silage fibre. Bioresour. Technol. Reports 9, 100357. doi:10.1016/j.biteb.2019.100357

Pollard, A.S., Rover, M.R., Brown, R.C., 2012. Pyrolysis Characterization of bio-oil recovered as stage fractions with unique chemical and physical properties. J. Anal. Appl. Pyrolysis 93, 129–138. doi:10.1016/j.jaap.2011.10.007

Pradhan, N., Dipasquale, L., D'Ippolito, G., Panico, A., Lens, P.N.L., Esposito, G., Fontana, A., 2017. Hydrogen and lactic acid synthesis by the wild-type and a laboratory strain of the hyperthermophilic bacterium Thermotoga neapolitana DSMZ 4359T under capnophilic lactic fermentation conditions. Int. J. Hydrogen Energy 42, 16023–16030. doi:10.1016/j.ijhydene.2017.05.052

Raj, T., Chandrasekhar, K., Kumar, A.N., Kim, S.-H., 2022. Lignocellulosic biomass as renewable feedstock for biodegradable and recyclable plastics production: A sustainable approach. Renew. Sustain. Energy Rev. 158, 112130. doi:10.1016/j.rser.2022.112130

Reddy, M.V., ElMekawy, A., Pant, D., 2018. Bioelectrochemical synthesis of caproate through chain elongation as a complementary technology to anaerobic digestion. Biofuels, Bioprod. Biorefining 12, 966–977. doi:10.1002/bbb.1924

Ren, S., Usman, M., Tsang, D.C.W., O-thong, S., Angelidaki, I., 2020. Hydrochar-Facilitated Anaerobic Digestion: Evidence for Direct Interspecies Electron Transfer Mediated through Surface Oxygen- Containing Functional Groups. Environ. Sci. Technol. 54, 5755−5766.

Rena, Zacharia, K.M. Bin, Yadav, S., Machhirake, N.P., Kim, S.-H., Lee, B.-D., Jeong, H., Singh, L., Kumar, S., Kumar, R., 2020. Bio-hydrogen and bio-methane potential analysis for production of bio-hythane using various agricultural residues. Bioresour. Technol. 309, 123297. doi:10.1016/j.biortech.2020.123297

Rodríguez-Valderrama, S., Escamilla-Alvarado, C., Magnin, J.-P., Rivas-García, P., Valdez-Vazquez, I., Ríos-Leal, E., 2020. Batch biohydrogen production from dilute acid hydrolyzates of fruits-and-vegetables wastes and corn stover as co-substrates. Biomass and Bioenergy 140, 105666. doi:10.1016/j.biombioe.2020.105666

Roghair, M., Hoogstad, T., Strik, D.P.B.T.B., Plugge, C.M., Timmers, P.H.A., Weusthuis, R.A., Bruins, M.E., Buisman, C.J.N., 2018a. Controlling Ethanol Use in Chain Elongation by CO2 Loading Rate. Environ. Sci. Technol. 52, 1496−1505. doi:10.1021/acs.est.7b04904

Roghair, M., Liu, Y., Adiatma, J.C., Weusthuis, R.A., Bruins, M.E., Buisman, C.J.N., Strik, D.P.B.T.B., 2018b. Effect of n-Caproate Concentration on Chain Elongation and Competing Processes. ACS

Sustain. Chem. Eng. 6, 7499−7506. doi:10.1021/acssuschemeng.8b00200

Rojas-Chamorro, J.A., Romero-garcía, J.M., Cara, C., Romero, I., Castro, E., 2020. Improved ethanol production from the slurry of pretreated brewers' spent grain through different co-fermentation strategies. Bioresour. Technol. 296, 122367. doi:10.1016/j.biortech.2019.122367

Rotaru, A.E., Shrestha, P.M., Liu, F., Shrestha, M., Shrestha, D., Embree, M., Zengler, K., Wardman, C., Nevin, K.P., Lovley, D.R., 2014. A new model for electron flow during anaerobic digestion: Direct interspecies electron transfer to Methanosaeta for the reduction of carbon dioxide to methane. Energy Environ. Sci. 7, 408–415. doi:10.1039/c3ee42189a

Saif, I., Salama, E.S., Usman, M., Lee, D.S., Malik, K., Liu, P., Li, X., 2021. Improved digestibility and biogas production from lignocellulosic biomass: Biochar addition and microbial response. Ind. Crops Prod. 171, 113851. doi:10.1016/j.indcrop.2021.113851

Sarkar, O., Rova, U., Christakopoulos, P., Matsakas, L., 2021. Ethanol addition promotes elongation of short-chain fatty acids to medium-chain fatty acids using brewery spent grains as substrate. J. Environ. Chem. Eng. 9, 105990. doi:10.1016/j.jece.2021.105990

Scarborough, M.J., Lynch, G., Dickson, M., Mcgee, M., Donohue, T.J., Noguera, D.R., 2018. Increasing the economic value of lignocellulosic stillage through medium - chain fatty acid production. Biotechnol. Biofuels 1–17. doi:10.1186/s13068-018-1193-x

Seengenyoung, J., Mamimin, C., Prasertsan, P., 2019. Pilot-scale of biohythane production from palm oil mill effluent by two-stage thermophilic anaerobic fermentation. Int. J. Hydrogen Energy 44, 3347–3355. doi:10.1016/j.ijhydene.2018.08.021

Shahab, R.L., Brethauer, S., Davey, M.P., Smith, A.G., Vignolini, S., Luterbacher, J.S., Studer, M.H., 2020. A heterogeneous microbial consortium producing short-chain fatty acids from lignocellulose. Science (80-.). 369. doi:10.1126/science.abb1214

Sharma, J., Kumar, V., Prasad, R., Gaur, N.A., 2022. Engineering of Saccharomyces cerevisiae as a consolidated bioprocessing host to produce cellulosic ethanol: Recent advancements and current challenges. Biotechnol. Adv. 56, 107925. doi:10.1016/j.biotechadv.2022.107925

Shen, Y., Yu, Y., Zhang, Y., Urgun-demirtas, M., Yuan, H., Zhu, N., Dai, X., 2021. Role of redox-active biochar with distinctive electrochemical properties to promote methane production in anaerobic digestion of waste activated sludge. J. Clean. Prod. 278, 123212. doi:10.1016/j.jclepro.2020.123212

Sheng, T., Meng, Q., Wen, X., Sun, C., Yang, L., Li, L., 2021. Bioaugmentation with Ruminiclostridium thermocellum M3 to enhance thermophilic hydrogen production from agricultural solid waste. J Chem Technol Biotechnol 96, 1623–1631. doi:10.1002/jctb.6682

Shi, Z., Campanaro, S., Usman, M., Treu, L., Basile, A., Angelidaki, I., 2021a. Genome-Centric Metatranscriptomics Analysis Reveals the Role of Hydrochar in Anaerobic Digestion of Waste Activated Sludge. Environ. Sci. Technol. 55, 8351−8361. doi:10.1021/acs.est.1c01995

Shi, Z., Usman, M., He, J., Chen, H., Zhang, S., Luo, G., 2021b. Combined microbial transcript and metabolic analysis reveals the different roles of hydrochar and biochar in promoting anaerobic digestion of waste activated sludge. Water Res. 205, 117679. doi:10.1016/j.watres.2021.117679

Singh, T., Alhazmi, A., Mohammad, A., Srivastava, N., Haque, S., 2021. Integrated biohydrogen production via lignocellulosic waste: Opportunity, challenges & future prospects. Bioresour. Technol. 338, 125511. doi:10.1016/j.biortech.2021.125511

Slininger, P.J., Dien, B.S., Kurtzman, C.P., Moser, B.R., Bakota, E.L., Thompson, S.R., O'Bryan, P.J., Cotta, M.A., Balan, V., Jin, M., Sousa, L. da C., Dale, B.E., 2016. Comparative lipid production by oleaginous yeasts in hydrolyzates of lignocellulosic biomass and process strategy for high titers. Biotechnol. Bioeng. 113, 1676–1690. doi:10.1002/bit.25928

Soares, J. F., Confortin, C., Todero, I., Mayer, D., Mazutti, M.A., 2020. Dark fermentative biohydrogen production from lignocellulosic biomass: Technological challenges and future prospects. Renew. Sustain. Energy Rev. 117. doi:10.1016/j.rser.2019.109484

Son, Y., Jeon, J., Kim, D., Yang, Y., Jin, Y., Cho, B., Kim, S., Kumar, S., Lee, B., Yoon, J., 2021. Improved bio-hydrogen production by overexpression of glucose-6-phosphate dehydrogenase and FeFe hydrogenase in Clostridium acetobutylicum. Int. J. Hydrogen Energy 46, 36687–36695. doi:10.1016/j.ijhydene.2021.08.222

Song, Y., Lee, Y.G., Lee, D.S., Nguyen, D.T., Bae, H.J., 2022. Utilization of bamboo biomass as a biofuels feedstocks: Process optimization with yeast immobilization and the sequential fermentation of glucose and xylose. Fuel 307, 121892. doi:10.1016/j.fuel.2021.121892

Souza, L. De, Shivakumar, S., Das, A., 2022. Dual phase statistical optimization of biological pre-treatment of sugarcane bagasse with Pycnoporus coccineus MScMS1 for polyhydroxyalkanoates production. J. Environ. Manage. 302, 113948. doi:10.1016/j.jenvman.2021.113948

Srivastava, N., Srivastava, M., Mishra, P.K., Adnan, M., Saeed, M., Gupta, V.K., Singh, R., Ramteke, P.W., 2020. Advances in nanomaterials induced biohydrogen production using waste biomass. Bioresour. Technol. 307, 123094. doi:10.1016/j.biortech.2020.123094

Stinner, W., Yuan, X., Cai, Y., Zheng, Z., Sch, F., Wang, H., Cui, Z., Wang, X., 2021. A review about pretreatment of lignocellulosic biomass in anaerobic digestion: Achievement and challenge in Germany and China. J. Clean. Prod. 299, 126885. doi:10.1016/j.jclepro.2021.126885

Su, T., Zhao, D., Khodadadi, M., Len, C., 2020. Lignocellulosic biomass for bioethanol: Recent advances, technology trends, and barriers to industrial development. Curr. Opin. Green Sustain. Chem. 24, 56–60. doi:10.1016/j.cogsc.2020.04.005

Ta, D.-T., Lin, C., Minh, T., Ta, N., Chu, C., 2020. Biohythane production via single-stage anaerobic fermentation using entrapped hydrogenic and methanogenic bacteria. Bioresour. Technol. 300, 122702. doi:10.1016/j.biortech.2019.122702

Taguchi, S., Matsumoto, K., 2021. Evolution of polyhydroxyalkanoate synthesizing systems toward a sustainable plastic industry. Polym. J. 67–79. doi:10.1038/s41428-020-00420-8

Ünyay, H., Yılmaz, F., Başar, İ.A., Altınay Perendeci, N., Çoban, I., Şahinkaya, E., 2022. Effects of organic loading rate on methane production from switchgrass in batch and semi-continuous stirred tank reactor system. Biomass and Bioenergy 156, 1–11. doi:10.1016/j.biombioe.2021.106306

Upcraft, T., Tu, W., Johnson, R., Finnigan, T., Hung, N. Van, Hallett, J., Guo, M., 2021. Protein from renewable resources: mycoprotein production from agricultural residues. Green Chem. 23, 5150–5165. doi:10.1039/d1gc01021b

Usmani, Z., Sharma, M., Kumar, A., Lukk, T., Tuohy, M.G., Gong, L., Nguyen-tri, P., Goddard, A.D., Bill, R.M., Nayak, S.C., Kumar, V., 2021. Lignocellulosic biorefineries: The current state of challenges and strategies for efficient commercialization. Renew. Sustain. Energy Rev. 148, 111258. doi:10.1016/j.rser.2021.111258

Uthandi, S., Kaliyaperumal, A., Srinivasan, N., Thangavelu, K., Muniraj, I.K., Zhan, X., Gathergood, N., Gupta, V.K., 2021. Microbial biodiesel production from lignocellulosic biomass: New insights and future challenges. Crit. Rev. Environ. Sci. Technol. 1–30. doi:10.1080/10643389.2021.1877045

Valdés, G., Mendonça, R.T., Parra, C., Aggelis, G., 2020. Patterns of Lignocellulosic Sugar Assimilation and Lipid Production by Newly Isolated Yeast Strains From Chilean Valdivian Forest. Appl. Biochem. Biotechnol. 192, 1124–1146. doi:10.1007/s12010-020-03398-4

Verma, D., Kumar, N.R., Subudhi, S., 2020. Isolation and characterization of a novel photoheterotrophic strain 'Rubrivivax benzoatilyticus TERI-CHL1': Photo fermentative hydrogen production from spent effluent. Int. J. Hydrogen Energy 45, 14245–14254. doi:10.1016/j.ijhydene.2020.03.133

Voutilainen, E., Pihlajaniemi, V., Parviainen, T., 2021. Economic comparison of food protein production with single-cell organisms from lignocellulose side-streams. Bioresour. Technol. Reports 14, 100683. doi:10.1016/j.biteb.2021.100683

Walker, D.J.F., Nevin, K.P., Holmes, D.E., Rotaru, A.E., Ward, J.E., Woodard, T.L., Zhu, J., Ueki, T., Nonnenmann, S.S., McInerney, M.J., Lovley, D.R., 2020. Syntrophus conductive pili demonstrate that common hydrogen-donating syntrophs can have a direct electron transfer option. ISME J. 14, 837–846. doi:10.1038/s41396-019-0575-9

Wang, J., Yin, Y., 2022. Biological production of medium-chain carboxylates through chain elongation: An overview. Biotechnol. Adv. 55, 107882. doi:10.1016/j.biotechadv.2021.107882

Wang, Y., Jing, Y., Lu, C., Kongjan, P., Wang, J., Kumar, M., Tahir, N., Zhang, Q., 2021. A syntrophic co-fermentation model for bio-hydrogen production. J. Clean. Prod. 317, 128288. doi:10.1016/j.jclepro.2021.128288

Wei, X., Feng, J., Cao, W., Li, Q., Guo, L., 2021. Photo-biological hydrogen production by a temperature-tolerant mutant of Rhodobacter capsulatus isolated by transposon mutagenesis. Bioresour. Technol. 320, 124286. doi:10.1016/j.biortech.2020.124286

Weidener, D., Klose, H., Westarp, W.G. Von, Jupke, A., Leitner, W., María, P.D. De, Grande, P.M., 2021. Selective lignin fractionation using CO2-expanded 2-methyltetrahydrofuran (2-MTHF). Green Chem. 23, 6330–6336. doi:10.1039/d1gc01651b

Wu, Q., Guo, W., Bao, X., Meng, X., Yin, R., Du, J., Zheng, H., Feng, X., Luo, H., Ren, N., 2018. Upgrading liquor-making wastewater into medium chain fatty acid: Insights into co-electron donors, key microflora, and energy harvest. Water Res. 145, 650–659. doi:10.1016/j.watres.2018.08.046

Wu, S., Luo, G., Sun, J., Wei, W., Song, L., Ni, B., 2021a. Medium chain fatty acids production from anaerobic fermentation of waste activated sludge. J. Clean. Prod. 279, 123482. doi:10.1016/j.jclepro.2020.123482

Wu, S., Sun, J., Chen, X., Wei, W., Song, L., Dai, X., Ni, B., 2020. Unveiling the mechanisms of medium-chain fatty acid production from waste activated sludge alkaline fermentation liquor through physiological, thermodynamic and metagenomic investigations. Water Res. 169, 115218. doi:10.1016/j.watres.2019.115218

Wu, S., Wei, W., Xu, Q., Huang, X., Sun, J., Dai, X., Ni, B., 2021b. Revealing the Mechanism of Biochar Enhancing the Production of Medium Chain Fatty Acids from Waste Activated Sludge Alkaline Fermentation Liquor. ACS EST Water 1, 1014–1024. doi:10.1021/acsestwater.0c00278

Xu, D., Lin, J., Ma, R., Fang, L., Sun, S., Luo, J., 2022. Microwave pyrolysis of biomass for low-oxygen bio-oil: Mechanisms of CO2-assisted in-situ deoxygenation. Renew. Energy 184, 124–133. doi:10.1016/j.renene.2021.11.069

Xu, J., Hao, J., Guzman, J.J.L., Spirito, C.M., Harroff, L.A., Angenent, L.T., 2018. Temperature-Phased Conversion of Acid Whey Waste Into Medium-Chain Carboxylic Acids via Lactic Acid: No External e-Donor. Joule 2, 280–295. doi:10.1016/j.joule.2017.11.008

Xu, Zhangyang, Pan, C., Li, X., Hao, N., Zhang, T., Gaffrey, M.J., Pu, Y., Cort, J.R., Ragauskas, A.J., Qian, W.J., Yang, B., 2021. Enhancement of polyhydroxyalkanoate production by co-feeding lignin derivatives with glycerol in Pseudomonas putida KT2440. Biotechnol. Biofuels 1–23. doi:10.1186/s13068-020-01861-2

Xu, Zhaoxian, Xu, M., Cai, C., Chen, S., Jin, M., 2021. Microbial polyhydroxyalkanoate production from lignin by Pseudomonas putida NX-1. Bioresour. Technol. 319, 124210. doi:10.1016/j.biortech.2020.124210

Yadav, M., Paritosh, K., Vivekanand, V., 2020. Lignocellulose to bio-hydrogen: An overview on recent developments. Int. J. Hydrogen Energy 45, 18195–18210. doi:10.1016/j.ijhydene.2019.10.027

Yadav, M., Vivekanand, V., 2021. Combined fungal and bacterial pretreatment of wheat and pearl millet straw for biogas production – A study from batch to continuous stirred tank reactors. Bioresour. Technol. 321, 124523. doi:10.1016/j.biortech.2020.124523

Yan, X., Li, D., Ma, X., Li, J., 2021. Bioconversion of renewable lignocellulosic biomass into multicomponent substrate via pressurized hot water pretreatment for bioplastic polyhydroxyalkanoate accumulation. Bioresour. Technol. 339, 125667. doi:10.1016/j.biortech.2021.125667

Yang, H., Si, B., Huang, S., Liu, Z., Zhang, Y., 2020a. Effect of pH control on biohythane production and microbial structure in an innovative multistage anaerobic hythane reactor (MAHR). Int. J. Hydrogen Energy 45, 4193–4204. doi:10.1016/j.ijhydene.2019.12.046

Yang, H., Zhang, C., Lai, N., Huang, B., Fei, P., Ding, D., Hu, P., Gu, Y., 2020b. Efficient isopropanol biosynthesis by engineered Escherichia coli using biologically produced acetate from syngas fermentation. Bioresour. Technol. 296, 122337. doi:10.1016/j.biortech.2019.122337

Yang, P., Leng, L., Tan, G.A., Dong, C., Leu, S., Chen, W., Lee, P., 2018. Upgrading lignocellulosic ethanol for caproate production via chain elongation fermentation. Int. Biodeterior. Biodegrad. 135, 103–109. doi:10.1016/j.ibiod.2018.09.011

Yang, P., Tan, G.Y.A., Aslam, M., Kim, J., Lee, P.H., 2019. Metatranscriptomic evidence for classical and RuBisCO-mediated CO 2 reduction to methane facilitated by direct interspecies electron transfer in a methanogenic system. Sci. Rep. 9, 4116. doi:10.1038/s41598-019-40830-0

Yu, J., Huang, Z., Wu, P., Zhao, M., Miao, H., 2019. Performance and microbial characterization of two-stage caproate fermentation from fruit and vegetable waste via anaerobic microbial consortia. Bioresour. Technol. 284, 398–405. doi:10.1016/j.biortech.2019.03.124

Zan, X., Sun, J., Chu, L., Cui, F., Huo, S., Song, Y., Koffas, M.A.G., 2021. Improved glucose and xylose co-utilization by overexpression of xylose isomerase and/or xylulokinase genes in oleaginous fungus Mucor circinelloides. Appl. Microbiol. Biotechnol. 105, 5565–5575. doi:10.1007/s00253-021-11392-x

Zhang, C., Yang, L., Huo, S., Su, Y., Zhang, Y., 2021. Optimization of the Cell Immobilization-Based

Chain-Elongation Process for E ffi cient n - Caproate Production. ACS Sustain. Chem. Eng. doi:10.1021/acssuschemeng.0c07281

Zhang, J., Zhao, W., Zhang, H., Wang, Z., Fan, C., Zang, L., 2018. Recent achievements in enhancing anaerobic digestion with carbon-based functional materials. Bioresour. Technol. 266, 555–567. doi:10.1016/j.biortech.2018.07.076

Zhang, Q., Xu, S., Li, Y., Ding, P., Zhang, Y., Zhao, P., 2021a. Green-synthesized nickel oxide nanoparticles enhances biohydrogen production of Klebsiella sp . WL1316 using lignocellulosic hydrolysate and its regulatory mechanism. Fuel 305, 121585. doi:10.1016/j.fuel.2021.121585

Zhang, Q., Zhang, Y., Li, Y., Ding, P., Xu, S., Cao, J., 2021b. Green synthesis of magnetite nanoparticle and its regulatory effect on fermentative hydrogen production from lignocellulosic hydrolysate by Klebsiella sp. Int. J. Hydrogen Energy 46, 20413–20424. doi:10.1016/j.ijhydene.2021.03.142

Zhang, T., Jiang, D., Zhang, H., Jing, Y., Tahir, N., 2020. Comparative study on bio-hydrogen production from corn stover: Photo-fermentation, dark-fermentation and dark-photo co-fermentation. Int. J. Hydrogen Energy 45, 3807–3814. doi:10.1016/j.ijhydene.2019.04.170

Zhang, Y., Zhang, H., Lee, D., Zhang, T., Jiang, D., Zhang, Z., 2020. Effect of enzymolysis time on biohydrogen production from photo-fermentation by using various energy grasses as substrates. Bioresour. Technol. 305, 123062. doi:10.1016/j.biortech.2020.123062

Zhao, L., Wang, Z., Ren, H., Chen, C., Nan, J., Cao, G., Yang, S., Ren, N., 2021. Residue cornstalk derived biochar promotes direct bio-hydrogen production from anaerobic fermentation of cornstalk. Bioresour. Technol. 320, 124338. doi:10.1016/j.biortech.2020.124338

Zheng, S., Liu, F., Wang, B., Zhang, Y., Lovley, D.R., 2020. Methanobacterium Capable of Direct Interspecies Electron Transfer. Environ. Sci. Technol. 54, 15347−15354. doi:10.1021/acs.est.0c05525

Zhou, H., Brown, R.C., Wen, Z., 2019. Anaerobic digestion of aqueous phase from pyrolysis of biomass: Reducing toxicity and improving microbial tolerance. Bioresour. Technol. 292, 121976. doi:10.1016/j.biortech.2019.121976

Chapter 3

Acidogenic fermentation of food waste to generate electron acceptors and donors towards medium-chain carboxylic acids production

S. G. Arhin, A. Cesaro, F. Di Capua, G. Esposito

Journal of Environmental Management 348 (2023) 119379

3.1. Introduction

The evolving human population and rapid socio-economic transformations are impacting the amount of food waste produced globally (Okoro-Shekwaga et al., 2021). Estimates indicate that the global food waste production of 1.95 gigatonnes estimated for 2011 will increase to 3.62 gigatonnes in 2030 (Byun et al., 2021). In Europe, around 173 kg of food waste is generated per inhabitant per year (van der Linden and Reichel, 2020). Although there are ongoing efforts to avoid or reduce food waste production, unavoidable losses may still occur along the supply chain (Ishangulyyev et al., 2019). Hence, from a circular bioeconomy viewpoint, exploring techniques to generate value from unavoidable food waste streams is one of the most crucial challenges faced by modern society.

Over the years, various technologies, including anaerobic digestion and composting have been used to valorize food waste and avoid the negative environmental impacts of food waste decomposition in landfills. Recent estimates suggest that the annual food waste treatment infrastructure capacity in Europe is about 38 million tonnes (van der Linden and Reichel, 2020). Of this, the installed capacity for composting is about 21 million tonnes while 17 million is for anaerobic digestion. Notwithstanding, anaerobic processes are gaining increasing attention because of their economic and environmental benefits (Wang et al., 2023). Among the numerous resources potentially coming from anaerobic processes, MCCAs featuring 6–12 carbon atoms, such as caproic acid (C6) and caprylic acid (C8), have emerged more recently as attractive products from food waste (Contreras-Dávila et al., 2020; Wu et al., 2022). The growing interest in MCCAs is because they have higher energy content and market value compared to conventional anaerobic products such as SCCAs and are relatively easier to recover from the fermentation broth (Arhin et al., 2023). Additionally, as versatile platform chemicals, MCCAs have diverse industrial applications, including those as precursors for biofuels, lubricants, bioplastics, and additives, among others (Liu et al., 2022).

The process route for MCCAs biosynthesis from food waste involves two main metabolic modes, which can be performed separately in a two-stage system (Yu et al., 2019) or may occur consecutively in a single-stage bioreactor (De Groof et al., 2021). The primary or acidogenic fermentation reactions generate SCCAs (typically VFAs), which act as electron acceptors for the formation of MCCAs (Cavalcante et al., 2017). Then, with the requisite participation of an electron donor, such as ethanol or lactic acid, the carbon chain lengths of the VFAs are elongated at each cycle with two-carbon atoms via reverse β-oxidation and/or fatty acid

biosynthesis in the secondary fermentation or chain elongation phase (Angenent et al., 2016; Arhin et al., 2023). The nature and concentration of SCCAs generated in the acidogenic fermentation phase influence the chain elongation efficiency and distribution of the chain elongation products. Although different C_2–C_5 VFAs could be synthesized during acidogenic fermentation, the simultaneous accumulation of even and odd-chain VFAs would create a competition for electron donors between even- and odd-chain elongation pathways (Cavalcante et al., 2017). Moreover, to prevent excessive consumption of electron donors during chain elongation, it is advisable to steer acidogenic fermentation reactions towards the production of longer-chain VFAs (e.g., butyric acid) rather than acetic acid (Angenent et al., 2016; Cavalcante et al., 2017). Meanwhile, it has also been observed that a mixture of acetic acid and butyric acid as co-electron acceptors could stimulate more caproic acid production than using either of these acids as the sole electron acceptor (San-Valero et al., 2019). Although butyric acid could accelerate caproic acid synthesis, it has a low energy harvest and thus might have a long-term competitive disadvantage in an energy-limited microbial ecosystem (Wu et al., 2018). In contrast, acetic acid could facilitate the growth rate of chain elongation bacteria (San-Valero et al., 2019), albeit it has a longer chain elongation route and requires twice more electron donors to form caproic acid. Thus, for an efficient chain elongation process, it is crucial to ensure the appropriate balance in the type and concentration of VFAs formed during acidogenic fermentation. Besides VFAs as electron acceptors, acidogenic fermentation reactions could also be tailored towards the production of electron donors such as lactic acid and ethanol, eliminating the need for expensive exogenous electron donors and their associated environmental impacts (Zhang et al., 2022).

However, the wide and complex product spectrum of anaerobic microbial communities makes it challenging to steer acidogenic fermentation reactions selectively toward the desired intermediates for maximizing MCCAs production. A key strategy to achieve process control and influence the product spectrum and concentration during acidogenic fermentation is by regulating environmental conditions, including pH, temperature, and organic loading (Asunis et al., 2019; De Groof et al., 2021; Yang et al., 2022; Zhao et al., 2021). Uptake of the substrate by competing microbial processes will occur if the environmental conditions are not tailored to suit the desired metabolic pathway. For instance, Strazzera et al. (2021) demonstrated that the pH, temperature, and organic loading rate could influence VFAs profile and microbial community structure during acidogenic fermentation of food waste. Rasi et al. (2022) also revealed that the pH and organic loading could modulate the microbial community composition

and activities. Moreover, Zhang et al. (2023) showed that pH adjustment could regulate lactic acid conversion to VFAs during acidogenic fermentation. Although several studies have been conducted to explore the influence of operational conditions on SCCAs production from food waste for various biobased applications, reported optimal settings remain inconsistent. For example, Arras et al. (2019) reported that thermophilic fermentation of food waste at 55 °C was optimal for VFAs accumulation with butyric acid as the dominant product. However, Yang et al. (2022) observed that thermophilic fermentation at 55 °C led to the accumulation of lactic acid. These inconsistencies could be attributed partly to the differences in the fermenting microbiome. At the same time, the range of conditions examined remains limited, while some studies determined the influence of these parameters in solitary (Tang et al., 2017). Even though different environmental conditions may influence SCCAs yield, their combination may induce specific metabolic pathways that could synergistically or antagonistically impact SCCAs production. Besides that, none of these studies aimed at producing SCCAs to be used purposely for MCCAs production. However, the utility of acidogenic fermentation products in chain elongation reactions is complex and MCCAs synthesis could be remarkably affected by several factors besides the concentration of reactants such as the stoichiometric distribution of electron acceptors and donors, the butyric acid-to-acetic acid ratio, the even-to-odd chain acids ratio, among others (Bao et al., 2019; Nzeteu et al., 2022). Thus, for an efficient chain elongation process, there is a need for a systematic study of the optimal settings for regulating the formation of SCCAs to be used as reactants for microbial chain elongation.

Based on these considerations, this study aimed to determine the optimal environmental conditions, including pH, temperature, and food-to-microorganisms (F/M) ratio for regulating the formation of VFAs and lactic acid to be used purposely as electron acceptors and donors for MCCAs production. Firstly, the influence of varying pHs in the range of 4–8 on the product spectrum and concentration during acidogenic fermentation at a mesophilic temperature (35 ± 1 °C) was examined. Afterward, the optimum temperature for generating VFAs (as electron acceptors) and lactic acid (as an electron donor) was investigated by performing experiments under thermophilic settings (50 ± 1 °C). Then, with the optimum pH and temperature, the F/M ratio was increased from 1 to 6 to assess the effect of increasing the organic loading on the production of electron acceptors and donors. Lastly, a preliminary techno-economic assessment was performed to investigate the feasibility of using the intermediates generated at the optimum conditions for MCCAs production.

3.2. Materials and methods

3.2.1. Substrate and inoculum

The food waste used as a substrate in this study was obtained from a food market in Naples (Campania, Italy). The food waste consisted of fruits and vegetables (79 %), bread and bakery (6 %), pasta, rice, cereals, and flour (5 %), meat and fish (8 %), and dairy products (2 %) and was akin to the typical composition of the food waste fraction of the municipal solid waste in Italy (Ariunbaatar et al., 2014; Fisgativa et al., 2016). After homogenizing into a slurry, the food waste was kept at −20 °C for long-term storage and thawed at room temperature before experimentation. The seed sludge was a mesophilic digestate obtained from the anaerobic digester of the municipal wastewater treatment plant of Nola (Campania, Italy). To inactivate methanogens and ensure the predominance of acidogenic bacteria, the microbial consortia were heat-shocked at 105 °C for 4 h before mixing with the food waste (Ghimire et al., 2015). The characteristics of the food waste and inoculum, including the TS, VS, and COD, among others, are presented in **Table 3.1**.

Table 3.1. Characteristics of the food waste substrate and inoculum used in the study. Data represent the mean ± standard deviation calculated on three replicates.

Parameter	Food waste (substrate)	Digestate (inoculum)
pH	4.9 ± 0.0	8.9 ± 0.2
TS (g TS/L)	216.1 ± 8.7	31.8 ± 1.8
VS (g VS/L)	200.5 ± 8.2	14.6 ± 0.7
Total COD (g COD/L)	432.6 ± 26.2	-
Soluble COD (g COD/L)	126.0 ± 7.2	-
Total carbohydrates (g/L)	151.8 ± 16.9	-
Soluble carbohydrates (g/L)	84.9 ± 7.8	-
Total proteins (g/L)	21.2 ± 5.8	-
Soluble proteins (g/L)	10.4 ± 0.3	-
Total VFAs (g/L)	0.2 ± 0.0	0.8 ± 0.1
Ethanol (g/L)	0.0 ± 0.0	0.0 ± 0.0
Lactic acid (g/L)	8.5 ± 0.3	0.1 ± 0.0
Alkalinity (g $CaCO_3$/L)	-	1.6 ± 0.4

3.2.2. Acidogenic fermentation experiments

Acidogenic fermentation of the food waste was conducted in triplicates in air-tight 500 mL borosilicate glass bottles (Schott Duran, Wertheim, Germany) placed in a thermostatic water

bath to maintain the desired mesophilic (35.0 ± 1.0 °C) or thermophilic (50.0 ± 1.0 °C) temperature. To maintain the desired pH level stable during acidogenic fermentation experiments, 200 mM of potassium phosphate buffer was added to the bioreactors at the onset of each experiment. The F/M ratio was defined as the ratio of VS contained in the food waste to those of the inoculum at the onset of each fermentation test. The experiments were conducted in three groups (**Table 3.2**). In the first group, the pH varied from 4 to 8 at 35.0 ± 1.0 °C and F/M ratio of 1.0. A test condition without the buffer was used as a control, denoted as uncontrolled test. After obtaining the optimum pH in group 1, the temperature was increased to 50.0 ± 1.0 °C in group 2 tests while maintaining the F/M ratio of 1.0 to investigate SCCAs production under thermophilic conditions. Lastly, with the optimum pH and temperature from groups 1 and 2, the F/M ratio was increased from 1 to 6 in group 3 tests. Each bioreactor received 150 mL of the inoculum. After feeding the required amount of food waste, inoculum, and buffer, distilled water was added to make the working volume of 300 mL. The bioreactors were sparged with argon gas for 5 min, tightly sealed, and placed in the water bath. A set of control bioreactors with the inoculum and water only (denoted as blank) was used to monitor the SCCAs, bioethanol, and biogas produced by the sole inoculum in each stage.

Table 3.2. Description of the operating conditions of the bioreactors for the various experimental groups.

Experimental Groups	**Bioreactor**	**pH**	**Temperature (°C)**	**F/M ratio (g VS/g VS)**	**Initial concentration of food waste (g VS)**
Group 1	UNC	Uncontrolled	35 ± 1	1	2.0
	pH4	4			
	pH5	5			
	pH6	6			
	pH7	7			
	pH8	8			
Group 2	pH5T	5	50 ± 1	1	2.0
	pH6T	6			
Group 3	F/M1	6	35 ± 1	1	2.0
Mesophilic	F/M2			2	3.9
	F/M3			3	5.9
	F/M4			4	7.9
	F/M5			5	9.8
	F/M6			6	11.8
Thermophilic	F/M1T	6	50 ± 1	1	2.0
	F/M2T			2	3.9
	F/M3T			3	5.9
	F/M4T			4	7.9
	F/M5T			5	9.8

F/M6T	6	11.8

3.2.3. Conversion of the metabolites into chemical energy

To quantitatively assess and compare the relative energy balance among the metabolites produced, the amount of chemical energy in the form of COD that was harvested as carboxylic acids, ethanol, and H_2 was computed. For H_2, the COD equivalent was calculated by considering 1 mol of H_2 to correspond to 16 g of COD, while for the carboxylic acids and ethanol the specific COD conversion coefficients (i.e., 1 g of acetic, formic, and lactic acid = 1.07g COD, 1 g of propionic acid = 1.51g COD, 1 g of butyric acid = 1.82 g COD, 1 g of valeric acid = 2.04 g COD, 1 g of caproic acid = 2.21 g COD, and 1 g of ethanol = 2.09 g COD) were adopted (Wu et al., 2020).

3.2.4. Techno-economic analysis

Following the approach described in previous works (Chowdhury, 2021; Hu et al., 2023), a preliminary techno-economic analysis was conducted to assess the potential profitability of three scenarios for food waste valorization (i.e., food waste valorization into VFAs, lactic acid, or caproic acid – the most readily produced MCCA via chain elongation). A schematic representation of these scenarios is shown in **Fig. 3.1**. The analysis was based on the anticipated profit per annum, rate of return, payback period, and net present value. The capital expenditure, which is determined by the plant size, location, infrastructure, equipment, etc., and the operating expenses, which include the maintenance costs, annual licensing, employees' salaries, transportation, etc., were calculated according to previous studies (Chowdhury, 2021; Hu et al., 2023). All the relevant equations regarding the calculation of the capital and operating expenditures, rate of return, payback period, net present value, and anticipated profits are shown in **Appendix A** (**Table A3.1**). Butyric acid was assumed as the technically extractable VFA in the first scenario because of its prevalence in the study. Thus, the maximum butyric acid yield of 0.542 g COD/g VS under mesophilic conditions at pH 6 and F/M ratio of 5 (**Fig. 3.4b**) was assumed in the calculations and its market price was estimated at 1600 €/t (Atasoy et al., 2018). Similarly, lactic acid was considered as the technically extractable acid in the second scenario under thermophilic settings, and a market value of 1300 €/t (Wei et al., 2018) and yield of 0.583 g COD/g VS (**Fig. 3.4d**) was assumed. Lastly, in the third scenario focusing on utilizing the VFAs and lactic acid produced via acidogenic fermentation as reactants for

caproic acid synthesis, a secondary fermentation of the produced acids at 37 °C and pH 5.5 was assumed, and a caproic acid yield of 0.40 g/g of

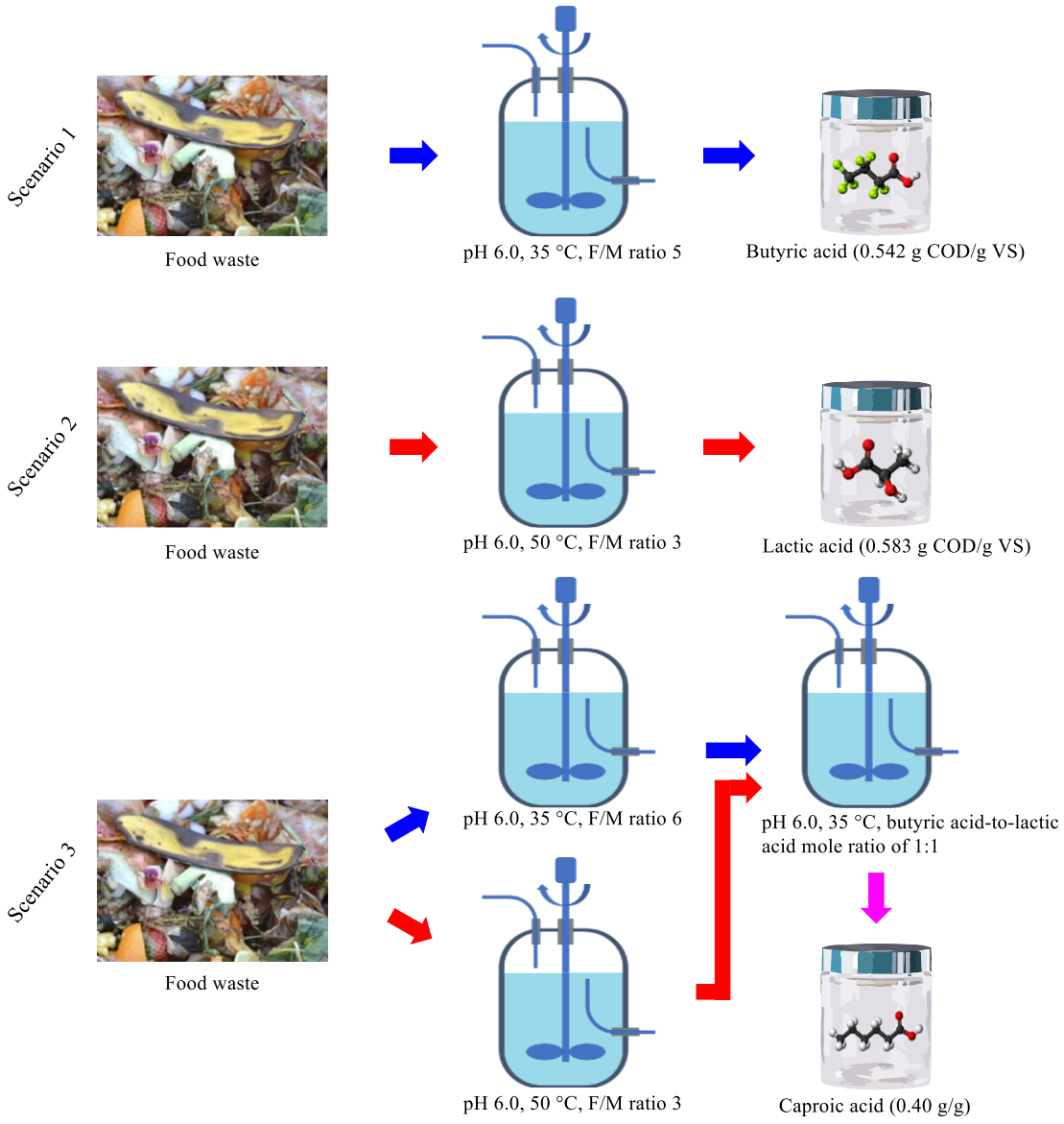

Fig. 3.1. Schematic representation of the three biorefinery scenarios for food waste valorization considered in the techno-economic analysis.

reactants (i.e., 0.50 g of butyric acid and 0.50 g of lactic acid) was considered based on the results of previous studies (Nzeteu et al., 2022). The main source of income considered in this scenario was the sales of caproic acid (3000 €/t) (Wu et al., 2020). An additional source of income emanating from gate fees paid when food waste arrives at the treatment facility (90 €/t; **Table A3.2, Appendix A**) (Chowdhury, 2021) was also considered for all three scenarios. Specific scenario-related costs such as the cost of an additional bioreactor for chain elongation (**Table A3.2, Appendix A**), carboxylic acids recovery and purification (500 €/t) (Woo and

Kim, 2019), chemicals for pH control (700 €/t) and methane inhibition during chain elongation (1000 €/t) (Wu et al., 2020) were also considered. The carboxylic acids recovery and purification approach proposed by Woo and Kim (2019) was considered because of its high product recovery efficiency (99 %), acid purity (99.5 %), and environmental friendliness compared to conventional separation processes. Briefly, the method uses hexyl acetate and nonyl acetate for the extraction of low-carbon and high-carbon-number carboxylic acids, respectively. The solvent is separated from the carboxylic acid and recycled to an extractor, and the carboxylic acid is purified via distillation. Based on previous studies, an additional heating cost of 4.18 × 103 kJ per m^3 per 1 °C increase in temperature was considered to cater for the extra heating required under thermophilic settings (Chen et al., 2019). Finally, a sensitivity analysis was conducted to assess the effect of different variables on the processes' economics. Since the global economic environment could flatulate during a plant's lifetime, the varying impacts of the capital expenditure, operating expenditure, product yield, gate fees, and selling price of products within ± 50 % at the beginning of the plant's lifetime on the process economics were independently evaluated. The net present value was used as an indicator at a 5 % discount rate and anticipated plant lifetime of 20 years (Kwan et al., 2018).

3.2.5. Analytical methods

TS, VS, and COD were analyzed according to standard methods (APHA, 2005). Carbohydrates and proteins were analyzed according to the Dubois phenol-sulfuric acid method and the Lowry method with glucose and bovine serum albumin as standards, respectively (Tabraiz et al., 2021). The solid dilution approach was employed in analyzing the total COD, carbohydrate, and protein content (Noguerol-Arias et al., 2012). The biogas accumulated in the headspace of the bioreactors was monitored with a volumetric displacement system comprised of a Drexel bottle containing 12 % NaOH (w/v) to serve as a CO_2 trap and a vessel containing distilled water to be displaced. The CO_2 trap allowed the H_2 to displace the water in the vessel to a volume equal to the amount of H_2 produced. The H_2 yield was then calculated by dividing the final cumulative H_2 production (normalized at 0 °C and 1 atm) by the amount of food waste (g VS) added at the onset of each experiment (Scotto di Perta et al., 2022). The gas composition was analyzed by a Star 3400 gas chromatograph (Varian, Palo Alto, CA, USA). Liquid samples (1 mL) were collected on days 0, 1, 2, 5, 6, and 7 to monitor the pH and concentration of SCCAs and bioethanol. For SCCAs and bioethanol analysis, the samples were centrifuged at 10,000 rpm for 10 min in a Mikro 22R centrifuge (Hettich, UK), followed by microfiltration

of the supernatant through 0.45 μm (ALWSCI Technologies, China) and 0.22 μm (AM&C, Italy) nylon membranes. The samples were then analyzed by high-performance liquid chromatography (UVD 340U HPLC system, Dionex, CA, USA) equipped with a diode array detector and a Metrosep organic acid column 250/7.8 (Metrohm, Herisau, Switzerland). The mobile phase consisted of 1% H_2SO_4 solution at a flow rate of 0.7 mL/min.

3.2.6. Statistical analysis

The statistical significance difference among the SCCAs formed in the pH experiment was assessed through a one-way analysis of variance followed by the Tukey post hoc test. The same statistical analysis was performed for the temperature, and F/M ratio experiments. IBM SPSS Statistics version 26 (IBM corporation, USA) was used for statistical analysis, and $p < 0.05$ was considered statistically significant. OriginPro 2021 (OriginLab Corporation, USA) was used for graphs and charts.

3.3. Results and discussion

3.3.1. Effect of pH on carboxylic acid production under mesophilic conditions

Fig. 3.2(a–d) shows the pH profiles, VFAs, and lactic acid yield (mg COD/g VS) during acidogenic fermentation of food waste at different pHs in the range of 4–8 under mesophilic conditions and F/M ratio of 1 (group 1 tests). In the control test without the buffer (i.e., uncontrolled pH), the pH dropped rapidly from 8.9 ± 0.1 to 6.3 ± 0.1 as carboxylic acids started to accumulate on day 1 and tended to be relatively stable thereafter (**Fig. 3.2a**). However, the pH in the bioreactors with the buffer was relatively stable throughout the experiment.

Regarding VFAs production, no significant difference ($p > 0.05$) was observed among the VFAs yield at pH 6 (719 ± 94 mg COD/g VS), pH 7 (703 ± 48 mg COD/g VS), pH 8 (696 ± 131 mg COD/g VS), and uncontrolled pH (615 ± 218 mg COD/g VS) (Fig. 2b). However, the distribution of the individual acids varied extensively. Acetic acid and butyric acid were the dominant VFAs detected in the bioreactors. The highest acetic acid yield (547 ± 100 mg COD/g VS) was observed at pH 8, while the highest butyric acid yield (448 ± 103 mg COD/g VS) was observed at pH 6 (**Fig. 3.2c**). The ratio of butyric acid-to-acetic acid (g COD/g COD equivalents) at pH 6, 7, 8, and uncontrolled pH was 2.2, 0.5, 0.2, and 0.4, respectively (**Fig. 3.2b**). A high butyric acid-to-acetic acid ratio is typically preferred for MCCAs production because butyric acid could be elongated to caproic acid via a one-cycle chain elongation process. Besides, a high butyric acid-to-acetic acid ratio would prevent unnecessary

consumption of electron donors in the chain elongation phase to generate the minimum butyric acid concentration required for MCCAs production (Angenent et al., 2016; Cavalcante et al., 2017). Therefore, even though the net VFAs yield at pH 6, 7, 8, and uncontrolled pH did not differ, the higher butyric acid-to-acetic acid ratio at pH 6 makes it a more suitable condition for generating VFAs to be used as electron acceptors for MCCAs production. This observation is consistent with the work of San-Valero et al. (2019), who demonstrated that combining 8.5 g/L of butyric acid (i.e., 15.5 g COD/L) and 5.3 g/L of acetic acid (i.e., 5.7 g COD/L, butyric acid-to-acetic acid ratio of ∼2.7 g COD/g COD) as electron acceptors could stimulate the highest caproic acid production.

At acidic pH 4 and 5, VFAs production was strongly inhibited (<50 mg COD/g VS) (**Fig. 3.2b**), and lactic acid accumulated as the dominant metabolite (**Fig. 3.2d**). This result is probably because low extracellular pH levels could inhibit the growth of VFA-producers, whereas lactic acid bacteria can tolerate acidic environments and produce antimicrobial compounds, including peptides alongside lactic acid that could impede the growth rate of VFA-producers (Tang et al., 2017; Zhang et al., 2022). The high accumulation of lactic acid at pH 5 (385 ± 53 mg COD/g VS) was consistent with the results of Tang et al. (2017), who also observed that pH 5 was the best pH for lactic acid production from food waste with three different inocula under mesophilic conditions. The lactic acid yield at pH 5 was not significantly different ($p > 0.05$) from that obtained at pH 4. However, considering that chain elongation bioreactors are typically operated at pHs ranging from 5.5 to 7.4 (Reddy et al., 2018), adopting pH 5 for lactic acid production would imply lesser chemicals input for pH adjustment at the onset of chain elongation compared to pH 4. It should also be noted that increasing the pH from 5 to 5.5 shifted the product spectrum from heterolactic fermentation to butyric-type fermentation, although the VFAs yield at pH 5.5 was lower than at pH 6 (**Fig. A3.1, Appendix A**).

Hence, based on the high lactic acid yield at pH 5 coupled with its minimal chemical demand for pH adjustment, and the high VFAs yield at pH 6 with a high butyric acid-to-acetic acid ratio, pH 5 and 6 were chosen for the subsequent experiment to maximize the yield of lactic acid and VFAs as electron donor and acceptors, respectively.

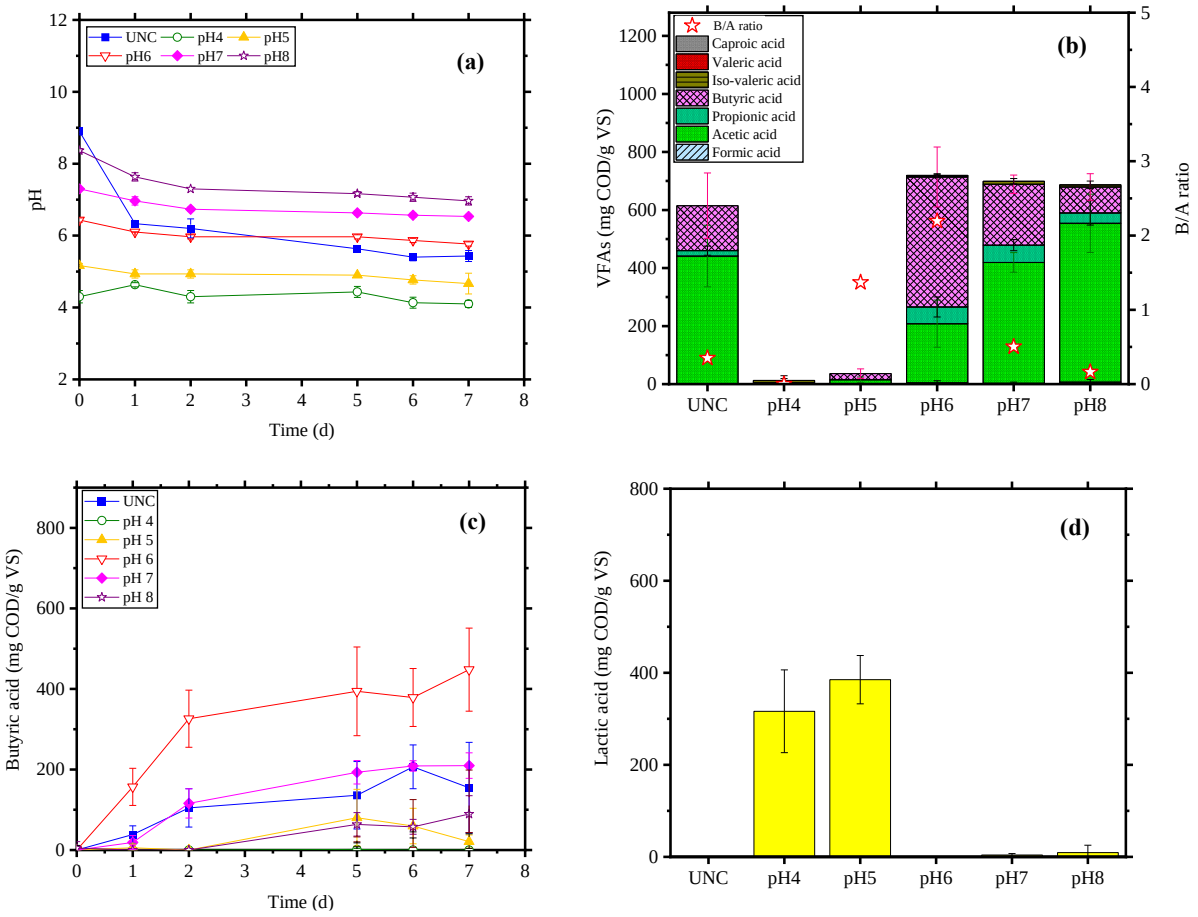

Fig. 3.2. pH profiles (a), VFAs yield (b), the evolution of butyric acid (c), and lactic acid yield (d) during acidogenic fermentation at pH 4 to 8 under mesophilic conditions and F/M ratio of 1. Carboxylic acid yields are expressed as mg COD/g VS of food waste added and the data represent the mean of three readings obtained after deducting the respective carboxylic acid produced by the sole inoculum. B/A ratio and UNC means butyric acid-to-acetic acid ratio and uncontrolled pH test, respectively. Error bars represent standard deviation.

3.3.2. Effect of temperature change on carboxylic acids production

Fig. 3.3(a and b) shows the pH profiles and carboxylic acid yield (mg COD/g VS) in the bioreactors under thermophilic conditions. As expected, the buffer ensured a stable pH throughout the fermentation process. Lactic acid was the sole product at pH 5. The lactic acid yield at pH 5 under thermophilic conditions (577 ± 36 mg COD/g VS) was 1.5 times higher than at the same pH under mesophilic conditions, indicating that the higher temperature was beneficial for lactic acid accumulation.

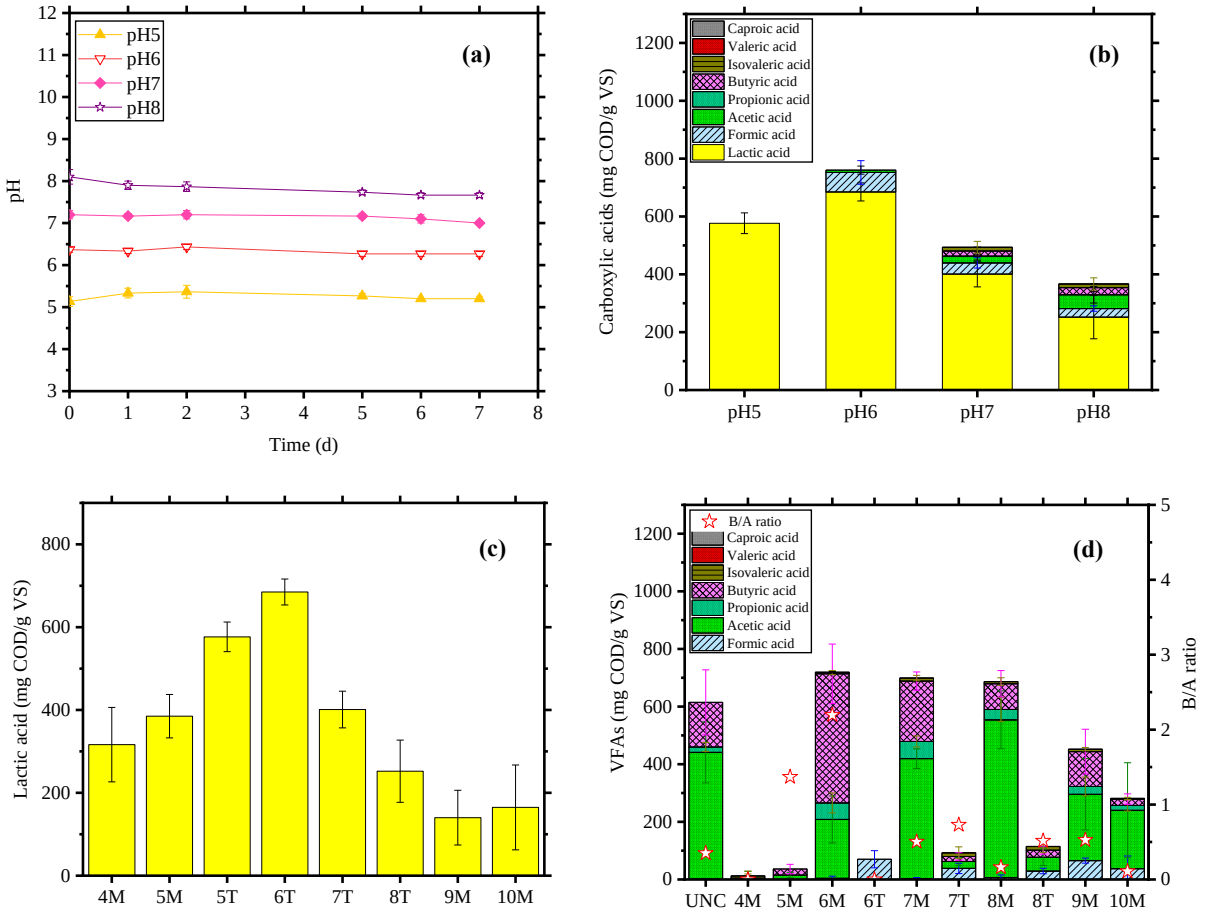

Fig. 3.3. pH profiles (a) and carboxylic acids yield (b) under thermophilic conditions at pH 5 to 8 and F/M ratio of 1, and lactic acid yield (c) and VFAs yield (d) under both thermophilic and mesophilic conditions. Carboxylic acid yields are expressed as mg COD/g VS of food waste added and the data represent the mean of three readings obtained after deducting the respective carboxylic acid produced by the sole inoculum. 4M implies pH 4 under mesophilic conditions, 5T implies pH 5 under thermophilic conditions, and so on. B/A ratio and UNC means butyric acid-to-acetic acid ratio and uncontrolled pH test, respectively. Error bars represent standard deviation.

Surprisingly, switching from mesophilic to thermophilic fermentation at pH 6 shifted the dominant product spectrum from butyrate-type fermentation to heterolactic fermentation. The lactic acid yield at pH 6 (684 ± 34 mg COD/g VS) was almost twice as much as that observed at pH 5 under mesophilic conditions. Moreover, the observed lactic acid yield at pH 6 was higher than the maximum values reported in the literature (**Table 3.3**). Considering that the VFAs yield at pH 6 to 8 did not differ significantly ($p > 0.05$) during the mesophilic experiments, additional experiments were performed at pH 7 and 8 under thermophilic settings

to ascertain the product spectrum. Nonetheless, pH 7 and 8 also yielded lactic acid as the dominant metabolite, which made up about 81 % and 69 % of the total carboxylic acids, respectively (**Fig. 3.3b**). These results imply that thermophilic fermentation at pH 5–8 selectively enhanced lactic acid accumulation over VFAs production. The observed predominance of lactic acid under thermophilic conditions may be because compared to mesophilic fermentation, thermophilic fermentation specifically promoted the proliferation of lactic acid bacteria over other functional groups as observed in previous studies (Yang et al., 2022).

Table 3.3. Comparison of the maximum lactic acid yield with the results of some recent studies on acidogenic fermentation of food waste for lactic acid production.

Food waste source	Inoculum source	Fermentation mode	Optimum operating conditions	Maximum lactic acid yield [a]	Lactic acid selectivity (%) [b]	Reference
Food market	Methanogenic sludge	Batch	pH 6.0, temperature 50 ± 1 ° C, F/M ratio of 1 g VS/g VS	684 ± 34 mg COD/g VS	90	This study
Simulated food waste	Methanogenic sludge	Batch	pH 6.0, temperature 50° C	590 ± 22 mg COD/g VS	87	Bühlmann et al. (2022)
Simulated food waste	Indigenous microbes in food waste	Semi-continuous	pH 5.5, temperature 52 ± 1 ° C, organic load rate (OLR) 19 g VS/(L·d)	610 mg COD/g VS	89	Yang et al. (2022)
Canteen	Microorganisms from Fresh FW	Batch	pH 5.0, temperature 37 ° C	524 mg COD/g TS	78	Tang et al. (2017)
Simulated food waste	Indigenous microbes in food waste	Batch	Uncontrolled pH, temperature 37 ° C, F/M ratio of 4 g VS/g VS	224 mg COD/g VS	93	Pau et al. (2022)
Household food waste	Axenic culture of *Lactobacillus rhamnosus* ATCC 7469	Batch	pH 6.8, temperature 37 ° C, 5–30% inoculum volume	524 mg COD/TCOD	N.A. [c]	Song et al. (2022)
Simulated food waste	Methanogenic sludge	Semi-continuous	Uncontrolled pH, temperature 36 ± 1 ° C, OLR 11.75 g VS/(L·d)	449 mg COD/g VS	84	Wang et al. (2021)

[a] Reported lactic acid yields have been converted to COD equivalents.

[b] Based on the net carboxylic acids yield.

[c] Not available

Combining the results of the mesophilic and thermophilic experiments revealed that the test performed at pH 6 under thermophilic conditions resulted in the highest lactic acid yield (**Fig. 3.3c**), whereas the test at pH 6 and mesophilic conditions yielded the highest VFAs concentration and butyric acid-to-acetic acid ratio (**Fig. 3.3d**). Hence, thermophilic fermentation and mesophilic fermentation at pH 6 were investigated further in the subsequent experiments by increasing the F/M ratio from 1 to 6 as these conditions would be beneficial to obtain electron acceptors and donors for subsequent use in chain elongation.

3.3.3. Effect of increasing food-to-microorganisms ratio on carboxylic acids production under mesophilic and thermophilic conditions

Fig. 3.4(a–c) shows the effect of increasing the F/M ratio on the pH, yield of carboxylic acids (mg COD/g VS), and total concentration (g COD/L) under mesophilic conditions at pH 6. Even though the operational pH dropped slightly with increasing F/M ratio (Fig. 4a), the F/M ratio had no significant ($p > 0.05$) impact on the yield of carboxylic acids, which remained in the range of 610 ± 45 to 719 ± 94 mg COD/g VS. Conversely, increasing the F/M ratio impacted the product spectrum, resulting in the butyric acid-to-acetic acid ratio increasing from 2.2 at an F/M ratio of 1 to 13.8 at an F/M ratio of 6 (**Fig. 3.4b**). Moreover, at high F/M ratios of 5 and 6, caproic acid began to accumulate in the bioreactors, reaching 39 ± 5 mg COD/g VS (~2 ± 0 g COD/L) at an F/M ratio of 6. These results suggest that high F/M ratios favoured the synthesis of C_4 and C_6 carboxylic acids during acidogenic fermentation. The net concentration of carboxylic acids (including caproic acid) reached 24 ± 2 g COD/L at an F/M ratio of 6 with acetic acid and butyric acid making up ~ 6 % and 81 %, respectively (**Fig. 3.4c**). While it was possible to further increase the concentrations of these acids by increasing the F/M ratio, at F/M ratios of 5 and 6 the pH dropped to 5 on day 1 and lactic acid began to accumulate in the bioreactors, reaching 59 ± 12 mg COD/g VS (~2 ± 0 g COD/L) at an F/M ratio of 6. Although the pH recovered slightly on day 5 at F/M 6, possibly due to the proton-consuming nature of the lactic acid-guided chain elongation process that led to the synthesis of caproic acid under this condition (**Eq. 3.1**), the F/M ratio was not increased further as a further drop in pH in the initial days could shift the product spectrum from butyric-type to heterolactic fermentation (Tang et al., 2017; Zhou et al., 2018).

$$C_3H_5O_3^- + C_4H_7O_2^- + H^+ \rightarrow C_6H_{11}O_2^- + H_2O + CO_2 \quad \textbf{(3.1)}$$

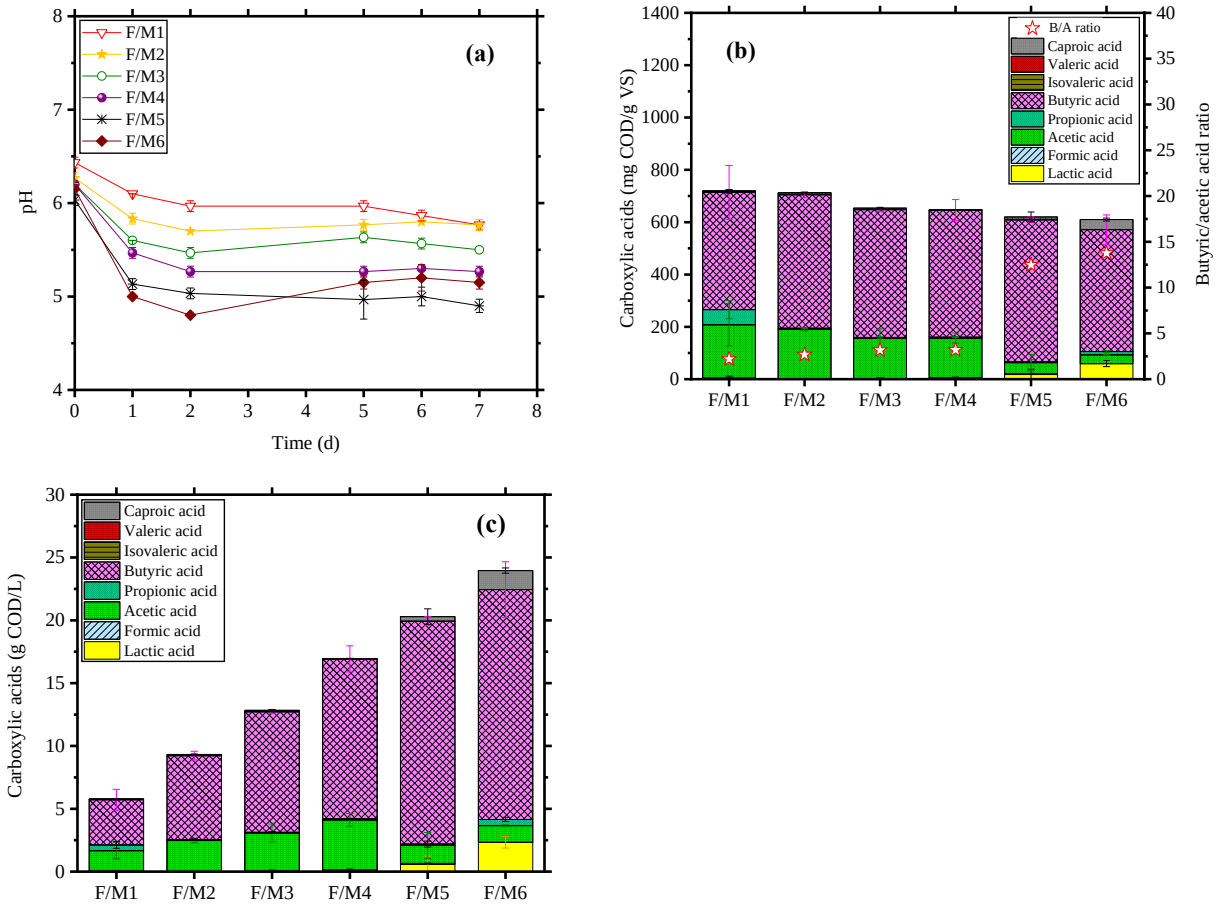

Fig. 3.4. pH profiles (a), carboxylic acids yield (mg COD/g VS) (b), and net carboxylic acids concentration in (g COD/L) (c) during mesophilic fermentation at pH 6 under varying F/M ratios of 1–6. B/A ratio means butyric acid-to-acetic acid ratio. Error bars represent standard deviation.

Overall, the positive correlation between F/M ratio and the butyric acid-to-acetic acid ratio observed under mesophilic conditions could be attributed to the fact that under high organic loading, anaerobic microbiomes would synthesize more butyric acid to make up for the large amounts of NADH produced via glycolysis as butyric acid synthesis could regenerate NAD^+ to help maintain the intracellular NADH/NAD^+ balance (Yu et al., 2019). Also, the synthesis of caproic acid at F/M ratios of 5 and 6 could be attributed to the accumulation of lactic acid under these conditions, which acted as the electron donor to drive the conversion of butyric acid to caproic acid. However, a significant fraction of the butyric acid was not converted to caproic acid due to the low concentration of lactic acid, highlighting the relevance of the electron donor to acceptor ratio to caproic acid synthesis.

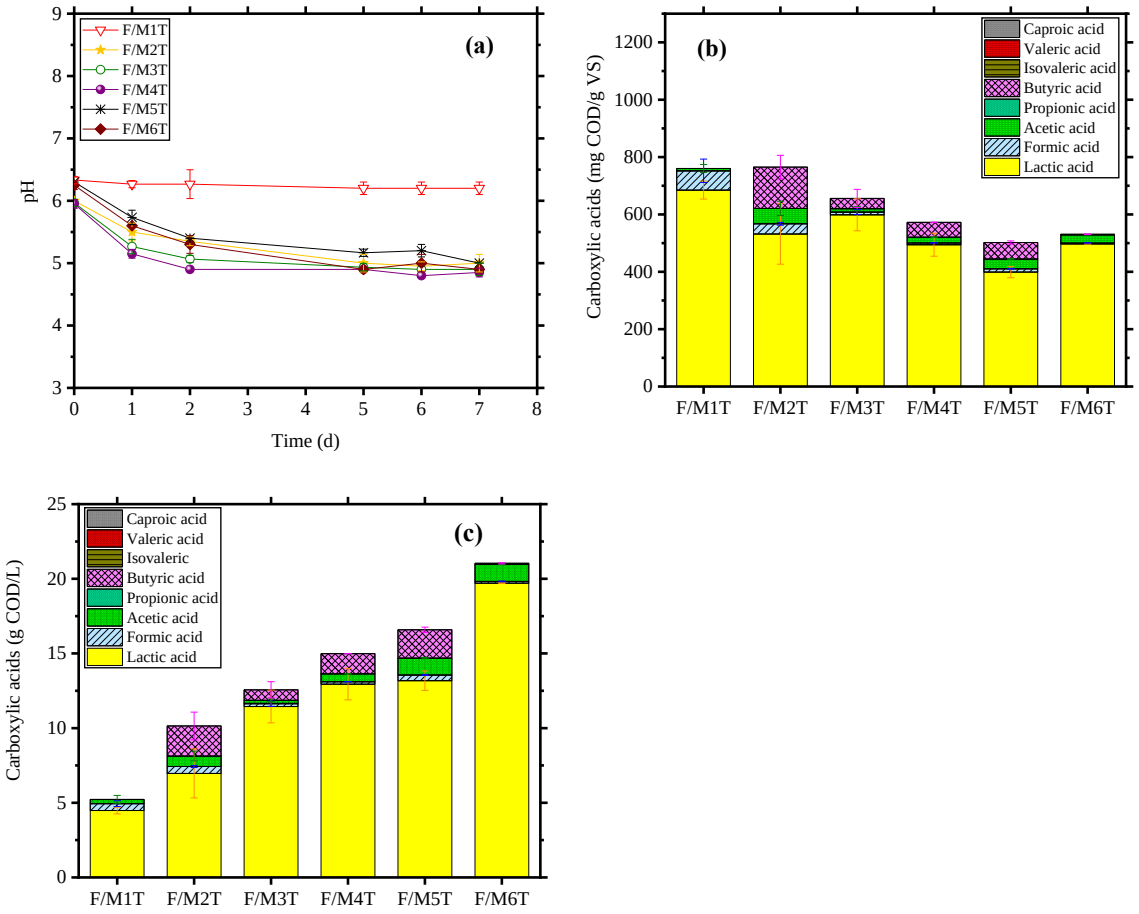

Fig. 3.5. pH profiles (a), carboxylic acids yield (mg COD/g VS) (b), and net carboxylic acids concentration in (g COD/L) (c) during thermophilic (T) fermentation at pH 6 under varying F/M ratios of 1–6. Error bars represent standard deviation.

Fig. 3.5(a–c) shows the influence of increasing F/M ratios on the pH, carboxylic acids yield (mg COD/g VS), and total concentration (g COD/L) under thermophilic conditions at pH 6. As expected, the operational pH dropped slightly with increasing F/M ratio (**Fig. 3.5a**). However, unlike mesophilic fermentation, the F/M ratio significantly ($p < 0.05$) impacted carboxylic acid yield under thermophilic settings (**Fig. 3.5b**). Even though there was no significant difference in the carboxylic acids yield among F/M ratios of 1, 2, and 3 ($p > 0.05$), higher F/M ratios (above 3) led to significant reductions in the yield of carboxylic acids. Moreover, lactic acid yields at F/M ratios of 1 and 3 did not differ significantly ($p > 0.05$), suggesting that an F/M ratio of 3 could be applied to treat the food waste to generate a high lactic acid concentration (11 ± 1 g COD/L, **Fig. 3.5c**) without affecting the yield per g VS of food waste added. However, beyond the F/M ratio of 3, lactic acid yield decreased significantly ($p < 0.05$). The poor response of the microbiome to the high F/M ratios of 4–6 under thermophilic conditions may

be attributed to the possibility that thermophilic fermentation lowered the relative abundance and diversity of the microbial community as observed in several previous studies (Bühlmann et al., 2022; Yang et al., 2022). Thus, the metabolic burden to break down and convert the food waste into carboxylic acids was distributed among a reduced community size, which led to the low yield observed at high organic loading (i.e., F/M ratios of 4–6).

3.3.4. Co-generation of hydrogen gas and ethanol during acidogenic fermentation

Besides carboxylic acids, other valuable metabolites, including H_2 and ethanol were synthesized during the open culture acidogenic fermentation, which could also serve as intermediates for MCCAs production. **Table 3.4** shows the H_2 and ethanol yield in the different bioreactors in the three experimental groups. Under mesophilic conditions, the highest H_2 yield (252 ± 20 mL H_2/g VS, i.e., 25.0 % relative COD equivalents) was observed at pH 6, while pH 8 generated the lowest yield (75 ± 15 mL H_2/g VS, i.e., 7.6 % relative COD equivalents). However, under thermophilic conditions, H_2 production was generally inhibited and less than 7 % of the COD in the food waste was converted into H_2. The low H_2 yield under thermophilic conditions is probably because lactic acid was the main product under thermophilic settings in the bioreactors (**Eqs. 3.2 and 3.3**) except at an F/M ratio of 2 (**Fig. 3.3d**), in which a substantial fraction of the lactic acid was consumed to generate butyric acid (**Eq. 3.4**), leading to a significantly higher H_2 yield (137 ± 14 mL/g VS or 12.7% relative COD equivalents, $p < 0.05$).

$$C_6H_{12}O_6 \rightarrow 2CH_3CHOHCOOH \quad \textbf{(3.2)}$$

$$2C_6H_{12}O_6 \rightarrow 3CH_3COOH + 2CH_3CHOHCOOH \quad \textbf{(3.3)}$$

$$2CH_3CHOHCOOH \rightarrow CH_3CH_2CH_2COOH + 2CO_2 + 2H_2 \quad \textbf{(3.4)}$$

$$C_6H_{12}O_6 + 2H_2O \rightarrow 2CH_3COOH + 2CO_2 + 4H_2 \quad \textbf{(3.5)}$$

$$C_6H_{12}O_6 \rightarrow CH_3CH_2CH_2COOH + 2CO_2 + 2H_2 \quad \textbf{(3.6)}$$

$$4H_2 + 2CO_2 \rightarrow CH_3COOH + 2H_2O \quad \textbf{(3.7)}$$

$$C_6H_{12}O_6 \rightarrow 3CH_3COOH \quad \textbf{(3.8)}$$

$$C_6H_{12}O_6 + 2H_2 \rightarrow 2CH_3CH_2COOH + 2H_2O \quad \textbf{(3.9)}$$

Table 3.4. Comparison of the fraction of COD converted to carboxylic acids, H_2, and ethanol at the end of the acidogenic fermentation experiments under different operational conditions. ΔH_2 represents the ratio between the experimental (exp.) and theoretical (theor.) H_2 yields, calculated as discussed in section 3.4. The final chemical energy in the form of COD recovered as H_2, ethanol, and carboxylic acids is reported as mg H_2-COD/g VS, mg EtOH-COD/g VS, and mg CA-COD/g VS, respectively. ΔE_1 and ΔE_2 show the amount of chemical energy recovered as H_2 (mg H_2-COD) and ethanol (mg EtOH-COD) in comparison with that obtained as carboxylic acids (mg CA-COD), respectively. ∑COD represent the total amount of chemical energy recovered as H_2, carboxylic acids, and ethanol.

Exp. Groups	Reactors	H_2 yield (mL H_2/g VS)		ΔH_2	H_2 yield (mg H_2-COD/g VS) [a]	Ethanol yield (mg EtOH-COD/g VS) [a]	Carboxylic acids yield (mg CA-COD/g VS) [a]	ΔE_1 (mg H_2-COD /mg CA-COD) [b]	ΔE_2 (mg EtOH-COD /mg CA-COD) [c]	∑COD (mg COD/g VS)
		Exp.	Theor.							
Group 1	UNC	219 ± 28	343 ± 105	64 %	156 ± 20	19 ± 4	615 ± 218	25.4 %	3.1 %	790
	pH4	90 ± 33	N/A [d]	N/A	65 ± 24	0 ± 0	324 ± 83	20.1 %	0.0 %	389
	pH5	138 ± 16	N/A	N/A	99 ± 12	0 ± 0	424 ± 36	23.3 %	0.0 %	523
	pH6	252 ± 20	244 ± 27	103 %	180 ± 13	4 ± 4	719 ± 94	25.0 %	0.6 %	903
	pH7	167 ± 41	321 ± 25	52 %	120 ± 30	0 ± 0	703 ± 48	17.1 %	0.0 %	823
	pH8	75 ± 15	388 ± 72	19 %	53 ± 11	0 ± 0	696 ± 131	7.6 %	0.0 %	748
Group 2	pH5T	27 ± 23	N/A	N/A	20 ± 16	0 ± 0	577 ± 36	3.5 %	0.0 %	597
	pH6T	38 ± 19	N/A	N/A	27 ± 17	69 ± 11	758 ± 81	3.6 %	9.1 %	854
Group 3	F/M1	252 ± 20	244 ± 27	103 %	180 ± 13	4 ± 4	719 ± 94	25.0 %	0.6 %	903
Mesophilic	F/M2	227 ± 1	274 ± 14	83 %	162 ± 1	16 ± 12	713 ± 32	22.7 %	2.2 %	890
	F/M3	238 ± 9	244 ± 25	98 %	169 ± 6	18 ± 14	654 ± 36	25.8 %	2.8 %	841
	F/M4	241 ± 9	241 ± 24	100 %	172 ± 6	13 ± 2	648 ± 59	26.5 %	2.0 %	833
	F/M5	139 ± 20	181 ± 24	77 %	100 ± 14	3 ± 0	621 ± 48	16.1 %	0.5 %	715
	F/M6	107 ± 14	151 ± 15	71 %	76 ± 10	2 ± 1	610 ± 45	12.5 %	0.3 %	688
Thermophilic	F/M1T	38 ± 19	N/A	N/A	27 ± 17	69 ± 11	758 ± 18	3.6 %	9.1 %	854
	F/M2T	137 ± 14	121 ± 16	113 %	98 ± 10	4 ± 1	771 ± 62	12.7 %	0.5 %	873
	F/M3T	30 ± 15	18 ± 13	167 %	21 ± 11	9 ± 4	640 ± 29	3.3 %	1.4 %	670
	F/M4T	21 ± 4	28 ± 0	75 %	15 ± 3	6 ± 1	572 ± 39	2.6 %	1.0 %	593
	F/M5T	48 ± 15	40 ± 2	120 %	34 ± 11	16 ± 1	502 ± 27	6.8 %	3.2 %	552
	F/M6T	16 ± 1	20 ± 0	80 %	12 ± 1	14 ± 0	531 ± 1	2.3 %	2.6 %	557

[a] Calculated as described in section 2.3, [b] CA= carboxylic acids, [c] EtOH = ethanol, [d] N/A = not applicable.

Overall, the high H_2 production could be associated with the accumulation of butyric acid as bioreactors with high butyric acid yields had higher H_2 yields compared to their counterparts with high acetic acid accumulation. In principle, acetic- and butyric-type fermentation of hexose-type carbohydrates would yield equal moles of H_2 (2 mol) per mole of either acid formed (**Eqs. 3.5** and **3.6**) (Akhlaghi et al., 2019). However, in open culture acidogenic fermentation, additional pathways for acetic acid synthesis or H_2 consumption, including autotrophic/heterotrophic homoacetogenesis (**Eqs. 3.7** and **3.8**), propionic acid fermentation (**Eq. 3.9**), and heterofermentative lactic acid and acetic acid production (**Eq. 3**), among others, may compete and sometimes overlap the hydrogenogenic pathways. Particularly, when methanogenic activities are suppressed (**Fig. A3.2, Appendix A**), homoacetogens could consume H_2 alongside CO_2 to generate acetic acid (**Eq. 7**). While the complexity of the biochemical process makes it difficult to quantify the specific contributions of individual metabolic pathways to the metabolites formed, the theoretical H_2 yield could be stoichiometrically calculated by considering the main processes related to H_2 production/consumption and the measured soluble metabolites. As depicted in **Table 3.4**, in bioreactors with butyric acid as the dominant product (i.e., pH 6 in group 1 and F/M ratios of 1–6 under mesophilic conditions in group 3), the ratio between the experimental and theoretical H_2 yield showed relatively high values, ranging from 71 to 103 %, which suggests that other metabolic pathways had minimal contributions to H_2 production/consumption. In contrast, the experimental H_2 yield ranged from 19 to 64 % of the theoretical values in bioreactors with acetic acid as the main VFA (i.e., controlled pH, pH 7, and pH 8 in group 1), which implies that a substantial proportion of the measured acetic acid may have been generated via other pathways. Thus, the potential formation of acetic acid via antagonistic pathways to hydrogenogenic reactions such as autotrophic homoacetogenesis, being supported by the relatively low CO_2 concentration in the biogas, especially at pH 8 (**Fig. A3.2, Appendix A**), could explain why butyric acid and not acetic acid accumulation aligned with high H_2 production.

Regarding ethanol, its production was notably low throughout the study with less than 10 % COD equivalents (**Table 3.4**). Under mesophilic conditions, the highest ethanol yield was observed under the uncontrolled pH condition, reaching only 19 ± 4 mg COD/g VS (i.e., 3.1 % relative COD conversion), while the highest yield under thermophilic conditions was at pH 6 and F/M ratio of 1, reaching 69 ± 11 mg COD/g VS (i.e., 9.1 % relative COD conversion).

3.3.5. Potential application for medium-chain carboxylic acid production

Following the approach discussed in section 3.2.4, the potential profitability of three biorefinery scenarios for food waste valorization was assessed based on the experimental yield of SCCAs obtained in the present study. The results of the techno-economic analysis in terms of the potential profits, rate of return, payback period, and net present value are graphically illustrated in **Fig. 3.6**, with further details in **Appendix A (Table A3.2)**. Overall, the three scenarios showed positive net present values (i.e., net present values > 0), which implies that all three production regimes would be profitable (Hu et al., 2023). Moreover, the principle of economy of scale was applicable in all three scenarios with larger plant capacities, seemingly, more profitable than smaller-scale plants. In the first scenario aimed at butyric acid synthesis, it was estimated that about 3.7–6.2 kt/y of butyric acid could be generated from the 60 to 100 kt/y plant, which could lead to a profit of about 395–421 €/t VS/y with rate of return, payback period, and net present value ranging from 13 to 17 %, 8 to 6 y, and 22 to 55 million euros, respectively. Similarly, in the second scenario, it was estimated that about 6.8–11.4 kt/y of lactic acid could be produced from the 60 to 100 kt/y plant, generating a profit of about 395–422 €/t VS/y with rate of return, payback period, and net present value from 13 to 17 %, 8 to 6 y, and 23 to 55 million euros, respectively. Even though the net product yield was higher under this scenario, the energy cost required to maintain the operating temperature at a thermophilic setting was a key cost element, making up about 15 % of the annual operating expenditure. Lastly, in the third scenario, it was estimated that about 2.2–3.6 kt/y of caproic acid could be generated leading to a profit of about 442–468 €/t VS/y with rate of return, payback period, and net present value from 14 to 18 %, 6 to 7 y, and 27 to 163 million euros.

Although the three scenarios seem profitable under the assumptions made, in principle, the extraction and purification of pure butyric acid and lactic acid from the mixed constituents, including other SCCAs, solid particulates, salts, microbes, etc., could pose a significant limitation to the scalability of the process from technical and economic viewpoints due to their high hydrophilicities (miscible in water) and the potential for the formation of water-acid azeotropes (Ramos-Suarez et al., 2021; Zhu et al., 2021). In contrast, the use of these acids as intermediates for producing caproic acid with a solubility of 10.82 g/L in water (Arhin et al., 2023), could provide a technical edge over the other products as it could be more readily separated from the fermentation broth. However, it is crucial to tailor the acidogenic fermentation reactions towards intermediates that are beneficial to caproic acid synthesis to maximize the profitability of the process. For instance, the high accumulation of odd-chain

electron acceptors such as propionic acid in the acidogenic fermentation phase could diverge carbon flux from caproic acid (Vonk et al., 2020) thus limiting the process output and overall profitability. As shown in the sensitivity analysis (**Fig. A3.3, Appendix A**), the main variables that could negatively impact the economics of the three food waste valorization scenarios were the operating expenses, the selling price of the products, gate fees, and the product yield. In the case of caproic acid production, a 50 % reduction in the estimated caproic acid yield, for example, could render the process unprofitable (net present value of −4.9 million euros) at a plant processing capacity of 60 kt/y (Fig. S3c). In summary, while SCCAs production from food waste is a promising biorefinery route, their use as reactants for MCCAs synthesis could enhance the economic gains of food waste biorefinery, offering a sustainable route to a circular bioeconomy. Yet, it is vital to design the primary fermentation process to enhance the synthesis of intermediates that are beneficial to the desired chain elongation pathway.

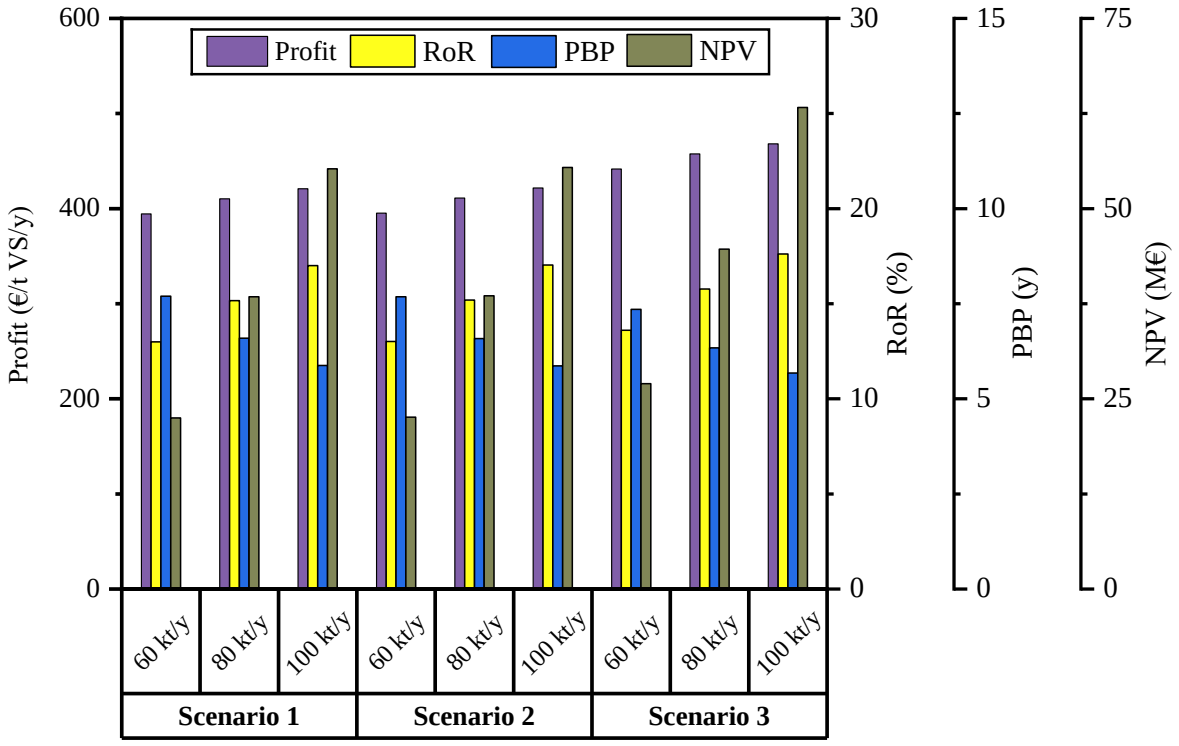

Fig. 3.6. Average potential profit, rate of return (RoR), payback period (PBP), and net present value (NPV) attainable at plant capacities of 60, 80, and 100 kt/y by valorizing food waste into lactic, butyric, and caproic acid. The profits are expressed as € per tonne VS per year and were calculated by diving the net annual profits by the quantity (in tonnes of VS) of food waste valorized. M€ implies million euros.

3.4. Conclusions

Manipulating the pH, temperature, and organic loading during acidogenic fermentation of food waste is a crucial process lever for regulating the formation of electron acceptors and donors in view of their utilization for MCCAs synthesis. The following conclusions could be drawn from the results of the study:

- Mesophilic fermentation at pH 6 favours the accumulation of VFAs as electron acceptors, yielding 719 ± 94 mg COD/g VS of VFAs with a butyric acid-to-acetic acid ratio of 2.2.
- Thermophilic fermentation at pH 6 yielded lactic acid (684 ± 34 mg COD/g VS) as an electron donor for potential MCCAs production.
- A high F/M ratio of 6 g VS/g VS could be applied to generate 22 ± 2 g COD/L of electron acceptors alongside 2 ± 0 g COD/L of caproic acid under mesophilic settings.
- F/M ratios above 3 g VS/g VS reduced lactic acid yield under thermophilic conditions.
- Based on the outcome of a preliminary techno-economic analysis, converting lactic acid and VFAs generated during acidogenic fermentation to MCCAs presents a technical and economically promising route for food waste valorization and could unlock 442 to 468 €/t VS/y.

References

Akhlaghi, M., Boni, M.R., Polettini, A., Pomi, R., Rossi, A., Gioannis, G. De, Muntoni, A., Spiga, D., 2019. Fermentative H2 production from food waste: Parametric analysis of factor effects. Bioresour. Technol. 276, 349–360. doi:10.1016/j.biortech.2019.01.012

Angenent, L.T., Richter, H., Buckel, W., Spirito, C.M., Steinbusch, K.J.J., Plugge, C.M., Strik, D.P.B.T.B., Grootscholten, T.I.M., Buisman, C.J.N., Hamelers, H.V.M., 2016. Chain Elongation with Reactor Microbiomes: Open-Culture Biotechnology To Produce Biochemicals. Environ. Sci. Technol. 50, 2796−2810. doi:10.1021/acs.est.5b04847

APHA, 2005. Standard Methods for the Examination of Water and Wastewater, 21st ed. American Public Health Association/American Water Works Association/Water Environment Federation, American Public Health Assn: Washington, DC.

Arhin, S.G., Cesaro, A., Capua, F. Di, Esposito, G., 2023. Recent progress and challenges in biotechnological valorization of lignocellulosic materials: Towards sustainable biofuels and platform chemicals synthesis. Sci. Total Environ. 857, 159333. doi:10.1016/j.scitotenv.2022.159333

Ariunbaatar, J., Panico, A., Frunzo, L., Esposito, G., Lens, P.N.L., Pirozzi, F., 2014. Enhanced anaerobic digestion of food waste by thermal and ozonation pretreatment methods. J. Environ. Manage. 146, 142–149. doi:10.1016/j.jenvman.2014.07.042

Arras, W., Hussain, A., Hausler, R., Guiot, S.R., 2019. Mesophilic, thermophilic and hyperthermophilic acidogenic fermentation of food waste in batch: Effect of inoculum source. Waste Manag. 87, 279–287. doi:10.1016/j.wasman.2019.02.011

Asunis, F., Gioannis, G. De, Isipato, M., Muntoni, A., Polettini, A., Pomi, R., Rossi, A., 2019. Control of fermentation duration and pH to orient biochemicals and biofuels production from cheese whey. Bioresour. Technol. 289, 121722. doi:10.1016/j.biortech.2019.121722

Atasoy, M., Owusu-Agyeman, I., Plaza, E., Cetecioglu, Z., 2018. Bio-based volatile fatty acid production and recovery from waste streams: Current status and future challenges. Bioresour. Technol. 268, 773–786. doi:10.1016/j.biortech.2018.07.042

Bao, S., Wang, Q., Zhang, P., Zhang, Q., Wu, Y., Li, F., Tao, X., Wang, S., Nabi, M., Zhou, Y., 2019. Effect of acid/ethanol ratio on medium chain carboxylate production with different VFAs as the electron acceptor: Insight into carbon balance and microbial community. Energies 12, 3720. doi:10.3390/en12193720

Bühlmann, C.H., Mickan, B.S., Tait, S., Batstone, D.J., Mercer, G.D., Bahri, P.A., 2022. Lactic acid from mixed food waste fermentation using an adapted inoculum: Influence of pH and temperature regulation on yield and product spectrum. J. Clean. Prod. 373, 133716. doi:10.1016/j.jclepro.2022.133716

Byun, J., Kwon, O., Park, H., Han, J., 2021. Food waste valorization to green energy vehicles: sustainability assessment. Energy Environ. Sci. 14, 3651. doi:10.1039/d1ee00850a

Cavalcante, W. de A., Leitão, R.C., Gehring, T.A., Angenent, L.T., Santaella, S.T., 2017. Anaerobic fermentation for n-caproic acid production: A review. Process Biochem. 54, 106–119. doi:10.1016/j.procbio.2016.12.024

Chen, R., Wen, W., Jiang, H., Lei, Z., Li, M., Li, Y.Y., 2019. Energy recovery potential of thermophilic high-solids co-digestion of coffee processing wastewater and waste activated sludge by anaerobic membrane bioreactor. Bioresour. Technol. 274, 127–133. doi:10.1016/j.biortech.2018.11.080

Chowdhury, T.H., 2021. Technical-economical analysis of anaerobic digestion process to produce clean energy. Energy Reports 7, 247–253. doi:10.1016/j.egyr.2020.12.024

Contreras-Dávila, C.A., Carrión, V.J., Vonk, V.R., Buisman, C.N.J., Strik, D.P.B.T.B., 2020. Consecutive lactate formation and chain elongation to reduce exogenous chemicals input in repeated-batch food waste fermentation. Water Res. 169, 115215. doi:10.1016/j.watres.2019.115215

De Groof, V., Coma, M., Arnot, T., Leak, D.J., Lanham, A.B., 2021. Selecting fermentation products for food waste valorisation with HRT and OLR as the key operational parameters. Waste Manag. 127, 80–89. doi:10.1016/j.wasman.2021.04.023

Fisgativa, H., Tremier, A., Dabert, P., 2016. Characterizing the variability of food waste quality: A need for efficient valorisation through anaerobic digestion. Waste Manag. 50, 264–274. doi:10.1016/j.wasman.2016.01.041

Ghimire, A., Frunzo, L., Pontoni, L., d'Antonio, G., Lens, P.N.L., Esposito, G., Pirozzi, F., 2015. Dark fermentation of complex waste biomass for biohydrogen production by pretreated thermophilic anaerobic digestate. J. Environ. Manage. 152, 43–48. doi:10.1016/j.jenvman.2014.12.049

Hu, Y., Liu, S., Wang, Xiaofan, Zhang, S., Hu, T., Wang, Xin, Wang, C., Wu, J., Xu, L., Xu, G., Hu, F., 2023. Enhanced anaerobic digestion of kitchen waste at different solids content by alkali pretreatment and bentonite addition: Methane production enhancement and microbial mechanism. Bioresour. Technol. 369, 128369. doi:10.1016/j.biortech.2022.128369

Ishangulyyev, R., Kim, S., Lee, S.H., 2019. Understanding Food Loss and Waste—Why Are We Losing and Wasting Food? Foods 8, 297. doi:10.3390/foods8080297

Kwan, T.H., Hu, Y., Lin, C.S.K., 2018. Techno-economic analysis of a food waste valorisation process for lactic acid, lactide and poly(lactic acid) production. J. Clean. Prod. 181, 72–87. doi:10.1016/j.jclepro.2018.01.179

Liu, C., Ji, J., Wu, W., Arhin, S.G., Papadakis, V.G., Goula, M.A., Zhang, S., Zhang, Y., Wang, W., 2022. Heterogeneous Catalyst-Microbiome Hybrids for Efficient CO-Driven C6 Carboxylic Acid Synthesis via Metabolic Pathway Manipulation. ACS Catal. 12, 5834–5845. doi:10.1021/acscatal.2c00768

Noguerol-Arias, J., Rodríguez-Abalde, A., Romero-Merino, E., Flotats, X., 2012. Determination of chemical oxygen demand in heterogeneous solid or semisolid samples using a novel method combining solid dilutions as a preparation step followed by optimized closed reflux and colorimetric measurement. Anal. Chem. 84, 5548–5555. doi:10.1021/ac3003566

Nzeteu, C. orline, Coelho, F., Trego, A.C., Abram, F., Ramiro-Garcia, J., Paulo, L., O'Flaherty, V., 2022. Development of an enhanced chain elongation process for caproic acid production from waste-derived lactic acid and butyric acid. J. Clean. Prod. 338, 130655. doi:10.1016/j.jclepro.2022.130655

Okoro-Shekwaga, C.K., Barry, A., Camargo-valero, M.A., 2021. Enhanced in-situ biomethanation of food waste by sequential inoculum acclimation: Energy efficiency and carbon savings analysis. Waste Manag. 130, 12–22. doi:10.1016/j.wasman.2021.04.053

Pau, S., Tan, L.C., Lens, P.N., 2022. Effect of pH on lactic acid fermentation of food waste using different mixed culture inocula. J Chem Technol Biotechnol 97, 950–961. doi:10.1002/jctb.6982

Ramos-suarez, M., Zhang, Y., Outram, V., 2021. Current perspectives on acidogenic fermentation to produce volatile fatty acids from waste, Reviews in Environmental Science and Bio/Technology. Springer Netherlands. doi:10.1007/s11157-021-09566-0

Rasi, S., Vainio, M., Blasco, L., Kahala, M., Leskinen, H., Tampio, E., 2022. Changes in volatile fatty acid production and microbiome during fermentation of food waste from hospitality sector. J Environ Manage 308. doi: 10.1016/j.jenvman.2022.114640

Reddy, M.V., ElMekawy, A., Pant, D., 2018. Bioelectrochemical synthesis of caproate through chain elongation as a complementary technology to anaerobic digestion. Biofuels, Bioprod. Biorefining, 12 (2018), pp. 966-977, 10.1002/bbb.1924

San-Valero, P., Fernández-Naveira, Veiga, M.C., Kennes, C., 2019. Influence of electron acceptors on hexanoic acid production by Clostridium kluyveri. J. Environ. Manage. 242, 515–521. doi:10.1016/j.jenvman.2019.04.093

Scotto di Perta, E., Cesaro, A., Pindozzi, S., Frunzo, L., Esposito, G., Papirio, S., 2022. Assessment of Hydrogen and Volatile Fatty Acid Production from Fruit and Vegetable Waste: A Case Study of Mediterranean Markets. Energies 15, 5032. doi:10.3390/EN15145032

Song, L., Liu, S., Liu, R., Yang, D., Dai, X., 2022. Direct lactic acid production from household food waste by lactic acid bacteria. Sci. Total Environ. 840, 156479. doi:10.1016/j.scitotenv.2022.156479

Strazzera, G., Battista, F., Tonanzi, B., Rossetti, S., Bolzonella, D., 2021. Optimization of short chain volatile fatty acids production from household food waste for biorefinery applications. Environ Technol Innov 23. https://doi.org/10.1016/j.eti.2021.101562

Tabraiz, S., Petropoulos, E., Shamurad, B., Quintela-Baluja, M., Mohapatra, S., Acharya, K., Charlton, A., Davenport, R.J., Dolfing, J., Sallis, P.J., 2021. Temperature and immigration effects on quorum sensing in the biofilms of anaerobic membrane bioreactors. J. Environ. Manage. 293, 112947. doi:10.1016/j.jenvman.2021.112947

Tang, J., Wang, X.C., Hu, Y., Zhang, Y., Li, Y., 2017. Effect of pH on lactic acid production from acidogenic fermentation of food waste with different types of inocula. Bioresour. Technol. 224, 544–552. doi:10.1016/j.biortech.2016.11.111

van der Linden, A., Reichel, A., 2020. Bio-waste in Europe: Turning challenges into opportunities, European Environment Agency Report.

Vonk, V.R., Buisman, C.N.J., Contreras-d, C.A., Strik, D.P.B.T.B., 2020. Consecutive lactate formation and chain elongation to reduce exogenous chemicals input in repeated-batch food waste fermentation. Water Res. 169. doi:10.1016/j.watres.2019.115215

Wang, Y., Fang, J., Lü, F., Zhang, H., He, P., 2023. Food waste anaerobic digestion plants: Underestimated air pollutants and control strategy. Sci. Total Environ. 903, 166143. doi:10.1016/j.scitotenv.2023.166143

Wang, Q., Yang, L., Feng, K., Li, H., Deng, Z., Liu, J., 2021. Promote lactic acid production from food waste fermentation using biogas slurry recirculation. Bioresour. Technol. 337, 125393. doi:10.1016/j.biortech.2021.125393

Wei, C., Liu, G., Zhang, J., Bao, J., 2018. Elevating fermentation yield of cellulosic lactic acid in calcium lactate form from corn stover feedstock. Ind. Crops Prod. 126, 415–420. doi:10.1016/j.indcrop.2018.10.041

Woo, H.C., Kim, Y.H., 2019. Eco-efficient recovery of bio-based volatile C2-6 fatty acids. Biotechnol. Biofuels 12, 1–11. doi:10.1186/s13068-019-1433-8

Wu, L., Wei, W., Liu, X., Wang, D., Ni, B.J., 2022. Potentiality of recovering bioresource from food waste through multi-stage Co-digestion with enzymatic pretreatment. J. Environ. Manage. 319, 115777. doi:10.1016/j.jenvman.2022.115777

Wu, Q., Guo, W., Bao, X., Meng, X., Yin, R., Du, J., Zheng, H., Feng, X., Luo, H., Ren, N., 2018. Upgrading liquor-making wastewater into medium chain fatty acid: Insights into co-electron donors, key microflora, and energy harvest. Water Res. 145, 650–659. doi:10.1016/j.watres.2018.08.046

Wu, S., Wei, W., Sun, J., Xu, Q., Dai, X., Ni, B., 2020. Medium-Chain fatty acids and long-chain alcohols production from waste activated sludge via two-stage anaerobic fermentation. Water Res. 186, 1–11. doi:10.1016/j.watres.2020.116381

Yang, L., Chen, L., Li, H., Deng, Z., Liu, J., 2022. Lactic acid production from mesophilic and thermophilic fermentation of food waste at different pH. J. Environ. Manage. 304, 114312. doi:10.1016/j.jenvman.2021.114312

Yu, J., Huang, Z., Wu, P., Zhao, M., Miao, H., 2019. Performance and microbial characterization of two-stage caproate fermentation from fruit and vegetable waste via anaerobic microbial consortia. Bioresour. Technol. 284, 398–405. doi:10.1016/j.biortech.2019.03.124

Zhang, M., Zhang, D., Du, J., Zhou, B., Wang, D., Liu, X., Yan, C., Liang, J., Zhou, L., 2023. Enhancing propionic acid production in the acidogenic fermentation of food waste facilitated by a fungal mash under neutral pH. J Environ Manage 327. https://doi.org/10.1016/j.jenvman.2022.116901

Zhang, W., Wang, S., Yin, F., Cao, Q., Lian, T., Zhang, H., Zhu, Z., Dong, H., 2022. Medium-chain carboxylates production from co-fermentation of swine manure and corn stalk silage via lactic acid: Without external electron donors. Chem. Eng. J. 439, 135751. doi:10.1016/j.cej.2022.135751

Zhao, Q., Arhin, S.G., Yang, Z., Liu, H., Li, Z., Anwar, N., Papadakis, V.G., Liu, G., Wang, W., 2021. pH regulation of the first phase could enhance the energy recovery from two-phase anaerobic digestion of food waste. Water Environ. Res. 1–11. doi:10.1002/wer.1527

Zhou, M., Yan, B., Wong, J.W.C., Zhang, Y., 2018. Enhanced volatile fatty acids production from anaerobic fermentation of food waste: A mini-review focusing on acidogenic metabolic pathways. Bioresour. Technol. 248, 68–78. doi:10.1016/j.biortech.2017.06.121

Zhu, X., Leininger, A., Jassby, D., Tsesmetzis, N., Ren, Z.J., 2021. Will Membranes Break Barriers on Volatile Fatty Acid Recovery from Anaerobic Digestion? ACS EST Engg 1, 141−153. doi:10.1021/acsestengg.0c00081

Chapter 4

Effect of carbon monoxide partial pressure on methanogenesis and medium-chain fatty acids production from food waste effluents via mixotrophic cultures

S. G. Arhin, A. Cesaro, F. Di Capua, V. Santala, M. Kokko, G. Esposito

Manuscript

4.1 Introduction

The sustainable generation of biochemicals from biowaste streams is regarded as a critical step in the development of a circular economy and averting the negative impacts of unsustainable sources, including fossil reserves and first-generation sources on the environment (L. Wu et al., 2023a). Food waste, making up over 60 % of the municipal biowaste in Europe (European Environment Agency, 2016), could be used as substrates for synthesizing various biochemicals via anaerobic fermentation with mixed microbial cultures (Sharma et al., 2020). Specifically, MCFAs consisting of aliphatic straight carbon chain with 6 to 2 carbons, including caproate, heptylate, and caprylate have risen to prominence (L. Wu et al., 2023b). Their versality as platform chemicals and relative ease of recovery compared to typical products such as short-chain fatty acids and alcohols make MCFAs one of the most attractive class of products from food waste (Zhang et al., 2023). MCFAs are produced via the so-called chain elongation process whereby the participation of an electron donor (e.g., ethanol, lactate) is a prerequisite to initiate the extension of the carbon chain length of VFAs acting as electron acceptors. Because electron donors and acceptors can be sustainable generated from food waste, thereby circumventing the cost and environmental implications of supplementing external reactants such as ethanol, food waste is considered an excellent resource for MCFAs production (Arhin et al., 2023; L. Wu et al., 2023b; Zhang et al., 2023)

Food waste bioconversion by typical mixed-culture anaerobic microbiomes involves hydrolysis, acidogenesis, acetogenesis, and methanogenesis. Methanogenesis is an electron sink in anaerobic environments that consumes intermediates such as VFAs and H_2 generated during fermentation (Leahy et al., 2022; Pereira et al., 2022; Wilson et al., 2017). Hence, to prevent carbon losses to methane production, selective inhibition of methanogens is usually practised during chain elongation. Specifically, bioactive chemicals such as 2-bromoethanesulfonate (BES) are mostly added to lab-scale chain elongation setups (Qiu et al., 2023). However, the potential cost implications associated with the use of such chemicals at scale remain a concern. Moreover, the use of such chemicals prevents the subsequent utilization of the nonconverted organics from the process as soil fertilizer upon composting (Roghair et al., 2018). Alternative strategies to prevent methanogenic growth during chain elongation include working at mildly acidic conditions (e.g., pH 5 – 5.5), which are typically unfavorable to methanogenic archaea. Yet, such relatively low pHs are close to the pka of MCFAs (e.g., 4.88 for caproate), resulting in a substantial fraction of the carboxylates existing in their undissociated form. Undissociated acids are toxic to microbiomes and could limit the MCFAs

production to moderate and low concentrations (Candry et al., 2020). Also, thermal treatment of the inoculum via heat-shocking (HS) has also been used as a method to suppress methanogenic growth during fatty acids production (Yin et al., 2021). However, HS is non-selective and could kill non-spore forming chain elongator or other functional groups related to chain elongation.

It is well-known that CO is more toxic to methanogenesis than hydrogenogenesis, acetogenesis, and solventogenesis (Oelgeschläger and Rother, 2008). Several anaerobic carboxidotrophs have been shown to metabolize CO directly into H_2, acetate, butyrate, and ethanol (Oelgeschläger and Rother, 2008). Moreover, recent studies have also shown that chain elongation microbiomes can effectively use CO to synthesize MCFAs (Liu et al., 2022). Therefore, syngas (consisting mainly of CO, H_2, and CO_2) derived from pyrolysis of recalcitrant residues such as LCMs or sludges could be used a co-substrate in chain elongation systems to inhibit methanogens and facilitated MCFAs production. However, CO has a low water solubility (0.04 mL/mL), and its gas-liquid mass transfer has been identified as one of the primary bottlenecks during fermentation (W. Wu et al., 2023). According to the Henry's law, increasing the CO partial pressure (P_{CO}) could enhance the gas-liquid mass transfer (Li et al., 2020). However, limited information exists on the impact of P_{CO} on chain elongation. Esquivel-Elizondo et al. (2018) studied the effect of P_{CO} 0.08 to 0.3 atm on methanogenesis and fatty acid production during ethanol fermentation and observed that $P_{CO} \geq 0.11$ atm could partially inhibit methanogenesis. Other studies suggest that methanogenic activities may be supressed at increased P_{CO} higher than 0.25 atm (Luo et al., 2013). Nonetheless, the impact of high P_{CO} on the bioconversion of food waste acidification products containing various electron donors (lactate, ethanol) and electron acceptors (acetate, propionate, butyrate, valerate) to MCFAs by a mixotrophic chain elongation microbiome remains unclear. Perhaps, higher P_{CO} ($\geq$ 0.25 bar) could completely inhibit methanogenesis, channelling the available electron towards MCFAs synthesis. At the same time, a high P_{CO} may overcome the CO tolerance threshed of chain elongators or induce specific metabolic pathways that may be detrimental to MCFAs synthesis.

Based on these considerations, this study aimed to understand the influence of CO supplementation on MCFAs production from food waste acidification products using a mixed microbial culture. The specific objectives were to (i) determine the impacts of varying P_{CO} of 0.00, 0.25, 0.50, and 1.00 bar on methanogenesis through continuous addition of CO, (ii)

determine the effect of varying P_{CO} of 0.00, 0.25, 0.50, and 1.00 on chain elongation and the product spectrum, (iii) compare the impact of CO with other strategies for inhibiting methanogenesis, specifically, HS and BES addition.

4.2 Materials and methods

4.2.1 Food waste substrate and inocula

The food waste used in this study is kitchen food waste obtained from the household of the staff at the Bio and Circular Economy Unit, Tampere University, Finland. The food waste consisted of fruits and vegetable waste (65 %), spent coffee grounds (22 %), eggshells (6 %), cereals (5 %), dairy products (1%), and bread (1 %). The food waste was shredded into a homogenous slurry upon receipt and stored at -20 °C for later use. The characteristics of the food waste, including TS, VS, COD, carbohydrate, and protein contents are summarized in **Table A4.2** (**Appendix B**).

The indigenous microbiota used for lactate production was obtained by shredding 200 g of fresh food waste into a slurry. Afterward, the TS and VS of the slurry were adjusted to 27.6 ± 0.3 g/L and 23.9 ± 0.4 g/L, respectively, with Milli-Q water based on previous studies (Tang et al., 2017). The pH and alkalinity of the fresh food waste inoculum were 6.8 ± 0.2 and 3.2 ± 0.5 g CaCO3/L, respectively.

The anaerobically digested sludge (ADS) used as inoculum for VFAs production was a mesophilic digestate obtained from the anaerobic digester of Hatanpää Wastewater Treatment Plant (Tampere, Finland). The seed sludge was pretreated by heating at 100 °C for 30 min to inhibit methanogenic archaea (Wang et al., 2022). The TS, VS, alkalinity, and pH of the ADS were 25.8 ± 1.7 g/L, 14.8 ± 1.1 g/L, 6.9 ± 0.2 g CaCO3/L and 9.1 ± 0.0, respectively.

The inoculum used for chain elongation was cultivated by feeding the ADS in a chain elongation bioreactor regularly with food waste effluent containing mixed VFAs (i.e., acetate, propionate, butyrate, and valerate), lactate, and ethanol at pH 6 and 35 °C. The inoculum was centrifuged at 4500 rpm for 15 mins and the precipitate was resuspended in Milli-Q water for the chain elongation experiments (Wang et al., 2022). The TS, VS, and pH of the chain elongation inoculum were 8.2 ± 0.1 g/L, 2.9 ± 0.2 g/L, and 6.8 ± 0.1, respectively.

4. 2.2 Experimental procedure

4.2.2.1 Lactate production via acidogenic fermentation

The indigenous microbiota in the fresh food waste was used as the inoculum for lactate production. The experiments were performed in triplicate in 2.0 L bottles with a working volume of 1.2 L. The F/M ratio (i.e., the ratio of the food waste substrate to that of the inoculum) was set at 10 g-VS/g-VS. 200 mM of potassium phosphate buffer at pH 6.0 was added at the onset of fermentation, and the pH was maintained at 6.0 ± 0.1 throughout the experiment via dropwise addition of 5 M KOH and H_3PO_4. The bottles were flushed with ultrapure N_2 for 5 min and incubated at 35 ± 1.0 °C in a static water bath. 1 mL of the liquid and 200 µL of the gas were sampled daily for analysis. The detailed operation of the acidogenic fermentation phase can be found in Arhin et al. (2023). After 5 d fermentation, the samples were centrifuged at 4500 rpm for 15 min and the supernatant (hereafter denoted as the lactate-rich effluent) was collected for the chain elongation experiments.

4.2.2.2 Volatile fatty acids production via acidogenic fermentation

The VFAs production from food waste was conducted in triplicates following a similar experimental procedure as described in **section 4.2.2.1**. However, the inoculum used for VFAs production was the ADS and the experiment lasted 8 d. The acidified liquid (denoted as the VFAs-rich effluent) was collected after fermentation for MCFAs production.

4.2.2.3 Chain elongation experiments

The chain elongation experiments were performed in triplicates in 550 mL serum bottles with a working volume of 200 mL. The lactate- and VFAs-rich effluents were mixed to a final concentration of lactate (10.0 g-COD/L), ethanol (3.2 g-COD/L), acetate (3.2 g-COD/L), propionate (1.2 g-COD/L), *n*-butyrate (5.4 g-COD/L), and *n*-valerate (1.4 g-COD/L) in each bottle. The bottles were inoculated with 5 g-VS/L of the chain elongation inoculum and a growth medium solution containing NH_4Cl (0.25 g/L), $MgSO_4 \cdot 7H_2O$ (0.20 g/L), KH_2PO_4 (0.23 g/L), K_2HPO_4 (0.31 g/L), NaCl (0.80 g/L), L-Cysteine-HCl·H_2O (0.25 g/L), trace elements solution (1 mL/L; **Text A4.1, Appendix B**), and vitamins solution (1 mL/L; **Text A4.2, Appendix B**) was added to each bottle (Zhu et al., 2015).

Two groups of long-term parallel chain elongation experiments were conducted (**Table A4.3, Appendix B**). In the first group, the effect of different CO partial pressures (P_{CO}) of 0.00, 0.25, 0.50, and 1.00 bar on methanogenesis and MCFAs production from the effluents was investigated. The bottles were sealed with butyl rubber stoppers and aluminum seals, and their headspaces were purged with CO and N_2 at different ratios to obtain the required initial P_{CO} (Esquivel-Elizondo et al., 2018; Jing et al., 2017). The P_{CO} was readjusted to the initial values at least once a week depending on the CO consumption rate after the liquid (1 mL) and gas (200 µL) sampling. In the second group, comparative experiments were performed to assess the effect of other methanogenic inhibiting strategies by adding 10 g/L of BES inhibitor (denoted as the BES) and heat-shocking the chain elongation inoculum at 100 °C for 10 min (denoted as the heat-shocked, HS). A set of bottles with the inoculum, medium, and Milli-Q water only was used as a negative control (denoted as Blank). The BES, HS, and Blank bottles were flushed with ultrapure N_2 to ensure anoxic conditions. All the bottles were incubated in an air bathe incubator at 35 °C and 150 rpm, and the pH was maintained at 6.0 ± 0.1 via dropwise addition of 5 M KOH and H_3PO_4.

4.2.3 Pathway verification assays

Batch CO conversion experiments were conducted at the end of the chain elongation experiments to determine the pathway for CO conversion. Serum bottles with total and working volumes of 120 and 40 mL, respectively, were supplied with CO as the sole carbon source at P_{CO} of 0.25, 0.50, and 1.00 bar. The other experimental parameters were as described in **section 4.2.2.3**.

Specific methanogenic activity (SMA) tests were also conducted to ascertain the pathway of methane production in the P_{CO} of 0.00 bar and HS groups following the procedure described in previous studies (Wu et al., 2023). Briefly, 120 mL serum bottles were filled with 20 mL of biomass retrieved from the corresponding bottles in **section 4.2.2.3** and 20 mL of the medium, trace elements, and vitamin solutions. After purging the bottles with ultrapure N_2 for 5 mins to ensure axenic conditions, acetate (1.2 g/L) or H_2/CO_2 mix (2 bar, H_2: CO_2 volumetric ratio of 4:1) were supplied as carbon sources and the bottles were incubated at 35 °C and 150 rpm.

4.2.4 Extracellular polymeric substances characterization

Extracellular polymeric substances (EPS) produced during chain elongation were extracted using the thermal method following previous studies (Qiu et al., 2023). Briefly, 30 mL of the sludge samples from the bottles were centrifuged at 3200 rpm for 30 min to remove the bulk solution. The supernatants were regarded as the soluble EPS fractions (S-EPS). The resulting sludge slurries were resuspended in 0.05 % NaCl solution to 12 mL and centrifuged at 9000 rpm for 20 min. The supernatants were collected as the loosely bound EPS fraction (LB-EPS). The remaining solid fractions were resuspended in 0.05 % NaCl solution to 12 mL and thermally treated at 80 °C for 45 min. After centrifugation at 10000 rpm for 20 min, the supernatant was collected as the tightly bound EPS (TB-EPS). The carbohydrate and protein contents of the EPS fractions were determined as detailed in **section 4.2.5**.

4.2.5 Analytical methods

TS, VS, COD, alkalinity, and volatile suspended solids (VSS) were analyzed using standard methods (APHA, 2005). The pH was measured with a WTW ProfiLine pH 3110 pH meter. The carbohydrate and protein content of the food waste and EPS samples were analyzed with the Dubois phenol-sulfuric acid and the Lowry methods using glucose and bovine serum albumin as standards, respectively, as described in our previous studies (Arhin et al., 2023).

The biogas produced during acidogenic fermentation was measured by the water displacement method (Kokko et al., 2018), while the biogas volume in the chain elongation, SMA, and batch CO conversion experiments was determined based on the pressure in the headspace (Sun et al., 2021) as detailed in the **Appendix B (Text A4.3)**. The H_2, CO_2, and CH_4 content was analyzed with a Shimadzu GC-2014 gas chromatograph equipped with a Porapak N 80-100 column and a thermal conductivity detector. Nitrogen was the carrier gas at a flow rate of 20 mL/min and the column, injector, and detector temperatures were 40, 110, and 110 °C, respectively. CO was also analyzed with a Shimadzu GC-2014 gas chromatograph equipped with a Carboxen-1000 60/80 column and a thermal conductivity detector. Helium was the carrier gas at a flow rate of 30 mL/min. The column, injector, and detector temperatures were 180, 180, and 190 °C, respectively.

The VFAs, MCFAs, and ethanol concentrations were analyzed with a Shimadzu gas chromatograph (GC-2010 Plus) equipped with a Zebron ZB-WAX Plus column and a flame

ionization detector as detailed in Kokko et al. (2018). Lactate concentration was analyzed with a Shimadzu high-performance liquid chromatograph equipped with a refractive index detector and a Rezex RHM-monosaccharide H+ (8%) column (Phenomenex, USA). The mobile phase consisted of 10 mM H_2SO_4 solution at 0.5 mL/min flow rate. Samples for carboxylates and ethanol analysis were centrifuged (10000 g for 10 min) and filtered through 0.2 μm syringe filters (Chromafil® Xtra PET-20/25, Macherey-Nagel, Germany).

4.2.6 Statistical analysis

A one-way analysis of variance followed by the Tukey post hoc test was used to compare the total MCFA production in the P_{CO} experiment. The same statistical test was employed for comparison of the EPS production. IBM SPSS statistics (version 26) was used for statistical analysis, and a $p < 0.05$ was considered statistically significant. The steady state was defined as the relative variation in substrate consumption or MCFA production of less than 10 %. The graphs and charts were created with OriginPro 2021 (OriginLab Corporation, USA).

4.3 Results and discussion

4.3.1 Impact of CO partial pressure on methane production during chain elongation

As mentioned in **section 4.2.1**, kitchen food waste was used for the experiments in this chapter. Generally, its characteristics were comparable that of the food waste obtained from the food retail market in Naples, Italy (**chapter 3**). However, appreciable differences in some properties, including the COD and total VFAs concentration were observed (**Table A4.2**, **Appendix B**). While these differences may have impacted the acidogenic fermentation reactions, such potential impacts were hard to establish due to differences in the fermenting microbiome.

As shown in **Fig. A4.1 (Appendix B**), the main end-products of the acidogenic fermentation reactions were lactate, VFAs, and ethanol, which were subsequently used as organic substrates for chain elongation. Lactate was the dominant product in the experiments with the indigenous microbiota in food waste as inoculum. Lactate concentration reached 18.6 ± 0.3 g-COD/L, alongside acetate (2.1 ± 0.2 g-COD/L), *n*-butyrate (0.2 ± 0.0 g-COD/L), *n*-caproate (0.2 ± 0.0 g-COD/L), and ethanol (2.6 ± 0.3 g-COD/L) as co-products. In contrast, with ADS as inoculum, *n*-butyrate accumulated as the main product (11.1 ± 8.2 g-COD/L) together with acetate (3.8 ± 2.3 g-COD/L), propionate (3.2 ± 2.5 g-COD/L), *iso*-butyrate (0.2 ± 0.0 g-COD/L), *n*-valerate (2.5 ± 3.3 g-COD/L), *n*-caproate (0.7 ± 0.2 g-COD/L), and ethanol (4.3 ±

0.0 g-COD/L). After acidogenic fermentation, the food waste acidification products were supplied once at the onset of chain elongation, but the P_{CO} was maintained throughout the experiment by the addition of CO.

The amount of CO injected and consumed are shown in **Table A4.4 (Appendix B). Fig. 4.1** also shows the cumulative methane production during chain elongation. In the control test without methanogenic inhibitors, methane begun to accumulate after day 7 and increased gradually till day 21reaching its peak. In contrast, methane production was completely inhibited at $P_{CO} \geq 0.25$ bar. This indicate that continuous supplementation of CO during chain elongation was adequate in supressing methanogenic activity. Similarly, the addition of 10 g/L of BES was also efficient in inhibiting methanogenic growth. However, thermally treating the chain elongation inoculum was not efficient in supressing the methanogenic archaea as trace amounts of methane were detected after day 14 and increased gradually till day 77 when the experiment was terminated.

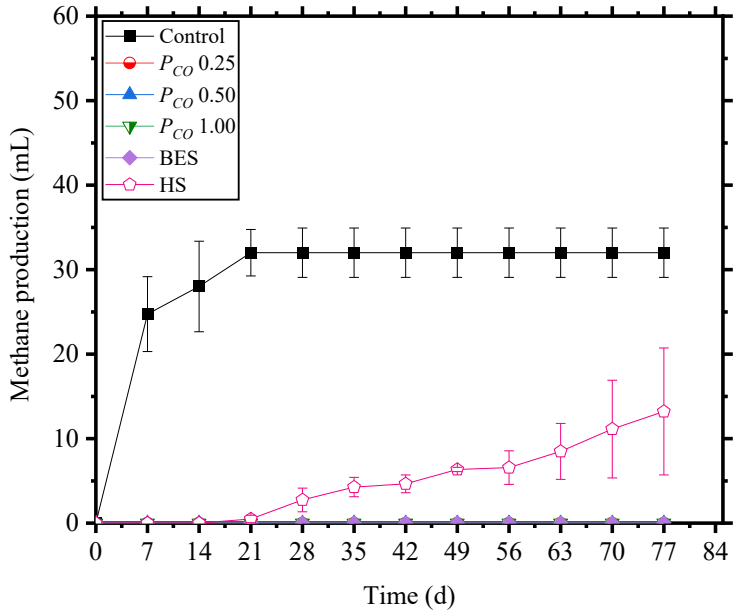

Fig. 4.1. Methane production during chain elongation.

4.3.2 Effect of CO partial pressure on medium-chain fatty acid production

Fig. 4.2 shows the products of chain elongation. Lactate, as a vital and versatile intermediate for the synthesis of various fatty acids (Shahab et al., 2020), was quickly consumed within 3 d in all the experimental groups. However, lactate consumption mainly led to an increase in SCFAs concentration. For instance, the average propionate concentrations increased from 1.2

± 0.0 g-COD/L to 2.7 ± 0.3 g-COD/L. More importantly, the concentrations of *n*-butyrate and *n*-valerate, possibly formed via the respective chain elongation pathways of acetate and propionate (Angenent et al., 2016), rose from 5.4 ± 0.2 g-COD/L and 1.4 ± 0.1 g-COD/L to 8.5 ± 0.6 g-COD/L and 5.4 ± 0.3 g-COD/L, respectively. *n*-Caproate (≤ 2.1 g-COD/L) was the only MCFA detected until lactate was depleted in all the system. At this stage, less than 20 % of the ethanol had been consumed in the different experimental condition. Hence, the remaining ethanol was used in the subsequent days as the main electron donor to extend the carbon chain length of the SCFAs to MCFAs, leading to the production of *n*-heptylate and *n*-caprylate besides *n*-caproate.

Unlike lactate, ethanol consumption varied across the various experimental groups. In the control test in group 1, ethanol was completely consumed by day 7 leading to an increase in *n*-caproate, *n*-heptylate, and *n*-caprylate concentrations to 5.2 ± 0.2 g-COD/L, 2.9 ± 0.0 g-COD/L, and 1.0 ± 0.0, respectively. After ethanol was depleted, steady-state conditions were observed with no significant change in the SCFAs and MCFAs concentrations. In contrast, when CO was supplemented at P_{CO} of 0.25, 0.50, and 1.00 bar, ethanol consumption occurred more slowly and *n*-caproate and *n*-heptylate peaks were observed on day 49 whereas *n*-caprylate reached its peak on days on day 14 at P_{CO} of 0.25 bar and day 21 at P_{CO} of 0.50 and 1.00 bar Ethanol consumption and MCFAs production in the BES test in group 2 followed as similar pattern as the control. The supplied ethanol was consumed within 7 d to generate *n*-caproate (4.7 ± 0.0 g-COD/L), *n*-heptylate (2.7 ± 0.1 g-COD/L), and *n*-caprylate (0.8 ± 0.1 g-COD/L). Steady-state conditions were attained after day 7 when ethanol was depleted. On the contrary, ethanol consumption was inhibited in the HS leading to poor MCFAs production. The peak concentrations of *n*-caproate, *n*-heptylate, and *n*-caprylate in the HS test was attained on day 28, reaching only 2.5 ± 1.5 g-COD/L, 1.0 ± 0.9 g-COD/L, and 0.3 ± 0.5 g-COD/L, respectively. These results imply that heat-shocking the chain elongation inoculum was not only poor in controlling methanogenic growth but led to adverse impact on ethanol utilization and MCFAs production.

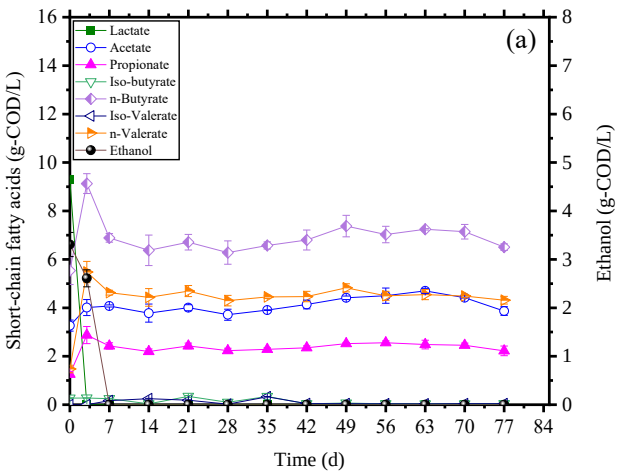
(a)
Lactate
Acetate
Propionate
Iso-butyrate
n-Butyrate
Iso-Valerate
n-Valerate
Ethanol
Short-chain fatty acids (g-COD/L)
Ethanol (g-COD/L)
Time (d)

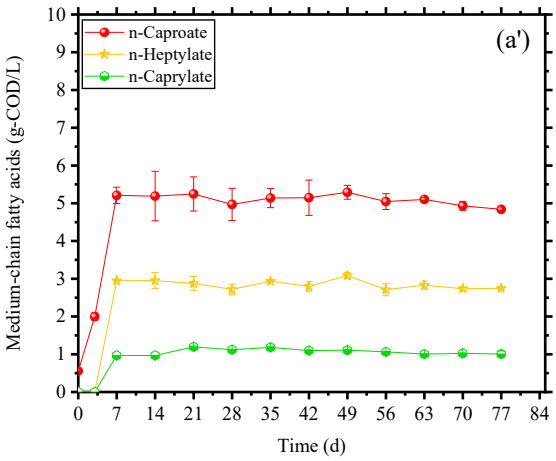
(a')
n-Caproate
n-Heptylate
n-Caprylate
Medium-chain fatty acids (g-COD/L)
Time (d)

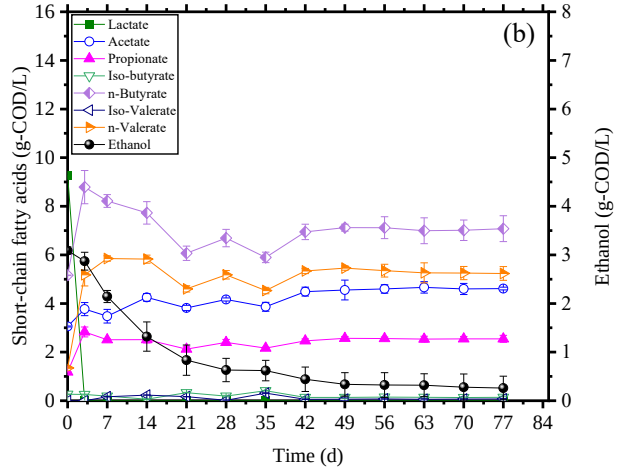
(b)
Lactate
Acetate
Propionate
Iso-butyrate
n-Butyrate
Iso-Valerate
n-Valerate
Ethanol
Short-chain fatty acids (g-COD/L)
Ethanol (g-COD/L)
Time (d)

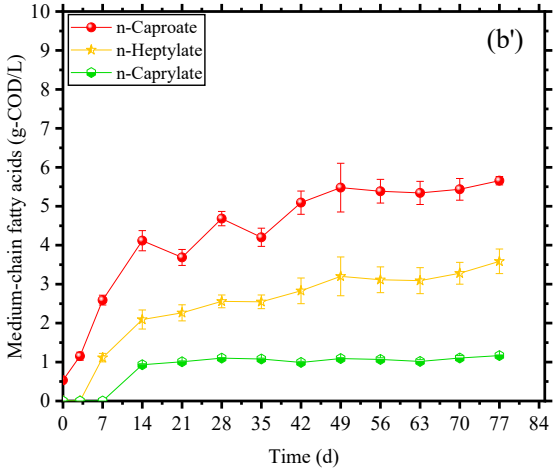
(b')
n-Caproate
n-Heptylate
n-Caprylate
Medium-chain fatty acids (g-COD/L)
Time (d)

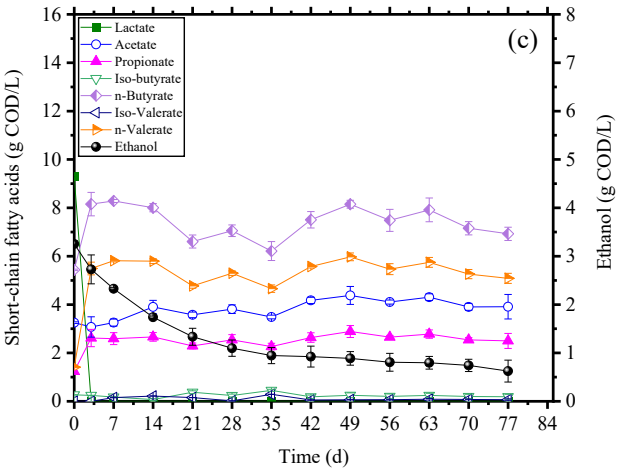
(c)
Lactate
Acetate
Propionate
Iso-butyrate
n-Butyrate
Iso-Valerate
n-Valerate
Ethanol
Short-chain fatty acids (g COD/L)
Ethanol (g COD/L)
Time (d)

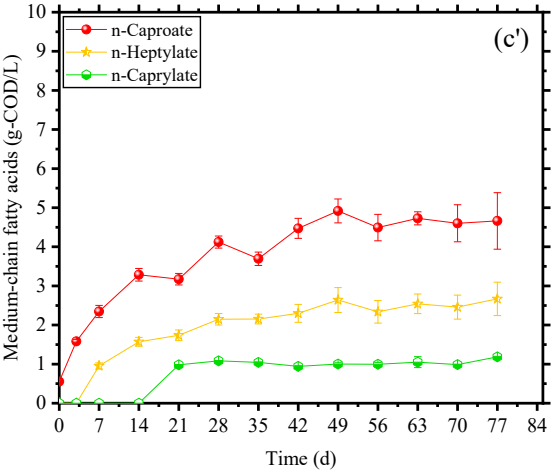
(c')
n-Caproate
n-Heptylate
n-Caprylate
Medium-chain fatty acids (g-COD/L)
Time (d)

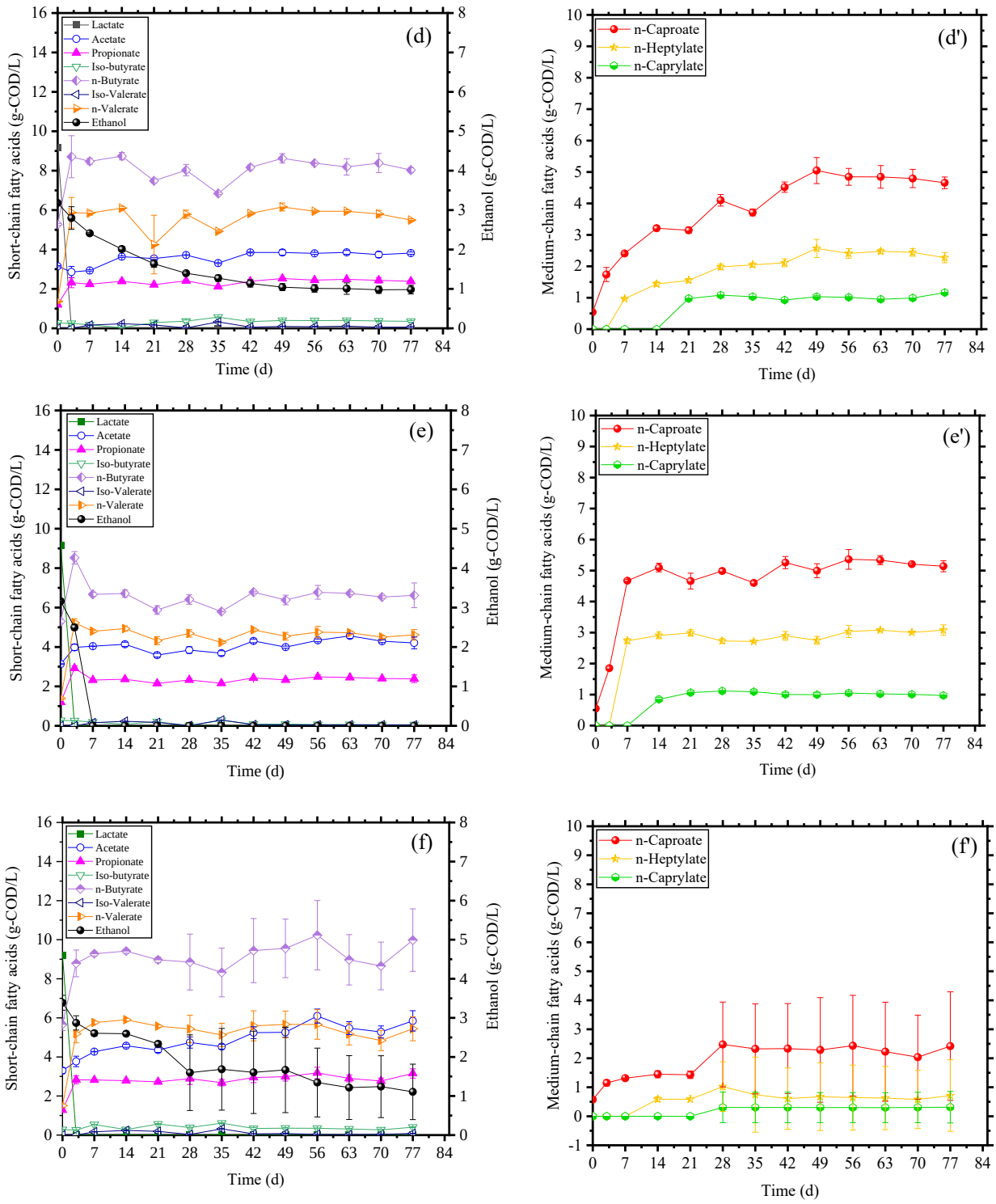

Fig. 4.2. Variations in short-chain fatty acids and ethanol (a-f) and medium-chain fatty acids production (a'-f') during chain elongation. (a, a') P_{CO} 0.00 bar. (b, b') P_{CO} 0.25 bar. (c, c') P_{CO} 0.50 bar. (d, d') P_{CO} 1.00 bar. (e, e') BES. (f, f') HS.

At the end of the chain elongation experiments on day 77, the highest total MCFAs accumulation was observed at a P_{CO} of 0.25, reaching 10.4 ± 0.4 g-COD/L (**Fig A4.2a, Appendix B).** An increasing trend in the accumulation of unfermented ethanol with increasing P_{CO} from 0.00 to 1.00 bar was observed in group 1 tests (**Fig A4.2b, Appendix B)**. The potential *n*-caproate yield from the unfermented ethanol was stoichiometrically estimated to be 0.6 ± 0.5, 1.2 ± 0.4, and 1.8 ± 0.2 g COD/L for P_{CO} of 0.25, 0.5, and 1.00 bar, respectively. The accumulation of ethanol with CO supplementation and the slow ethanol consumption in the presence of CO could possibly be because the microbial community had not acclimated to CO, thus, its potential toxicity may have inhibited certain functional groups within the community leading to slow ethanol assimilation. On the other hand, additional ethanol may have been produced from CO, which lead to the observed scenario. To verify this, batch CO conversion experiments were conducted, and the results are presented in **section 4.3.3.**

4.3.3 Verification of CO conversion pathway

The supplied CO may be used as a substrate to synthesize acetate (**Eq. 4.1**), ethanol (**Eq. 4.2**), H_2 (**Eq. 4.3**), or other intermediates by autotrophs, which could impact MCFA production (Baleeiro et al., 2023; Esquivel-Elizondo et al., 2018; Jing et al., 2017; Liu et al., 2022; Wu et al., 2023). Therefore, the pathways for CO conversion catalyzed by the microbiome under the P_{CO} of 0.25, 0.50, and 1.00 bar were determined. As depicted in **Fig. 4.3(a-c)**, CO consumption occurred rapidly at a P_{CO} of 0.25 compared to 0.50 and 1.00 bar. H_2 production was negligible (< 300 µL) in the initial 4 d and no H_2 was detected at the end of fermentation (6 d) in all three systems. At the P_{CO} of 0.25 bar, CO was quickly consumed within 2 d to produce acetate (233.5 ± 17.2 mg-COD/L) as the main product (**Fig. 4.3a**). However, when CO was depleted in the system, methanogenesis began to occur and methane accumulated as the sole product by day 4. Similarly, acetate was the main product from CO conversion at a P_{CO} of 0.50 bar, reaching a concentration of 630.9 ± 55.9 mg-COD/L on day 6, and methane (< 1 mL) was detected on days 4 and 6 when CO was depleted (**Fig. 4.3b**). Interestingly, with more CO available to the microbiome at a P_{CO} of 1.00 bar, the product spectrum included acetate (772.5 ± 100.4 mg-COD/L), ethanol (229.2 ± 101.1 mg-COD/L), and n-butyrate (24.0 ± 5.6 mg-COD/L) (Fig. 3c). Trace amounts of methane (< 500 µL) were once again detected on days 4 and 6 when CO was depleted.

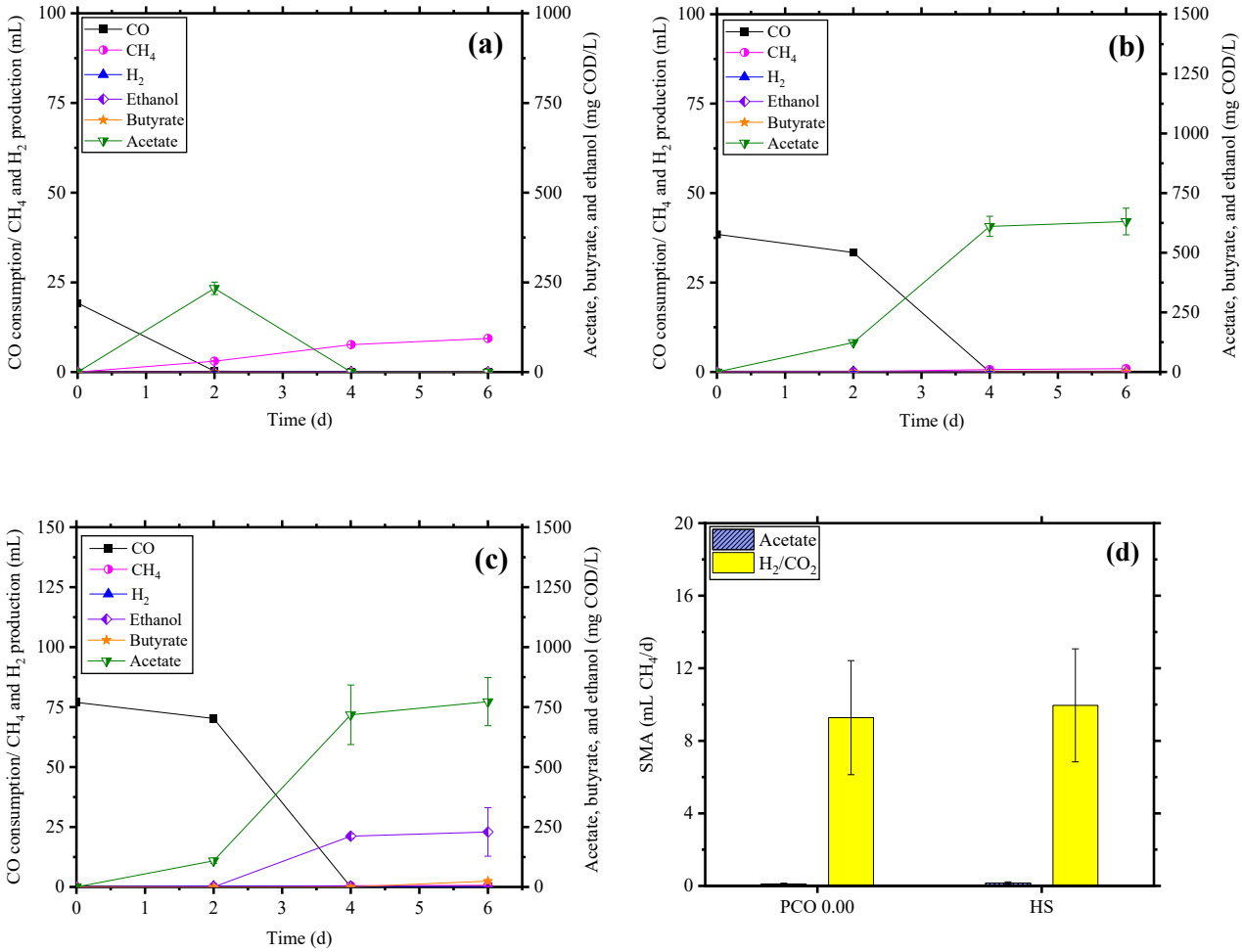

Fig. 4.3. Pathway verification assay with CO as the sole carbon source and specific methanogenesis activity (SMA) tests with acetate or H_2 as substrate. (a) CO conversion test at a P_{CO} of 0.25 bar, (b) 0.50 bar, and (c) 1.00 bar. (d) Acetate- and H_2-based SMA tests.

Overall, the results of the CO conversion assays corroborated the findings of the chain elongation experiments that the presence of CO in our system inhibited methanogenic growth and availed more carbons for the synthesis of MCFA via intermediates such as acetate. The results also suggest that ethanol production from CO (Eq. 4.2) occurred with increasing availability of CO, which was consistent with the accumulation of ethanol at increasing P_{CO} in the chain elongation experiments.

$$4CO + 2H_2O \rightarrow CH_3COOH + 2CO_2 \ (\Delta G^o = \text{-}154.6 \text{ kJ/mol}) \quad (4.1)$$

$$6CO + 3H_2O \rightarrow C_2H_5OH + 4CO_2 \ (\Delta G^o = \text{-}217.4 \text{ kJ/mol}) \quad (4.2)$$

$$CO + H_2O \rightarrow H_2 + CO_2 \ (\Delta G^o = \text{-}20.1 \text{ kJ/mol}) \quad (4.3)$$

To understand the pathway for methane generation in the absence of CO (P_{CO} 0.00 bar) and HS groups, batch SMA assays were also performed. As shown in **Fig. 4.3(d)**, the H_2-based SMA was higher than the acetate-based SMA in both systems suggesting that hydrogenotrophic methanogenesis was the dominant pathway for methane formation. These findings were in line with those of the chain elongation experiments, which showed that methane production in the Control and HS groups mainly occurred with H_2 consumption in our systems.

4.4 Extracellular polymeric substances production during chain elongation

The EPS produced by the microbiome in response to CO, BES, and HS treatment is shown in **Fig. 4.4.** Altogether, CO supplementation resulted in a decreasing trend in the carbohydrate and protein content, leading to a lower total EPS content. Compared to the control (P_{CO} of 0.00 bar), the total EPS produced at P_{CO} of 0.25, 0.50, and 1.00 bar was reduced by 17.0 ± 0.3 %, 24.1 ± 1.0 %, and 37.3 ± 0.6 %, respectively. However, regarding the EPS subtypes, CO supplementation had varying impacts on the carbohydrate and protein content. For instance, significant reductions ($p < 0.05$) in the carbohydrate and protein content of the TB-EPS fraction were observed with increasing P_{CO} from 0.25 to 1.00 bar. However, such trends were not evident in the carbohydrate and protein content of the S-EPS and LB-EPS fractions.

The addition of BES also lowered the carbohydrate and protein content, leading to a 25.5 ± 0.5 % reduction in the total EPS content compared to the control. In contrast, heat-shocking the inoculum resulted in the overproduction of EPS. Even though the carbohydrate content of the HS group decreased by 13.8 ± 3.7 % compared to the control, the protein content increased by 13.3 ± 2.0 %, resulting in an overall higher EPS content (10.3 ± 2.1%).

These results imply that the inhibited methane production observed in the CO and BES groups may partly be due to the suppressed overall EPS secretion caused by CO- and BES-induced stress. Similar observations were reported by Qiu et al. (2023) were BES-induced stress limited the overall EPS secretion leading to inhibited methanogenesis. Meanwhile, the overproduction of EPS in the control and HS groups ensured a stable environment for methanogenesis as observed in past studies where EPS overproduction was associated with enhanced methanogenesis (Jing et al., 2017; Li et al., 2022).

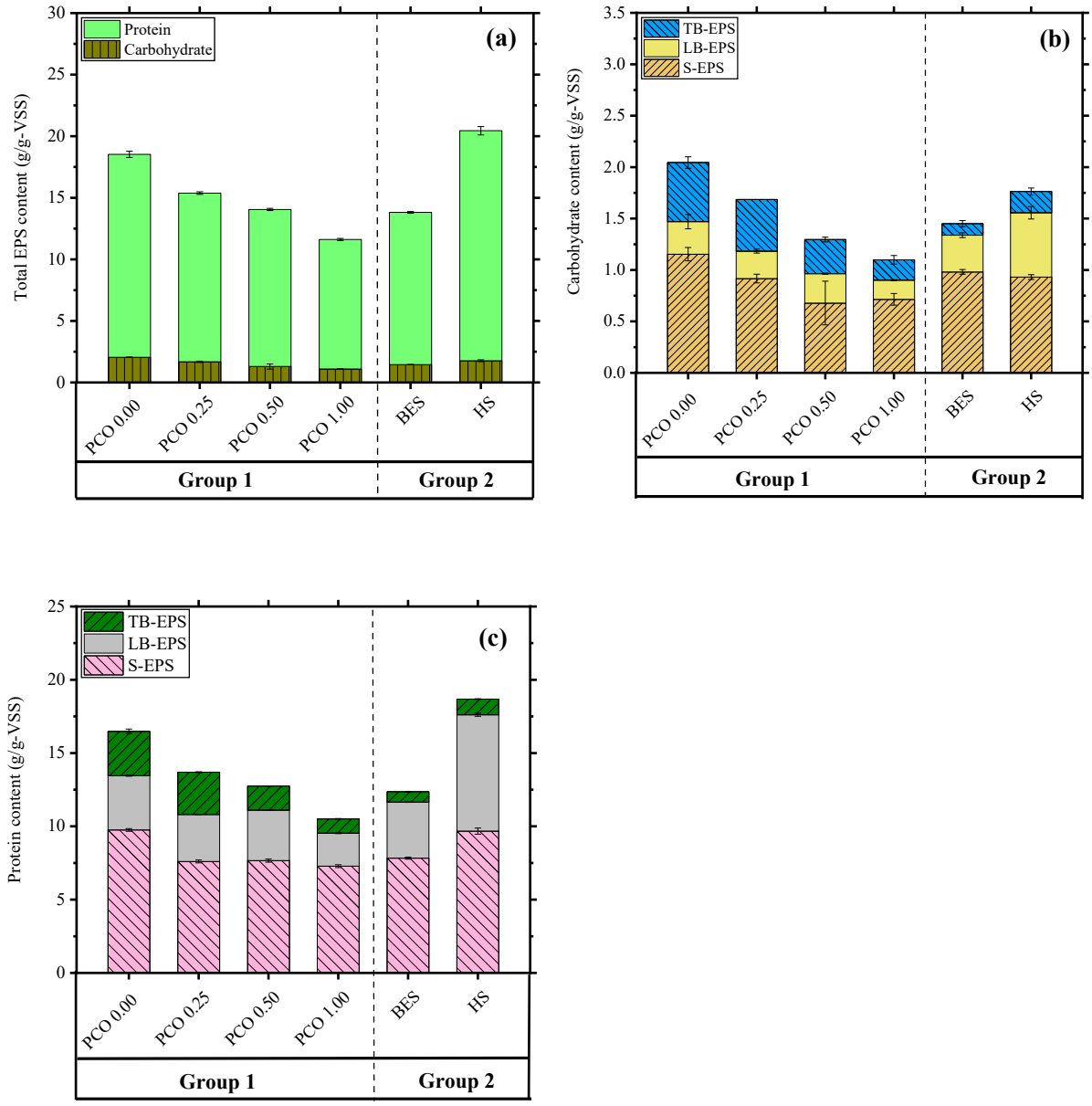

Fig 4.4. Extracellular polymeric substances (EPS) production in the chain elongation systems. (a) Total EPS content, (b) carbohydrate content of the EPS subtypes, and (c) protein content of the EPS subtypes.

4.4 Conclusions

In this study, the effect of varying P_{CO} of 0.00, 0.25, 0.50, 1.00 bar on methanogenesis and MCFAs production from food waste acidogenic fermentation products were assessed and compared with HS and BES supplementation. The following conclusions could be drawn from the finding of the study:

- CO could be co-fermented with organic substrates for MCFA production.
- CO partial pressure of 0.25 could completely inhibit methanogenesis and increase the total MCFA concentration paving the way to sustainably generate MCFA from food waste without the need for industrial chemicals (e.g., BES) to control methanogenic growth.
- Higher CO partial pressure (0.5 and 1.0) could inhibit methanogenesis but did not improve chain elongation due to ethanol accumulation.
- Further studies should be conducted to enhance the resilience of chain elongators under high CO stress.

Reference

Angenent, L.T., Richter, H., Buckel, W., Spirito, C.M., Steinbusch, K.J.J., Plugge, C.M., Strik, D.P.B.T.B., Grootscholten, T.I.M., Buisman, C.J.N., Hamelers, H.V.M., 2016. Chain Elongation with Reactor Microbiomes: Open-Culture Biotechnology to Produce Biochemicals. Environ Sci Technol. https://doi.org/10.1021/acs.est.5b04847

APHA, 2005. Standard Methods for the Examination of Water and Wastewater. American Public Health Association/American Water Works Association/ Water Environment Federation, Washington, DC.

Arhin, S.G., Cesaro, A., Di Capua, F., Esposito, G., 2023. Acidogenic fermentation of food waste to generate electron acceptors and donors towards medium-chain carboxylic acids production. J Environ Manage 348, 119379. https://doi.org/10.1016/j.jenvman.2023.119379

Baleeiro, F.C.F., Raab, J., Kleinsteuber, S., Neumann, A., Sträuber, H., 2023. Mixotrophic chain elongation with syngas and lactate as electron donors. Microb Biotechnol 16, 322–336. https://doi.org/10.1111/1751-7915.14163

Candry, P., Huang, S., Carvajal-Arroyo, J.M., Rabaey, K., Ganigue, R., 2020. Enrichment and characterisation of ethanol chain elongating communities from natural and engineered environments. Sci Rep 10. https://doi.org/10.1038/s41598-020-60052-z

Esquivel-Elizondo, S., Miceli, J., Torres, C.I., Krajmalnik-Brown, R., 2018. Impact of carbon monoxide partial pressures on methanogenesis and medium chain fatty acids production during ethanol fermentation. Biotechnol Bioeng 115, 341–350. https://doi.org/10.1002/bit.26471

European Environment Agency, 2016. Municipal waste management across European countries [WWW Document]. URL http://www.mzp.cz.

Jing, Y., Campanaro, S., Kougias, P., Treu, L., Angelidaki, I., Zhang, S., Luo, G., 2017. Anaerobic granular sludge for simultaneous biomethanation of synthetic wastewater and CO with focus on the identification of CO-converting microorganisms. Water Res 126, 19–28. https://doi.org/10.1016/j.watres.2017.09.018

Kokko, M., Koskue, V., Rintala, J., 2018. Anaerobic digestion of 30−100-year-old boreal lake sedimented fibre from the pulp industry: Extrapolating methane production potential to a practical scale. Water Res 133, 218–226. https://doi.org/10.1016/j.watres.2018.01.041

Leahy, S.C., Janssen, P.H., Attwood, G.T., Mackie, R.I., Mcallister, T.A., Kelly, W.J., 2022. Electron flow: key to mitigating ruminant methanogenesis. Trends Microbiol 30.

Li, S., Zhang, Y., Duan, W., Deng, R., Gu, L., Shi, D., 2022. Insights into the resistance of different extracellular polymeric substance (EPS) layers to the fermentation environment in sludge anaerobic digestion. Chemical Engineering Journal 449. https://doi.org/10.1016/j.cej.2022.137844

Li, Y., Wang, Z., He, Z., Luo, S., Su, D., Jiang, H., Zhou, H., Xu, Q., 2020. Effects of temperature, hydrogen/carbon monoxide ratio and trace element addition on methane production performance from syngas biomethanation. Bioresour Technol 295. https://doi.org/10.1016/j.biortech.2019.122296

Liu, C., Ji, J., Wu, W., Arhin, S.G., Papadakis, V.G., Goula, M.A., Zhang, S., Zhang, Y., Wang, W., 2022. Heterogeneous Catalyst-Microbiome Hybrids for Efficient CO-Driven C6 Carboxylic Acid Synthesis via Metabolic Pathway Manipulation. ACS Catal 5834–5845. https://doi.org/10.1021/acscatal.2c00768

Luo, G., Wang, W., Angelidaki, I., 2013. Anaerobic digestion for simultaneous sewage sludge treatment and CO biomethanation: Process performance and microbial ecology. Environ Sci Technol 47, 10685–10693. https://doi.org/10.1021/es401018d

Oelgeschläger, E., Rother, M., 2008. Carbon monoxide-dependent energy metabolism in anaerobic bacteria and archaea. Arch Microbiol. https://doi.org/10.1007/s00203-008-0382-6

Pereira, A.M., de Lurdes Nunes Enes Dapkevicius, M., Borba, A.E.S., 2022. Alternative pathways for hydrogen sink originated from the ruminal fermentation of carbohydrates: Which microorganisms are involved in lowering methane emission? Anim Microbiome. https://doi.org/10.1186/s42523-021-00153-w

Qiu, S., Xia, W., Xu, J., Li, Z., Ge, S., 2023. Impacts of 2-bromoethanesulfonic sodium on methanogenesis: Methanogen metabolism and community structure. Water Res 230. https://doi.org/10.1016/j.watres.2022.119527

Roghair, M., Liu, Y., Adiatma, J.C., Weusthuis, R.A., Bruins, M.E., Buisman, C.J.N., Strik, D.P.B.T.B., 2018. Effect of n-Caproate Concentration on Chain Elongation and Competing Processes. ACS Sustain Chem Eng 6, 7499–7506. https://doi.org/10.1021/acssuschemeng.8b00200

Shahab, R.L., Brethauer, S., Davey, M.P., Smith, A.G., Vignolini, S., Luterbacher, J.S., Studer, M.H., 2020. A heterogeneous microbial consortium producing short-chain fatty acids from lignocellulose. Science (1979) 369. https://doi.org/10.1126/science.abb1214

Sharma, P., Gaur, V.K., Kim, S.H., Pandey, A., 2020. Microbial strategies for bio-transforming food waste into resources. Bioresour Technol 299. https://doi.org/10.1016/j.biortech.2019.122580

Sun, H., Yang, Z., Shi, G., Arhin, S.G., Papadakis, V.G., Goula, M.A., Zhou, L., Zhang, Y., Liu, G., Wang, W., 2021. Methane production from acetate, formate and H2/CO2 under high ammonia level: Modified ADM1 simulation and microbial characterization. Science of the Total Environment 783. https://doi.org/10.1016/j.scitotenv.2021.147581

Tang, J., Wang, X.C., Hu, Y., Zhang, Y., Li, Y., 2017. Effect of pH on lactic acid production from acidogenic fermentation of food waste with different types of inocula. Bioresour Technol 224, 544–552. https://doi.org/10.1016/j.biortech.2016.11.111

Wang, Q., Zhang, G., Wang, X., Fang, W., Zhang, P., Yang, N., Wu, Y., Ma, W., Fu, C., 2022. Promoting chain elongation efficiency from food waste by refluxing chain elongation fermentation liquid. J Clean Prod 368. https://doi.org/10.1016/j.jclepro.2022.133220

Wilson, R.M., Tfaily, M.M., Rich, V.I., Keller, J.K., Bridgham, S.D., Zalman, C.M., Meredith, L., Hanson, P.J., Hines, M., Pfeifer-Meister, L., Saleska, S.R., Crill, P., Cooper, W.T., Chanton, J.P., Kostka, J.E., 2017. Hydrogenation of organic matter as a terminal electron sink sustains high CO2:CH4 production ratios during anaerobic decomposition. Org Geochem 112, 22–32. https://doi.org/10.1016/j.orggeochem.2017.06.011

Wu, L., Wei, W., Chen, Z., Shi, X., Wang, D., Chen, X., Ni, B.J., 2023a. Medium chain fatty acids production from anaerobic fermentation of food wastes: The role of fermentation pH in metabolic pathways. Chemical Engineering Journal 472. https://doi.org/10.1016/j.cej.2023.144824

Wu, L., Wei, W., Qian, J., Chen, X., Ni, B.-J., 2023b. Converting Food Waste into High-value Medium Chain Fatty Acids and Long Chain Alcohols via Chain Elongation with Internally Produced Electron Donor. Green Chemistry. https://doi.org/10.1039/d3gc03614f

Wu, W., Arhin, S.G., Sun, H., Li, Z., Yang, Z., Liu, G., Wang, W., 2023. Facilitated CO biomethanation by exogenous materials via inducing specific methanogenic pathways. Chemical Engineering Journal 460. https://doi.org/10.1016/j.cej.2023.141736

Yin, D. min, Mahboubi, A., Wainaina, S., Qiao, W., Taherzadeh, M.J., 2021. The effect of mono- and multiple fermentation parameters on volatile fatty acids (VFAs) production from chicken manure via anaerobic digestion. Bioresour Technol 330. https://doi.org/10.1016/j.biortech.2021.124992

Zhang, Y., Bai, J., Zuo, J., 2023. Performance and mechanisms of medium-chain fatty acid production by anaerobic fermentation of food waste without external electron donors. Bioresour Technol 374. https://doi.org/10.1016/j.biortech.2023.128735

Zhu, X., Tao, Y., Liang, C., Li, X., Wei, N., Zhang, W., Zhou, Y., Yang, Y., Bo, T., 2015. The synthesis of n-caproate from lactate: a new efficient process for medium-chain carboxylates production. Sci Rep 5, 14360. https://doi.org/10.1038/srep14360

Chapter 5

Facilitated medium-chain fatty acids production from food waste and ethanol co-fermentation: impact of lactate to ethanol ratio of chain elongation product spectrum

S. G. Arhin, A. Cesaro, F. Di Capua, G. Esposito

Manuscript

5.1 Introduction

Due to the growing human population and urbanization in recent years, municipalities are faced with the challenge of solid waste management and an urgent need for research on economically attractive and sustainable strategies to recover resources from them. Biowaste, composed of food and garden waste, remains a key component of the solid waste stream in many regions, including Europe (Dalke et al., 2021; European Environment Agency, 2020). Due to its significant proportion, biowaste valorization to value-added products is a crucial node in the implementation of a circular economy and realizing the goals of modern environmental policies such as the European Green Deal, which seeks to achieve a carbon neutral Europe by 2050 (European Commission, 2019).

Over the years, anaerobic microbiomes as biocatalysts have been used to convert biowaste into various products, including short-chain fatty acids (SCFAs) with 2–5 carbon atoms, hydrogen (H_2), and carbon dioxide (CO_2) (Akhlaghi et al., 2019; Hafid et al., 2022; Spirito et al., 2014). In anaerobic digesters with long cell residence times, the end-product of the bioconversion process is methane (CH_4) (Angenent et al., 2016). However, CH_4 has relatively low monetary value and, in the absence of governmental policies and subsidies, its production may be economically uninviting (Spirito et al., 2014; Yu et al., 2019). Fortunately, under certain environmental conditions (e.g., the presence of a reduced substrate and/or by inhibiting methanogenesis) other fermentation products with higher monetary value, including MCFAs can be produced (Wu et al., 2023b). Compared to conventional anaerobic products such as CH_4 and SCFAs, MCFAs such as caproate are deemed more profitable and are rapidly gaining attention in the literature (Zhu et al., 2015). MCFAs carry more energy due to their higher carbon-oxygen-ratio and have better separation properties due to their longer hydrophobic carbon chains (Wang et al., 2020). Moreover, their versatility as platform chemicals gives them a wide range of industrial applications, including food additives, fragrances, aviation fuels, biodiesel, bioplastics, and lubricants.

MCFAs can be produced via chain elongation, a nascent biorefinery process for the carboxylate platform based on the RBO or FAB metabolic pathways. In chain elongation reactions, SCFA are elongated at each cycle with two-carbon units derived from a reduced substrate, the electron donor. Due to the role of the electron donor in the requisite intermediate acetyl-CoA (RBO) or malonyl-ACP (FAB) formation, it is considered an indispensable metabolic requirement in the

chain elongation process. Therefore, several studies have explored various electron donors, including ethanol, methanol, propanol, lactate, galactitol, H_2, and CO, as carbon and energy sources for the chain elongation bacteria (Fernando-Foncillas and Varrone, 2021; Seung et al., 2013; Steinbusch et al., 2011; Xu et al., 2018). The data suggests ethanol and lactate as the two most preferred electron donors for high-rate chain elongation (Wu et al., 2018). However, both ethanol and lactate exhibit their respective limitations. High concentrations of ethanol, for example, could be toxic to microbiomes and inhibit MCFAs synthesis (Liu et al., 2017). Also, past studies have demonstrated that for every five chain elongation reactions, one extra mol of ethanol is oxidized to acetate to generate energy (ATP) via substrate-level phosphorylation (Eqs. 1 and 2) (Seedorf et al., 2008). However, ethanol oxidation to acetate at ratios higher than 5:1 has been observed (Grootscholten et al., 2014; Roghair et al., 2018a). This phenomenon, known as excessive ethanol oxidation (EEO, Eq. 3), is performed by ethanol-oxidizing bacteria that do not participate in chain elongation but compete to diverge ethanol use towards MCFAs synthesis (Roghair et al., 2018b). EEO also acidifies the fermentation broth and leads to extra base supplementations, which adds to operation costs. Another limitation of the ethanol-guided pathway is the cost implications of constantly supplementing CO_2 to the bioreactor to sustain the growth of chain elongators (Reddy et al., 2020). On the other hand, the dispersive lactate-carbon flow is also a challenge in the lactate-guided pathway. Over 30% of the carbon in lactate – converted to CO_2 in the necessary step of lactate oxidization to acetyl-CoA – becomes redundant. Furthermore, some carbons are converted to propionate via the competing acrylate pathway, further reducing MCFAs selectivity (Wu et al., 2019). Also, a constant supply of chemicals is required to keep the pH ideal for the chain elongators as lactate-guided chain elongation consumes protons (Eqs. 4 and 5).

Considering the limitations of solely employing either ethanol or lactate as the electron donor, combining them as co-electron donors to drive chain elongation reactions could have a synergistic influence on MCFAs production (Wu et al., 2018). Lactate could compensate for the low ethanol concentrations in the ethanol-guided route. Superfluous CO_2 released in the lactate-guided process could also make up for the CO_2 required in the ethanol-guided pathway. Furthermore, this study postulates that at the optimum ratio, the net proton consuming behavior of the lactate-guided process (Eq 4 and 5) could compensate for the net proton release in the ethanol-guided process because of chain elongation (Eq. 1 and 2) or EEO (Eq. 3) to bypass the

requirement of a buffering again during chain elongation. However, limited information exists on the ratio of lactate and ethanol needed to realize these potential benefits.

$$6C_2H_5O + 4C_2H_3O_2^- \rightarrow 5C_4H_7O_2^- + C_2H_3O_2^- + 4H_2O + 2H_2 + H^+, \Delta G^O = -182.5\ \text{kJ/mol} \quad (1)$$

$$6C_2H_5O + 5C_4H_7O_2^- \rightarrow 5C_6H_{11}O_2^- + C_2H_3O_2^- + 4H_2O + 2H_2 + H^+, \Delta G^O = -183.5\ \text{kJ/mol} \quad (2)$$

$$C_2H_6O + H_2O \rightarrow C_2H_3O_2^- + 2H_2 + H^+, \Delta G^O = -49.6\ \text{kJ/mol} \quad (3)$$

$$C_3H_5O_3^- + C_2H_3O_2^- + H^+ \rightarrow C_4H_7O_2^- + H_2O + CO_2,\ \Delta G^O = -97.7\ \text{kJ/mol} \quad (4)$$

$$C_3H_5O_3^- + C_4H_7O_2^- + H^+ \rightarrow C_6H_{11}O_2^- + H_2O + CO_2,\ \Delta G^O = -97.9\ \text{kJ/mol} \quad (5)$$

Besides the cost and environmental impacts associated with the use of commercial chemicals for pH control, another major bottleneck in the chain elongation process is the use of commercial reactants such as ethanol (Roghair et al., 2018a). Therefore, from an economic and environmental sustainability perspective, in-situ generation of electron acceptors and donors from organic residues is gaining attention (Reddy et al., 2020). In chapter 3, it was demonstrated that food waste is a viable substrate for the synthesis of electron acceptor and donors for MCFAs production (Arhin et al., 2023). Nonetheless, given the complex biochemical reactions, in-situ generation of ethanol was overshadowed by lactate and VFA-producing pathways in the mixed culture system. Ethanol yield could be improved by bioaugmentation with pure cultures (Wu et al., 2023c). Alternatively, ethanol could be generated from another waste stream such as lignocellulosic biomass (e.g., wheat straw) (Karagöz and Özkan, 2014) and co-fermented with the food waste acidification products. However, the co-utilization of different waste streams for MCFAs has received less attention in the literature. Nonetheless, co-fermentation of different organic residues could improve MCFAs yield compared to mono-fermentation (Fernando-Foncillas and Varrone, 2021).

Based on the above considerations, the study aimed to shed light into the valorization of biowaste into MCFAs by assessing the potential cooperative effect of co-fermenting lactate and ethanol as co-electron donors for MCFA biosynthesis. To this end, preliminary acidogenic fermentation experiments aimed at lactate synthesis from food waste and ethanol from wheat straw were performed. Lactate and ethanol were then feed at various molar ratios to obtain the

optimum lactate-ethanol-ratio. The potential synergistic effects of lactate and ethanol as co-electron donors on pH stabilization and MCFAs production were assessed.

5.2 Materials and methods

5.2.1 Substrates and inocula

The food waste was collected from a food retail market in Naples (Campania, Italy), and it comprised of fruits and vegetables waste (79 %), stale bread (6 %), pasta/rice/cereal/flour residue (5 %), meat residue (8 %), and cheese residue (2 %) as shown in Arhin et al. (2023). The food waste was immediately homogenized into a uniform slurry upon receipt with a kitchen food processor and store at −20 °C. The total solid (TS) and volatile solid (VS) contents of the food waste were 21.6 ± 0.5 % and 20.6 ± 0.2 %, respectively.

The wheat straw used for ethanol production was obtained from an agricultural field in the Campania region of Italy. The wheat straw was dried to a moisture content of 10 %, milled to pass through a 1 mm-mesh sieve, and stored until processing. The TS and VS contents of the wheat straw were 92.9 ± 0.2 % and 85.5 ± 0.2 %, respectively.

The inoculum used for acidogenic fermentation of food waste was a mesophilic digestate sampled from the anaerobic digester at the wastewater treatment plant (WWTP) in Mercato San Severino (Campania, Italy). The TS and VS contents of the inoculum were 10.0 ± 0.0 % and 2.2 ± 0.0 %, respectively.

The inoculum for chain elongation was cultivated in our lab by feeding the digestate from the WWTP regularly with acetate, butyrate, lactate, and ethanol at pH 6.0 ± 0.2 and 37 ± 1.0 °C. After chain elongators were activated, the inoculum was centrifuged at 6000 rpm for 10 mins and the precipitate was washed 3 times and resuspended in distilled water for the chain elongation experiments (Wang et al., 2022). The TS and VS contents of the chain elongation inoculum were 5.2 ± 0.2 % and 1.0 ± 0.0 %, respectively.

5.2.2 Lactate production from food waste via acidogenic fermentation

Lactate production from the food waste was conducted in triplicate in air-tight 1.0 L borosilicate glass bottles (Schott Duran, Wertheim, Germany) with a working volume of 0.6 L. The mass of food waste to that of the inoculum was set at 10 g VS/g VS. The bottles were flushed with ultrapure argon for 5 min after adding the food waste and inoculum and placed in

a thermostatic water bath at a mesophilic temperature (37.0 ± 1.0 °C) without pH adjustment. After 4 d fermentation, the samples were centrifuged at 6000 rpm for 10 min and the lactate-rich supernatant was collected for the chain elongation experiments.

5.2.3 Ethanol production from wheat straw

The pretreatment process for ethanol production from wheat straw was optimized by testing three different conditions: direct biomass conversion without pretreatment, dilute sulfuric acid (H_2SO_4) pretreatment, and mild alkaline (NaOH) deacetylation coupled with dilute H_2SO_4 pretreatment. The experimental conditions for the dilute H_2SO_4 pretreatment were 0.5% v/v H_2SO_4 at 140 °C for 15 min and a solid-to-liquid ratio of 1:10. Mild alkaline deacetylation was also performed with 0.4% w/v NaOH at 70 °C for 3 h and a solid-to-liquid ratio of 1:12 followed by the dilute H_2SO_4 treatment as described.

Triplicate semi simultaneous saccharification and fermentation experiments were carried out in a 500 mL flask by loading only the pretreated substrate and enzyme for 10 h at 50 °C. An enzyme combination of cellulase and β-Glucosidase at a ratio of 3:1 unit was used. After 10 h, the temperature was reduced to 35 °C for fermentation with *Saccharomyces cerevisiae* (YSC2, Merck, Germany), which was added at a 5 % substrate loading. The pH was maintained at pH 5 throughout fermentation. Glucose release and ethanol production were monitored regularly during fermentation. Ethanol yield from wheat straw was calculated according to Eq. (6) (Karagöz and Özkan, 2014):

$$Y_{ethanol}\ (\%) = \frac{Ethanol\ produced\ (^{g}/_{L})}{Raw\ biomass\ (g)} \times 100 \qquad (6)$$

5.2.4 Experimental set up for chain elongation

The chain elongation experiments were performed in triplicate in 250 mL serum bottles with a working volume of 150 mL. The lactate-rich supernatant from the food waste acidogenic fermentation and ethanol were mixed to a final concentration of electron donors (i.e., lactate and/or ethanol) and acceptors as shown in **Table 5.1**. The bottles were inoculated with 5 g VS/L of the chain elongation inoculum and a growth medium solution containing NH_4Cl (1.5 g/L), $MgSO_4 \cdot 7H_2O$ (0.20 g/L), NaH_2PO_4 (1.0 g/L), KCl (0.15 g/L), $MgCl_2 \cdot 6H_2O$ (0.33 g/L), $CaCl_2$ (0.2 g/L), 2-bromosulfonate (10 g/L), and 1 mL/L of trace elements solution (Nzeteu et al., 2022). The trace element solution contained the following per liter of distilled water: nitrilotriacetic acid 2.0 g; $MnSO_4.H_2O$ 1.0 g; $Fe(SO_4)_2(NH4)_2.6H_2O$ 0.8 g; $CoCl_2.6H_2O$ 0.2 g;

$ZnSO_4.7H_2O$ 0.2 mg; $CuCl_2.2H_2O$ 20.0 mg; $NiCl_2.6H_2O$ 20.0 mg; $Na_2MoO_4.2H_2O$ 20.0 mg; Na_2SeO_4 20.0 mg; Na2WO4 20.0 mg. A set of bottles with the inoculum, medium, and distilled water only was used as a negative control (denoted as Blank). The initial pH was adjusted to 6.0 ± 0.1. The bottles were sealed with butyl rubber stoppers and aluminium seals, and their headspaces were purged with ultrapure argon for 5 mins to ensure anoxic conditions. All the bottles were incubated in a thermostatic water bath at a mesophilic temperature (37.0 ± 1.0 °C) without operational pH adjustment. The biogas volume and composition, pH, and carboxylates production were monitored at regular time interval during fermentation.

Table 5.1. Experimental setup for chain elongation with lactate and ethanol as co-electron donors (Co-EDs). The lactate-to-ethanol mole ratio in each test is indicated in parentheses.

Test groups	Concentration of electron donors and acceptors
Blank (negative control)	-
Co-ED1(4.0)	334 mM lactate + 89 mM ethanol + 62 mM acetate + 9 mM propionate + 3 mM *iso*-butyrate + 33 mM *n*-butyrate + 2 mM *iso*-valerate + 94 mM *n*-valerate
Co-ED2 (1.5)	205 mM lactate + 134 mM ethanol + 39 mM acetate + 4 propionate + 1 mM *iso*-butyrate + 21 mM *n*-butyrate + 1 mM *iso*-valerate + 57 mM *n*-valerate
Co-ED3 (0.9)	137 mM lactate + 153 mM ethanol + 25 mM acetate + 4 propionate + 1 mM *iso*-butyrate + 13 mM *n*-butyrate + 1 mM *iso*-valerate + 38 mM *n*-valerate
Co-ED4 (0.6)	90 mM lactate + 159 mM ethanol + 15 mM acetate + 2 propionate + 0.2 mM *iso*-butyrate + 8 mM *n*-butyrate + 0.6 mM *iso*-valerate + 27 mM *n*-valerate
Co-ED5 (0.4)	68 mM lactate + 167 mM ethanol + 11 mM acetate + 2 propionate + 0.2 mM *iso*-butyrate + 6 mM *n*-butyrate + 0.4 mM iso-valerate + 19 mM *n*-valerate
SE [*] (0)	200 mM ethanol + 16 mM acetate + 13 mM propionate + 18 mM *n*-butyrate + 2 mM *iso*-valerate

[*] SE implies ethanol as the sole electron donor.

5.2.5 Analytical methods

TS and VS were analyzed using standard methods (APHA, 2005). The pH was measured with a WTW ProfiLine pH 3110 pH meter. The biogas produced during acidogenic fermentation was collected into air-tight gas bags and the biogas volume was measured by the water displacement method. Meanwhile, biogas volume in the chain elongation experiments was determined based on the pressure in the headspace (Sun et al., 2021). The gas composition was

analyzed by a Star 3400 gas chromatograph (Varian, Palo Alto, CA, USA). Samples for carboxylates and ethanol analysis were centrifuged at 10,000 rpm for 10 min in a Mikro 22R centrifuge (Hettich, UK), followed by microfiltration of the supernatant through 0.45 μm (ALWSCI Technologies, China) and 0.22 μm (AM&C, Italy) nylon membranes. The samples were then analyzed by high-performance liquid chromatography (UVD 340U HPLC system, Dionex, CA, USA) equipped with a diode array detector and a Metrosep organic acid column 250/7.8 (Metrohm, Herisau, Switzerland). The mobile phase consisted of 1% H_2SO_4 solution at a flow rate of 0.7 mL/min.

5.2.6. Statistical analysis and calculations

The statistical significance difference among the carboxylates formed in the chain elongation experiment was assessed through a one-way analysis of variance followed by the Tukey post hoc test. IBM SPSS Statistics version 26 (IBM corporation, USA) was used for statistical analysis, and $p < 0.05$ was considered statistically significant. OriginPro 2021 (OriginLab Corporation, USA) was used for graphs and charts.

To quantitatively assess and compare the relative energy balance among the metabolites produced, the amount of chemical energy in the form of COD was computed. For H_2, the COD equivalent was calculated by considering 1 mol of H_2 to correspond to 16 g of COD, while for the carboxylic acids and ethanol the specific COD conversion coefficients (i.e., 1 g of acetate, formate, and lactate = 1.07g COD, 1 g of propionate = 1.51g COD, 1 g of butyrate = 1.82 g COD, 1 g of valerate = 2.04 g COD, 1 g of caproate = 2.21 g COD, and 1 g of ethanol = 2.09 g COD) were adopted (Wu et al., 2020).

5.3 Results and discussion

5.3.1 Acidogenic fermentation without pH adjustment favoured lactate production

Fig. 5.1(a-c) shows the pH trend, carboxylates spectrum, and biogas composition in the acidogenic fermentation experiment targeting lactate from food waste for subsequent utilization as an electron donor in the chain elongation experiment. As shown in **Fig 5.1a**, the pH dropped rapidly from 5.2 ± 0.1 to 3.5 ± 0.0 by day 3 because no exogenous buffering agent was supplemented. The pH remained at 3.5 ± 0.0 by the end of day 4 when the experiment was terminated. As expected, the relatively low pH in the system facilitated the accumulation of lactate over other carboxylates (**Fig 5.1b)**. The lactate concentration reached 50.1 ± 0.4 g/L.

Lactate constituted about 80 % of the carboxylates produced. In contrast, VFAs such as acetate, propionate, and butyrate remained low. The main VFAs produced alongside lactate were acetate, propionate, *n*-butyrate, *iso*-butyrate, *iso*-valerate, and *n*-valerate. Besides the carboxylates, the relatively low pH in the acidogenic fermentation system also facilitated solventogenesis, leading to ethanol production. The ethanol concentration reached 6.7 ± 0.3 g/L on day 4. As shown in **Fig. 5.1c**, the H_2 content of the biogas in the acidogenic fermentation phase remained low with a volumetric production of 174.0 ± 0.1 mL (1.9 mg-H_2 COD/g VS). CH_4 was not detected even though no methane inhibiting strategy was implemented.

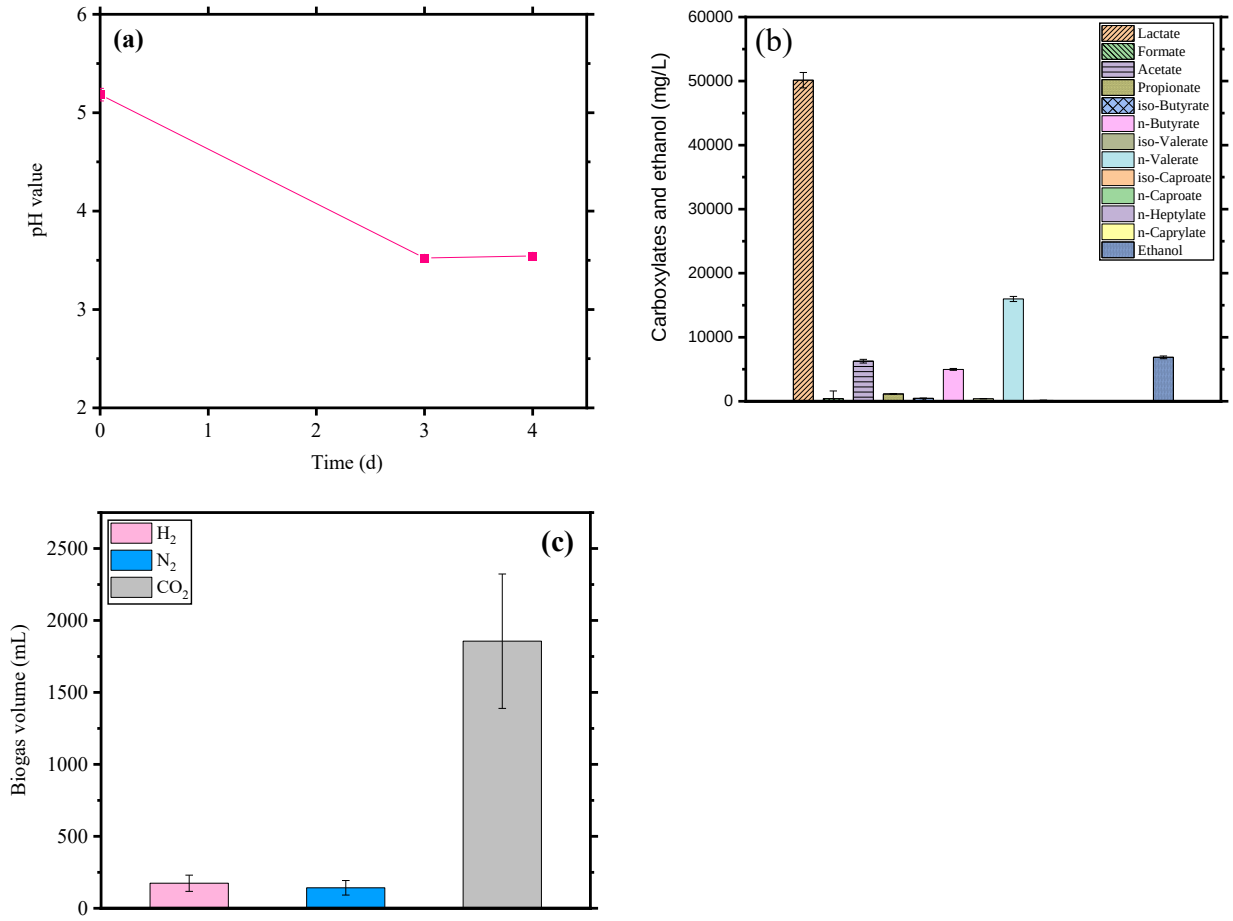

Fig. 5.1. Profiles of (a) pH, (b) carboxylates profile, and (c) biogas composition during acidogenic fermentation of food waste at a mesophilic temperature without pH control

Altogether, these results suggest that the acidic pH in the acidogenic fermentation phase enriched lactic acid bacteria (LBA) over other functional groups, including methanogens and VFA-producers. LBA are known to tolerate acidic environments and could produce antimicrobial compounds, including peptides alongside lactate that could impede the growth

of methanogens and VFA-producers (Zhang et al., 2022). The enrichment of LBA and the dominance of lactate-type fermentation over acetate- and butyrate-type fermentation, which are typically associated with H_2 production (Akhlaghi et al., 2019), could also explain why H_2 production in the acidogenic fermentation phase remained low.

5.3.2 Mild alkaline deacetylation promoted ethanol generation from wheat straw

Fig. 5.2 displays the glucose production and ethanol yield from wheat straw. The semi-simultaneous saccharification and fermentation approach was used to prevent glucose accumulation and facilitate its conversion to ethanol. Hence, at the onset of fermentation, varying amounts of glucose had been released from the wheat straw for fermentation by *S. cerevisiae*. The raw biomass seemingly had the highest glucose concentration (198.4 ± 76.3 mg/L) at this point. This is possibly because some of the finer particles obtained after milling that could be more readily converted by the enzymes were lost through the pretreatment and washing procedures. Nonetheless, this did not seem to have had a significant impact on ethanol yield as similar ethanol yields were obtained within the first 12 h of fermentation. After 12 h, a notable difference in ethanol yield was observed. Compared to the direct fermentation of the raw wheat straw without pretreatment, the ethanol yield almost doubled with mild alkaline deacetylation coupled with dilute sulfuric acid pretreatment (53.5 %) while implementing only dilute sulfuric acid pretreatment did not seem to have benefitted ethanol yield. After 72 h, the ethanol yields remained stable under all the three conditions until the experiment was terminated at 168 h. At the end of the experiment, only 21.0 ± 36.4 mg/L glucose remained in the systems with mild alkaline deacetylation coupled with dilute sulfuric acid pretreatment while significantly higher concentration remained in the other two systems. Therefore, mild alkaline deacetylation followed by dilute sulfuric acid was chosen as the optimum treatment for ethanol production from wheat straw.

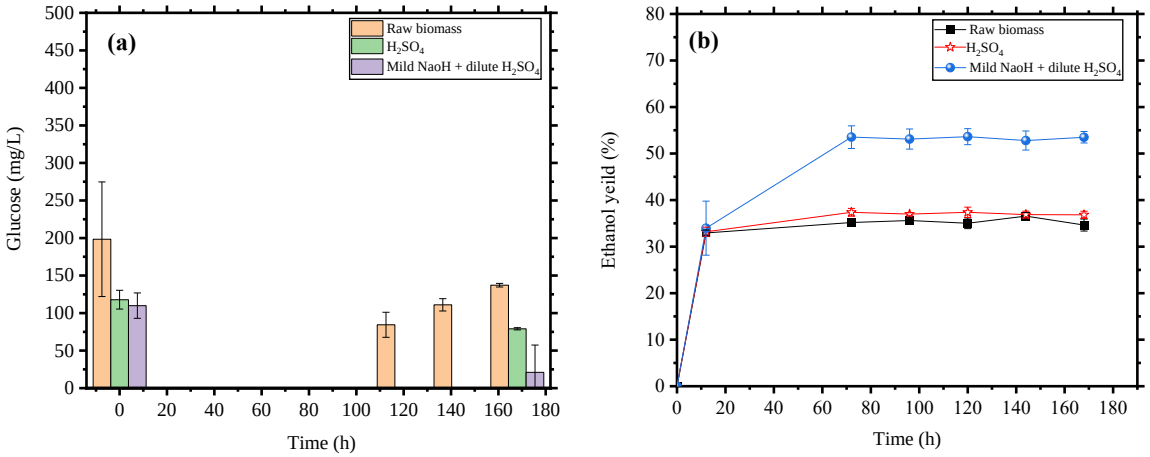

Fig. 5.2. (a) Glucose accumulation and (b) ethanol yield from wheat straw via semi simultaneous saccharification and fermentation with the raw biomass, dilute sulfuric acid pretreatment, and mild alkaline deacetylation coupled with dilute sulfuric acid pretreatment.

5.3.3. Higher lactate-to-ethanol ratios ensured pH stability during chain elongation

Fig. 5.3 shows the pH profile during chain elongation with lactate and ethanol as co-electron donors at different ratio. Because the lactate-rich solution from the acidogenic fermentation phase had a low pH of 3.5, which is below the pH range of 5.0 – 7.4 typically associated with chain elongation (Reddy et al., 2018), the initial pH was adjusted to 6.0 ± 0.1 to create a conducive environment for chain elongation to start. Afterward, the potential buffering capacity of the combined lactate and ethanol processes was relied on to maintain a stable environment for chain elongators to proliferate. As displayed in **Fig. 5.3**, the operational pH in all the bioreactors remained in the range of about 5.0 – 6.5, which is tolerable to chain elongators. Higher lactate concentrations ensured a more stable pH, while the pH seemed to have decreased rather rapidly with higher ethanol concentration, except when 200 mM of ethanol was used as the sole electron donor (SE), in which case no notable activity seemed to have occurred possibly due to the toxicity of ethanol (Liu et al., 2017). However, when lactate and ethanol were used as co-electron donors (Co-ED1), chain elongation occurred but the pH remained relatively stable round pH 6.0, reaching a final value of 6.0 ± 0.2 on day 6. When lactate and ethanol were supplied at a ratio of 1.5 (Co-ED2), the pH dropped slightly to 5.8 ± 0.1 on day 1, increased to 6.4 ± 0.1 of day 2, and decreased again to 5.6 ± 0.7 by day 6. A similar trend was observed with Co-ED3, whereby the pH dropped to 5.8 ± 0.1 on day 1, increases to 6.3 ± 0.0 on day 2, and then decreased to 5.1 ± 0.1 on day 6. In contrast, when the lactate concentration was significantly lower than that of ethanol (i.e., Co-ED4 and Co-ED5),

the pH dropped continuously from day 1 to 6, reaching 5.0 ± 0.0 on day 6. These results suggest that stable pH conditions could be attained during chain elongation with lactate and ethanol as co-electron donors by adjusting their ratios to capitalize on their respective proton consuming and releasing behaviour to cutdown on operational costs associated with the supplementation of buffering agents.

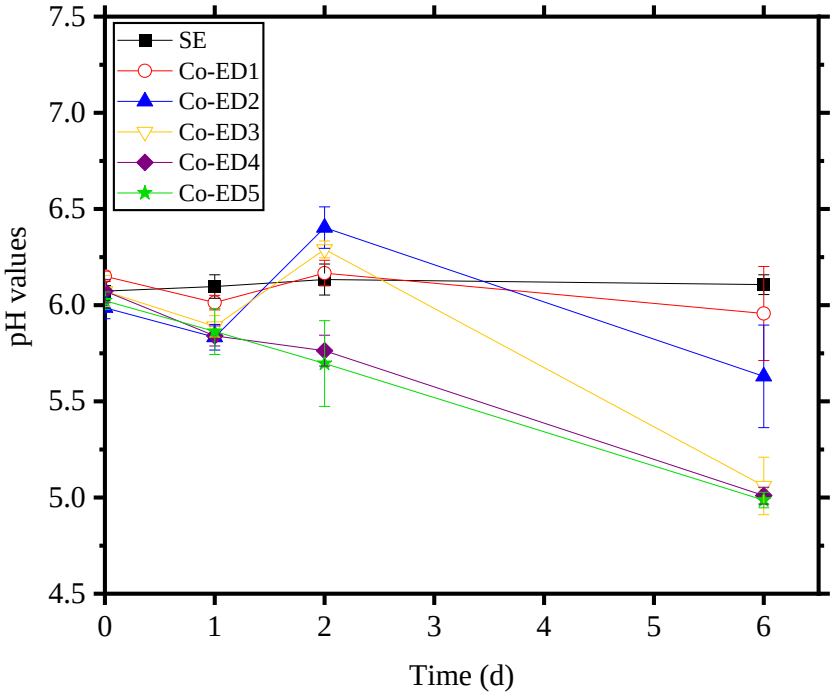

Fig. 5.3. pH profile of the chain elongation bioreactors with different lactate-ethanol ratios.

5.3.4 Higher lactate-to-ethanol ratios enhanced medium-chain fatty acids production

Fig. 5.4(a-f) shows the carboxylates spectrum with lactate and ethanol as electron donors. Chain elongation reactions typically start with lactate oxidation to acetate and CO_2 as the side product when lactate is supplied as the electron donor, and the reaction is favoured in slightly acidic conditions (pH 5.0 – 5.5) (Duber et al., 2022). However, at a slightly higher pH (e.g., pH 6), competing pathways including the acrylate, propanediol, and methylmalonyl-CoA pathways could be activated, leading to propionate formation, and subsequently, creating a competition for the remaining lactate usage between odd and even chain elongation pathways. As discussed in **section 5.3.3**, the pH was maintained at around pH 6 in the initials 24 h of fermentation with Co-ED1. Therefore, propionate production was facilitated, and the product spectrum after chain elongation consisted of even and odd chain carboxylates, including acetate, propionate, *n*-butyrate, *n*-valerate, *n*-caproate, with *n*-heptylate accumulating as the

main products (**Fig. 5.4a**). However, when lactate was combined with ethanol as co-electron donors at Co-ED2 to Co-ED5 the pH dropped below 6 on day 1, decreasing with increasing ethanol concentration. This phenomenon reduced propionate synthesis and the subsequent production of odd chain carboxylates chain elongation (**Fig. 5.4 b-e)**. Hence, a substantial fraction of the electron donors after the initial oxidation reactions were more readily directed towards the pathway for caproate production, resulting in the highest caproate concentration of in Co-ED2 (**Fig. 5.4b**). These results were consistent the work of Candry et al. (2020) who observed that propionate producers outcompeted chain elongator for lactate use at pH 6 and above, but pH lower than 6 stimulated lactate-based chain elongation to even chain carboxylates. It must be stated that even though the highest caproate concentration was observed with Co-ED2, n-heptylate remained the dominant product on day 6 because n-valerate was the main electron acceptor in the onset of chain elongation.

Although propionate production and subsequent competition for electron donors between the even- and odd-chain elongation pathways were limited in Co-ED3, Co-ED4, and Co-ED5 caproate production was lower than Co-ED1. A possible explanation is that the high ethanol concentrations (>150 mM) in these bottles may have affected chain elongation. It was observed that ethanol concentration of 40 mM and above could inhibit acidogenic bacteria that perform ethanol oxidation to initiate chain elongation (Liu et al., 2017). However, several studies have also reported high-rate chain elongation with ethanol concentrations above 40 mM. For example, Yang et al. (2018) reported caproate concentrations ranging from 6.5 – 8.6 g COD/L with 150 mM of ethanol and 50 mM of acetate as carbon sources. Angenent et al. (2016) suggest that the threshold ethanol concentration at which an acclimated microbiome may become inhibited is ∼200−400 mM. Considering that the chain elongation inoculum was cultivated by feeding a medium containing ethanol, it is unlikely that ethanol concentrations ranging from 153 –167 mM inhibited the activities of the microbiome. However, as noted in **section 5.3.3**, it appears that ethanol concentration of 200 mM in the sole ethanol-driven chain elongation situation was the threshold concentration at which the microbiome became inhibited in this study, with caproate production below 0.02 g COD/L.

Another explanation for the limited caproate and overall MCFAs concentrations in Co-ED3, Co-ED4, and Co-ED5 could be due to products-induced toxicity due to the low pH (∼5) observed under these conditions. Although pH 5 could limit competition for chain elongators and electron donor use, it is close to the pka of carboxylates (e.g., 4.88 for *n*-caproate), and

therefore, a substantial proportion of the carboxylates exist as undissociated acids at this pH (Candry et al., 2020a). Undissociated *n*-caproate is known to be extremely toxic to microbiomes, limiting its own production. For instance, Vasudevan et al. (2014) suggest that 0.2 g/L of undissociated *n*-caproate is the threshold concentration for severe inhibition to occur in an unacclimated culture, while Ge et al. (2015) reported that undissociated *n*-caproate concentrations above 0.85 g/L could cause severe inhibition in an acclimated biomass. Thus, the potential formation of undissociated *n*-caproate at the low pH observed in Co-ED3, Co-ED4, and Co-ED5 could explain why caproate production was low in these lactate-to-ethanol ratios. This phenomenon may have affected ethanol use for chain elongation, leading to the accumulation of ethanol in under these conditions.

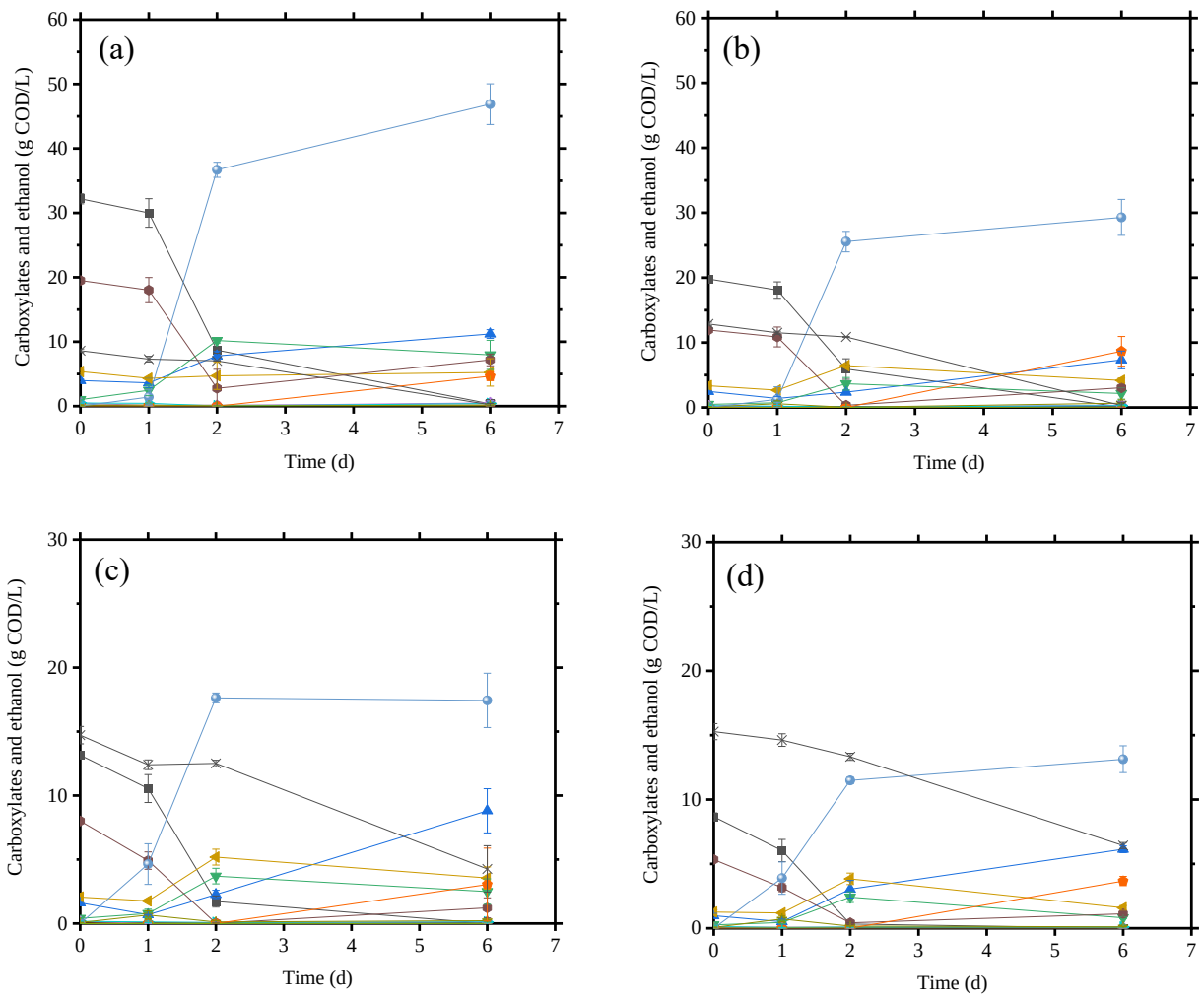

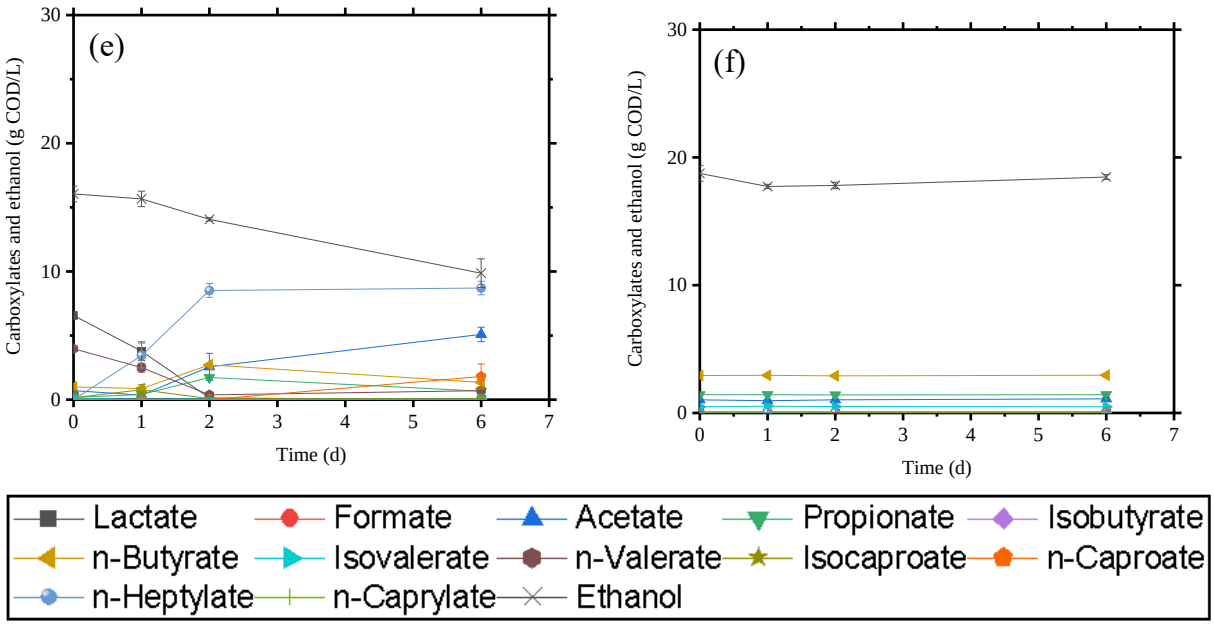

Fig. 5.4. Carboxylates profile at the end of chain elongation with lactate and ethanol as electron donors. ((a) Co-ED1, (b) Co-ED2, (c) Co-ED3, (d) 2 Co-ED4, (e) Co-ED5, and (f) sole ethanol as electron donor.

5.3.5 High lactate concentration facilitated H_2 and CO_2 production

The biogas produced in the chain elongation experiment with lactate and/or ethanol is shown in **Fig. 5.5**. Altogether, the biogas volume increased with increasing lactate concentration. The highest H_2 production rate (382 ± 19 mL/d) and cumulative H_2 volume (442 ± 22 mL) was observed with Co-ED1. Similarly, the highest CO_2 production rate (120 ± 25 mL/d) was recorded with lactate as the sole electron donor. The high H_2 production with increasing lactate concentration could be due to the release of H_2 through dehydrogenase in the lactate-driven chain elongation (Tang et al., 2023). Also, the positive correlation between the CO_2 volume and lactate concentration could be explained by the release of CO_2 in the requisite step of lactate oxidation to acetyl-COA during chain elongation (Wu et al., 2019).

H_2 and CO_2 produced during chain elongation are beneficial for MCFAs production. CO_2 is known to be essential for the growth of ethanol chain elongating bacteria, and a high CO_2 loading rate was associated with high MCFAs production in a previous study (Roghair et al., 2018). Similarly, high H_2 partial pressures could prevent the EEO, and H_2 partial pressure higher than 0.03 atm may avoid the oxidation of the carboxylates produced (Wu et al., 2023a). The beneficial roles of H_2 and CO_2 were evident in the co-electron donor situation, particularly Co-ED1 and Co-ED2 that had the highest *n*-heptylate and *n*-caproate production, respectively,

as H_2 and CO_2 generated in the initial fermentation days were later utilized to facilitate caproate production. In contrast, no apparent production nor utilization of H_2 and CO_2 was observed with ethanol as the sole electron donor.

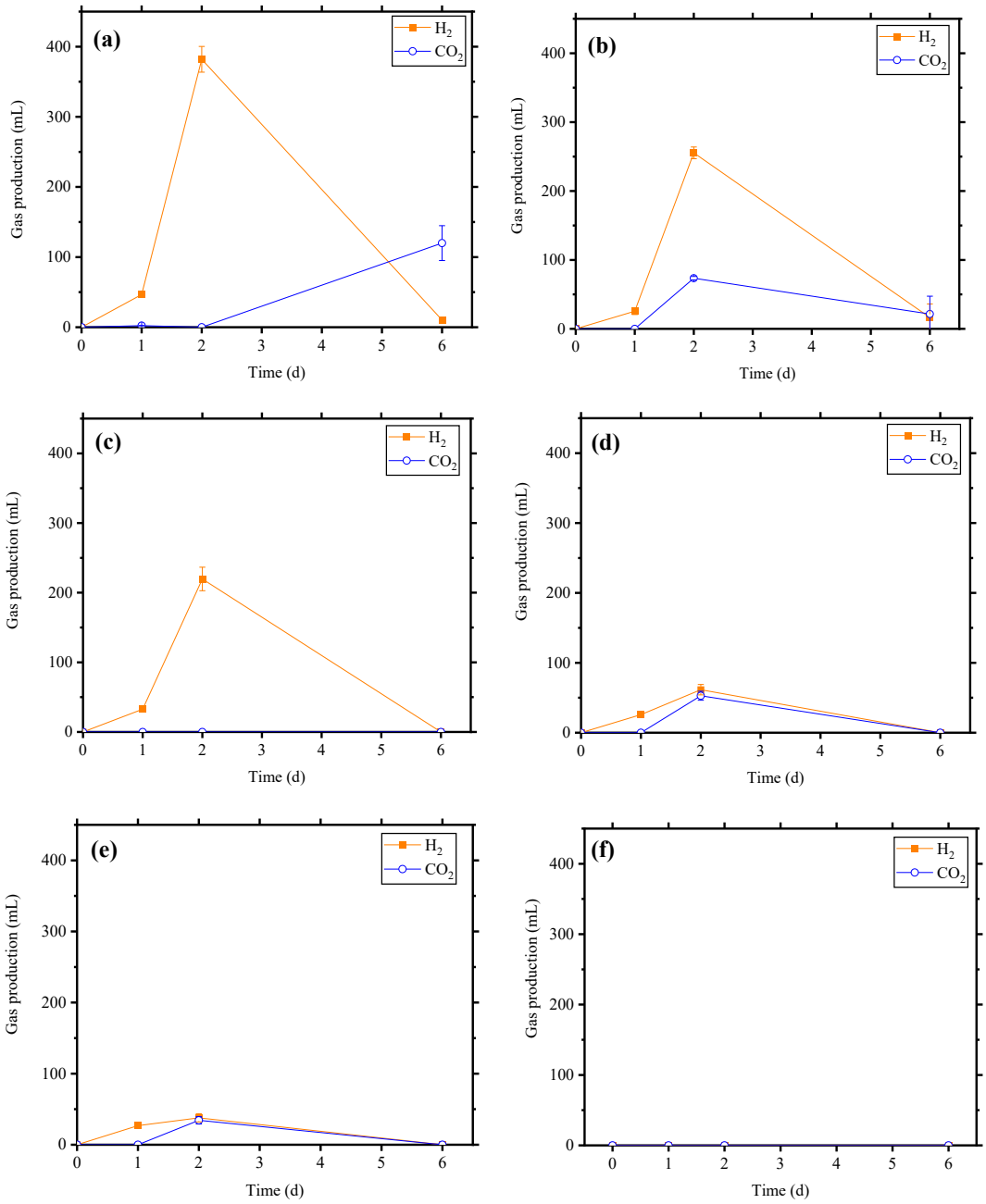

Fig. 5.5. Biogas production during chain elongation with lactate and/or ethanol as electron donors. (a) Co-ED1, (b) Co-ED2, (c) Co-ED3, (d) 2 Co-ED4, (e) Co-ED5, and (f) sole ethanol as electron donor.

Conclusions

In this study the potential synergistic effects of using waste-derived lactate and ethanol as co-electron donors for MCFAs biosynthesis were assessed. The following conclusions could be drawn from the study:

- Combining lactate and ethanol at a high lactate-to-ethanol mole ratio of c.a. 4 (Co-ED1) was the optimum ratio for activating the self-buffering capacity of the combined lactate and ethanol chain elongation processes, maintaining a relatively stable pH (≥ 6), thereby facilitating propionate production from lactate and the subsequent odd-chain elongation pathway, leading to the highest n-heptylate production.
- Lactate-to-ethanol ratio of c.a. 1.5 (Co-ED2) maintained the right pH conditions to limit propionate induced competitions and facilitate *n*-caproate generation, leading to the highest *n*-caproate concentration.
- Higher ratios of ethanol to lactate (i.e., lactate-to-ethanol ratios below 1) limited propionate formation by shifting the operation pH towards a mildly acidic condition. However, the relatively low pH (~5) led to low ethanol utilization and MCFAs production, possibly due to product inhibition caused by undissociated MCFAs.

References

Akhlaghi, M., Boni, M.R., Polettini, A., Pomi, R., Rossi, A., De Gioannis, G., Muntoni, A., Spiga, D., 2019. Fermentative H2 production from food waste: Parametric analysis of factor effects. Bioresour Technol 276, 349–360. https://doi.org/10.1016/j.biortech.2019.01.012

Angenent, L.T., Richter, H., Buckel, W., Spirito, C.M., Steinbusch, K.J.J., Plugge, C.M., Strik, D.P.B.T.B., Grootscholten, T.I.M., Buisman, C.J.N., Hamelers, H.V.M., 2016. Chain Elongation with Reactor Microbiomes: Open-Culture Biotechnology To Produce Biochemicals. Environ. Sci. Technol. 50, 2796−2810. https://doi.org/10.1021/acs.est.5b04847

APHA, 2005. Standard Methods for the Examination of Water and Wastewater. American Public Health Association/American Water Works Association/ Water Environment Federation, Washington, DC.

Arhin, S.G., Cesaro, A., Di Capua, F., Esposito, G., 2023. Acidogenic fermentation of food waste to generate electron acceptors and donors towards medium-chain carboxylic acids production. J Environ Manage 348, 119379. https://doi.org/10.1016/j.jenvman.2023.119379

Candry, P., Huang, S., Carvajal-Arroyo, J.M., Rabaey, K., Ganigue, R., 2020a. Enrichment and characterisation of ethanol chain elongating communities from natural and engineered environments. Sci Rep 10. https://doi.org/10.1038/s41598-020-60052-z

Candry, P., Radić, L., Favere, J., Carvajal-Arroyo, J.M., Rabaey, K., Ganigué, R., 2020b. Mildly acidic pH selects for chain elongation to caproic acid over alternative pathways during lactic acid fermentation. Water Res 186. https://doi.org/10.1016/j.watres.2020.116396

Dalke, R., Demro, D., Khalid, Y., Wu, H., Urgun-Demirtas, M., 2021. Current status of anaerobic digestion of food waste in the United States. Renewable and Sustainable Energy Reviews 151. https://doi.org/10.1016/j.rser.2021.111554

Duber, A., Zagrodnik, R., Gutowska, N., Oleskowicz-Popiel, P., 2022. Lactate and Ethanol Chain Elongation in the Presence of Lactose: Insight into Product Selectivity and Microbiome Composition. ACS Sustainable Chem. Eng. 3407–3416. https://doi.org/10.1021/acssuschemeng.1c05869

European Commission, 2019. The European Green Deal.

European Environment Agency, 2020. Bio-waste in Europe - turning challenges into opportunities.

Fernando-Foncillas, C., Varrone, C., 2021. Effect of reactor operating conditions on carboxylate production and chain elongation from co-fermented sludge and food waste. J Clean Prod 292, 126009. https://doi.org/10.1016/j.jclepro.2021.126009

Ge, S., Usack, J.G., Spirito, C.M., Angenent, L.T., 2015. Long-Term n-Caproic Acid Production from Yeast-Fermentation Beer in an Anaerobic Bioreactor with Continuous Product Extraction. Environ Sci Technol 49, 8012–8021. https://doi.org/10.1021/acs.est.5b00238

Grootscholten, T.I.M., Strik, D.P.B.T.B., Steinbusch, K.J.J., Buisman, C.J.N., Hamelers, H.V.M., 2014. Two-stage medium chain fatty acid (MCFA) production from municipal solid waste and ethanol. Appl Energy 116, 223–229. https://doi.org/10.1016/j.apenergy.2013.11.061

Hafid, H.S., Omar, F.N., Abdul Rahman, N., Wakisaka, M., 2022. Innovative conversion of food waste into biofuel in integrated waste management system. Crit Rev Environ Sci Technol. https://doi.org/10.1080/10643389.2021.1923976

Karagöz, P., Özkan, M., 2014. Ethanol production from wheat straw by Saccharomyces cerevisiae and Scheffersomyces stipitis co-culture in batch and continuous system. Bioresour Technol 158, 286–293. https://doi.org/10.1016/J.BIORTECH.2014.02.022

Liu, Y., He, P., Shao, L., Zhang, H., Lü, F., 2017. Significant enhancement by biochar of caproate production via chain elongation. Water Res 119, 150–159. https://doi.org/10.1016/j.watres.2017.04.050

Nzeteu, C. orline, Coelho, F., Trego, A.C., Abram, F., Ramiro-Garcia, J., Paulo, L., O'Flaherty, V., 2022. Development of an enhanced chain elongation process for caproic acid production from waste-derived lactic acid and butyric acid. J Clean Prod 338. https://doi.org/10.1016/j.jclepro.2022.130655

Reddy, M.V., ElMekawy, A., Pant, D., 2018. Bioelectrochemical synthesis of caproate through chain elongation as a complementary technology to anaerobic digestion. Biofuels, Bioproducts and Biorefining 12, 966–977. https://doi.org/10.1002/bbb.1924

Reddy, M.V., Kumar, G., Mohanakrishna, G., Shobana, S., Al-raoush, R.I., 2020. Review on the production of medium and small chain fatty acids through waste valorization and CO2 fixation. Bioresour Technol 309, 123400. https://doi.org/10.1016/j.biortech.2020.123400

Roghair, M., Hoogstad, T., Strik, D.P.B.T.B., Plugge, C.M., Timmers, P.H.A., Weusthuis, R.A., Bruins, M.E., Buisman, C.J.N., 2018a. Controlling Ethanol Use in Chain Elongation by CO2 Loading Rate. Environ. Sci. Technol. 52, 1496−1505. https://doi.org/10.1021/acs.est.7b04904

Roghair, M., Liu, Y., Adiatma, J.C., Weusthuis, R.A., Bruins, M.E., Buisman, C.J.N., Strik, D.P.B.T.B., 2018b. Effect of n-Caproate Concentration on Chain Elongation and Competing Processes. ACS Sustainable Chem. Eng. 6, 7499−7506. https://doi.org/10.1021/acssuschemeng.8b00200

Seedorf, H., Fricke, W.F., Veith, B., Bruggemann, H., Liesegang, H., Strittmatter, A., Miethke, M., Buckel, W., Hinderberger, J., Li, F., Hagemeier, C., Thauer, R.K., Gottschalk, G., 2008. The genome of Clostridium kluyveri , a strict anaerobe. Proc. Natl. Acad. Sci. 105. https://doi.org/10.1073/pnas.07110 93105

Seung, B., Moon, C., Kim, B., Kim, H., Um, Y., Sang, B., 2013. In situ extractive fermentation for the production of hexanoic acid from galactitol by Clostridium sp . BS-1. Enzyme Microb Technol 53, 143–151. https://doi.org/10.1016/j.enzmictec.2013.02.008

Spirito, C.M., Richter, H., Rabaey, K., Stams, A.J.M., Angenent, L.T., 2014. Chain elongation in anaerobic reactor microbiomes to recover resources from waste. Curr Opin Biotechnol 27, 115–122. https://doi.org/10.1016/j.copbio.2014.01.003

Steinbusch, K.J.J., Hamelers, H.V.M., Plugge, M., Buisman, C.J.N., 2011. Biological formation of caproate and caprylate from acetate: fuel and chemical production from low grade biomassSteinbusch, K.J.J., Hamelers, H.V.M., Plugge, M., Buisman, C.J.N., 2011. Biological formation of caproate and caprylate from acetate: fuel and . Energy Environ Sci 216–224. https://doi.org/10.1039/c0ee00282h

Sun, H., Yang, Z., Shi, G., Arhin, S.G., Papadakis, V.G., Goula, M.A., Zhou, L., Zhang, Y., Liu, G., Wang, W., 2021. Methane production from acetate, formate and H2/CO2 under high ammonia level: Modified ADM1 simulation and microbial characterization. Science of the Total Environment 783. https://doi.org/10.1016/j.scitotenv.2021.147581

Tang, J., Yang, H., Pu, Y., Hu, Y., Huang, J., Jin, N., He, X., Wang, X.C., 2023. Caproic acid production from food waste using indigenous microbiota: Performance and mechanisms. Bioresour Technol 387. https://doi.org/10.1016/j.biortech.2023.129687

Vasudevan, D., Richter, H., Angenent, L.T., 2014. Upgrading dilute ethanol from syngas fermentation to n-caproate with reactor microbiomes. Bioresour Technol 151, 378–382. https://doi.org/10.1016/j.biortech.2013.09.105

Wang, Y., Wei, W., Wu, S., Ni, B., 2020. Zerovalent Iron Effectively Enhances Medium-Chain Fatty Acids Production from Waste Activated Sludge through Improving Sludge Biodegradability and Electron Transfer E ffi ciency. Environ. Sci. Technol. 54, 10904−10915. https://doi.org/10.1021/acs.est.0c03029

Wu, L., Wei, W., Chen, Z., Chen, X., Ni, B.J., 2023a. Long-chain alcohol production in open culture anaerobic fermentation. Chemical Engineering Journal. https://doi.org/10.1016/j.cej.2022.139225

Wu, L., Wei, W., Chen, Z., Shi, X., Wang, D., Chen, X., Ni, B.J., 2023b. Medium chain fatty acids production from anaerobic fermentation of food wastes: The role of fermentation pH in metabolic pathways. Chemical Engineering Journal 472. https://doi.org/10.1016/j.cej.2023.144824

Wu, L., Wei, W., Qian, J., Chen, X., Ni, B.-J., 2023c. Converting Food Waste into High-value Medium Chain Fatty Acids and Long Chain Alcohols via Chain Elongation with Internally Produced Electron Donor. Green Chemistry. https://doi.org/10.1039/d3gc03614f

Wu, Q., Bao, X., Guo, W., Wang, B., Li, Y., Luo, H., Wang, H., 2019. Medium chain carboxylic acids production from waste biomass: Current advances and perspectives. Biotechnol Adv 37, 599–615. https://doi.org/10.1016/j.biotechadv.2019.03.003

Wu, Q., Guo, W., Bao, X., Meng, X., Yin, R., Du, J., Zheng, H., Feng, X., Luo, H., Ren, N., 2018. Upgrading liquor-making wastewater into medium chain fatty acid: Insights into co-electron donors, key microflora, and energy harvest. Water Res 145, 650–659. https://doi.org/10.1016/j.watres.2018.08.046

Xu, J., Hao, J., Guzman, J.J.L., Spirito, C.M., Harroff, L.A., Angenent, L.T., 2018. Temperature-Phased Conversion of Acid Whey Waste Into Medium-Chain Carboxylic Acids via Lactic Acid: No External e-Donor. Joule 2, 280–295. https://doi.org/10.1016/j.joule.2017.11.008

Yang, P., Leng, L., Tan, G.Y.A., Dong, C., Leu, S.Y., Chen, W.H., Lee, P.H., 2018. Upgrading lignocellulosic ethanol for caproate production via chain elongation fermentation. Int Biodeterior Biodegradation 135, 103–109. https://doi.org/10.1016/j.ibiod.2018.09.011

Yu, J., Huang, Z., Wu, P., Zhao, M., Miao, H., 2019. Performance and microbial characterization of two-stage caproate fermentation from fruit and vegetable waste via anaerobic microbial consortia. Bioresour Technol 284, 398–405. https://doi.org/10.1016/j.biortech.2019.03.124

Zhang, W., Wang, S., Yin, F., Cao, Q., Lian, T., Zhang, H., Zhu, Z., Dong, H., 2022. Medium-chain carboxylates production from co-fermentation of swine manure and corn stalk silage via lactic acid: Without external electron donors. Chemical Engineering Journal 439. https://doi.org/10.1016/j.cej.2022.135751

Zhu, X., Tao, Y., Liang, C., Li, X., Wei, N., Zhang, W., Zhou, Y., 2015. The synthesis of n-caproate from lactate: a new efficient process for medium-chain carboxylates production. Nature Publishing Group 1–9. https://doi.org/10.1038/srep14360

Chapter 6

General discussion, future perspectives, and concluding remarks

6.1 General discussion

The main goal of this PhD thesis was to investigate the valorization of food waste via the nascent chain elongation process to generate MCFAs and optimize the process via the addition of LCMs to unveil the potential synergistic effects of utilizing these waste streams for medium chain fatty acids production. To this extent, this thesis begun by conducting a comprehensive review of the recent literature on potential biological valorization routes of solid waste by focusing on LCMs. The experimental phase was then channelled towards the synthesis of MCFAs via chain elongation with mixed culture fermentation using food waste and intermediates from LCMs as co-substrates. The fermentation reactions involved in MCFAs production from organic residues are centred around two key functional groups, acidogenic bacteria and chain elongators. Hence, the study sought to address some key bottlenecks related to their performance. The initial experiments aimed to optimize the acidogenic fermentation process to maximize the production of VFAs as electron acceptors and lactate as an electron donor from food waste. Afterward, electron donor and acceptors derived food waste acidogenic fermentation were co-fermented with CO to evaluate the impact of CO on methanogenesis and MCFAs production. Lastly, the potential co-operative effect of utilizing food waste and LCMs for MCFAs production was evaluated by using food waste-derived lactate and ethanol from LCMs as co-electron donors for chain elongation. The results showed that food waste and LCMs were viable substrates for MCFAs production and co-fermenting electron acceptors and donors generated from these two solid waste streams had a positive impact in chain elongation.

6.1.1 Manipulating the pH, temperature and substrate loading enhanced the generation of electron acceptors and donors

In the preliminary experiments to optimize the acidogenic fermentation phase, it was revealed that by manipulating the environmental conditions the biochemical reactions of acidogenic fermentation could be tailored towards the synthesis of specific intermediates to produce MCFAs with even or odd carbon chain lengths. The results demonstrate that the selection of pH, temperature, and substrate loading could induce various metabolic pathways towards the production of electron donors or acceptors with even or odd carbon chain lengths, which could subsequently affect the type of MCFA produced in the chain elongation stage. After a series of optimization experiments it was shown that VFAs and lactate, respectively as electron acceptors and electron donor, could be generated from food waste at high concentrations to

facilitate MCFAs production. However, ethanol producers were suppressed under the conditions examined, resulting in less than 10 % of the COD in food waste converted to ethanol under all the conditions studied. Consequently, it was deemed imperative to introduce ethanol from another waste stream to reach desirable levels for the purposes of this study.

6.1.2 Co-fermenting CO and food waste acidogenic fermentation products improves medium-chain fatty acids production

After the initial optimization process, the acidogenic fermentation products from food waste were co-fermented with CO, which could be derived from recalcitrant waste-streams such as lignocelluloses. It is known that CO may act as a potential substrate for the synthesis of ethanol or VFAs that may benefit MCFAs production. However, considering that CO is also an inhibitor to competitors such as methanogens, the dual role of CO in chain elongation systems was studied. The results demonstrated that carbon losses to methanogenesis could be prevented by co-fermenting the acidogenic fermentation products from food waste with CO. A P_{CO} of 0.25 bar was adequate to completely inhibit the growth of methanogenic archaea while availing extra carbon towards the production of MCFAs. CO induced stress created an unstable environment for methanogens to proliferate, which was supported by the low EPS contents in the presence of CO. However, CO could be converted by acidogenic bacteria to VFAs and ethanol that would be metabolized by chain elongators. Consequently, over 10 g COD/L of MCFAs could be produced without the supplementation of bioactive chemicals such as BES to inhibit methanogenic archaea.

6.1.2 Lactate and ethanol co-driven chain elongation ensures pH stability and facilitates chain elongation

Considering that a key bottleneck in chain elongation is the operational cost associated with the use of commercial buffering agents, it was postulated that lactate and ethanol as co-electron donors could synergize to maintain the right pH environment for chain elongators. When combined at the appropriate ratio, the potential for self-buffering could be induced by capitalizing on the respective net proton consuming and net proton releasing behaviours of the lactate- and ethanol-driven chain elongation processes. Meanwhile, combining lactate and ethanol could also synergize to improve MCFAs yield by compensating for their individual limitations. It was observed in this thesis that the optimum lactate-to-ethanol ratio was c.a. 4.

At this ratio, relatively stable operational pH conditions were attained to facilitate chain elongation. The self-buffering capacity of the co-electron donor chain elongation system at lactate-to-ethanol ratio of 4 ensured a highly selective *n*-heptylate production while avoiding potential MCFAs self-inhibition from the accumulation of undissociated acid.

6.2 Future perspectives

This thesis focused on a strategy to valorize food waste and lignocelluloses into high-value MCFAs for potential industrial applications. Currently, the main food waste management strategies employed in Europe includes composting and anaerobic digestion for nutrients and energy recovery. However, considering that food waste could be sustainably converted to green chemicals such as MCFAs, the recovery of MCFAs should also be included in efforts to move towards a circular economy. This is of particular importance since MCFAs used in industrial applications are currently mainly derived from unsustainable sources including fossil reserves and plants- and animals-based sources.

In this study, food waste was demonstrated as a viable substrate for MCFAs production. Yet, the sustainable utilization of the food waste fraction of municipal biowaste as a resource for MCFAs production depends highly on proper waste sorting, which takes places at the household level. Thus, there is the need for the continuous education and awareness creation on the significance of waste sorting to the sustainability of the resources at our disposal. For simplicity and research purposes, carefully selected food waste from a food retail market and kitchen waste were used for this thesis. However, for practical applications, it would be necessary to focus on municipal biowastes that may contain other components in addition to food waste.

It was demonstrated in this thesis that co-fermenting food waste acidogenic fermentation products with CO could enhance MCFAs production while supressing the activities on methanogens, which typical compete to divert carbon use towards MCFAs. To understand the specific role of CO, pure CO was used instead of syngas, which comprises other gases beside CO such as H_2, CO_2, CH_4. From the perspective of ‘real world’ applications, the use of real waste-derived syngas on chain elongation systems needs to be investigated. It was observed that CO partial pressures of 0.5 and 1.0 bar could successfully inhibit methanogenesis but did not improve MCFAs production due to the activation of an ethanolic pathway, leading to the accumulation of ethanol. Considering that the CO content of real waste-derived syngas is

typically around 30–60 %, there is the need to explore strategies to enhance the robustness of chain elongators and related functional groups to high CO stress in order to establish a real mixotrophic chain elongation system.

It was also revealed in this thesis that the use of lactate and ethanol as co-electron donors in chain elongation could surmount the limitations of employing either of them as the sole driver for chain elongation and provide extra benefits such as the potential for self-buffering to cut back on the use of exogenous chemicals for pH control and their associated operational costs. The lactate and ethanol used were generated separately and combined in the chain elongation stage. However, for real world applications, a less complex system that permits the simultaneous generation of lactate and ethanol at the desired ratio in a single process should be explored. Moreover, further research on the self-pH control strategy of the co-lactate and ethanol driven chain elongation in a continuous system is needed.

To establish process control, the valorization approach employed for MCFAs in this study focused on two-stage fermentation, in which acidogenesis and chain elongation are carried out in two separate systems. However, considering that these two processes could occur simultaneously in a single-stage system, the use of the 'one-pot' approach may provide some economic and technical benefits over the two-stage process. Yet, because of the complexity of the biochemical processes involved and the possibility to activate antagonistic pathways to chain elongation, single-stage chain elongation systems typically reduce MCFAs production to moderate and low concentrations. In this context, there is the need to explore strategies to enhance MCFAs yield in single stage systems. Additionally, in the complex biochemical process, it was shown that MCFAs production occurred simultaneously with other biobased products including VFAs, H_2, and alcohols. Therefore, future approaches should consider an integrated biorefinery system where multiple products are recovered from chain elongation systems alongside the valorization of nonconverted organics via pyrolysis or composting for nutrients recovery. In this context, there is the need for in depth life cycle and cost assessments to unveil the full potential of chain elongation.

6.3 Concluding remarks

Solid waste streams such as food waste and LCMs can be sustainably converted to MCFAs using mixed culture fermentation. In the acidogenic fermentation phase, the pH, temperature,

and substrate loading are critical environmental factors that control the product yield and spectrum. The optimization of these factors could lead to the synthesis of electron donors and acceptors that yield MCFAs with even or odd carbon length. In the chain elongation phase, it was discovered that CO supplementation at the appropriate level supressed the growth of methanogens and availed more carbon towards the chain elongation. This result provides a sustainable pathway to overcome the bottleneck of using bioactive chemicals such BES to control methanogenesis during chain elongation. Nonetheless, beyond the threshold partial pressure, CO supplementation may not improve MCFAs production. When used as co-electron donors, lactate and ethanol could synergize to increase MCFAs yield during chain elongation, and their respective ratios control the product spectrum. Chain elongation with lactate and ethanol as co-electron donors could also induce an in-situ buffering capacity from their respective net proton consuming and net proton releasing behaviours. This phenomenon is beneficial for reducing operating costs and improving MCFAs yield.

ACKNOWLEDGEMENTS

This thesis has been supported by the 36th PhD cycle scholarship of the University of Naples Federico II funded by the Italian Ministry of Education, University and Research (MIUR) in the frame of the research project entitled “Dipartimenti di Eccellenza” per Ingegneria Civile Edile e Ambientale- 1 CUP E65D18000820006. The author is also grateful to the Bio and Circular Economy Unit, Tampere University, Finland for hosting and supporting his research period abroad.

Appendices

Appendix A (chapter 3)

Table A3.1. General equations considered in the economic analysis.

Number	Equations	Notes
S1	$Y_1=35000*\omega^{0.6}$	Y_1 (€) is the capital expenditure (CAPEX) related to land, equipment, and engineering, ω (t/y) is the plant capacity. [a]
S2	$Y_2 = 493601 * (V_r/1000)^{0.7202}$	Y_2 (€) is the capital cost of an additional bioreactor that may be required depending on the processing scenario, V_r is the volume of the bioreactor (m^3).
S3	$Y = Y_1 + Y_2$	Y is the total CAPEX (€)
S4	$X_1 = 17000*\omega^{0.39}$	X_1 (€/y) is the operating expenditure (OPEX) related to employees' salaries, maintenance, transportation, and annual license. [a]
S5	$X_2 = \sum_{i=1}^{n} X_{2i}$	X_2 is the miscellaneous operating costs associated with the different scenarios (€/y) such as chemical costs for pH control, ethanol supply, the cost of caproic acid extraction, and the cost of a methanogenic inhibitor.
S6	$X = X_1 + X_2$	X is the total OPEX (€/y).
S7	$I_1 = V_c*P_1$	I_1 (€/y) is the income generated from caproic acid production, V_c (t/y) is the quantity of caproic acid produced, P_1 (€/t) is the price of caproic acid.
S8	$I_2=\omega*P_2$	I_2 (€/y) is the income from gate fees, ω (t/y) is the plant capacity, and P_2 (€/t) is the gate fees.
S9	$I = I_1 + I_2$	I (€/y) is the net income.
S10	$N = I - X$	N (€/y) is the net profit.
S11	$RoR(\%) = \frac{N}{Y}*100$	RoR (%) is the rate of return.
S12	$PBP = \frac{Y}{N}$	PBP (y) is the payback period.
S13	$NPV = \sum_{t=1}^{T} \frac{N}{(1+d)^t} - Y$	NPV (€) is the net present value, T (20 y) is the plant lifetime, and d (5%) is the discount rate.

[a] Information online suggests the inflation rate of the Euro from 2003 to 2023 is 48%. Therefore, the capital and operating expenditure values were adjusted by a factor of 1.48 to cater for inflation since the original capital and operating expenditure equations were formulated based on the 2003-euro rate (Chowdhury, 2021).

2003-euro rate: https://www.in2013dollars.com/europe/inflation/2003?amount=100.

Table A3.2. Parameters and results of the economic analysis of the three biorefinery scenarios considered.

Item	Estimation assumption		
Plant location	Naples, Italy		
Food waste production (population equivalent of Naples) (Mt/y)	67.5 [a]		
Plant capacity of food waste (kt/y)	60, 80, 100		
Feedstock	Food waste		
Main products	Scenario 1 – Butyric acid		
	Scenario 2 – Lactic acid		
	Scenario 3 – Caproic acid		
Butyric acid yield (t COD/t VS)	0.542		
Lactic acid yield (t COD/t VS)	0.583		
Caproic acid yield (t/t reactants)	0.400		
Gate fees (€/t)	90.0 [b]		
Cost of KH_2PO_4 (€/t VS)	246 [c]		
Cost of K_2HPO_4 (€/t VS)	19 [c]		
Cost of methane inhibitor (2-BES) (€/t VS)	53.7 [c]		
Cost of carboxylic acid extraction (€/t)	500 [d]		
Electricity costs (€/kWh)	0.51 [e]		
SCENARIO 1			
Plant processing capacity (kt/y)	**60**	**80**	**100**
Net capital expenditure (Y) (€)	38125936	45308924.34	51800000
Net operating expenditure(X) (€/y)	6429610	8306397.332	10162066
Net Income (I) (€/y)	11383637	15178182.77	18972728
Net profit (N) (€/y)	4954027	6871785.436	8810662
Profit per tonne VS (€/t VS/y)	394.4946	410.405801	420.9616
Rate of return (%)	12.99385	15.16651639	17.009
Payback period (y)	7.695948	6.593471925	5.87924
Net present value (€)	22487803	38408296.37	55238408

SCENARIO 2

Plant processing capacity (kt/y)	**60**	**80**	**100**
Net capital expenditure (Y) (€)	38125936	45308924	51800000
Net operating expenditure(X) (€/y)	9331905	12176118	14999221
Net Income (I) (€/y)	14294991	19059987	23824984
Net profit (N) (€/y)	4963086	6883870	8825763
Profit per tonne VS (€/t VS/y)	395.2339	411.1462	421.7022
Rate of return (%)	13.01761	15.19319	17.03815
Payback period (y)	7.681901	6.581897	5.869181
Net present value (€)	22595321	38551723	55417639

SCENARIO 3

Plant processing capacity (kt/y)	**60**	**80**	**100**
Net capital expenditure (Y) (€)	40763902	48554189	55611050
Net operating expenditure(X) (€/y)	6309886	8146765	9962525
Net Income (I) (€/y)	11854998	15806665	19758331
Net profit (N) (€/y)	5545113	7659900	9795805
Profit per tonne VS (€/t VS/y)	441.5834	457.4954	468.0516
Rate of return (%)	13.603	15.77598	17.61485
Payback period (y)	7.35132	6.33875	5.677027
Net present value (€)	26990916	44671517	63301271

[a] The quantity of food waste produced in Naples was estimated based on the average yearly per capita food waste production of **30,956 kg in Italy.** Source: https://montenapodaily.com/en/2022/03/23/nel-2022-gli-italiani-stanno-gia-sprecando-piu-cibo/

[b] A typical gate fee of 90 €/t is charged when food waste is transported to the treatment facility. Source: https://www.eea.europa.eu/data-and-maps/figures/typical-charge-gate-fee-and.

[c] The average price of Sodium 2-bromoethanesulfonate (i.e., 2-BES, 1000 €/t), caproic acid (3000 €/t), KH_2PO_4 (700 €/t) and K_2HPO_4 (700 €/t) was taken from http://www.alibaba.com/.

[d] Based on Woo and Kim (2019).

[e] Source: https://www.globalpetrolprices.com/Italy/electricity_prices

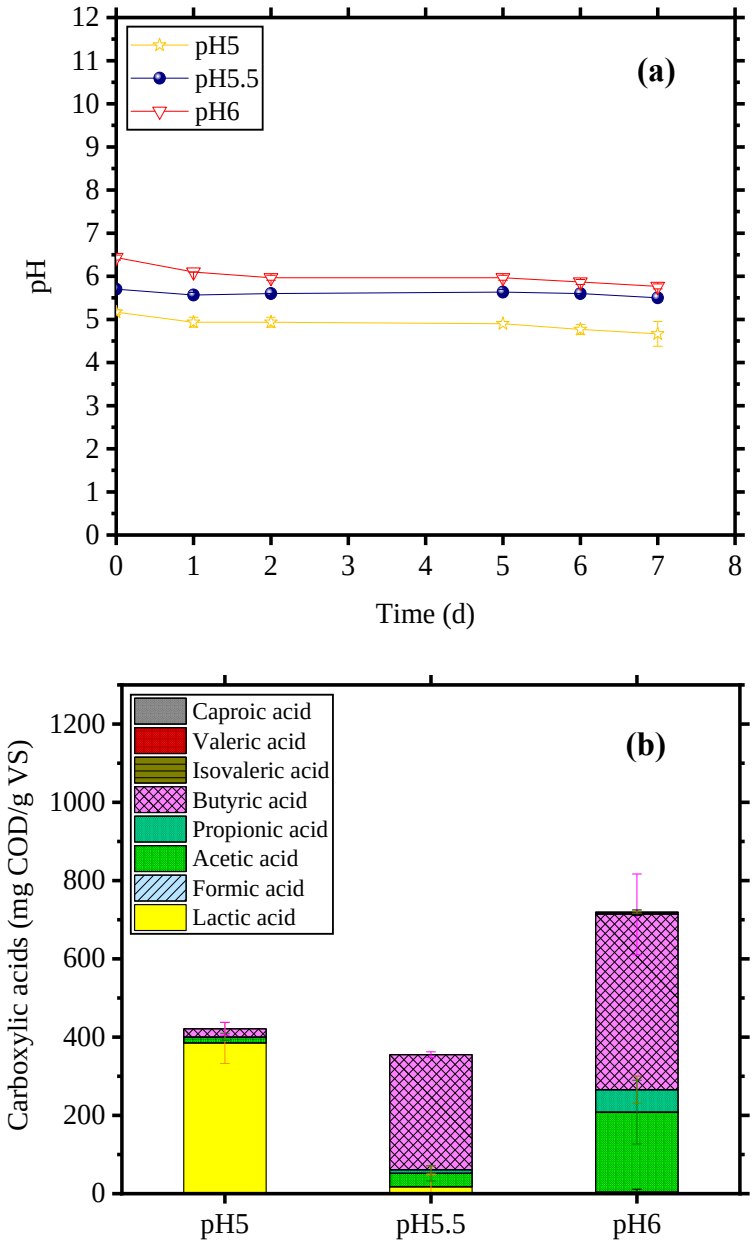

Fig. A3.1. pH profiles (a) and carboxylic acids yield (b) at pH 5, 5.5, and 6 under mesophilic conditions and F/M ratio of 1.

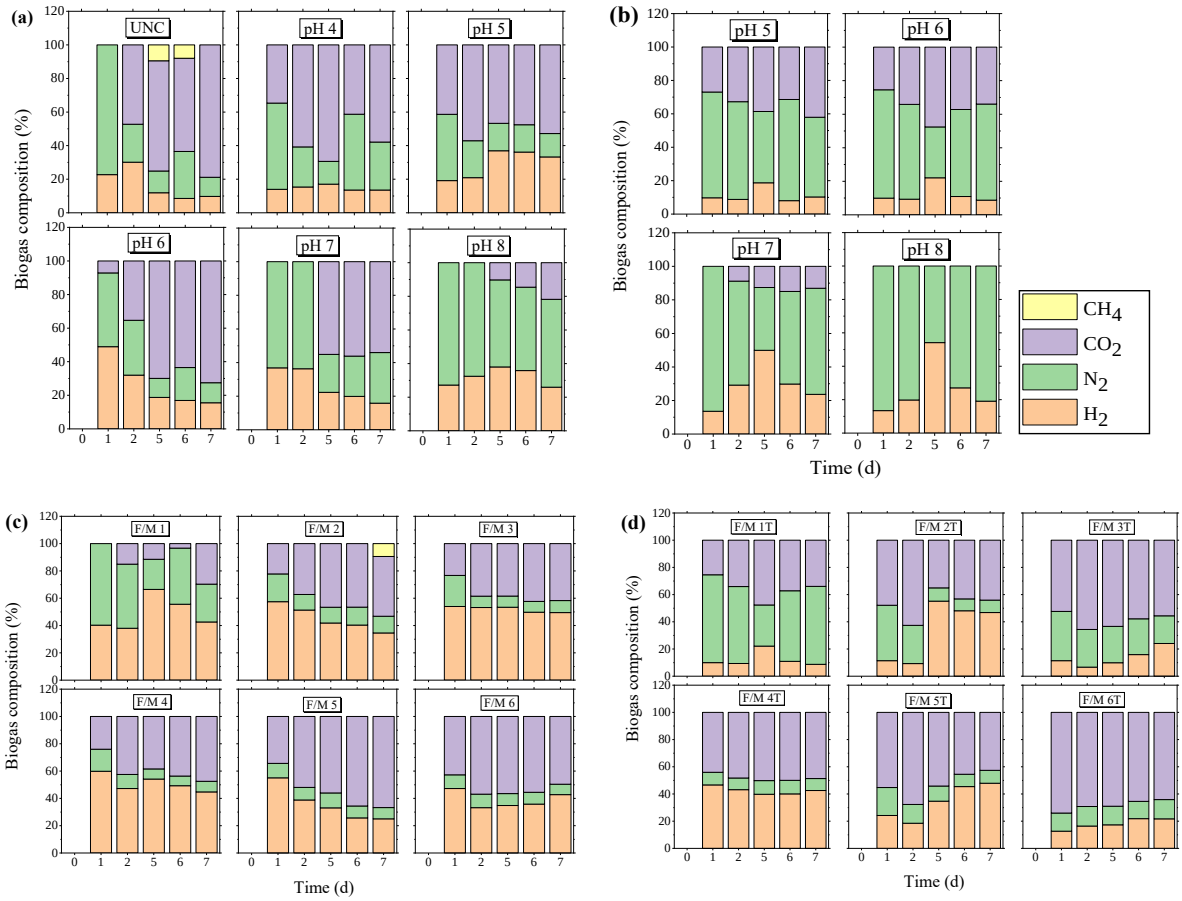

Fig. A3.2. Gas composition in the headspace of the bioreactors at pH 4 to 8 under mesophilic conditions and F/M ratio of 1 (a), pH 5 to 8 under thermophilic conditions and F/M ratio of 1 (b), during mesophilic fermentation at pH 6 and varying F/M ratios of 1 to 6 (c), and during thermophilic fermentation pH 6 and varying F/M ratios of 1 to 6 (d).

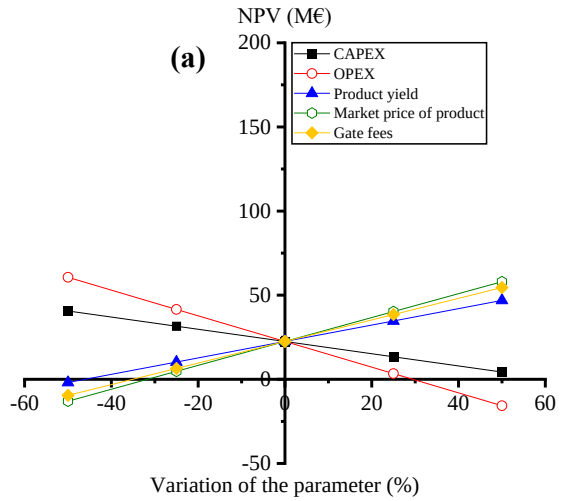
(a)
NPV (M€)
CAPEX
OPEX
Product yield
Market price of product
Gate fees
Variation of the parameter (%)

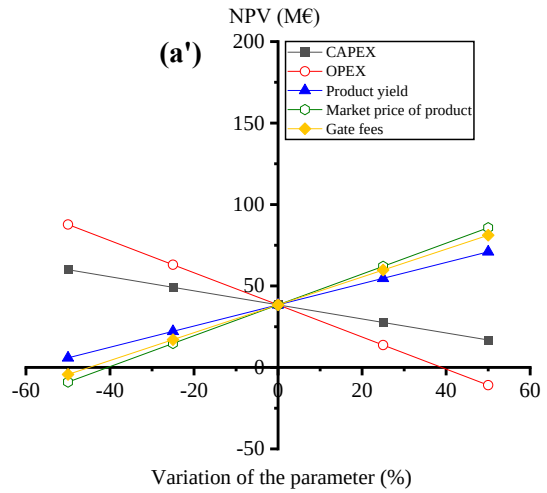
(a')
NPV (M€)
CAPEX
OPEX
Product yield
Market price of product
Gate fees
Variation of the parameter (%)

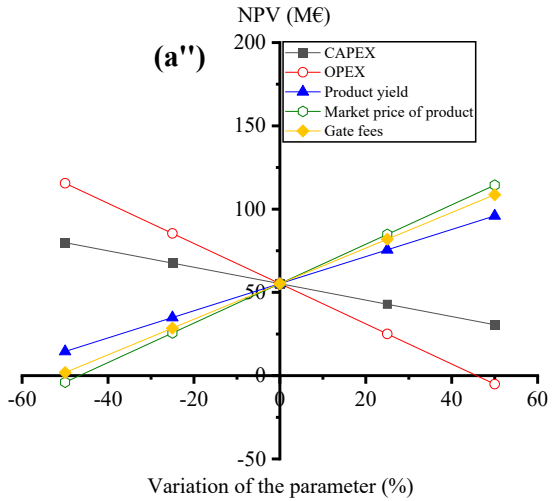
(a'')
NPV (M€)
CAPEX
OPEX
Product yield
Market price of product
Gate fees
Variation of the parameter (%)

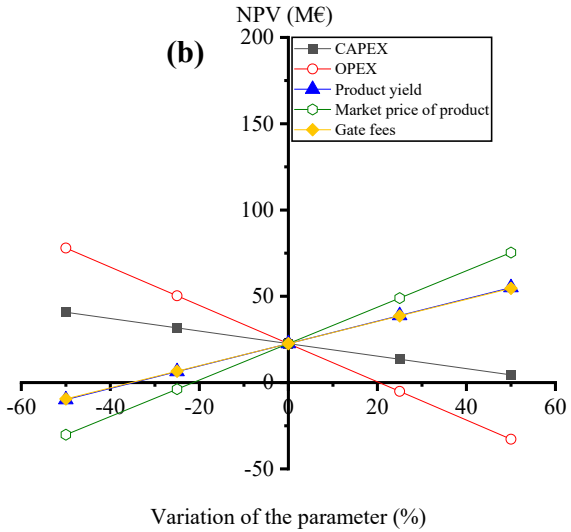
(b)
NPV (M€)
CAPEX
OPEX
Product yield
Market price of product
Gate fees
Variation of the parameter (%)

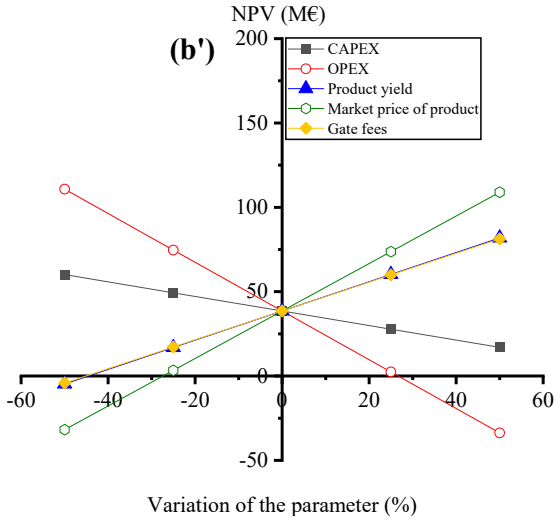
(b')
NPV (M€)
CAPEX
OPEX
Product yield
Market price of product
Gate fees
Variation of the parameter (%)

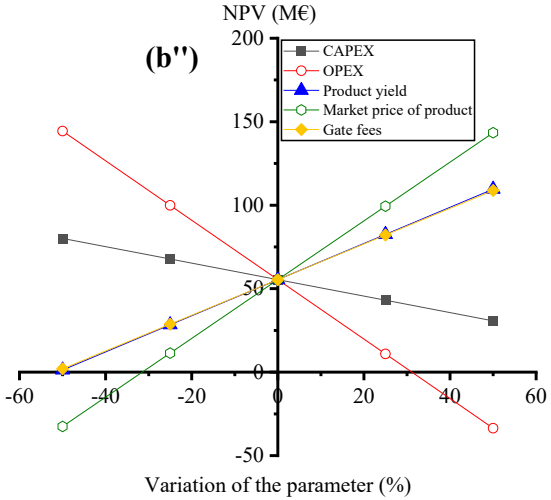
(b'')
NPV (M€)
CAPEX
OPEX
Product yield
Market price of product
Gate fees
Variation of the parameter (%)

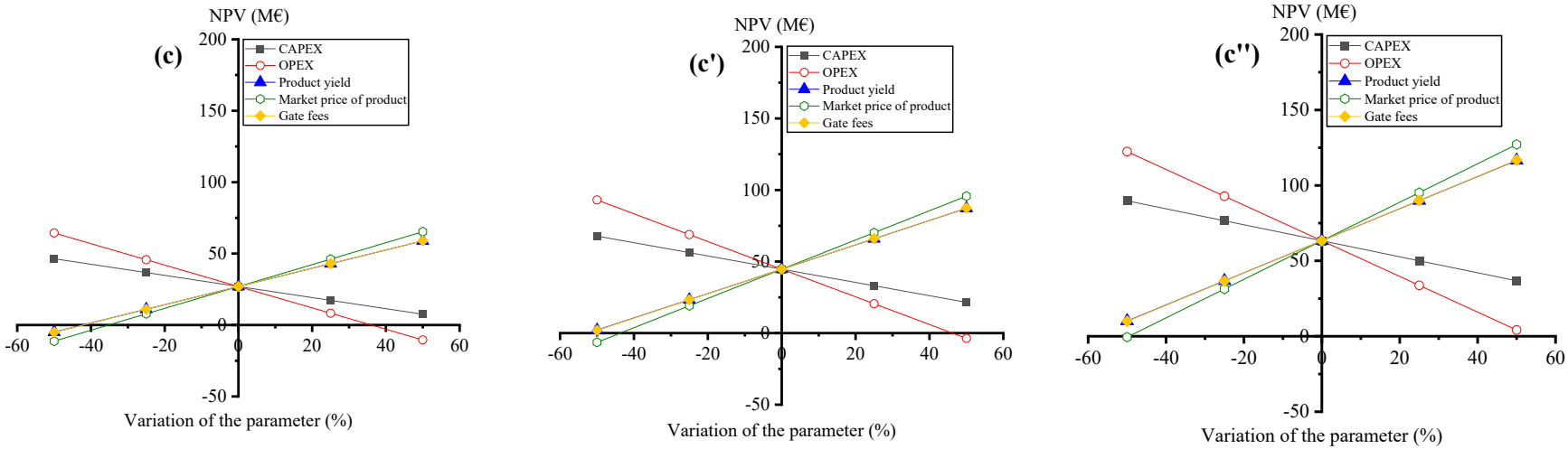

Fig. A3.3. Sensitivity analysis of the influence of varying cost parameters on the net present values (NPVs) of scenario 1 (a) 60 kt/y, (a') 80 kt/y, (a'') 100 kt/y, scenario 2 (b) 60 kt/y, (b') 80 kt/y, (b'') 100 kt/y, and scenario 3 (c) 60 kt/y, (c') 80 kt/y, (c'') 100 kt/y. CAPEX and OPEX means capital expenses and operating expenses, respectively.

Appendix B (chapter 4)

Text A4.1. Trace element solution

The trace element solution contained the following per liter of Milli-Q water: nitrilotriacetic acid 2.0 g; $MnSO_4.H^2O$ 1.0 g; $Fe(SO_4)_2(NH4)_2.6H_2O$ 0.8 g; $CoCl_2.6H_2O$ 0.2 g; $ZnSO_4.7H_2O$ 0.2 mg; $CuCl_2.2H_2O$ 20.0 mg; $NiCl_2.6H_2O$ 20.0 mg; $Na_2MoO_4.2H_2O$ 20.0 mg; Na_2SeO_4 20.0 mg; Na2WO4 20.0 mg.

Text A4.2. Vitamin solution

The vitamin solution contained the following per liter of Milli-Q water: vitamin B12, 100.0 mg; p-aminobenzoic acid 80.0 mg; D(+)-biotin 20.0 mg; nicotinic acid 200.0 mg; calcium pantothenate 100.0 mg; pyridoxine hydrochloride 300.0 mg; thiamine-HCl × 2 H_2O 200.0 mg.

Text A4.3. Analytical methods for biogas volume

The biogas produced during acidogenic fermentation was collected in air-tight gas bags connected to the bottles. After fermentation, the gas bags were removed and connected with tubing to an air-tight water column, which was opened from the bottom. The gas released from the gas bags displaced a certain amount of water from the water column. The displaced water was weighed, and the mass was converted to volume at standard temperature (273. 15 K) and pressure (1 bar).

Meanwhile, the biogas volumes in the chain elongation, SMA, and batch CO conversion experiments were determined based on the pressure in the headspace. The gas pressure was measured by a digital manometer (LEO 1, KELLER Pressure, Switzerland). After measuring the gas pressure (referred to as P_1, mbar), the biogas was released under water to prevent gas exchange, and the pressure was then measured again (referred to as P_2 for the next day, mbar). The volume of biogas produced was calculated as

$$V_{biogas} = \frac{(P_1 - P_2) \times V_{head} \times M}{R \times T} \quad \text{(S1)}$$

Where V_{biogas} refers to the daily biogas volume (L), V_{head} is the volume of the headspace (L), M is the molar volume (22.41 L/mol), R is the universal gas constant (83.14 L mbar/K/mol), and T is the absolute temperature (K).

Text A4.4.: Stochiometric estimation of the amount of potential MCFAs yield from the unfermented ethanol.

The amount of MCFAs (caproate) that could have been generated from the unfermented ethanol was stoichiometrically estimated using equation S2:

$$6C_2H_5O + 5C_4H_7O_2^- \rightarrow 5C_6H_{11}O_2^- + C_2H_3O_2^- + 4H_2O + 2H_2 + H^+, \Delta G^O = -183.5\ kJ/mol \quad (S2)$$

Table A4.1. n-caproate yield from unfermented ethanol.

CO partial pressure	n-Caproate yield from unfermented ethanol (g COD/L)
P_{co} 0.25	0.6 ± 0.5
P_{co} 0.5	1.2 ± 0.4
P_{co} 1.00	1.8 ± 0.2

Table A4.2. Characteristics of the food waste substrate in comparison with those of previous studies.

Parameter	This study	Arhin et al. (2023)	Contreras-Davila et al. (2020)	Okoro-Shekwaga et al. (2021)
pH	5.5 ± 0.0	4.9 ± 0.0	6.0	4.80
Total solids (g/L)	253.6 ± 7.4	216.1 ± 8.7	200.2 ± 2.2	295.0 ± 0.3
Volatile solids (g/L)	209.7 ± 5.6	200.5 ± 8.2	179.4 ± 1.1	314.3 ± 0.2
Total COD (g/L)	321.4 ± 42.2	432.6 ± 26.2	276.6 ± 52.5	469.7 ± 0.0
Soluble COD (g/L)	90.7 ± 5.2	126.0 ± 7.2	125.2 ± 0.6	-
Total carbohydrates (g/L)	115.6 ± 11.1	151.8 ± 16.9	83.5 ± 4.2	-
Soluble carbohydrates (g/L)	86.2 ± 1.9	84.9 ± 7.8	-	-
Total proteins (g/L)	44.3 ± 8.6	21.2 ± 5.8	-	-
Soluble proteins (g/L)	8.9 ± 0.5	10.4 ± 0.3	-	-
Total volatile fatty acids (g/L)	7.1 ± 1.2	0.2 ± 0.0	7.35 ± 0.4	5.1 ± 3.5
Ethanol (g/L)	0.6 ± 0.2	0.0 ± 0.0	4.4 ± 0.0	-
Lactate (g/L)	14.3 ± 0.1	8.5 ± 0.3	18.6 ± 1.3	-
Alkalinity (g $CaCO_3$/L)	2.1 ± 0.2	-	6.7 ± 0.4	-

- Implies unavailable data.

Table A4.3. Experimental setup for chain elongation.

Group 1	**Group 2**	**Negative control**
P_{CO} 0.00 (control) #	2-Bromoethanesulfonate addition (BES, 10 g/L)	Blank (no substrate)
P_{CO} 0.25	Heat-shocking of inoculum (HS, 100 ° C for 10 min)	
P_{CO} 0.50		
P_{CO} 1.00		

P_{CO} = Carbon monoxide partial pressure (bar).

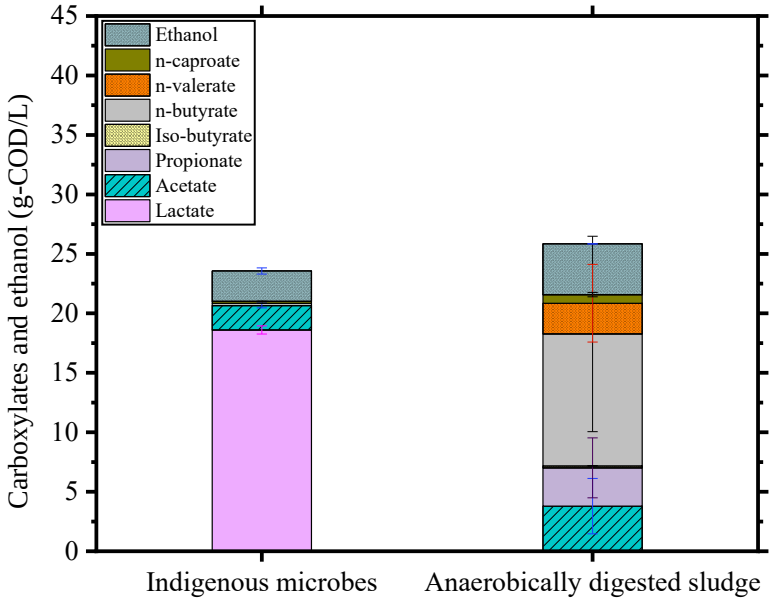

Fig. A4.1. Carboxylates and ethanol profile in the acidogenic fermentation reactions with the indigenous microbiota in food waste or anaerobically digested sludge as inoculum.

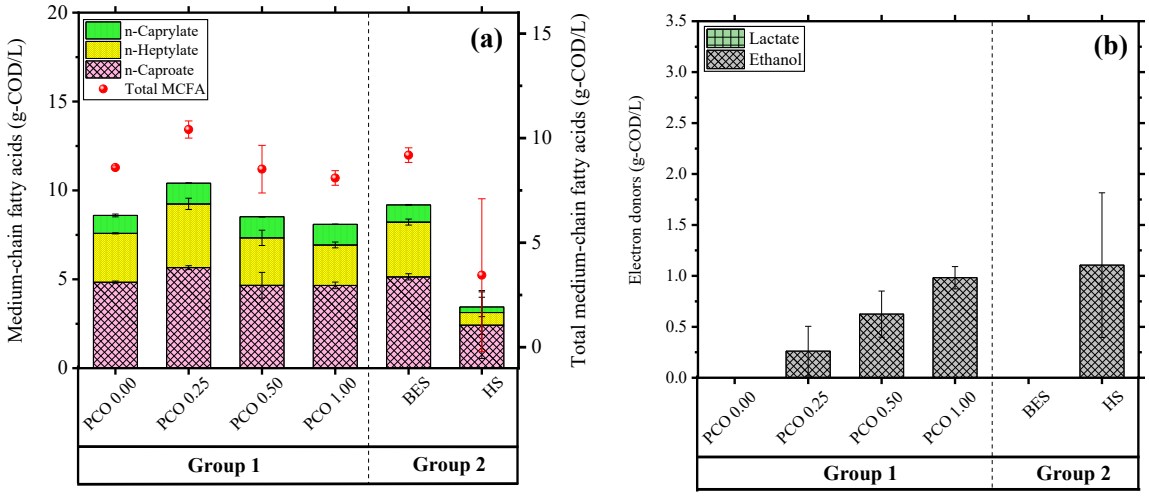

Fig. A4.2. (a) Total medium-chain fatty acids and (b) ethanol accumulation the end of chain elongation.